PREDATOR-PREY INTERACTIONS IN AEROBIC GRNAULATION SYSTEMS CHAN SIEW HERNG 2018

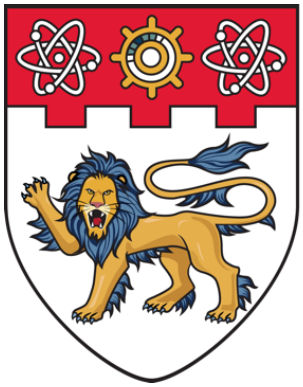

NANYANG TECHNOLOGICAL UNIVERSITY
SINGAPORE

PREDATOR-PREY INTERACTIONS IN AEROBIC GRANULATION SYSTEMS

CHAN SIEW HERNG

Interdisciplinary Graduate School

Singapore Centre for Environmental Life Sciences Engineering

2018

PREDATOR-PREY INTERACTIONS IN AEROBIC GRANULATION SYSTEMS

CHAN SIEW HERNG

Interdisciplinary Graduate School

Singapore Centre for Environmental Life Sciences Engineering

A thesis submitted to the Nanyang Technological University
in partial fulfilment of the requirement for the degree of

Doctor of Philosophy

2018

ACKNOWLEDGEMENTS

I would like to express my utmost gratitude to my supervisor, Assoc. Prof Scott Rice, for giving me this opportunity to be part of this exciting work. He has been absolutely encouraging and I sincerely appreciate his tremendous support and guidance throughout the thesis. His enthusiasm and contributions to my work are greatly appreciated. It has been a pleasant and fruitful experience and I hope I have achieved your expectations.

I thank Assoc. Prof. Diane McDougald for her guidance and encouragements during the process of my PhD. The harmonious teamwork between Scott and Diane has been essential for the completion of this thesis. The constructive feedback and criticisms of my writing has also helped to improve my scientific writing skills.

I also wish to thank Prof. Stefan Wuertz for his supervision and contributions towards my PhD journey.

I am extremely grateful to Dr. Grant Tan for his great patience and willingness to render assistance throughout the project. I appreciate his time and efforts in mentoring and helping me to plan out the structure of my thesis. Without his help, the operation of bioreactors and the subsequent processing of results would have been a tedious one.

I am also especially grateful to Muhammad Hafiz for his efforts during the operation of the bioreactors. He has always been a great team player and teaming up with him has made the bioreactor work much more enjoyable. His key role in the bioinformatics part of my project is also greatly appreciated.

Special thanks to Dr. Henriette Lyng Røder for her close collaboration in the single and mixed species biofilm work. Her efforts in the laboratory and manuscript writing were important contributions towards the completion of Chapter 4 and an ongoing manuscript.

Also, special thanks to Dr. Kelvin Lee for his useful advice and guidance during our single and mixed species biofilm work.

I would also like to thank the Interdisciplinary Graduate School, NTU and Singapore Centre for Environmental Life Sciences Engineering for their assistance and valuable resources to facilitate this work.

I would like to thank Shi Ming, Peiyi, Yan Hong, Adelicia, Wee Han, Dan and many others for their friendship and making the laboratory a friendly place to work at.

I also express my deepest gratitude to my family members and friends for all their undying support and encouragements.

Lastly, my heartfelt thanks and gratitude to my loving partner, Wai Kae, whose unwavering love and support has been the greatest motivation and driving force during my PhD candidature. I look forward to the upcoming arrival of our little one with much excitement.

TABLE OF CONTENTS

LIST OF TABLES

LIST OF FIGURES

LIST OF ABBREVIATIONS

AI	Autoinducer
AHL	Acyl homoserine lactone
ANOVA	Analysis of variance
AOB	Ammonia oxidizing bacteria
BALO	*Bdellovibrio* and like organisms
CAFB	Continuous flow airlift fluidized bed reactor
CLSM	Confocal light scanning microscope
COD	Chemical oxygen demand
DMSO	Dimethyl sulfoxide
DO	Dissolved oxygen
DPAO	Denitrifying polyphosphate accumulating organism
EBPR	Enhanced biological phosphorus removal
EPS	Extracellular polymeric substances
FA	Free ammonia
g	Grams
h	Hour
L	Litre
LB	Luria-Bertani
MBBR	Moving bed biofilm reactor
MDS	Multidimensional scaling
mSBRs	Mini-sequencing batch reactors
min	Minute
mL	Mililitre

MLSS	Mixed liquor suspended solids
MLVSS	Mixed liquor volatile suspended solids
NOB	Nitrite oxidizing bacteria
OTU	Operational taxonomic unit
PE	Paired-end
PAO	Polyphosphate accumulating organism
PERMANOVA	Permutational multivariate analysis of variance
PHAs	Poly-β-hydroxyalkanoates
PMNs	Polymorphonuclear leukocytes
PS/PN	Polysaccharide/protein ratio
QS	Quorum sensing
SBR	Sequencing batch reactor
SDS	Sodium dodecyl sulphate
SND	Simultaneous nitrification-denitrification
SNDPR	Simultaneous nitrification-denitrification phosphorus removal
SUAV	Superficial upflow air velocity
SVI	Sludge volumetric index
T3SS	Type III secretion system
T6SS	Type VI secretion system
VFA	Volatile fatty acids
WT	Wild type

LIST OF PUBLICATIONS

Manuscripts

1. **Chan, S. H.,** Røder, H. L., Madsen, J. S., Lee, K. W. K., Sørensen, S. J., Givskov, M., Burmølle, M., Rice, S. A. and McDougald, D. "Associational resistance to predation by protists in a multispecies biofilm" (Manuscript in preparation)

2. **Chan, S. H.,** Tan, C. H. G., Ismail, M. H., Rice, S. A., McDougald, D. "Predator-prey interactions in aerobic granular sludge" (Manuscript in preparation)

Conferences

1. **Chan, S. H.,** Røder, H. L., Lee, K. W. K., Sørensen, S. J., Burmølle, M., Rice, S. A. and McDougald, D. "*Pseudomonas aeruginosa confers resistance to predation in mixed species biofilms*" Conference presentation at 7th ASM Conference on Biofilms 2015, Chicago, USA. (Poster presentation)

2. **Chan, S. H.,** Tan, C. H. G., Ismail, M. H., Rice, S. A., McDougald, D. "Predator-prey interactions in aerobic granular sludge" Conference presentation at IWA Specialist Conference Microbial Ecology and Water Engineering 2016, Copenhagen, Denmark. (Poster presentation)

ABSTRACT

Predation by protozoa can impact bacterial communities by controlling their biomass and alter the community species composition. Bacterial communities are essential for the functioning of most ecosystems including engineered systems such as activated floccular sludge, where bacteria are responsible for biological nutrient removal and flocculation. Activated floccular sludge is often utilized to cultivate aerobic granules over long periods of time. Although the formation of granules has been optimized by controlling physical factors, the instability of aerobic granules remains a challenge for its implementation in full-scale wastewater treatment systems. While it has been hypothesised that protozoa are important in the formation of granules, no studies have characterized the abundance and diversity of protozoa during aerobic granulation.

In this study, the impact of protozoa on microbial communities was monitored. Sessile ciliates were reported to be the most abundant protozoa that colonized the surfaces of granules. These ciliates consume suspended bacteria and are also hypothesized to act as a form of substratum for bacteria; colonization. Here, four bioreactors seeded with activated floccular sludge were operated for aerobic granulation for 11 weeks to better understand the roles of protozoa during the formation of aerobic granules. The abundance and diversity of protozoa decreased initially due to reduction in settling time. Upon the formation of granules, sessile ciliates became the dominant group of protozoa with gradual increase in abundance. However, microbial community analysis and correlation studies demonstrated that protozoa did not have a significant role in granule formation. In

contrast, bacteria, particularly *Candidatus Accumulibacter*, were suggested to have a greater role in the formation of granules.

The role of predation by protozoa on the formation of granules was further explored through the inhibition of protozoa in floccular sludge performed to investigate if aerobic granulation would be affected without protozoa. The absence of protozoa did not significantly affect the formation of granules from floccular sludge. Similar to the experiments following the changes in the community composition, it was also observed that *Candidatus Accumulibacter* was highly dominant when granules were formed in the treated sludge. In addition, inhibition of protozoa, including sessile ciliates on the surface of pre-formed granules, also did not result in disintegration of granules. Granules with and without sessile ciliates continued to maintain their granular appearance and size. Overall, the data suggested that protozoa did not play a dominant role in granulation and it was the change in sludge morphology that selected for the dominance of sessile ciliates in granules.

Aerobic granules and activated floccular sludge comprised of high species diversity. Therefore, to better define the mechanisms that drive the interaction between microbial communities and predators, a mixed species biofilm system composed of *Pseudomonas aeruginosa*, *Klebsiella pneumoniae* and *Pseudomonas protegens* was subjected to protozoan grazing by the model ciliate, *Tetrahymena pyriformis*. It was found that grazing sensitive strains, *K. pneumoniae* and *P. protogens*, gained associational resistance from the grazing resistant *P. aeruginosa*. This resistance was partly due to the production of

rhamnolipids, however results showed that there were other unidentified factors that provide *P. aeruginosa* resistance to predation.

Chapter 1: LITERATURE REVIEW

1.1. Bacterial biofilms

Bacteria generally exist as single cells in planktonic populations or as biofilms, which are immobile bacterial communities that adhere to surfaces. Biofilms are an assemblage of microorganisms that are enclosed in extracellular polymeric substances (EPS). The biofilm lifecycle consists of transitions from single cells to mature microcolonies to subsequent dispersal of highly motile and differentiated cells from these microcolonies (Hall-Stoodley et al. 2004). During the attachment phase, free swimming bacteria use their flagella or pili to loosely attach themselves to surfaces. This attachment becomes irreversible when EPS is being produced by the attached bacteria. The presence of EPS mediates adhesion for bacterial cells to surfaces and immobilizes them, keeping them in close proximity which allows for interactions between cells such as cell-cell communication and horizontal gene transfer.

The EPS is made up of polysaccharides, glycoproteins, glycolipids, nucleic acids, humic substances and water (Flemming et al. 2007, Flemming and Wingender 2010). The EPS composition depends on the environmental conditions, stresses, bacterial species and the surface on which biofilms are formed (Branda et al. 2005). Within the EPS matrix, bacteria continue to propagate which expands the biofilm to maturation. After maturation, the biofilm can enter the final stage where some bacterial cells disperse from the biofilm into its surroundings.

Active dispersal from the biofilm is a highly regulated process that is initiated by the bacteria and can be triggered by modifications to several environmental factors, such as

temperature, nutrients, oxygen and metabolite concentrations (McDougald et al. 2012). Genes associated with cell motility and polysaccharide degradation, such as flagella biosynthesis and dispersin secretion, respectively, are upregulated in active dispersal, while genes responsible for production of EPS, i.e. polysaccharide synthesis, were downregulated (McDougald et al. 2012, Toyofuku et al. 2016). In contrast to active dispersal, passive dispersal refers to the detachment of biofilm cells that involves physical forces such as hydrodynamic shear and protozoan grazing (Kaplan 2010). The formation and dispersal of biofilms can also be influenced by quorum sensing, which is a form of communication between cells for the coordination of group behaviours between bacterial populations.

Quorum sensing (QS) in bacteria depends on sensing and responding to small biochemical signalling molecules known as autoinducers (AI). These signalling molecules are constitutively produced and released into the environment, where the concentration of these signalling molecules are highly dependent on cell density and local diffusion parameters (Hense et al. 2007, Solano et al. 2014). Signalling molecules such as autoinducing peptides (AIPs) are utilized by Gram positive bacteria while acyl-homoserine lactone (AHLs) are produced by Gram negative bacteria. All QS systems are dependent on three basic principles, although they differ in the specific regulatory components and mechanisms (Rutherford and Bassler 2012). First, the bacterial members in the community produce AIs and the concentration of AIs are dependent on the cell density. At low cell density, the AIs will be present at concentrations below the detection threshold and hence would not elicit any cooperative response. In contrast, a high cell density would result in high concentrations of AI that enables detection and induction of a

collective response from the bacterial populations. Second, receptors present in the bacterial cytoplasm or membrane are responsible for detecting AIs. Third, the detection of AIs results in the induction of genes that is associated with the specific QS response, e.g. biofilm formation or virulence factor expression.

In addition to biofilm formation and dispersal, quorum sensing systems are also responsible for controlling processes such as bioluminescence (Nealson et al. 1970) and expression of virulence factors (de Kievit and Iglewski 2000). For example, there are two major QS pathways in the Gram negative bacterium, *Pseudomonas aeruginosa*, the *las* and *rhl* systems consisting of the response regulators, LasR and RhlR and the signal synthases, LasI and RhlI (Pearson et al. 2000). These quorum sensing pathways regulate the expression of several virulence factors. The loss of virulence was observed in mouse models infected with a *lasI* mutant, where a *rhlI* mutant, and a *lasI rhlI* double mutant in mouse models of infection demonstrated significant loss of virulence, with the double mutant showing the least virulence (Pearson et al. 2000). Mutations in these quorum sensing pathways also led to reduced recovery of bacteria in contrast to the wild type strain from the organs of the mouse. In addition, complementation of *lasI*, *rhlI*, or both *lasI* and *rhlI* in the double mutant significantly increased the *in vivo* virulence in the mouse model (Pearson et al. 2000). Hence, these studies demonstrated that QS can regulate the level of virulence in *P. aeruginosa.*

Biofilm formation is also regulated by QS. The formation of biofilms provides a form of protected growth for bacteria against a diverse range of stresses such as antibiotics and ultraviolet light. Cells within biofilms are also at least 100 to 1000 times more resistant

than planktonic cells to antibiotics and disinfecting agents (Stewart and William Costerton 2001). For example, a *mutant P. aeruginosa* biofilm that does not produce the *las* signal molecule, 3-oxo-C_{12}-HSL, was significantly thinner than the wild type strain (Davies et al. 1998). Moreover, the mutant strain appeared to grow as continuous, flat biofilms compared to the distinctive microcolonies of the wild type strain. The mutant strain was also sensitive to sodium dodecyl sulfate (SDS) and was removed upon exposure to the surfactant, unlike the wild type strain biofilm that remained after SDS treatment. However, the mutant biofilms regained resistance to SDS upon the exogenous addition of 3-oxo-C_{12}-HSL (Davies et al. 1998). Therefore, quorum sensing is essential for biofilm formation and differentiation.

Biofilm formation has negative implications in food processing environments where biofilms have significantly contributed to food spoilage or transmission of diseases (Van Houdt and Michiels 2010). Hence, the inherent resistance to antimicrobials has contributed to the persistence and chronic nature of biofilm associated infections and diseases. However, there are also beneficial applications of biofilms where they play important roles in bioremediation and wastewater treatment. Bioremediation is an emerging *in situ* technology utilising microbes to reduce and degrade contaminants that pose environmental and human risks. Indigenous biofilms from soil, water and sediments constantly perform bioremediation as part of the global nutrient cycling (Edwards and Kjellerup 2013). In comparison to bioremediation with planktonic microorganisms, biofilm mediated bioremediation is more effective, as cells within biofilms are protected by the matrix (Edwards and Kjellerup 2013, Singh et al. 2006). When both biofilm associated cells and planktonic cells of *Pseudomonas stutzeri* T102

were tested in natural petroleum contaminated soils over a period of 10 weeks, only the biofilm cells survived. Higher naphthalene degradation activity was also detected in soils inoculated with *P. stutzeri* T102 biofilms than soils with planktonic cells (Shimada et al. 2012).

Biofilms are also favoured over activated floccular sludge in wastewater treatment. The long residence time of biofilms is suitable for waste treatment processes that require slow growing organisms with poor biomass yield (Wilderer et al. 2000). Wastewater biofilms can be further enhanced by growing them on a range of support materials which can be suspended or fixed in bioreactors. Hence, biofilms do not require the long settling times observed in activated floccular sludge to retain high concentration of sludge while maintaining similar nutrient removal efficiency (Arnold et al. 2000). For example, specially designed polyethylene biofilm carriers utilized in moving bed biofilm reactors (MBBRs) provide a large surface area for micro-organisms to form biofilms and perform specific biological treatment functions (Biswas and Turner 2012). Therefore, the use of biofilm carriers provides a very compact configuration while achieving a highly active biomass concentration in the MBBRs and a low settling load in the downstream solids separation process. The addition of plastic nets into the aeration tanks can also serve as surfaces for bacterial attachment and their subsequent biofilm formation, which can enhance nutrient removal efficiency in the activated sludge process (Gebara 1999). This approach is useful to increase the overall biomass concentration in the aeration tank. Hence, the combination of both biofilms and suspended microorganisms considerably increased the efficiency of biochemical oxygen demand removal and a reduced sludge settling time in synthetic wastewater (Gebara 1999).

1.2. Activated sludge wastewater systems

Activated sludge is a biological wastewater treatment process that utilizes microorganisms to remove organic and inorganic matter. These microorganisms typically exist as a form of suspended biomass aggregates known as flocs which are responsible for nutrient and organic removal from wastewater. These flocs are suspended biofilms that can be separated from the effluent by gravitational settling over a period of time. This settling process produces quality effluents that are relatively free of suspended solids and organic matter. As flocs have poor settling characteristics, large aeration tanks and secondary clarifiers are required to provide large reaction volumes needed to retain sufficient floccular biomass for the targeted level of nutrient removal efficiency (Sadrzadeh and Dulekgurgen 2014). Hence, activated sludge systems typically need large areas to accommodate such requirements. Activated sludge treatment plants are typically operated for nutrient removal such as nitrogen and phosphorus prior to effluent discharge. The removal of these nutrients is central in preventing algal blooms and excessive growth of other photosynthetic microorganisms in aquatic environments (Cloete and Bosch 1994). Both enhanced biological phosphorus removal and simultaneous nitrification-denitrification and phosphorus removal are two common wastewater technologies utilized for biological nutrient removal in activated sludge.

1.2.1. Enhanced biological phosphorus removal

In activated sludge, enhanced biological phosphorus removal (EBPR) is commonly utilized for carbon and phosphorus removal without the need for chemical additives, and is achieved through the alternation between anaerobic and aerobic conditions. Biological

phosphorus removal largely relies on microorganisms known as polyphosphate accumulating organisms (PAOs) which can accumulate phosphate intracellularly. These microorganisms can assimilate volatile fatty acids (VFAs) anaerobically while degrading polyphosphate to for the storage of intracellular VFAs such as poly-β-hydroxyalkanoates (PHAs) (Figure 1.1). Under aerobic conditions, PAOs metabolize the intracellular PHAs to provide the energy for phosphate assimilation from the wastewater into intracellular polyphosphate (Figure 1.1). This intracellular accumulation of phosphate in PAOs and their subsequent discharge in the waste sludge leads to phosphorus being removed from the wastewater.

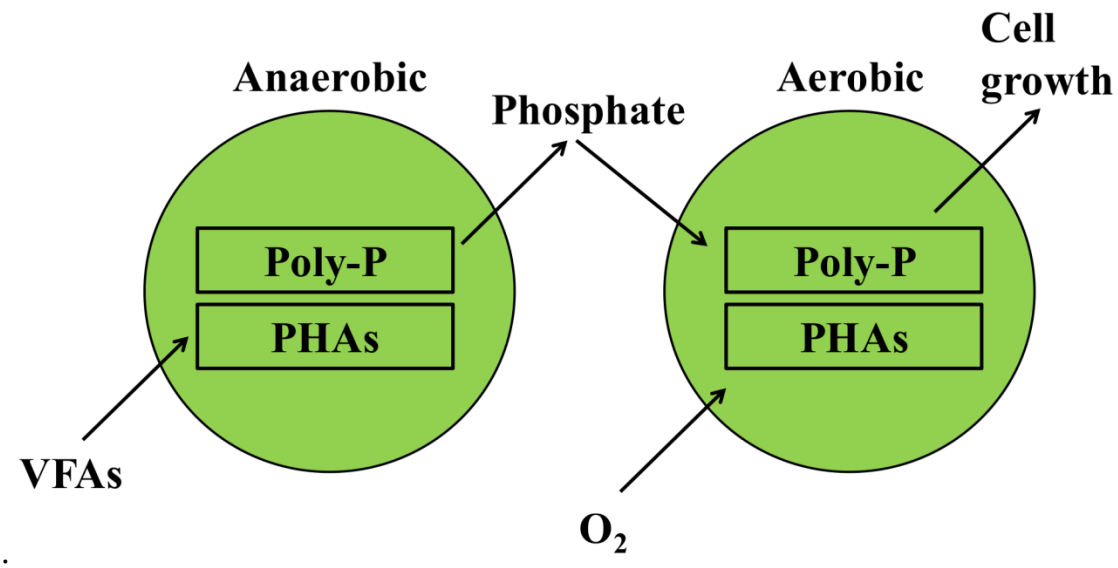

Figure 1.1: Metabolism of PAOs during anaerobic and aerobic phases in the EBPR process. During the anaerobic phase, VFAs from wastewater are taken up by PAOs for assimilation in PHAs while poly-P is degraded and released as phosphate. During the aerobic phase, PHAs are hydrolysed to provide the energy required for phosphate assimilation from the wastewater and store them as intracellular polyphosphate.

The most common PAOs identified in EBPR bioreactors and full-scaled EBPR plants were the Candidatus *Accumulibacter phosphatis (He et al. 2007, He and McMahon 2011)* . Other PAO candidates belonging to the genera *Actinobacteria* (Kawakoshi et al. 2012) and *Tetrasphaera* (Kristiansen et al. 2013, Nielsen et al. 2012) were also associated with phosphorus removal, despite their physiological differences compared to *Accumulibacter*. Alternating between anaerobic and aerobic phases can enrich for PAOs, which enhances the performance of phosphorus removal. However, the conditions for PAO enrichment are also fitting for the growth of glycogen accumulating organisms (GAOs). Like PAOs, GAOs such as Candidatus *Competibacter phosphatis*, can compete with PAOs for carbon sources anaerobically to store that carbon as PHAs, which are subsequently used under aerobic conditions for energy generation and growth (Crocetti et al. 2002). However, unlike the PAOs, GAOs neither degrade polyphosphate anaerobically nor accumulate phosphate aerobically (Oehmen et al. 2006). The EBPR process deteriorates when GAOs outcompete and dominate over PAOs (Saunders et al. 2003).

Hence, GAOs are widely regarded as a competitor of PAOs and detrimental towards the efficiency of EBPR systems. As the efficiency of EBPR correlates to the abundance of PAOs, several methods have been utilized to better enrich for PAOs such as alternating carbon sources between acetate and propionate (Lu et al. 2006, Oehmen et al. 2006), maintaining the EBPR process at relatively high temperature of 28^{o}C (Ong et al. 2016) or at a high pH (~7.5-8.0) (Oehmen et al. 2005a)

1.2.2. Simultaneous nitrification and denitrification

Biological elimination of nitrogen is achieved via a two stage process of nitrification and denitrification. Ammonium is converted to nitrite and nitrate by ammonium oxidizing bacteria (AOB) and nitrite oxidizing bacteria (NOB) during nitrification, respectively. During denitrification, denitrifying bacteria reduce nitrate to nitrogen gas (Helmer and Kunst 1998) (Figure 1.2a). However, both nitrification and denitrification have been demonstrated to occur concurrently within a bioreactor under conditions of low dissolved oxygen (DO) (Bertanza 1997, Münch et al. 1996, Pochana and Keller 1999). This process is known as simultaneous nitrification-denitrification (SND) (Figure 1.2b).

During the SND process, ammonium is partially oxidized to nitrite before being subjected to denitrification to nitrogen gas (Yoo et al. 1999). The SND process is more energy efficient as 40% less chemical oxygen demand (COD) is required compared to the two-step nitrification and denitrification system. This process also produces lower biomass yield and higher denitrification rates during aerobic growth (Turk and Mavinic 1986, Turk and Mavinic 1989).

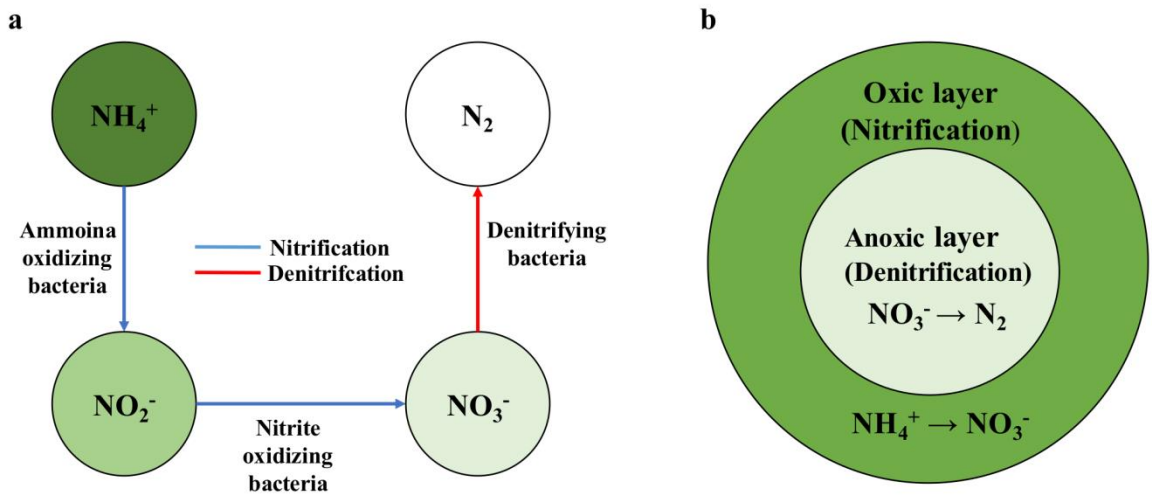

Figure 1.2: Biological elimination of ammonium by bacteria. (a) Ammonium is first oxidized to nitrite by AOB before being further oxidized by NOB to nitrate. Nitrogen gas is formed from the reduction of nitrate during denitrification. (b) For simultaneous nitrification and denitrification, ammonium is partially oxidized to nitrite in the oxic layer before being subjected to denitrification in the anoxic layer to nitrogen gas.

Interestingly, denitrification in anaerobic-anoxic EBPR systems can also be mediated by a novel group of PAOs known as denitrifying PAOs (DPAOs) (van Loosdrecht et al. 1998). These DPAOs are capable of simultaneous nitrate and nitrite reduction coupled with phosphate uptake using the same COD (Kerrn-Jespersen et al. 1994, Kuba et al. 1994). Nitrate is utilized by DPAOs as an electron acceptor instead of oxygen although they are less energy efficient, resulting in approximately 20% lower biomass yield (Murnleitner et al. 1997). Although DPAOs are less energy efficient, bench-scaled reactors enriched with DPAOs reported sufficient levels of phosphorus removal to be used commercially (Peng et al. 2006). Therefore, DPAOs are beneficial in biological nutrient removal systems for lowering COD demand, reduced cost of aeration and reduction in sludge production.

1.2.3. Simultaneous nitrification, denitrification and phosphorus removal

Recently, both processes of SND and EBPR have been integrated to obtain a cost-effective and efficient option for nutrient removal from wastewater. This integrated process is termed simultaneous nitrification, denitrification and phosphorus removal (SNDPR). The feasibility of SNDPR has been shown in laboratory-scaled systems (Fu et al. 2009, Meyer et al. 2005, Rahimi et al. 2011, Zeng et al. 2003) and in a full scale wastewater reclamation plant (Yang et al. 2016). Acetate is consumed during the anaerobic phase of SNDPR followed by the release of phosphorus. Thereafter, phosphorus is assimilated aerobically while ammonium is converted into nitrogen gas without the accumulation of nitrites and nitrates (Lemaire et al. 2006). However, the SNDPR process could be unstable in floccular sludge systems if both aerobic and anoxic zones are not formed in the microbial aggregates, resulting in poor coupling between nitrification and denitrification (Meyer et al. 2005). Hence, aerobic granules was suggested to be beneficial for the SNDPR process (de Kreuk et al. 2005).

Aerobic granules are large and compact microbial aggregates with spherical-like shape. The dense and compact structure of granules facilitates the formation of aerobic and anoxic zones in the granular core due to limitations in the mass transfer of oxygen. The formation of such aerobic and anoxic zones is essential for reliable SNDPR systems (de Kreuk et al. 2005, Lemaire et al. 2006). Several studies have successfully implemented aerobic granular sludge to operate and maintain SNDPR in sequencing batch reactors (SBRs) (Bassin et al. 2012, de Kreuk et al. 2005, Lemaire et al. 2008b, Lu et al. 2016, Yilmaz et al. 2008).

Analysis of the microbial community of the granules revealed that *Accumulibacter* spp. and *Competibacter* spp. were the most abundant members and that both were capable of denitrification (Lemaire et al. 2008b). Structural analysis of the granules indicated that *Accumulibacter* spp. dominated the outer 200 µm layer of the granule, while *Competibacter* spp. were localized in the granular core (Lemaire et al. 2008b). It was concluded that *Competibacter* spp. was responsible for the denitrification process within the SBR instead of *Accumulibacter* spp. (Lemaire et al. 2008b). Previous studies also demonstrated that *Competibacter* spp. was the main denitrifying population in laboratory-scaled SBRs (Lemaire et al. 2006, Zeng et al. 2003). However, microbial communities dominated by *Competibacter* spp. would be undesirable as they are unable to perform phosphorus removal while they compete against *Accumulibacter* spp. for carbon sources. Interestingly, these granules were cultured with only acetate as the carbon source. However, when the granules were exposed to real abattoir wastewater, the abundance of *Competibacter* spp. was significantly reduced (Yilmaz et al. 2008). The reduction in *Competibacter* spp. led to a lower carbon demand with *Accumulibacter* spp. as the dominant denitrification and phosphorus removal population (Yilmaz et al. 2008).

1.2.4. Aerobic granular sludge: a novel technology in biological wastewater treatment

Aerobic granular sludge is an alternative over the conventional activated sludge to treat and remove dissolved organic nutrients from wastewater. Aerobic granules are typically formed without any need for carrier materials by the aggregation of flocs under certain selective conditions (Morgenroth et al. 1997, Weissbrodt et al. 2012). Granules are

differentiated from flocs by their dense and compact structures (Figure 1.3). While flocs are characterized as having an average particle size between 30 to 100 µm, granules have an average particle size between 100 µm to 2000 µm (Barr et al. 2010a). The large particle size and high density of these granules result in fast settling properties and a low sludge volume index (Lemaire et al. 2008a). Improved settling of granules reduces the time required to separate the biomass from the effluent and also prevents them from being washed out of wastewater treatment systems. As a result, a high concentration of biomass is often retained within these systems.

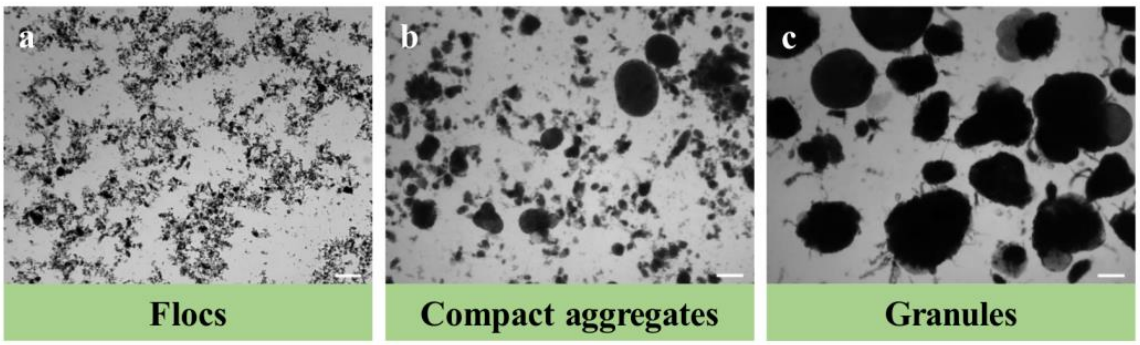

Figure 1.3: Micrographs of sludge morphology during the aerobic granulation process. The aerobic granulation process occurred over a period of 8 weeks with floccular sludge (a) as the seeding sludge. (b) Compact aggregates form after approximately 4 weeks and (c) expanding into granules. Magnification x 40 (bar, 200 µm).

Granules are readily separated from the effluent, which also contributes to the clarity and quality of the treated effluent. Therefore, these factors contribute to a relatively smaller biological footprint compared to conventional floccular systems (de Bruin et al. 2004). Furthermore, aerobic granular sludge also exhibits other advantageous attributes such as high tolerance to high organic loading and toxicity (Adav et al. 2008a). Hence, aerobic

granules have been successfully utilized to treat wastewater contaminated with a wide range of toxic compounds such as phenols, pyridines, heavy metals, chloroanilines to dyes (Maszenan et al. 2011). Recent successes in establishing aerobic granular sludge at the pilot scale (Isanta et al. 2012, Morales et al. 2013) and a full scale plant treating domestic sewage (Pronk et al. 2015) demonstrated the potential of this technology as a replacement for established wastewater treatment technologies.

Despite these recent successes, the inadequate stability of aerobic granules is a limitation towards to the full scale application of aerobic granular sludge due to disintegration of aerobic granules after extended periods of operation. Several mechanisms including filamentous overgrowth, excessive organic loading rates and breakdown of the anaerobic core contributes towards the instability of aerobic granules (Adav et al. 2008b, Adav et al. 2010a, Aqeel et al. 2016, de Kreuk et al. 2007, Liu and Liu 2006, Zheng et al. 2006). These factors contribute to the instability of granules, which can lead to poor settling and separation of aerobic granules from the treated water, resulting in their subsequent washout from the wastewater systems and collapse in reactors' performance.

1.2.5. Factors impacting the formation of aerobic granules

1.2.5.1. Operational parameters

Aerobic granulation is a process whereby floccular sludge is gradually converted to compact aggregates followed by the formation of aerobic granules and finally mature granules under certain operating conditions. These physical operating conditions have been widely studied and implemented in laboratory SBRs to exert selection pressure to obtain aerobic granules. In SBRs, settling time can exert selective pressure on sludge to

retain only sludge with fast settling characteristics. Sludge particles that failed to settle within the required timing are discharged. The role of settling time on aerobic granule formation was studied by Qin et al. (2004) where four SBRs had different settling times of 5, 10, 15 and 20 min, respectively. Although all SBRs eventually formed aerobic granules, the formation of aerobic granules were first observed in SBR 4, which had a 5 min settling time (Qin et al. 2004). Moreover, the proportion of aerobic granules in SBR 4 was the highest amongst all of the SBRs (Figure 1.4). The remaining reactors had varying concentrations of suspended flocs mixed with aerobic granules. This phenomenon was also observed in two SBRs operating at 10 and 2 min settling times where only the SBR operating at the 2 min settling time had completely granular sludge (McSwain et al. 2004). Hence, granules formation can be enhanced by a short settling time which selects for quick settling sludge particles.

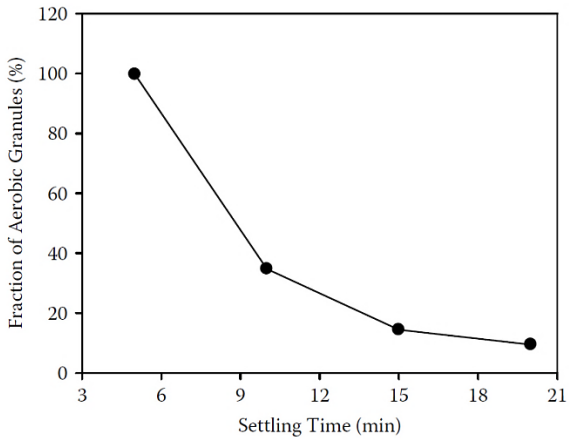

Figure 1.4: Fraction of aerobic granules in SBRs operating at various settling times. A short settling time provides strong selective pressure for only fast settling sludge particles. When the settling time was 20 min, the proportion of aerobic granules was ~10% compared to a ~ 100% when the settling time was 5 min (Qin et al. 2004).

In addition to settling time, shear forces between sludge particles also aid the formation and structure of aerobic granules. These shear forces are a result of hydrodynamic turbulence created by the intermittent upflow sparging of air and nitrogen during SBR operation and are measured by the superficial upflow air velocity (SUAV). The importance of shear forces in granule formation was demonstrated in four SBRs where aerobic granules were only observed in SBRs that operated at 1.2, 2.4 and 3.6 cm s^{-1} while flocs only were observed in the SBR operating at 0.3 cm s^{-1} after 4 weeks (Tay et al. 2001c). Another study also reported the formation of granules only in the SBR operating at a high SUAV of 2.5 cm s^{-1} and only fluffy flocs in another SBR operating at a low SUAV of 0.8 cm s^{-1} (Tay et al. 2001a). Hence, it is necessary to exert a minimum amount of shear force to induce aerobic granules formation. However, a high SUAV within the SBR could create more frequent collisions between sludge particles or granules, resulting in biomass detachment (Gjaltema et al. 1997), that would cause the mean size of granules to decrease (Gjaltema et al. 1997). The thickness of biofilms was also affected by hydrodynamic shear where a thinner biofilm will be formed under strong shear force (Tay et al. 2001c, van Loosdrecht et al. 1995).

Despite reduction in the size and thickness of biofilms, the presence of a high shear force increased the density of the biofilms, which is essential for maintaining the settleability of granules (Chang et al. 1991). The role of shear forces in promoting granule formation was further demonstrated when granules were formed in a continuous flow airlift fluidized bed reactor (CAFB) within 12 days from activated sludge (Zhou et al. 2013). The shear forces exerted by inner circulation of mixed liquor in CAFB were calculated to be a hundred times stronger than in the conventional SBR which utilises the flow of air

bubbles. Furthermore, these granules were formed without other established granulation factors such as settling time and starvation time (Zhou et al. 2013).

1.2.5.2. Biological factors

The presence of shear forces also simulates the production of extracellular polysaccharides (EPS) by the bacterial cells. EPS are sticky materials that accumulate on the surface of bacterial cells and consist of several organic compounds such as exopolysaccharides, proteins, lipids, uronic acid, humic-like substances and nucleic acids (Wang et al. 2006). These EPS mediate the cohesion and adhesion between cells which promotes the initial formation of microbial aggregates (Tay et al. 2001b). The development of aerobic granules was shown to be coupled to an increase in EPS production as a ratio of polysaccharides (PS) to proteins (PN) (Tay et al. 2001b, Tay et al. 2001c). It was demonstrated that floccular sludge was maintained by a low SUAV of 0.3 cm s^{-1}, which resulted in a low PS/PN ratio of 3. However, when aerobic granules were formed under high SUAV, between 1.2 and 3.6 cm s^{-1}, the PS/PN ratio increased from 3 to a range of 9 to 15. Hence, the formation of aerobic granules is clearly dependent on EPS production. Furthermore, EPS can be produced by bacterial cells in sludge as a protective response against stress. The operation of SBRs for aerobic granulation involves cycles of feast-famine, short settling times, short discharge times and high hydrodynamic shear forces which represent specific stress conditions. These stress conditions have been positively correlated to EPS production and the subsequent formation of granules (Adav et al. 2008a).

However, there are also stress conditions such as high concentrations of free ammonia (FA) that are negatively correlated to the production of EPS. It was shown that the cultivation of aerobic granules can be disrupted by high concentrations of FA which blocks EPS production (Yang et al. 2004). Free ammonia was suggested to repress EPS production as the PS/PN ratio declined steadily with an increase in FA concentration. In addition to the formation of granules, EPS is also essential in preserving the architecture of the aerobic granules. Extracellular polysaccharides produced by aerobic granules had both biodegradable and non-biodegradable components (Wang et al. 2007). These non-biodegradable EPS were suggested to belong to the family of beta-linked PS which were also shown to act as the backbone of biofilm structures (Wang et al. 2005). A study by Wang et al. (2005) demonstrated that aerobic granules that were starved for 20 days did not disintegrate despite the granular core being hollowed out. This was due to the non-biodegradable EPS that was localized at the outermost layer of the granule, while the biodegradable EPS on the granule interior was utilized as a form of energy during the starvation period. Hence, the role of EPS production is crucial for the formation of aerobic granules and the subsequent maintenance of granular structure.

Quorum sensing has been established as a mechanism responsible for the production of EPS in bacteria during aerobic granulation (Wang et al. 2017). A study by Tan et al. (2014) demonstrated that EPS production was correlated positively with AHL concentration and granulation, which suggested a close association between these processes. Quantification of EPS showed increases in both polysaccharides and proteins as floccular sludge began to transform into granules. Interestingly, the polysaccharide to protein ratio (PS/PN) was also positively correlated with the accumulation of AHLs in the

sludge. Moreover, the exogenous addition of various AHLs identified from the sludge supernatant significantly increased EPS production by approximately 14 - 36% and proteins by approximately 7 - 16% by the floccular sludge community after 1 h of incubation (Tan et al. 2014).

Furthermore, total RNA sequencing of the sludge biomass revealed that more than half of the top 50 community members had positive correlations with AHL concentration. A large number of genera, e.g. *Nitrosomonas*, *Burkholderiales* and *Xanthomonadaceae*, have been demonstrated to be AHL producers (Tan et al. 2014). Another study by Ren et al. (2010) found that the addition of both extracellular and intracellular substances extracted from granules into floccular sludge could greatly accelerate the formation of aerobic granules. The acceleration effect was most significant in flocs with the addition of granular intracellular substances as the size of flocs increased in size from 0.1 to 0.5 mm within a period 5 days. Based on mass spectrometry, both extracellular and intracellular substances were putatively identified as AHLs (Ren et al. 2010). Hence, it was suggested AHL mediated QS played an important role for aerobic granules development.

The formation of granules and their stability can also be affected by other microorganisms or entities such as protozoa and bacteriophage. Protozoa, particularly sessile ciliates, have been frequently found to exist in high abundance on mature granules (Lemaire et al. 2008a, Schwarzenbeck et al. 2004a). Furthermore, these sessile ciliates were suggested to act as a substratum for bacteria attachment, which would subsequently increase granular size (Weber et al. 2007). Bacteriophage were also found to be responsible for the collapse in performance of a working EBPR granular SBR

(Barr et al. 2010b). Predatory bacteria were also found to significantly reduce both microbial activity and total biomass in aerobic granular sludge (Feng et al. 2017). Therefore, it appears that predation could have an impact on the aerobic granulation process.

1.3. Predators of bacteria

Predation is defined as a biological interaction where a predator feeds on its prey. In all ecosystems, predation can have major impacts on the prey population dynamics (Lima 1998). Mortality in bacterial communities can be attributed to predation, which also exerts strong selective pressure on both phenotypic and taxonomic structure of these communities (Jürgens and Matz 2002). Bacteria in the environment are often exposed to predation by bacteriophages, predatory bacteria and heterotrophic protists.

1.3.1. Bacteriophage

Bacteriophage (phage) are a group of non-living, biological agents enveloped in a protein capsid consisting of a DNA or RNA genome. Phages are obligate intracellular parasites that do not have any intrinsic metabolism and can only function by manipulating the cellular machinery of their bacterial prey. Phages are also abundant and ubiquitous in nature where they typically outnumber bacteria by about 10 fold (Brüssow and Hendrix 2002). Phage predation on bacteria is initiated by the passive diffusion of phage and adsorption to specific surface receptors present on bacterial cell surfaces. These surface receptors may be surface proteins, polysaccharides or lipopolysaccharides (Samson et al. 2013). The infection cycle begins with the introduction of the phage genome into the host bacteria (Fuhrman 1999).

Phages generally reproduce by undergoing the lytic or lysogenic life cycle. Injection of the phage genome into the prey cell during the lytic cycle redirects the host bacterial cell to the production of phage progeny (Figure 1.5a). Phages are subsequently released by bacterial cell lysis. In contrast, the phage genome integrates itself into the host chromosomal DNA during the lysogenic phase, resulting in a dormant prophage (Figure 1.5b). The repression of phage lytic genes maintains the lysogenic state where the prophage are replicated with the host chromosomes. However, certain environmental cues or stressors, such as exposure to UV, will cause the phage to enter the lytic cycle (Weinbauer 2004).

Pseudolysogeny is another phage life cycle which occurs when the phage genome fails to integrate into the bacterial host chromosome to establish either the lytic or lysogenic life cycle (Figure 1.5c) (Feiner et al. 2015). Hence, the phage genome does not become integrated and does not replicate. This phenomenon can occur during nutrient starvation conditions when DNA synthesis or replication is not supported by bacterial cells. However, upon restoration of the nutritional status, the phage will either enter the lytic or lysogenic life cycle.

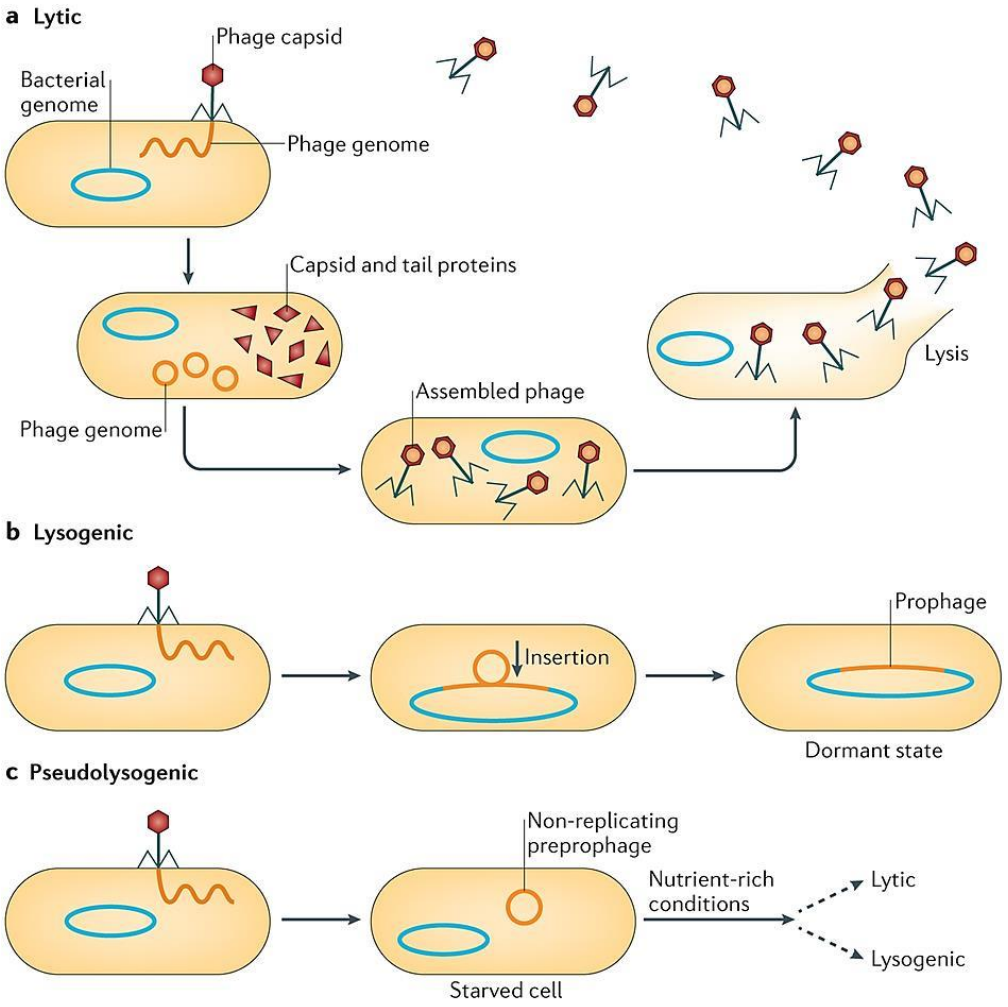

Figure 1.5: Three different types of phage life cycles. a) In the lytic cycle, the bacterial host cellular machinery is directed by the infecting phage to replicate the phage genome. The phage capsids and tails proteins are synthesized, assembled and liberated through bacterial cell lysis**.** b) In the lysogenic cycle, the phage genome integrates itself into the host chromosomal DNA during the lysogenic phase, resulting in a dormant prophage. c) For the pseudolysogenic cycle, the phage genome is unable to replicate or integrate into the bacterial host chromosome under nutrient-deprived conditions (Feiner et al. 2015).

Bacteria are constantly confronted with the threat of phage predation due to the prevalence and high abundance of phage in the environment. Phage predation is known to shape microbial communities in a process known as "kill the winner" strategy, where an increase in a bacterial or archaeal population is followed by an increase in phages specific for the dominant host populations (Breitbart 2012). Ultimately, the abundant host population is killed off or significantly reduced in numbers, which allows another host population to become dominant in the system. This strategy results in the co-existence of closely related, but distinct microbial populations and plays a role in maintaining high microbial diversity within the community (Withey et al. 2005).

Phages also exist in high abundance in both full-scaled wastewater treatment systems (Wu and Liu 2009) and laboratory scaled SBRs (Shapiro et al. 2009). The high abundance of phages in these systems suggests phage predation can significantly impact the sludge microbial community which can negatively affect the process stability of wastewater treatment. In laboratory EBPR SBRs, Candidatus *Accumulibacter phosphatis* are often enriched for their ability to remove phosphorus efficiently from wastewater (Lu et al. 2006, Martin et al. 2006). Hence, these bacteria populations are often present in high density and clonal which makes them natural targets for the "kill the winner" phenomenon. A study by Kunin et al. (2008) found that populations of Candidatus *Accumulibacter phosphatis* in EBPR sludge were exposed to persistent phage predation. Analysis of metagenomic data sets targeting both phage and bacterial genes revealed multiple genes that originated from the phage metagenome. In addition, there was high expression of certain genes in the bacterial metagenome that were hypothetically of prophage origin. These genes encoded proteins that were linked to the phage tail

assembly and a phage-specific endonuclease and terminase, indicating the presence of active phage populations in the EBPR sludge (Kunin et al. 2008).

Phage infections were found to cause deterioration of phosphorus removal performance in laboratory-scaled EBPR floccular and granular sludge bioreactors (Barr et al. 2010b). Proteomic analysis of proteins extracted from a crashed Granular SBR also identified the three most prominent proteins as phage tail sheath proteins (Barr et al. 2010b). In well performing EBPR SBRs, bacteriophage proteins were not in high abundance (Wilmes et al. 2008). When supernatant obtained from the crashed granular SBR were inoculated into healthy floccular and granular sludge SBRs, a drastic decline in the *Accumulibacter* spp. population and phosphorus removal was observed (Barr et al. 2010b). The decline in *Accumulibacter* spp. abundance also led to an increase of *Competibacter* spp. populations and the loss of VFA uptake during the anaerobic phase. These observations indicated that phages specific for *Accumulibacter* spp. were present in the failing granular SBR and the subsequent inoculation of its supernatant into healthy floccular and granular SBRs resulted in phage-induced cell lysis, which led to the failure of the EBPR process.

While phage predation has been demonstrated to negatively impact the bacterial populations and disrupt nutrient removal processes, recent studies have also suggested the potential of phage predation as a form of biocontrol against excessive filamentous bacterial growth (Choi et al. 2011, Jassim et al. 2016, Liu et al. 2015). Filamentous bacteria overgrowth often results in the foaming and bulking of the sludge biomass at the surface of wastewater treatment systems. Bulking and foaming of the sludge are common problems that occur in activated floccular sludge (Sezgin et al. 1978) and prevents

adequate flocculation, resulting in poor settleability of the floccular sludge. The filamentous bacterium, *Sphaerotilus natans*, plays a significant role in filamentous bulking in sludge (Choi et al. 2011). A lytic phage specific to *S. natans* isolated from wastewater and inoculated into sludge consisting of *S. natans* resulted in significant improvement of the sludge volume index and reduced the effluent turbidity (Choi et al. 2011). Live-dead staining of the phage infected samples also indicated that the lytic phage had only lysed *S. natans* (Choi et al. 2011). Phage infection also did not significantly affect the nutrient removal performance in both the controls and phage infected samples.

1.3.2. Predatory bacteria

While predation of bacteria by protists and phage has been well studied, there are relatively fewer studies of microbial predators of bacteria. The myxobacteria are known to feed on bacteria by the release of extracellular hydrolases. In contrast, the *Bdellovibrio* and *Bdellovibrio*-like organisms (BALOs), for which *Bdellovibrio bacteriovorus* has been well-studied, feed by penetrating the periplasm of bacteria and reproducing intracellularly.

Bdellovibrio spp. are Gram negative and their high motility allow the bacteria to predate primarily on other Gram negative bacteria (Stolp and Starr 1963). The motility of *Bdellovibrio* spp. derives from the active expression of six genes encoding for the flagella filament and three pairs of genes for flagella motor rotation. In comparison, a non-predatory *E. coli* K12 only has a single gene for the flagella filament and a pair of genes for flagella motor rotation. The number of motility genes in *Bdellovibrio* spp. indicates that motility plays a crucial role in the predation process.

Predation begins when highly motile *Bdellovibrio* spp. randomly collide with prey bacteria. *Bdellovibrio* spp. subsequently attach and penetrate the periplasm of these prey bacteria to form bdelloplasts (Figure 1.6). Hydrolytic enzymes are synthesized by the invasive *Bdellovibrio* spp. to degrade the cellular contents of the host cells. Previous genome sequencing of *B. bacteriovorus* HD100 revealed twenty DNases and nine RNases (Rendulic et al. 2004). In addition, there are approximately 15 genes responsible for synthesizing lipases, 10 genes encoding glycanases, 150 genes responsible for peptidases or proteases synthesis and 89 other genes encoding for other hydrolytic genes (Sockett 2009). Hence, the *Bdellovibrio* genome encodes for more hydrolytic enzymes than other bacteria such as the non-predatory *E. coli* MG1655, which has only 8 annotated RNase genes, 3 DNases, 2 lipases, and 60 proteases (Sockett 2009). The expression of these *Bdellovibrio* hydrolytic genes degrades the prey cell entirely to provide nutrients for the growth of the predator. These predatory bacteria grow filamentously within the bdelloplasts and septate into several progeny cells when the bdelloplasts resources are exhausted. Progeny cells lyse their host cells and are released into the environment where they continue their lifecycle (Figure 1.6).

The *Micavibrio* spp. are also Gram negative uniflagellated predatory bacteria with high motility. However, *Micavibrio* spp. do not invade the periplasmic space of their prey bacteria and instead attack their prey bacteria in an epibiotic manner (Dashiff et al. 2010, Wang et al. 2011). In the attack phase, the motile *Micavibrios* seek out their prey and attach irreversibly to the presurface. The attached *Micavibrio* consumes their prey and reproduce via binary fission. Once the infected prey die, the progenies would seek out new prey cells and continue their lifecycles.

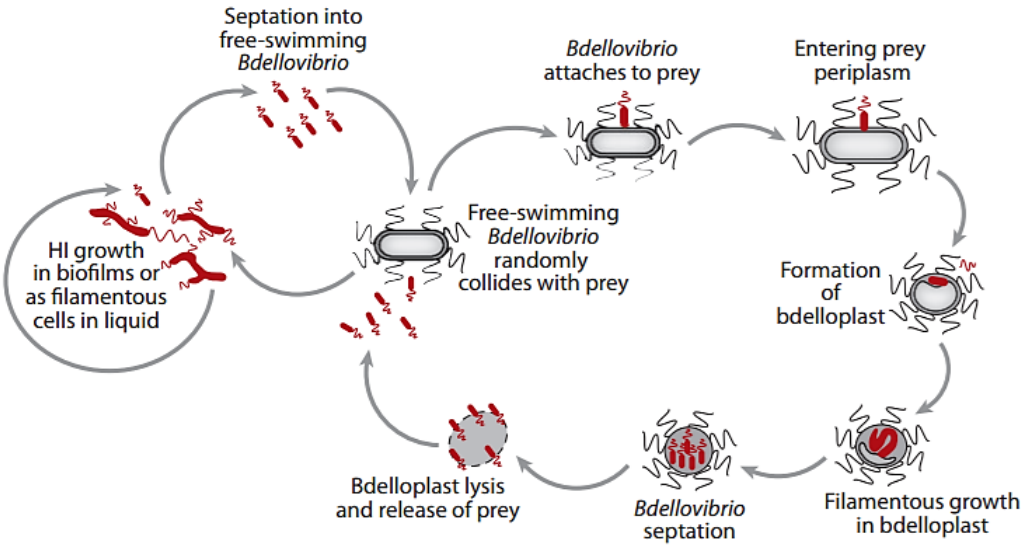

Figure 1.6: Predatory and host-independent lifecycles of *Bdellovibrio*. During its predatory lifecycle, the motile *Bdellovibrio* do not undergo binary fission to replicate. Instead, these predatory bacteria collide and attach to the prey bacteria where they subsequently enter the periplasm. Once inside the periplasm, the predatory bacteria and the prey cell form a bdelloplast which allows the filamentous growth of *Bdellovibrio*. Once the bdelloplast resources are exhausted, *Bdellovibrio* will undergo septation and subsequently lyse the bdelloplast to relase the progeny cells. These progeny cells can undergo the same predatory lifecycle again or an alternative host independent lifecycle. The switch from predatory to host independent lifecycle requires high concentrations of amino acids and presence of cofactors. The occurrence of host independent lifecycle is less frequent at an approximately rate of 1 in 10^7 attack-phase *Bdellovibrio* (Sockett 2009).

As *Micavibrio* are obligate predators that require prey cells for multiplication, they do not have a host independent lifecycle (Wang et al. 2011). In addition, *Micavibrio* are highly host specific where *Micavibrio aeruginosavorus* strain ARL-13 preys only on *P.*

aeruginosa, *Burkholderia cepacia* and *Klebsiella pneumoniae* (Kadouri et al. 2007). A portion of the *M. aeruginosavorus* genome is responsible for the synthesis of hydrolytic enzymes that comprise of 49 proteases and peptidases, 12 lipases, 2 DNases, 4 RNases and 37 other hydrolases. These predatory bacteria have a broad host range and can attack a broad range of medically relevant Gram negative pathogens (Dashiff et al. 2010). Both *Bdellovibrio* and *Micavibrio* can attack and reduce multidrug resistant pathogenic bacteria in both planktonic cultures and biofilms (Dashiff et al. 2010, Kadouri et al. 2007). Hence, predatory bacteria are suggested to serve as biological agents that can be used for controlling and eradicating biofilms.

In activated sludge systems, strong predation pressure exerted by predatory bacteria may affect the native bacterial community and could potentially upset the performance of wastewater treatment systems. A BALO strain, *B. bacterivorous* UP, isolated from activated sludge, was found to predate on Gram-negative bacteria including *Bacteriodetes* and *Proteobacteria* from activated sludge (Feng et al. 2016). These two classes consist of many bacterial groups, such as ammonia-oxidizing and phosphate accumulating bacteria which are essential for nutrient removal processes. This observation suggests that bacteria from these two classes could be natural targets for predation by *B. bacteriovorous* (Feng et al. 2016). One species of Gram negative bacteria, *Ochrobacterum anthropi*, was shown to be resistant to *B. bacteriovorous* predation, although the mechanism of resistance was not determined (Feng et al. 2016). To test if the predation resistant *O. anthropi* could protect other bacterial members in sludge, it was co-cultured in dual species planktonic communities or biofilms. Although *O. anthropic* co-existed with the other bacterial

isolates tested, it did not confer protection to the other bacteria present in the co-culture (Feng et al. 2016). Hence, there was selective predation by *B. bacterivorous*.

Another study demonstrated that predation by *B. bacterivorous* UP can significantly alter the microbial biomass and microbial community composition in both floccular and granular sludge (Feng et al. 2017). The total biomass of both floccular and granular sludge were found to be significantly reduced and an approximate reduction of total protein by 50% within 24 h when co-cultured with *B. bacterivorous* (Feng et al. 2017). The majority of the bacteria groups that were reduced in relative abundance by *B. bacterivorous* belonged to *Bacteroidetes* and *Proteobacteria*. Some of the functional bacterial groups such as *Nitrospira* and *Acinetobacter* which are responsible for oxidation of nitrite and phosphate removal respectively were reduced in abundance due to *B. bacterivorous* predation. As a result, it is possible that the activated sludge community could have a reduction in both nitrogen and phosphate removal. Interestingly, the analysis of mRNA revealed that *B. bacterivorous* predation did not significantly affect the expression of functional genes in either floccular or granular sludge (Feng et al. 2017). The limited changes in community mRNA expression after predation indicated that sludge communities had high levels of functional redundancy and resilience.

1.3.3. Protozoa

Protozoa is a common term used to describe unicellular, heterotrophic protists which range in size from approximately 1 to 200 µm (Finlay 2001). Protists can be autotrophic, heterotrophic or mixotrophic. Protists are ubiquitous in aquatic environments such as fresh and sea water, and in both soils and sediments. In these environments, protozoa are

responsible for controlling the abundance of bacteria by predation and for the recycling of nutrients for use by other organisms (Barcina et al. 1991, Rønn et al. 2002, Sherr and Sherr 1987, Trap et al. 2016). For example, protozoan numbers per gram at a soil site were 162,400 (123,000 amoebae, 27,300 flagellates and 12,100 small ciliates) (Anderson 2001). Protozoa that are parasitic by nature can be pathogenic to humans, animals and plants. The family *Trypanosomatidae* consists of severe vector-borne protozoan parasites of humans, including *Trypanosoma cruzi* and *Trypanosoma brucei*, which causes Chagas disease and African sleeping sickness, respectively (Hughes and Piontkivska 2003).

Protozoa are generally classified into three morphological groups of flagellates, ciliates and amoeba (Madoni 2003) (Figure 1.7). Flagellates are a heterogeneous group distinguished by the existence of one or more flagella which are used for mainly locomotion, feeding and attachment to surfaces (Figure 1.7a). Flagellated protozoa are ubiquitous on a global scale and have a wide size range between 1 – 450 μm (Jeuck and Arndt 2013). As they display all of the basic trophic strategies from primary producers to heterotrophic feeders, flagellates are also important predators in the aquatic food web. Photoautotrophic flagellates employ a range of pigment combinations for photosynthesis. Many species of flagellates are heterotrophic and graze on bacteria or take up soluble organic molecules as food sources. These heterotrophic flagellates are highly abundant and are regarded to be principal consumers of bacteria in aquatic habitats (Patterson 2001). When there are fluctuations of nutrient levels in the environment, some flagellates may form cysts or sharply reduce their metabolism and produce smaller cells which require lesser energy in order to survive.

Amoeba are characterized by the presence of pseudopodia that extend out from the periphery of the cells (Figure 1.7b). The contraction and extension of pseudopodia allow the amoeba to move by cytoplasmic streaming on surfaces. Pseudopodia of the amoeba can also be an apparatus for engulfing prey. Amoeba are categorized into two broad groups, namely the naked amoeba and testate amoeba. Naked amoeba can alter their cell shape through any motion of the pseudopodia as they lack any skeletal structure. Unlike the naked amoeba, testate amoeba are enclosed in elaborate organic shells with distinct pores for pseudopodia extension and prey ingestion.

Ciliates are the largest group of protozoa that are characterized by several major features such as nuclear dimorphism, sexual conjugation and the possession of cilia during certain stages of their life cycle (Figure 1.7c) (Lynn 2001). The cilia are categorized into somatic and oral cilia. Somatic cilia envelop the cell's surface in extensive rows and are responsible for propelling the protozoa through water. Somatic cilia close to the oral region also assist in prey capture. Oral cilia are responsible for drawing in water by the creation of feeding currents due to the beating motion of the cilia, and subsequently filtering out the food particles from the water for ingestion. In addition, certain groups of ciliates use specialised ventral cilia known as cirri, to swim around surfaces. Ciliates are known predators of bacteria and other smaller protozoa and in turn are predated by larger microorganisms such as zooplankton and fish.

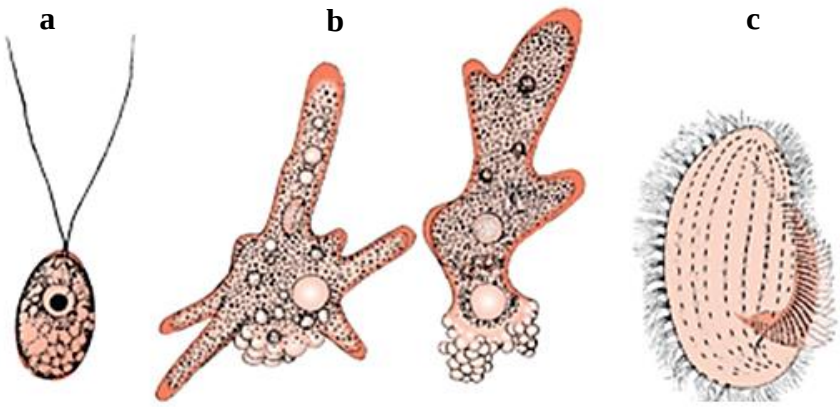

Figure 1.7: Different groups of protozoa. (a) Flagellate, (b) naked amoeba and (c) ciliate. The figure is reproduced from (Anderson 2001).

1.3.3.1. Feeding Types

Protozoa can prey on bacteria that are either in the suspended state or attached to a surface. Prey bacteria are generally consumed through phagocytosis, which involves the prey bacteria being enclosed in a vacuole formed by the invagination of the cell membrane (Ronn et al. 2012). Protozoa use a variety of feeding mechanisms for consumption of bacterial prey. The types of protozoan feeding are categorized into diffusion, filter, and direct interception or raptorial feeders (Lynn 2001).

Diffusion feeders rely on both the motility and high density of prey for effective feeding. This form of feeding is found among many types of sarcodines which are amoeba-like organisms. Diffusion feeders typically wait for their prey to make contact before capturing and immobilizing them with excreted mucus or networks of pseudopodia.

Filter feeding involves the creation of water currents by the protozoa which allow bacteria to be trapped by the cilia. Filter feeders predominately feed on suspended bacteria and

this mode of feeding is common in ciliates and flagellates. Filter feeding ciliates such as *Vorticella* sp. and *Stentor* sp. are usually found to attach to surfaces which allows for better capture rates of suspended bacteria. Filter feeding flagellates such as choanoflagellates use their single flagellum to produce currents to draw water through the microvilli at the outside of their collar, which filters out bacteria and food particles (Pettitt et al. 2002).

Lastly, raptorial or direct interception feeders are characterized by the generation of water currents by their anterior flagellum where prey bacteria are intercepted and phagocytized. Unlike filter feeders, which only capture prey bacteria of the correct size, these raptorial predators discriminate their prey bacteria based on their type and size. Raptorial feeding has been suggested as the most common mode of feeding and is widespread in many small flagellates and amoeba (Sanders 1991). For example, a heterotrophic flagellate, *Bodo saltans,* uses the tip of its trailing flagellum to attach to a surface while its anterior flagellum creates sweeping currents to propel prey bacteria towards its cytostome for phagocytosis (Mitchell et al. 1988).

1.3.3.2. Protozoa in biofilms

Protozoan predation is a significant mortality factor for bacteria in both planktonic phase and biofilms in the environment (Matz and Kjelleberg 2005). Biofilms are frequently colonised by diverse groups of protozoa such as naked amoeba (Barbeau and Buhler 2001), heterotrophic flagellates (Zubkov and Sleigh 1999) and ciliates (Dopheide et al. 2011a). In activated floccular sludge, protozoa are plentiful and can constitute approximately 5% of the sludge biomass (Madoni 2003). Protozoan grazing also clarifies

the effluent by removing suspended bacteria and loosely attached bacteria in wastewater systems (Madoni 2010). Ciliates are particularly important in the removal of suspended solids and bacteria and the increases in ciliates numbers have been demonstrated to correlate positively with good effluent quality (Esteban et al. 1991).

In the early stages of activated sludge formation, suspended bacteria are plentiful and protozoa such as flagellates and swimming ciliates predominate. Swimming ciliates are able to move freely within the sludge and can consume large quantities of suspended bacteria. As activated floccular sludge mature, the amount of suspended bacteria decreases and the size of flocs increases due to predation pressure by protozoan grazing. The increase in size confers protection to the bacteria embedded within the flocs against protozoan grazers. This change in availability and type of food resources results in the decline of flagellates and swimming ciliates (Madoni 2010) and an increase in crawling ciliates which attach to the flocs. Sessile ciliates of the subclass *Peritrichia* are also observed to grow on the surfaces of larger flocs, where they filter wastewater to ingest suspended bacteria (Curds 1982, Madoni 2003).

During the conversion from flocs to granules, the types of protozoa would also be expected to change as bacteria begin to form larger aggregates. Indeed, several studies have observed a high abundance of sessile ciliates on the surface of mature granules (Lemaire et al. 2008a, Li et al. 2013, Weber et al. 2007, Winkler et al. 2012). Sessile ciliates are filter-feeders that attach to surfaces and create feeding currents with oral cilia that sweep suspended bacteria into their oral region. For example, *Epistylis chrysemydis*, *Trochiliaminuta* and *Vorticella* spp. were identified on the fluffy outer layer of mature granules (Schwarzenbeck et al. 2004a). To elucidate their role in aerobic granulation,

aerobic granules were incubated with fluorescent polystyrene beads, which were ingested by the sessile ciliates. The authors hypothesized that predation by these ciliates helps to remove suspended bacteria and particulate organic matter while releasing waste products used as nutrients by the surrounding bacterial communities (Schwarzenbeck et al. 2004a). Another study also observed 'bouquets' of sessile ciliates (likely to be *Opercularia)* on the surfaces of almost all granules (Lemaire et al. 2008a). Using transmission electron microscopy, they also observed internalized bacteria in the food vacuoles of these sessile ciliates. Similarly, sessile ciliates were shown to reduce the concentration of suspended solids during discharge, which would help to reduce post-treatment. The role of sessile ciliates in removing suspended solids was also established in another study where high numbers of *Vorticella* on aerobic granules markedly improved the clarity of effluent (Li et al. 2013). Overall, these studies have demonstrated that protozoan grazing by sessile ciliates play a role in removing suspended bacteria and solids.

1.4. Bacterial adaptations to and defences against protozoan predation

Heterotrophic protists are known grazers of bacteria in aquatic and terrestrial environments (Jürgens 2007). Predation of bacteria usually occurs by contact between predator and prey, prey capture and finally ingestion. After ingestion, the bacterial cell is enclosed in a food vacuole where digestion occurs. Hence, bacterial mechanisms for resistance to predation can occur before ingestion (e.g. toxin production or increased swimming speed) or after ingestion (e.g. ability to survive digestion).

Morphological plasticity is one of the extracellular defence mechanisms that bacteria have acquired in response to predation (Justice et al. 2008). Predation by heterotrophic protists

is generally size selective where medium-sized bacterial cells are usually preferentially grazed (Boenigk et al. 2004, Chrzanowski and Šimek 1990). For example, smalls cells (< 0.4 µm) are less affected by grazing, medium sized bacteria (0.4 to 1.6 µm) are vulnerable to grazing, while bacteria between 1.6 to 2.4 µm are described as being grazing suppressed and larger cells (> 2.4 µm) are termed grazing resistant (Pernthaler et al. 1996). Bacteria can acquire a large and bulky morphology which protects them from being engulfed. Cells that can form filaments are larger than the edible size range of bacterivorous protists which substantially reduces the rate of grazing. For example, co-incubation of *Flectobacillus* spp. and the flagellate, *Ochromonas* spp. resulted in enrichment of grazing resistant filamentous cells (Hahn and Höfle 2001). These filamentous cells made up at least 80% of the *Flectobacillus* sp. population and averaged 18.6 µm in length. In contrast, *Flectobacillus* spp. that were grown in the absence of *Ochromonas* spp. mostly had rod-shaped morphology of 4 to 7 µm in length and a significantly low proportion of filamentous cells. Hence, the formation of filaments is regarded as an efficient means of protection against protozoan predation.

Another adaptive trait is the increase in bacterial motility. Motility is an important attribute of bacteria and most planktonic bacteria in marine environments are highly motile (Fenchel 2001, Hans-Peter et al. 2001). Previous studies demonstrated that feeding rates by protozoa were higher on motile and live cells compared to non-motile heat killed bacteria (Gonzalez and Suttle 1993, Monger and Landry 1992). Hence, it was proposed that motile bacterial cells had a higher encounter rate with protozoa and consequently resulted in higher ingestion rates. However, Matz and Jurgens (2005) discovered that although encounter rates with heterotrophic flagellates were high for motile bacteria, the

ingestion rates remained low due to the handling problems of motile bacteria, subsequently leading to capture failure. As a consequence, capture and handling efficiencies by heterotrophic flagellates were reduced for highly motile bacteria that had swimming speeds exceeding 30 µm s^{-1} (Matz and Jurgens 2005). A 'run and reversal' swimming pattern was also observed in highly motile marine bacteria which allows a rapid retreat upon encountering protozoa with long reaction times (Mitchell et al. 1995b). The prevalence of high swimming speeds observed in marine bacteria indicates that high motility could be an effective mechanism against capture by protozoan grazers (Mitchell et al. 1995a).

The formation of biofilms is another effective mechanism that bacteria have adapted to resist protozoan predation. Unlike planktonic bacteria that are capable of escaping predation through motility and morphology changes, biofilms are exposed to intense predation pressure as they are unable to avoid and escape predators. However, biofilms still persist and accumulate despite the existence of grazers, which shows that biofilms have developed anti-predator mechanisms. Development of these anti-predator mechanisms can be attributed to the close interaction and cooperation of bacterial cells in the biofilms.

The benefits of the biofilm mode of life were observed in co-cultures of *Pseudomonas* spp. and heterotrophic flagellates (Hahn et al. 2000, Matz et al. 2004). The presence of heterotrophic flagellates was suggested to increase the formation of grazing resistant microcolonies of *Pseudomonas* sp. MWH1 (Hahn et al. 2000) while elimination of flagellates resulted in a significant decline in microcolonies. However, microcolonies of

two different *P. aeruginosa* strains did not prove to be effective against the swimming ciliate, *Tetrahymena* spp. or the amoeba, *Acanthamoeba polyphaga* (Weitere et al. 2005). Microcolony populations of both strains were reduced by at least 70% by *Tetrahymena* spp. and completely removed by *A. polyphaga*. The flagellate, *B. saltans* did not affect microcolony formation of a toxic strain of *P. aeruginosa*, but there was an increase in microcolony abundance for the non-toxic strain. Hence, it was interpreted that the formation of microcolonies is a successful grazing-defence strategy against flagellates but ineffective against ciliates and amoeba.

Genes regulated by quorum sensing such as *rhlR* and *lasR* were determined to confer toxicity to *P. aeruginosa* biofilms (Matz et al. 2004). Biofilms of *P. aeruginosa rhlR* and *lasR* mutants did not exhibit the same level of toxicity to flagellates as the wild type. Furthermore, the *las* and *rhl* QS systems controls the expression of several virulence factors, including rhamnolipids and pyocyanins (Matz et al. 2004). The secretion of antiprotozoal factors by *V. cholerae* biofilms are also controlled by quorum sensing (Matz et al. 2005a). Supernatants collected from the mutant strain biofilms showed significantly lower inhibitory effects against the feeding activity of *Rhynchomonas nasuta*. Therefore, the absence of quorum sensing will cause deficiencies in predation resistance of biofilms. There are also some bacterial strains that are able to resist digestion by producing highly toxic chemicals such as violacein (Matz et al. 2008b). The release of violacein into the food vacuoles of the protozoan predators resulted in immediate death.

1.5. Research aims

Predation by protozoa is known to have a significant role in controlling the abundance of bacteria in many environments. In activated sludge, protozoan predation is responsible for removing suspended bacteria which improves the quality of the wastewater effluent. Furthermore, predatory pressure by protozoa can also be beneficial for the formation of flocs. However, their role in the aerobic granulation process has only been hypothesized. Hence, the focus of this thesis is to address the role of protozoan predators on driving flocs towards the initiation of aerobic granulation and subsequent maintenance of mature granules. In addition, the effects of protozoan predation on biofilm formation and resistance were also further investigated using mixed species biofilms. The specific aims of the research presented here are:

Chapter 2: To develop mature aerobic granules performing simultaneous nitrification, denitrification and phosphorous removal from floccular sludge using SBRs. In addition, the bacteria communities in floccular and granular sludge are also characterized. The role of protozoan predation in driving aerobic granulation is elucidated by tracking the ciliate community throughout the granulation process.

Chapter 3: To determine if the presence or absence of protozoa has a role in the development of aerobic granules and the maintenance of mature granules, as well as identifying the types of protozoa involved in aerobic granulation.

Chapter 4: To investigate the mechanisms of grazing resistance of model, mixed and single species biofilms formed by *Pseudomonas aeruginosa*, *Pseudomonas protegens* and *Klebsiella pneumoniae* against the heterotrophic protozoa, *Tetrahymena pyriformis*.

Chapter 2: AEROBIC GRANULAR SLUDGE – CHARACTERIZATION OF BACTERIAL AND EUKARYOTIC COMMUNITIES

2.1. Introduction

Aerobic granular sludge is a complex, man-made ecosystem consisting of highly diverse and functional microbial communities that are utilized for specific biological functions. These densely packed biofilm aggregates are typically developed from activated floccular sludge. Using laboratory sequencing batch reactors (SBRs), operational conditions can be adjusted accordingly to actively select for granule formation. The process for the formation of aerobic granules from flocs has been improved based on an increased understanding of the effects of operating conditions such as hydrodynamic shear force, settling time, hydraulic retention time and discharging time (Liu 2008, McSwain et al. 2004, Qin et al. 2004, Tay et al. 2001c, Winkler et al. 2012). The formation of aerobic granules can be achieved within a shorter timeframe by inoculating reactors with crushed pre-formed granules, suggesting that such pre-formed granules may either serve to nucleate granule production or may produce signals or other factors that drive the conversion of floccular biomass into granules (Pijuan et al. 2011).

In contrast to the impact of physical factors, the biological processes that drive granule formation are less well understood. For example, N-acyl-homoserine-lactone (AHL) mediated quorum sensing was found to positively correlate with the formation of granules from floccular sludge (Tan et al. 2014). It was demonstrated that AHLs correlated with the initiation of granulation were strongly upregulated (Tan et al. 2014). Furthermore, the addback of these AHLs markedly increased the production of EPS, which mediated the

attachment between bacterial cells (Tan et al. 2014, Tay et al. 2001b). However, other biological factors are also known to affect the formation of biofilms, such as protozoan predation (Matz and Kjelleberg 2005, Scherwass et al. 2016). Free-living protozoa are observed regularly in activated floccular sludge, which is generally utilized as the seed sludge for aerobic granulation. Protozoa are generally assumed to aid the clarification of the effluent through the predation of suspended and loosely attached bacteria. Predation on those free living bacteria may represent a strong pressure that selects for those bacteria that are tightly embedded in the waste-water biomass and hence are protected from predation. Further, there are several reports showing that there is a relatively high abundance of protozoa associated with aerobic granules, although their role has not been explicitly studied (Lemaire et al. 2008a, Li et al. 2013, Schwarzenbeck et al. 2004b, Weber et al. 2007).

Protozoa are the most abundant and species rich group in activated floccular sludge after bacteria. There are approximately 230 species of protozoa have been identified in activated sludge plants (Madoni 2003). The phylum *Ciliophora* is commonly the most dominant and diverse group of protozoa in activated floccular sludge as it accounts for 160 of the 230 species (Augustin and Foissner 1992). There can be up to 10 different species of ciliates in the sludge community and the number of individuals can range from 10^6 to 10^7 L^{-1} in the mixed liquor of activated sludge (Madoni 2010). Previous studies on the succession of protozoa have demonstrated that different functional groups are present during the establishment of activated sludge (Madoni 1994). For example, swimming ciliates are dominant during the initial start-up phase when flocs are uncommon and suspended bacteria are most abundant. However, these swimming ciliates are later

replaced with crawling ciliates which are proficient at grazing on loosely attached bacteria present on flocs. The increased surface area may also provide a substratum for the growth and attachment of sessile ciliates.

Interactions between protozoa and bacteria are considered to be beneficial for the formation of flocs (Bossier and Verstraete 1996). This is supported by previous studies that demonstrated that predatory pressure exerted by protozoa stimulated bacterial biofilm formation (Matz and Kjelleberg 2005, Scherwass et al. 2016). Hence, it is likely that the aggregation of suspended bacteria into flocs is also correlated with a shift in protozoan functional groups. Previous studies have demonstrated that the composition of the bacterial communities in activated sludge and aerobic granules are dissimilar despite exhibiting the same level of functionality (Winkler et al. 2013). Bacteria such as *Nitrospira* and *Sphingobacteriales* that were dominant in the floccular sludge were gradually replaced by other bacteria such as *Zoogloea* (Weissbrodt et al. 2012). However, there have been no reports correlating the shift in bacterial communities with shifts in protozoan communities. Furthermore, the dynamics and progression of different functional protozoan groups throughout the aerobic granulation process have not been studied.

Here, both bacterial and protozoan communities were characterized throughout the aerobic granulation process in four SBRs seeded with activated floccular sludge that were operated for the simultaneous nitrification, denitrification and phosphorus removal (SNDPR) process. In particular, the study aimed to track the succession of protozoan communities during the aerobic granulation process and to investigate the potential role

of protozoan predation in driving aerobic granulation. Therefore, Ribotagger analysis of the total RNA sequencing datasets was performed on samples obtained from an independent experiment of aerobic granulation over a period of 11 weeks.

2.2. Materials and Methods

2.2.1. Reactor setup and operation

Four sequencing batch reactors (SBRs) were seeded with activated floccular sludge from the Ulu Pandan Wastewater Treatment Plant. Each SBR had a final working volume of 2 L and were enhanced for simultaneous nitrification, denitrification and phosphorus removal (SNDPR performance at 21 to 22^{o}C (Zhou et al. 2010). Each SBR was operated in a 6 h cycle comprising two different phases: Phase I - feeding (8 min), anaerobic (60 min), aerobic (80 min at day 0, with a gradual increase to 95 min by week 5) and anoxic (40 min at day 0, with a gradual increase to 50 min by week 5); Phase II - feeding (2 min), anaerobic (30 min), aerobic (40 min at day 0 and gradual increase to 70 min by week 5) and anoxic (30 min). Each cycle was completed with a settling stage (120 min at day 0, with a gradual decrease to 5 min by the end of week 6) and a 10 min decanting stage. The settling time was maintained at 5 min per cycle from week 6 onwards.

A volume of 1 L of synthetic wastewater was supplied to each SBR during each phase and 1 L of effluent was discharged at the completion of each cycle. Synthetic wastewater was prepared as previously described (Smolders et al. 1994, Zhou et al. 2010). Nitrogen was sparged intermittently into the SBRs at a flow rate of 1.0 L min^{-1} throughout the cycles except during settling and decanting. Dissolved oxygen (DO) levels in the SBRs were maintained at 3.0 to 4.0 mg L^{-1} by sparging air during the aerobic phases. Sparging

of both nitrogen and air provided complete mixing of the sludge and the hydrodynamic shear force required for aerobic granulation. The pH of each SBR was kept in the range of 6.8 to 8.2 by dosing 0.1 M HCl and 0.1 M NaOH when required. Both pH and DO levels were monitored online by probes connected to a programmable logic controller (PLC).

2.2.2. Performance (cycle) studies of aerobic granulation SBRs

Cycle studies evaluating the performance of the granulation process were performed on a weekly basis. Mixed liquor suspended solids (MLSS) and mixed liquor volatile suspended solids (MLVSS), as well as concentrations of ammonia, nitrite, nitrate and orthophosphate were determined using APHA standard engineering methods (Eaton et al. 2005). Sludge density and compactness was measured by sludge volumetric index at 5 min (SVI_5) as described by Liu (Liu 2008). A low SVI_5 value is an indicator of a sludge that has desirable settling properties. Particle size of the sludge was determined using a laser diffraction particle size analyser (SALD-3101, Shimadzu, Japan). The morphology of the sludge particles was observed using a stereomicroscope or bench top microscope (Carl Zeiss, Germany). At the end of each cycle study, well-mixed sludge samples of 1 mL were collected from each reactor at the end of anoxic stage (Phase II). These sludge samples were centrifuged at 8,000 x g for 5 min and snap frozen in liquid nitrogen prior to storage at -80^{o}C.

2.2.3. RNA extractions for total RNA sequencing and analysis

Total RNA was extracted from sludge samples using the Soil, Fecal and Plant RNA kit (Zymo Research, USA) as shown in previous sludge studies (Feng et al. 2017, Law et al. 2016), according to manufacturer's guidelines. Extracted RNA underwent a single round

of DNase treatment to remove residual DNA (TURBO™ DNase kit; Invitrogen, Singapore). The quality of the extracted RNA was measured by spectrophotometry (Nanodrop; Thermo Scientific, USA). The concentration of RNA and residual DNA was quantified by fluorometry (Qubit® 2.0 Fluorometer; Invitrogen, USA), with Qubit® RNA broad range assay kit (Invitrogen, USA) and Qubit® DNA high sensitivity range assay kit respectively, following the manufacturer's guidelines. In addition, the integrity of the RNA was determined using the RNA Analysis ScreenTape and 2200 Tapestation instrument (Agilent Technologies, Singapore) and reported as the RNA Integrity Number (RIN). These RNA samples were subsequently sent for RNA library preparation prior to pooling and sequencing on an Illumnina HiSeq 2500 System (Illumina Inc.) using 100 bp paired-end (PE) sequencing as per the manufacturer's guidelines.

2.2.4. Total RNA sequencing and analysis

The microbial composition of the floccular and granular sludge was determined by analysis of the sequence data using the Ribotagger fast tag-based approach (Xie et al. 2016). Ribotagger data was generated by Muhammad Hafiz. Briefly, universal recognition profiles that target bacteria, *Archaea* and eukaryot*es* were selected for each of the hypervariable regions of both 16S and 18S rRNA (e.g. V4, V5, V6 and V7) (Xie *et al*. 2016). These universal recognition profiles were used to scan the sequencing reads to obtain 33 nucleotides (nt) downstream of the primers (Xie *et al*. 2016). Each of these 33 nt tags were defined as a ribotag and each ribotag was scanned in the SILVA database to map it to a known organism. Hence, each ribotag was used as a signature sequence to represent one operational taxonomic unit (OTU). Here, only the sequencing reads from

the V5 regions of both 16S and 18S rRNA were used to represent the abundance of both bacterial and protozoal communities. By quantifying the number of sequencing reads per OTU, the changes in composition of the microbial communities were compared using three factors, weeks, phases and SBRs (replicate reactors). Unidentified OTUs were not used for this analysis. Using multidimensional scaling (MDS) algorithm analysis based on a Bray-Curtis dissimilarity index, the differences in the microbial communities between replicates, weeks and phases were plotted in a two-dimensional space where each factor would be represented by a single point. Hence, the proximity between each point would indicate their degree of similarity.

Richness and diversity of both bacterial and eukaryotic communities were measured using Menhinick's Index and Shannon-Wiener Index respectively. The Menhinick's Index (D = s/sqrt(N)) is based on the ratio of the number of species (S) against the square root of the total number of individuals (N). Here, the number of species was represented by the number of OTUs present for each reactor week while the total number of individuals was represented by the total number of sequencing reads from each reactor week. Unidentified OTUs were also not used for this analysis. The Shannon-Wiener Index was calculated by the equation H' = $-\sum_{i=1}^{s} = Pi \times \ln(Pi)$, where Pi represented the proportion of each individual based on the sequencing reads in a single OTU, while s represented the total number of sequencing reads in V5 tags. Using the Shannon Wiener Index, the Shannon Equitability Index which represented the evenness of the bacterial and eukaryotic communities could be calculated by the division of H' against H_{max}. The factor H_{max} represented the maximum diversity value that could be obtained from each community.

Hence, equitability assumes a value between 0 and 1, where 1 indicates complete evenness in a community.

2.2.5. Statistical analysis

Permutational multivariate analysis of variance (PERMANOVA) using distance matrices were performed on all V5 OTUs to determine if any of the three factors namely time (weeks), replicates and phases played a role in the change in microbial communites. PERMANOVA was performed on RStudio (RStudio, Inc.) using the Adonis function from the R-vegan library. Correlation studies were performed by calculating Pearson correlation coefficient using RStudio (RStudio, Inc.). The resulting matrixes were clustered hierarchically based on Euclidean distance using Gene Cluster 3.0 (de Hoon et al. 2004) and visualized on Java Treeview (Saldanha 2004). False discovery rates corrections were also performed for all correlations.

2.3. Results

2.3.1. Development and performance of aerobic granular sludge

Activated floccular sludge was used to seed the SBRs which were operated under conditions optimal for the aerobic granulation process over a period of 11 weeks. The granulation process is defined by five distinct phases, floccular, initiation, maturation, maintenance and dispersal based on previous work (Tan et al. 2014). In the experiments reported here, only floccular, initiation and maturation phases were observed (Figure 2.1a). Weekly micrographs of the sludge from each SBR were also obtained to track the conversion of flocs to granules over time (Figure A2.1a to d). The 50^{th} percentile of the

particle size and the SVI_5 were used to determine if the floccular sludge had granulated. During the floccular phase, the sludge biomass had a mean particle size of 51.3 ± 2.2 µm (50^{th} percentile) (Figure 2.1b). Aerobic granules are dense and compact aggregates characterized by a minimum particle size of 100 µm and a SVI_5 of 50 mL g^{-1}or less (Barr et al. 2010a).

Initial decreases in settling time from 120 to 56 min resulted in a 10.5% average loss of biomass (MLSS decreased from 5.0 ± 0.1 to 4.1 ± 0.1 g L^{-1}) by the end of week 1 (Figure 2.1c). The SVI_5 of the floccular sludge increased from 190.8 ± 2. to 221.8 ± 5.4 mL g^{-1}, which indicated poor settling of the floccular sludge (Figure 2.1b). By week 4, compact aggregates were observed in the floccular sludge and the mean particle size was 96.2 µm (50^{th} percentile) (Figure 2.1b). Subsequent decreases in settling time from 56 to 24 min did not result in a decrease in overall biomass until week 4 (MLSS increased from 4.9 ± 0.4 to 5.1 ± 0.4 g L^{-1}) when the sludge biomass entered the initiation phase. From weeks 4 to 6, the settling time was reduced from 24 to 5 min which resulted in an average of 23.7% loss of biomass (MLSS decreased from 5.1 ± 0.4 to 3.9 ± 0.5 g L^{-1}) (Figure 2.1b).

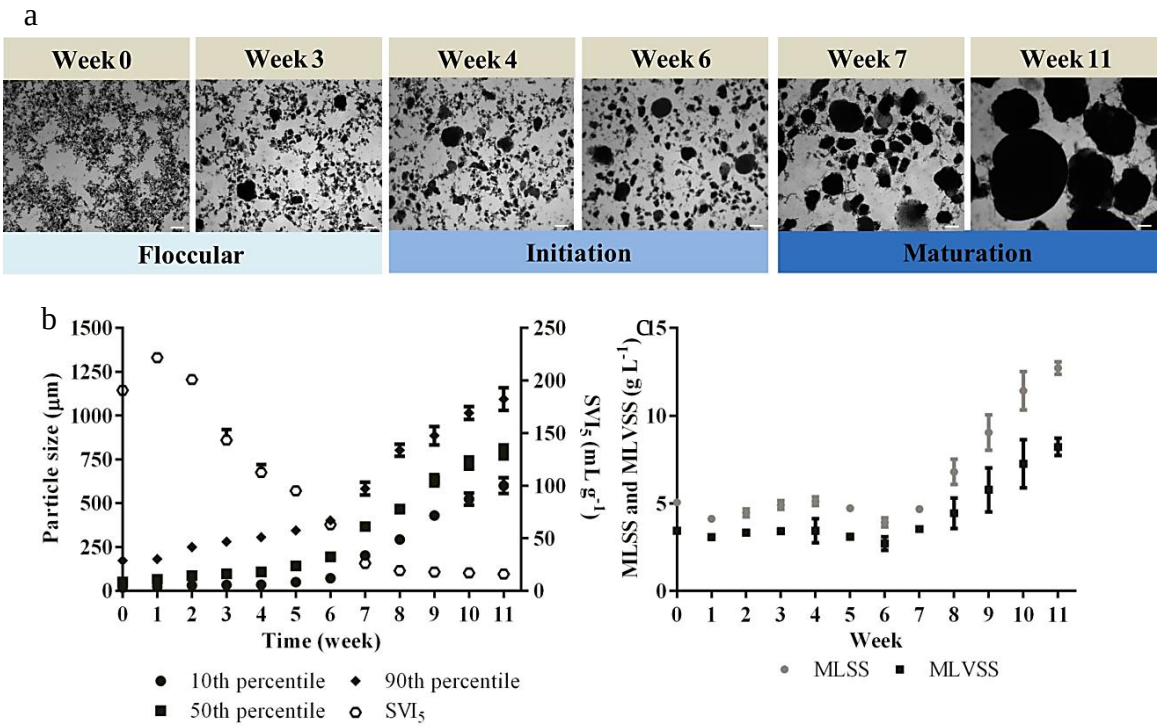

Figure 2.1: Development of granules from floccular sludge. (a) Development of small granules from floccular sludge over 11 weeks based on microscopic visualizations of sludge samples. (b) Average particle size distribution and SVI_5 in 4 SBRs. 10^{th} percentile (filled circle), 50^{th} percentile (filled square), 90^{th} percentile (filled diamond) represent the percentage of total particles below the corresponding size distribution respectively and the compactness of sludge particles is measured by SVI_5 (open circle). (c) Concentration of sludge biomass. Average sludge biomass concentrations are represented by both mixed liquor suspended solids (filled circle) and mixed liquor volatile suspended solids (filled squares). Error bars represent standard deviations (n = 4).

This reduction in settling time also coincided with an increase of mean particle size from 108.5 ± 6.9 to 193.0 ± 16.7 µm (50^{th} percentile) (Figure 2.1b). In addition, the SVI_5 also indicated a sharp decrease of 44% from 112.5 ± 13.2 to 63.0 ± 6.5 mL g^{-1} (Figure 2.1b). By week 7, the sludge biomass had entered the maturation phase of the aerobic

granulation process. Mean particle size of the sludge biomass had increased 90% from 193.0 ± 16.7 µm in week 6 to 367.0 ± 68.1 µm in Week 7 (50^{th} percentile) (Figure 2.1b). The particle size and SVI_5 of the sludge biomass continued to increase and decrease, respectively, over the remaining weeks. The MLSS of the sludge also showed a steady increase from week 7 onwards (Figure 2.1c). Over the entire run of 11 weeks, the reduction in settling time from 120 to 5 min was correlated with the appearance of high density and compact sludge particles. This resulted in a marked increase of the mean particle size of the sludge biomass from 51.3 ± 2.2 to 792.4 ± 130.6 µm (Figure 2.1b). Similarly, the SVI_5 also decreased significantly from 190.8 ± 2.5 to 16.0 ± 2.1 mL g^{-1} (Figure 2.1b). In addition, the MLSS of the sludge also increased to from 3.9 ± 0.5 in week 6 to 12.7 ± 0.6 mL g^{-1} by the end of week 11.

In this study, all SBRs were operated under conditions to achieve SNDPR. In terms of reactor performance across all SBRs, the average level of phosphorus removal had increased to 84% by week 4 when compact aggregates were observed (Figure 2.2a). From weeks 4 to 11, the average level of phosphorus removal was maintained in the range of 55 to 75% (Figure 2.2a) with the exception of SBR 3, which experienced a sharp decline in efficiency (21%) in week 8 (Figure A2.2a). Although the efficiency of phosphorus removal in SBR 3 recovered to 76% in week 9, a sharp decline in efficiency to 30.5% was again observed in week 10. The average nitrogen removal across all SBRs was relatively stable within the range of 67% to 79% from weeks 1 to 11 (Figure 2.2b). Interestingly, SBR 3 experienced a sudden increase in nitrogen removal (96%) in week 8 before declining to 75% in week 9 (Figure A2.2b).

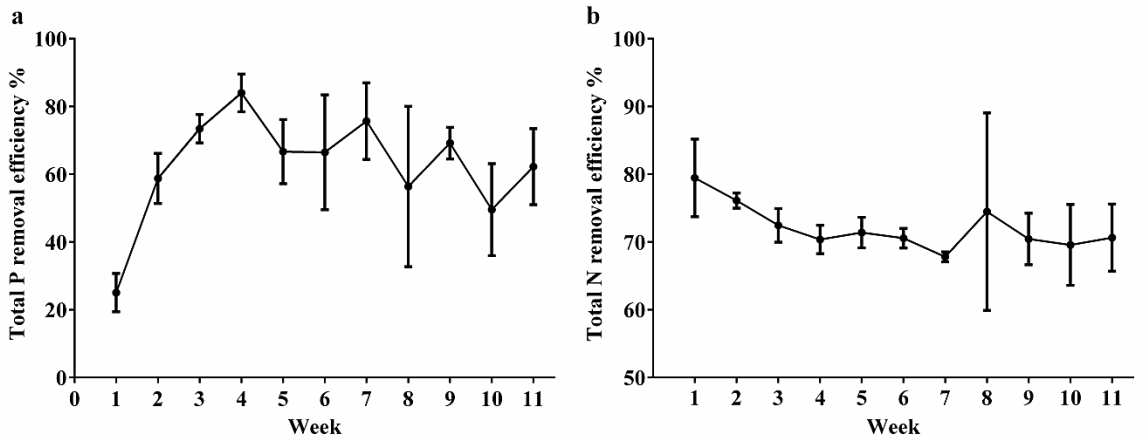

Figure 2.2: Nutrient removal profile of the sludge community in four SBRs over a period of 11 weeks. (a) Mean of the total phosphorous removal and (b) total ammonia removal. The nutrient removal profile for both P and N in each SBR can be found in Fig A2.2. Error bars represent standard deviations (n = 4).

2.3.2. Microscopic observations of floccular and granular sludge

Microscopic observations of the inoculum of activated sludge indicated several types of protozoa and metazoa existed within the sludge. Swimming ciliates that were most likely to be *Paramecium* spp. were observed within the floccular sludge (Figure 2.3a). Sessile ciliates, which were possibly *Epistylis* spp. (Figure 2.3b) were observed to be attached on the surfaces of the flocs. These sessile ciliates from the genus *Epistylis* have 'vase-shaped' heads and are colonial by nature with multiple heads growing on a single stalk. Metazoa such as tardigardes and rotifers were occasionally observed to move around freely within the sludge (Figure 2.3c and d) although rotifers were typically observed only in floccular sludge. Large rotifers that were likely from the genus *Euchlanis* were also attached to flocs by their rear "toes", which allows them to feed by filtering bacteria in the liquid phase (Figure 2.3d). Crawling ciliates that were likely from the genera *Aspidisca* or

Euplotes were also observed circling the flocs as they fed on loose bacteria around the floc surface (Figure 2.3e). These observations clearly indicated that the initial floccular sludge used as the inoculum, had a diverse community of protozoa present prior to seeding into the SBRs for these experiments. By the end of week 4, there were no swimming ciliates or tardigrades observed, although rotifers were still present. Upon granule formation after week 6, sessile ciliates which were likely *Vorticella* spp. were constantly observed on the granule surfaces (Figure 2.3f and g). These sessile ciliates were characterized by their "bell-shaped" heads and a single stalk containing a single head. Furthermore, the frequent twitching and contraction of the stalks strongly suggested that these sessile ciliates belonged to the genus *Vorticella*. Crawling ciliates that were previously common in floccular sludge became rare. Interestingly, large worm-like microorganisms known as bristle worms, possibly from the phylum *Annelids* were also found "coiling" around the granules (Figure 2.3h).

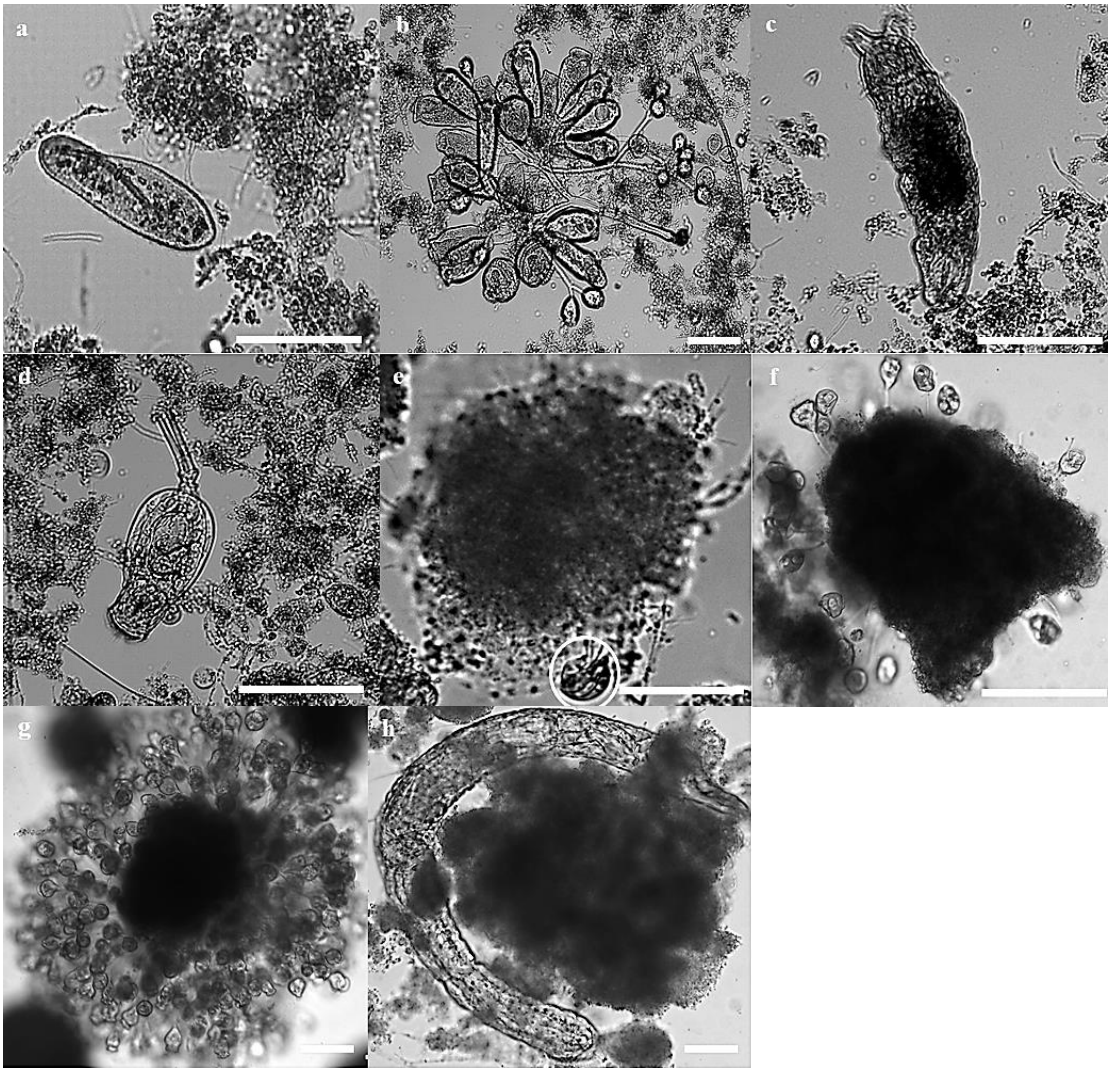

Figure 2.3: Micrographs of protozoa and metazoa in floccular and granular sludge. (a) A swimming ciliate, *Paramecium* spp. and (b) sessile ciliates likely from the genus *Epistylis*. **(c)** Metazoa such as tardigardes and (d) large rotifers from the genus *Euchlanis*. (e) Crawling ciliates (circled in white) were commonly sighted. (f and g) Sessile ciliates such as *Vorticella* attached on the surface of granules. (h) Large worms such as bristle worms crawling around the granules during the maturation phase. (Bar, 50 µm).

2.3.3. Microbial community composition of floccular and granular sludge

Microscopic observations of the sludge provided insights into the presence of several protozoa types in floccular sludge and the succession of protozoa as flocs granulated. However, microscopic observations were insufficient to specifically identify these different protozoa types. Total RNA sequencing was performed for sludge samples obtained from the four SBRs throughout the aerobic granulation process. Sequencing reads were processed using the Ribotagger method, which mapped individual sequence reads to a known operational taxonomic unit (OTU) (Xie et al. 2016). Sequencing reads that could not be identified and mapped to a known OTU were labelled as unidentified. Eukarya OTUs were mostly represented by protozoa, metazoa and fungi. The abundance of the microbial populations was represented by the number of sequencing reads detected per OTU. Relative abundance of these microorganisms would allow tracking of their diversity and abundance over time as the granulation process takes place.

On average, the number of sequencing reads from sludge samples in each SBR was between 127909 ± 11632 to 194963 ± 10410 throughout the 11 weeks (Table 2.1). The exact number of sequencing reads for each SBR per week is shown in Tables A2.1 to A2.4. Initial Ribotagger analysis indicated that there were shifts in the relative abundance of both bacterial and eukaryotic microbial communities throughout the different phases of aerobic granulation.

Table 2.1: Mean number and percentage of sequencing reads across 4 SBRs

Week	Total Reads	% Bacteria	% Eukarya	% Archaea	% Unidentified
0	194963 ± 10410	35.28 ± 1.91	42.96 ± 2.14	0.40 ± 0.03	21.36 ± 0.88
1	160625 ± 6946	58.01 ± 4.05	24.90 ± 4.38	0.14 ± 0.01	16.94 ± 1.06
2	127909 ± 11632	76.98 ± 0.59	4.17 ± 0.48	0.12 ± 0.01	18.72 ± 0.26
3	155099 ± 23904	77.36 ± 3.78	2.33 ± 1.52	0.05 ± 0.01	20.26 ± 2.80
4	164060 ± 33809	75.32 ± 3.60	3.47 ± 2.97	0.03 ± 0.01	21.19 ± 0.89
5	149674 ± 28158	84.15 ± 1.36	2.34 ± 0.74	0.01	13.50 ± 0.74
6	141215 ± 5591	83.59 ± 1.56	3.28 ± 1.49	0.01	13.13 ± 1.10
7	139970 ± 11834	83.86 ± 2.56	5.52 ± 1.87	0.00	10.62 ± 2.14
8	152613 ± 9397	82.60 ± 3.02	6.11 ± 4.38	0.00	11.29 ± 3.30
9	158572 ± 27949	83.60 ± 4.60	4.67 ± 4.24	0.00	11.73 ± 4.86
10	165334 ± 14405	82.93 ± 2.79	5.64 ± 3.73	0.00	11.43 ± 3.84
11	164654 ± 5799	84.06 ± 5.10	4.53 ± 5.35	0.00	11.41 ± 2.39

From weeks 0 to 6 (Phases 1 and 2), the close clustering of the four replicates suggested that the overall microbial communities appeared to change in a similar pattern for all four replicate SBRs (Figure 2.4a). SBR 4, during week 6 began to diverge from the other three SBRs and from week 7, all four SBRs began to show slightly different community abundance patterns (Figure 2.4a). The microbial communities showed 56.41% dissimilarity between weeks 0 to 11 (Figure 2.4a). PERMANOVA analysis also indicated that the microbial communities were highly dissimilar between phases (Pr = 0.001) and weeks (Pr = 0.001). However, there microbial communities were similar between each replicate (Pr = 0.286).

To better understand the similarities or dissimilarities of the microbial communities during aerobic granulation, all OTUs were separated and grouped accordingly into Bacteria (Figure 2.4b), Eukarya (Figure 2.5a) or Protozoa (Figure 2.5b). For Bacteria, all of the data displayed a similar clustering trend (Figure 2.4b) as observed in the MDS plot for the overall microbial communities (Figure 2.4a). This is likely due to Bacteria being the most abundant microorganisms in both the floccular and granular sludge. Bacterial communities showed high levels of dissimilarity of 65.31% between weeks 0 to 11 (Figure 2.4b). PERMANOVA analysis indicated that bacterial communities were significantly dissimilar between phases (Pr = 0.001) and weeks (Pr = 0.001). However, bacterial communities showed no significant difference between the replicates (Pr = 0.286) during the aerobic granulation process.

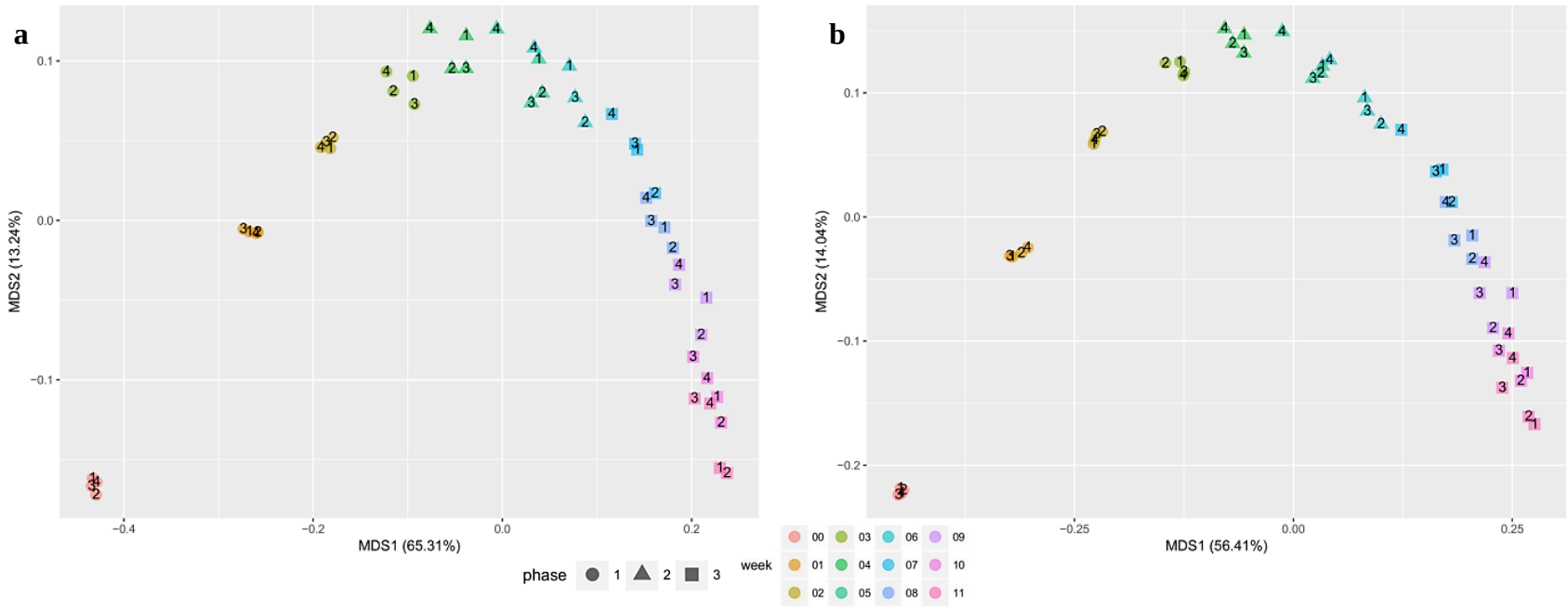

Figure 2.4: Multi-dimensional scaling (MDS) plots for different groups of microorganisms in floccular and granular sludge. The data were square root transformed for principal component analysis. Each symbol labelled 1 to 4 refers to a replicate SBR and its shape indicates the phase while each week is represented by a unique colour. (a) MDS plot for the whole sludge community including bacteria, eukaryotes and archaea (b) Bacteria only.

For Eukarya, there was close clustering of the points for the first two weeks (Figure 2.5a). However, from week 3 onwards, replicates began to diverge from each other. In particular, there were two distinct clusters, where SBRs 2 and 4 were grouped together while SBRs 1 and 3 were more similar to each other (Figure 2.5a). This suggested that the eukaryotic communities in SBRs 2 and 4 were more similar to each other than that of SBRs 1 and 3 and vice versa. PERMANOVA analysis indicated that eukaryotic communities were highly dissimilar between SBRs (Pr = 0.044), phases (Pr = 0.001) and weeks (Pr = 0.001). Eukaryotic communities showed a dissimilarity of 42.83% from weeks 0 to 11. As protozoa are eukaryotic predators of bacteria, it was of interest to investigate their change in composition during aerobic granulation.

MDS plot of protozoa indicated that there was close clustering of points from weeks 0 to 1 (Figure 2.5b). However, each replicate started to diverge from each other from week 2 onwards. From week 4 onwards, SBRs 2 and 4 were grouped close together. From week 6 onwards, SBRs 1 and 3 were clustered close together which indicated the similarity between their protozoal communities but distinctly dissimilar from those in SBRs 2 and 4 (Figure 2.5b). Protozoal communities also showed a dissimilarity **o**f 53.62% from weeks 0 to 11 (Figure 2.5b). PERMANOVA analysis also indicated that protozoal communities were highly dissimilar between SBRs (Pr = 0.009), phases (Pr = 0.001) and weeks (Pr = 0.001).

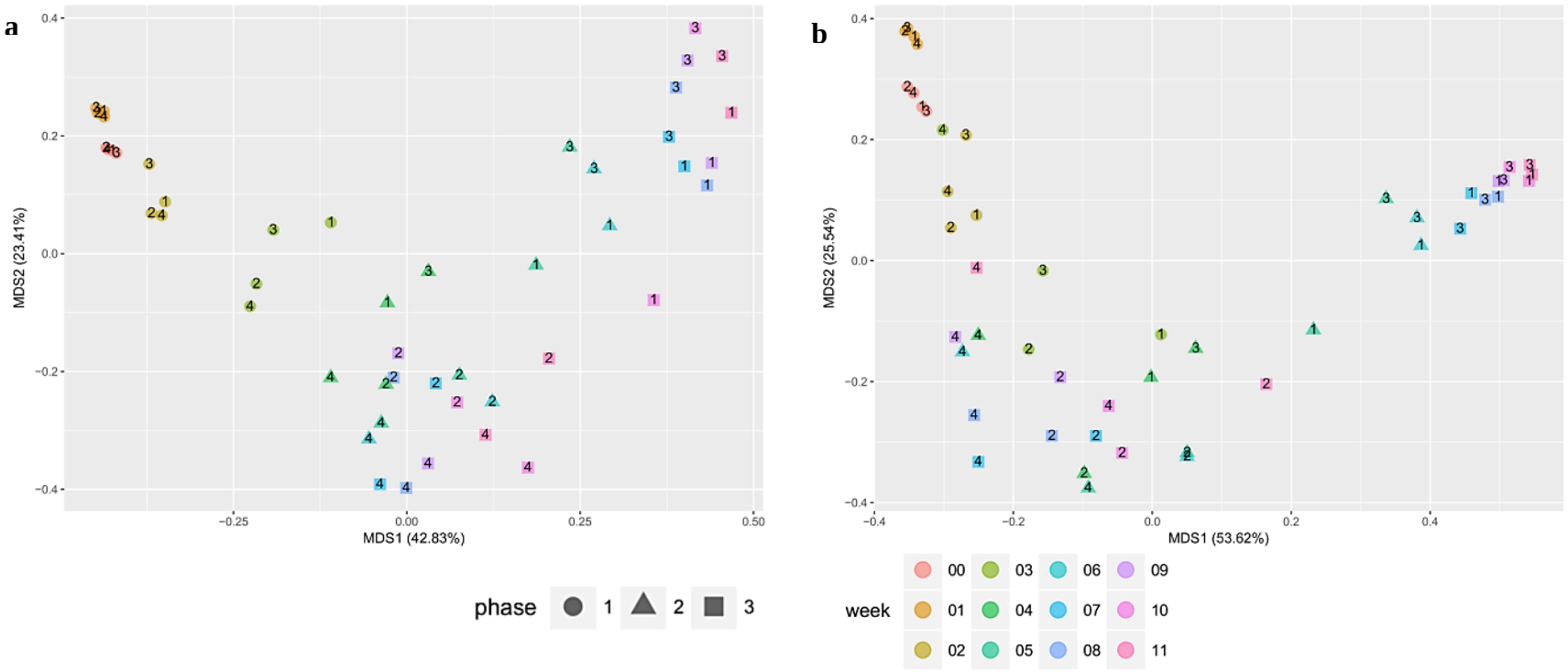

Figure 2.5: Multi-dimensional scaling (MDS) plots for different groups of microorganisms in floccular and granular sludge. The data were square root transformed for principal component analysis. Each symbol labelled 1 to 4 refers to a replicate SBR and its shape indicates the phase while each week is represented by a unique colour. (a) MDS plot for eukaryotes only and (b) protozoa only.

It was apparent that the abundance of eukaryotes declined in contrast to the increasing abundance of bacteria as floccular sludge transformed to granular sludge (Table 2.1). A total of 400 bacterial OTUs were selected as they represented approximately 90 to 95% of the sequencing reads from Bacteria. In general, the phylum *Proteobacteria* was the most dominant group throughout the 11 weeks in all four SBRs ranging from 64 to 90% of all Bacteria sequencing reads while other dominant groups were *Nitrospira, Bacteriodetes, Planctomycetes, Chloroflexi* and *Acidobacteria* (Figure 2.6). The relative abundance of dominant bacterial groups in each SBR is shown in Figure A2.3. Bacteria from *Verrucomicrobia*, *Actinobacteria, Firmicutes* and *Spirochaetes* were present at approximately 2.17, 1.90, 1.63 and 0.88% respectively at week 0 (Figure 2.6). However, the relative abundance of *Verrucomicrobia* and *Spirochaetes* gradually declined throughout the aerobic granulation process. The relative abundance of *Firmicutes* and *Actinobacteria* decreased sharply by week 1 and were less than 0.05% by weeks 4 to 6, respectively (Figure 2.6). This trend was also observed in all 4 replicates except for SBR 3, which showed an increase in *Acidobacteria* during weeks 10 and 11 (Figure A2.3d).

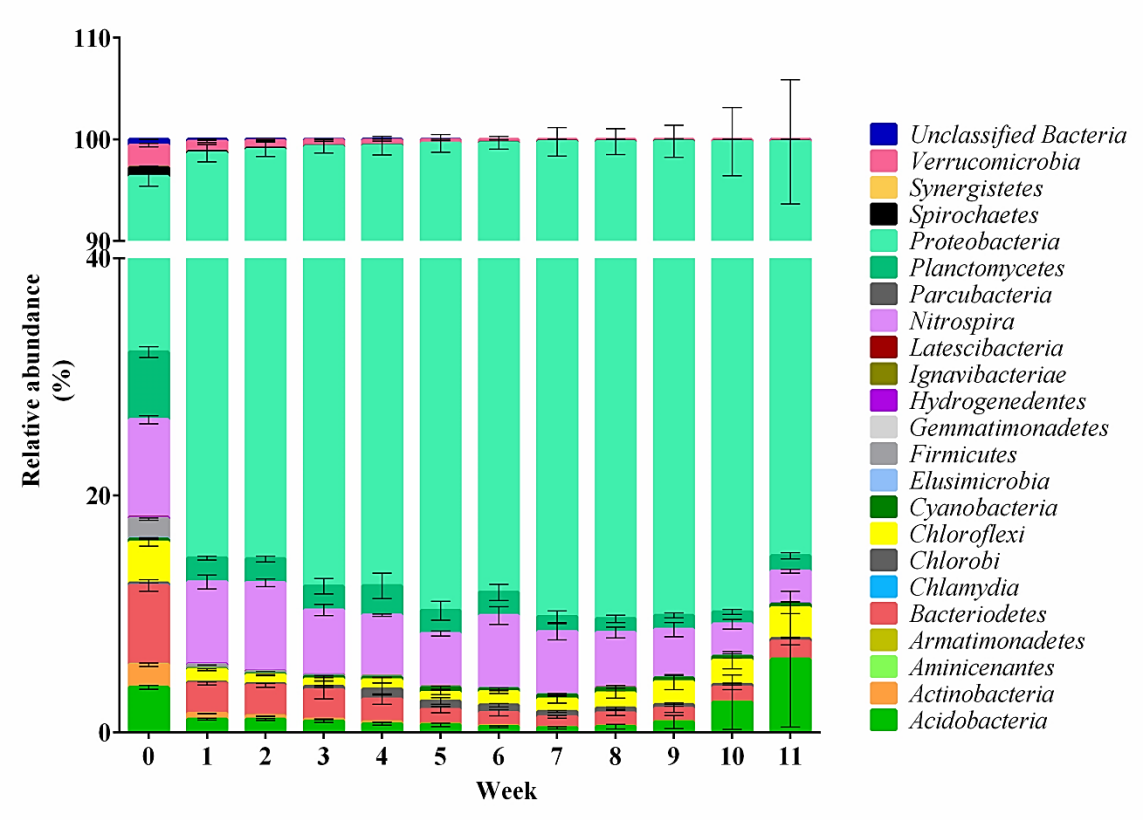

Figure 2.6: Relative abundance of the dominant bacteria groups in floccular and granular sludge. A total of 400 OTUs were selected from each SBR, which represented approximately 90 to 95% of the Bacteria sequencing reads. Error bars represent standard deviations (n = 4).

On average, there were approximately 200 *Proteobacteria* OTUs observed from each SBR. Within the phylum *Proteobacteria*, there were two key groups of bacteria, *Candidatus Accumulibacter* and *Candidatus Competibacter*. *Candidatus Accumulibacter* is a polyphosphate accumulating organism (PAO), which had a relative abundance of approximately 12% at week 0 (Figure 2.7). *Candidatus Competibacter*, which is a direct competitor of *Candidatus Accumulibacter* for carbon sources, was present at 6% at week 0 (Figure 2.7). By week 1, there were about 35% *Candidatus Competibacter* and only 20% *Candidatus Accumulibacter*. At week 11, *Candidatus Accumulibacter* was the most dominant group of *Proteobacteria* at approximately 65% whereas *Canndidatus*

Competibacter was only present at 7% (Figure 2.7). The particle sizes of the granules were also highest during week 11 (Figure 2.1b). Denitrifiers such as *Zoogloea* were present at approximately 8% at week 0 before progressively decreasing to 1.5% by week 11 (Figure 2.7). In contrast, *Thauera* increased in relative abundance from 1.7% to 6%. *Members from the family* ***Xanthomonadaceae*** maintained a relative abundance of 1% to 5% (Figure 2.7). The relative abundance of dominant bacteria groups in each SBR is shown in Figure A2.4.

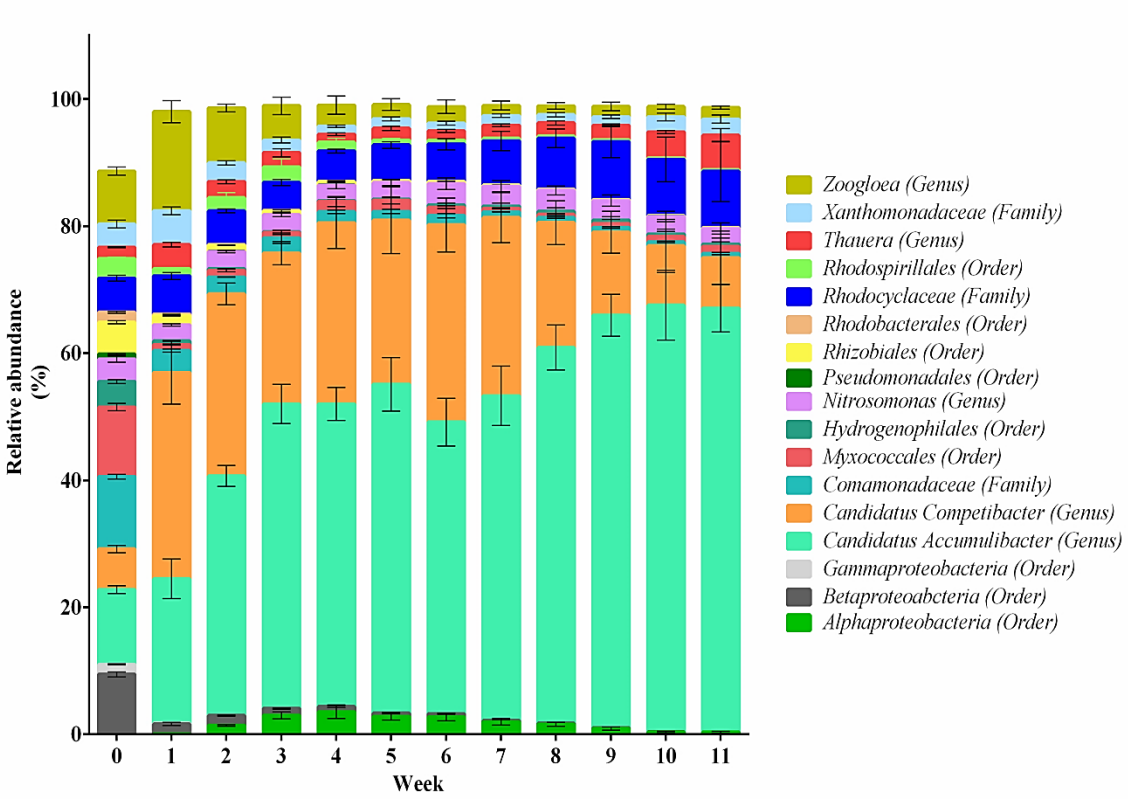

Figure 2.7: Relative abundance of the dominant bacteria groups within *Proteobacteria*. Approximately 200 OTUs from *Proteobacteria* were analyzed and grouped accordingly. Error bars represent standard deviations (n = 4).

The richness and diversity of the bacterial communities during the aerobic granulation process were examined using Menhinick's Index and Shannon-Wiener Index respectively. Bacterial communities were more diverse with a value of 0.815 ± 0.004 at week 0 and

were observed to gradually decline to 0.372 ± 0.024 at week 11 (Figure 2.8a). Equitability values also showed that the evenness of the bacteria communities decreased over time (Figure 2.8a). The Menhinick's Index was at 1.43 ± 0.033 at week 0 but decreased to 0.635 ± 0.046 by week 11 (Figure 2.8b). The loss of diversity appeared to be correlated with the loss of species richness.

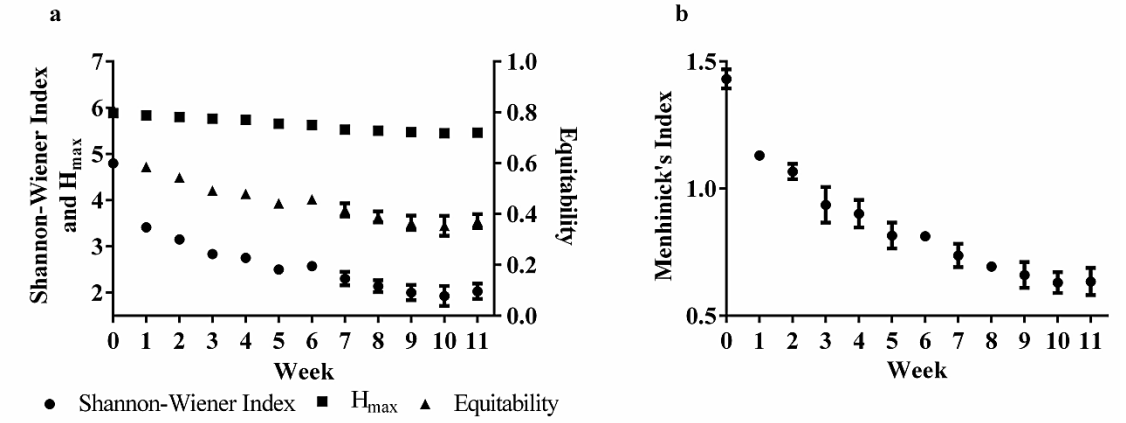

Figure 2.8: Mean diversity and richness indices for bacterial communities in 4 SBRs throughout aerobic granulation. (a) Shannon-Wiener Index, H_{max} and equitability of bacteria communities. (b) Menhinick's Index. Error bars represent standard deviations (n = 4).

Granulation is defined by a high sludge particle size (>100 µm) and low SVI_5 (50 mL g^{-1}). The relationship between the abundance of the top 400 bacterial OTUs in each reactor and the two measurements of granulation including 50th percentile of the sludge particle size and SVI_5 were determined using the Pearson correlation coefficient method (Figure 2.9). These correlation studies were to determine which bacterial groups were correlated to the formation of granules. Most of the bacterial reads are grouped based on the phylum level with the exception of the phylum *Proteobacteria,* which was differentiated into lower levels of classification due to their strong dominance within the sludge.

Correlation matrixes of four SBRs were grouped into three clusters depending on their Euclidean distance. The abundance of the bacterial OTUs has a positive relationship with the particle size as particle size increased over time during granulation. Most of the members in Cluster 1 were mostly not correlated to granulation in SBRs 1, 2 and 4 (Figure 2.9a). In SBR 3, all members except *Aminicenantes* were positively correlated with granulation. These members were very low in relative abundance except for the family *Xanthomonadaceae*.

In contrast, members of Cluster 2 showed strong, positive correlation with granulation. These members include *Candidatus Accumulibacter*, *Nitrosomonas* and *Thauera*, which also play important roles in phosphorus removal, ammonia oxidization and denitrification. Other members included *Rhodocyclaceae* and *Chloroflexi*. The family *Rhodocyclaceae* includes bacteria groups that are important for removal of different types of nutrients (Tsuneda et al. 2005). Both *Candidatus Accumulibacter* and *Thauera* belong to the family of *Rhodocyclaceae*. The phylum *Chloroflexi* consists of filamentous bacteria that are frequently associated with bulking or foaming of sludge (Kragelund et al. 2007), although they were also suggested to play a role in denitrification (McIlroy et al. 2016). The positive correlation between the particle size of the sludge and members of Cluster 2 indicated their importance for the formation of granules. For example, *Candidatus Accumulibacter* was found to dominate the aerobic zone which lies in the outer layers of the granules (Lemaire et al. 2008a). Hence, *Candidatus Accumulibacter* would be responsible for the continual expansion of granules in phosphorus removal systems. Members of Cluster 3 were mostly negatively correlated to granulation (Figure 2.9a). The competitor of *Candidatus Accumulibacter*, *Candidatus Competibacter*, which was also dominant in relative abundance from weeks 1 to 11, was found in Cluster 3 (Figure 2.9a). In addition, the phylum *Nitrospira*, which performs nitrite oxidation, was also found in

Cluster 3. Despite the high abundance of both *Nitrospira* and *Candidatus Competibacter* during the floccular, initiation and early maturation phase (Figure 2.6 and 2.7), these bacterial groups may only be needed for nutrient removal as specified during SBR operation and may not be necessary for granulation.

The sludge volumetric index (SVI_5) is another determinant of granulation. However, there is an inverse relationship between particle size and SVI_5. The formation of granules is demonstrated by the increasing particle size of the sludge biomass and the decrease of SVI_5 over time (Figure 2.1b). Hence, the abundance of bacterial members would have a negative relationship with SVI_5. The correlation matrixes for SVI_5 were grouped into 3 clusters (Figure 2.9b). Cluster 1 consisted of members that were negatively correlated SVI_5.

Furthermore, several of these members including *Candidatus Accumulibacter, Nitrosomonas* and *Rhodocyclaceae* were determined to be significant contributors towards the decrease in SVI_5. In contrast Members of Cluster 2 showed mixed correlations with SVI_5 while Cluster 3 are positively correlated with SVI_5. The genus *Candidatus Competibacter* which was suggested to localize in the core of granules (Lemaire et al. 2008b) did not significantly contribute to the decrease in SVI_5 (Figure 2.9b). The similar correlation matrixes in both particle size and SVI_5 showed reproducibility within four reactors.

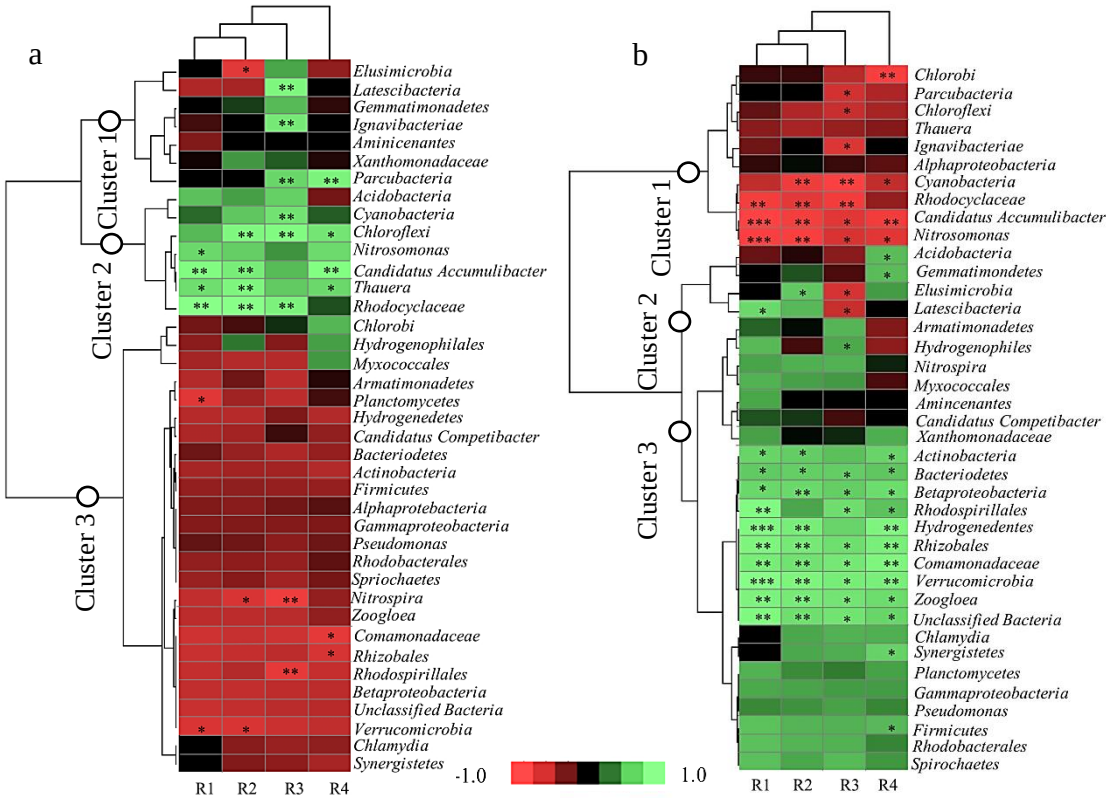

Figure 2.9: Clustering of the top 400 bacterial OTUs in each SBR with two measurements of granulation properties, (a) 50th percentile of particle size and (b) SVI_5. The relationship between the abundance of top 400 bacterial OTUs and granulation measurements over 11 weeks (12 time points) were determined using Pearson's correlation coefficient. The correlation matrixes were clustered based on Euclidean distance with complete linkage method. The correlation matrixes are color-coded where green and red indicate positive and negative correlations, respectively. False discovery rate corrections were also performed for multiple correlations. *, ** and *** denote significant difference where *P*-value $\leq$ 0.05, 0.01 and 0.001, respectively.

For Eukarya, a total of 100 OTUs were selected as they represented approximately 99% of all sequencing reads from Eukarya. In general, the phylum *Ciliophora* was the most dominant Eukarya group throughout the entire aerobic granulation process ranging from 60 to 95% in all replicates (Figure 2.10). Other less dominant members were from the phyla of *Rotifera* and *Tubulinea* which were observed from weeks 1 to 5 in most replicates. For SBR1, there was a sudden drop in the relative abundance of *Ciliophora* at week 11 where it was replaced by an increase in the relative abundance of *Ascomycota* (Figure 2.10a). The eukaryotic community in SBR 2 was relatively similar to SBR 1 except that there was no sudden increase in the fungi *Ascomycota* at week 10 (Figure 2.10b). In SBR 3, *Ciliophora* was observed to be the dominant group throughout 11 weeks (Figure 2.10c). For SBR 4, there was a rapid increase in the relative abundance of *Ascomycota*, which replaced *Ciliophora* as the dominant member from week 8 onwards (Figure 2.9d).

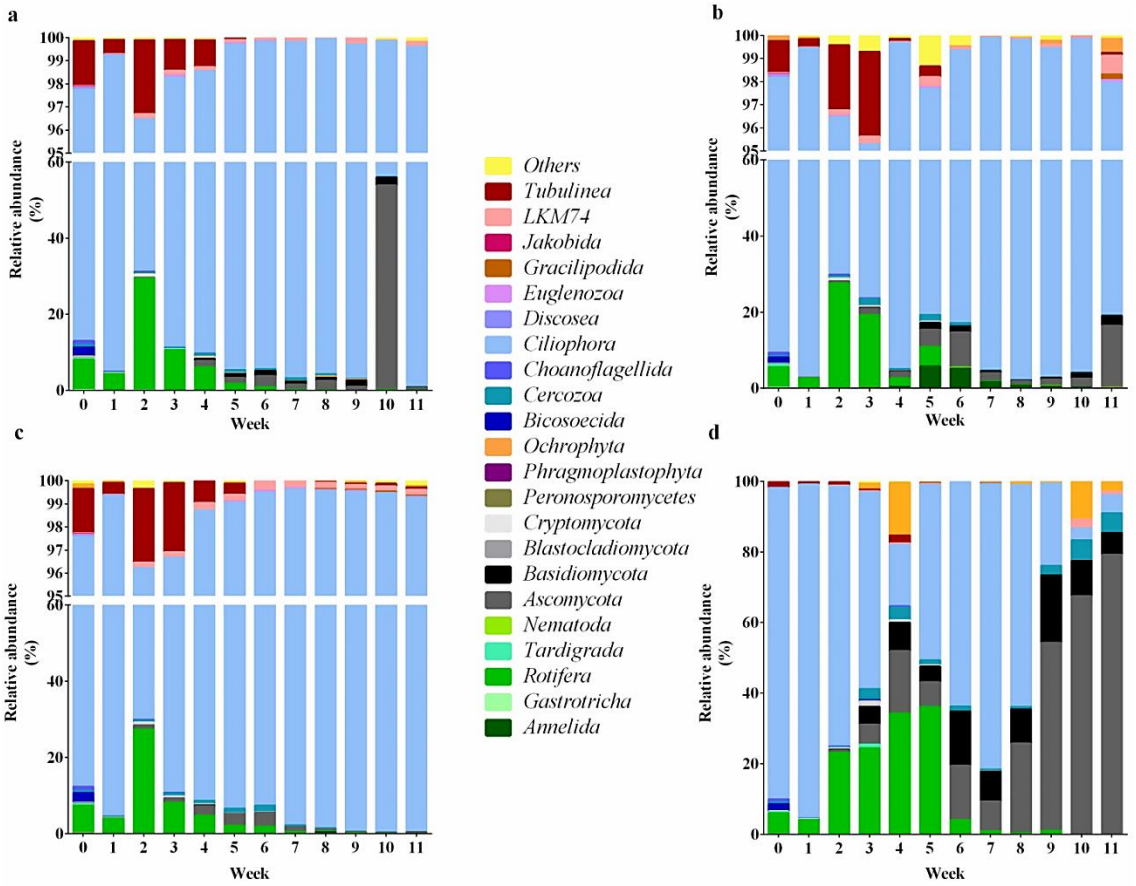

Figure 2.10: Relative abundance of dominant Eukarya groups in floccular and granular sludge. A total of 100 OTUs were selected from (a) SBR 1 (b) SBR 2 (c) SBR 3 (d) SBR 4. These OTUs represented approximately 99% of all sequencing reads from Eukarya. These groups were grouped together based on their phylum.

Within the *Ciliophora*, the family *Oligohymenophorea* was observed to be the most dominant (Figure 2.11). At week 0, its relative abundance was at 58.44 ± 4.78% in contrast to the genus *Telotrochidium* with a relative abundance of 41.33 ± 4.74% (Figure 2.11). The relative abundance of *Telotrochidium* continued to decrease weekly and was not detected from week 4 onwards (Figure 2.11). The two other genera, *Amphileptus* and *Pseudochilodonopsis*, were consistently present only during weeks 0 to 5 and during weeks 0 to 1 respectively (Figure 2.11). However, their relative abundance during these

periods was low ranging from 0.14 to 2% for *Amphileptus* and 0.01 to 0.08% *Pseudochilodonopsis.*

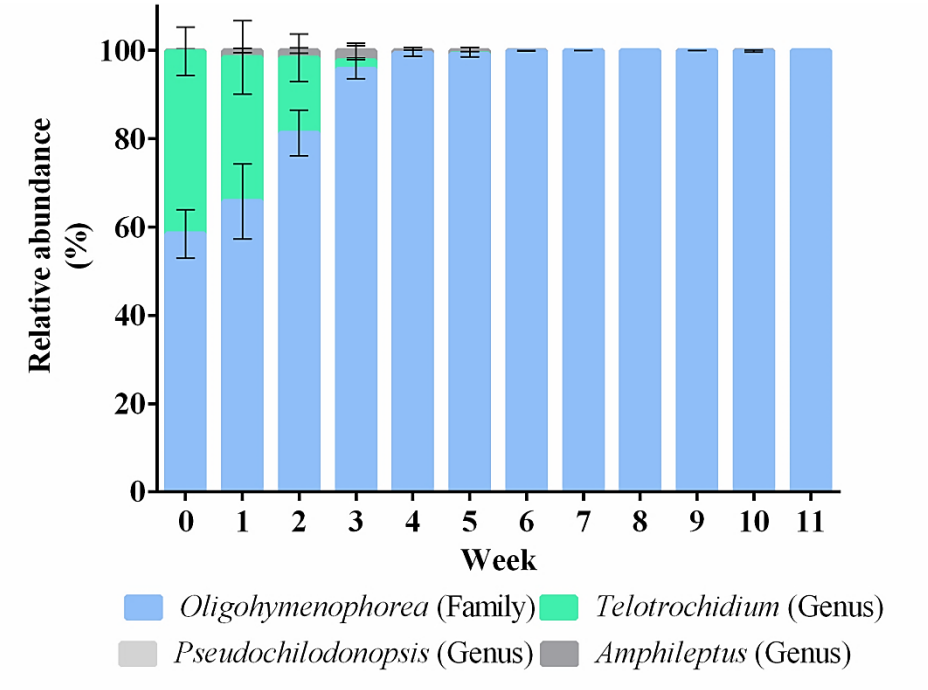

Figure 2.11: Relative abundance of ciliate groups within the phylum *Ciliophora.* Error bars represent standard deviations (n = 4).

The richness and diversity of the eukaryotic communities during the aerobic granulation process were also examined using Menhinick's Index and Shannon-Wiener Index respectively. Eukaryotic communities were more diverse, with a value of 0.815 ± 0.004 at week 0 and gradually declined to 0.372 ± 0.024 by week 11 (Figure 2.12a). Species richness of the eukaryotic communities also declined with the progression of the aerobic granulation process. The Menhinick's Index was at 1.43 ± 0.033 at week 0 but decreased to 0.635 ± 0.046 by week 11 (Figure 2.12b).

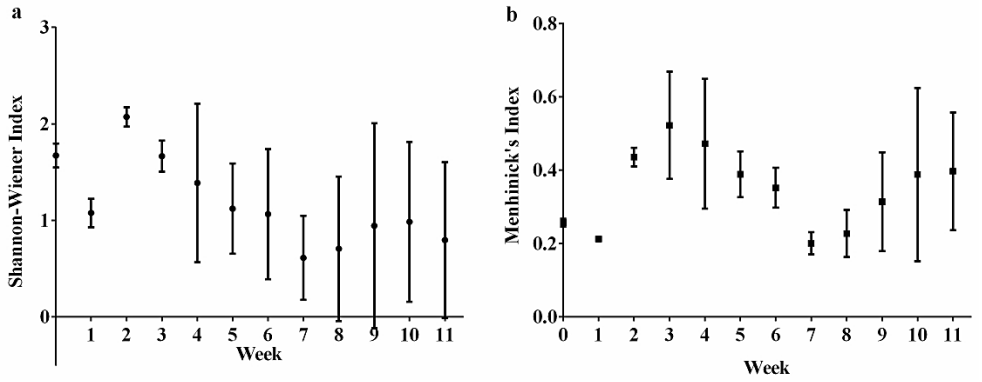

Figure 2.12: Mean diversity and richness indices for eukaryotic communities in 4 SBRs throughout aerobic granulation. (a) The Shannon-Wiener Index and (b) Menhinick's Index. Error bars represent standard deviations (n = 4).

The relationship between the abundance of the top 100 eukaryotes OTUs in each reactor and the four measurements of granulation including the 10, 50, 90th percentile of the sludge particle size and SVI_5 were determined using the Pearson correlation coefficient method (Figure 2.13). These correlation studies were to determine if protozoa were correlated to the formation of granules. Most of the eukaryotic reads are grouped based on the phylum level with the exception of the phylum *Ciliophora,* which was differentiated into lower levels of classification due to their strong dominance within the sludge. These correlations were grouped into two different clusters based on their Euclidean distance. For the 50th percentile of the particle size, members of Cluster 1 showed mixed correlations with granulation (Figure 2.13a). In SBRs 1 and 2, the members that were positively correlated were from *Ascomycota, Basidiomycota, Tetrahymena* and *Gracilipodida.* In contrast, only 1 member each from SBRs 3 and 4 in Cluster 1 was correlated with granulation (Figure 2.13a). The remaining members had negative correlations or no correlation with granulation in SBRs 4 and 3. The phyla *Ascomycota* and *Basidiomycota* are fungi that are able to form networks of filaments known as hyphae. These hyphae could be utilized by bacteria for particle size expansion (Weber et al. 2007).

Although both *Tetrahymena* and *Gracilipodida* showed strong correlation with granulation, both were present in extremely low numbers or not at all (Figure 2.10 and 2.11), *Tetrahymena* and *Gracilipodida* are swimming ciliate and naked amoebae, respectively (Lahr et al. 2012, Orias et al. 2011). In Cluster 2, most members in all four SBRs had negative correlation with granulation except *Oligohymenophorea* and *Annelida* in SBR 3 and *Nematoda* in SBR 1 (Figure 2.13a). Similarly, members in Cluster 3 demonstrated negative correlations with granulation in four reactors. Most of the protozoa including non-*Ciliophora* groups such *Bicosoecida, Choanoflagellida, Colpodea, Cercozoa, Discosea, Euglenozoa, Heterobolosea* and *Tubulinea* demonstrated negative correlations with granulation in four SBRs. As described in Section 2.33, particle size has a negative relationship with $SVI_{5.}$ Hence, in Cluster 1 of SVI_5, most of the members that were positively correlated to particle size were negatively correlated to SVI_5 (Figure 2.13b).

Both *Ascomycota* and *Basidiomycota* displayed negative correlations with the decreasing trend of SVI_5 (Figure 2.13b). This suggested that these fungal groups were closely associated with both flocs and granules during aerobic granulation (More et al. 2010). Previous studies have shown that fungi are closely associated with granules where long fungal filaments can entangle among themselves and also protrude out from the surface of the granules (Schwarzenbeck et al. 2005, Yang et al. 2008). Fungal filaments could also be observed by FISH in cross-sections of aerobic granules (Weber et al. 2007). Unlike fungi, protozoa with positive correlations with SVI_5 implied that these protozoa were not closely associated with the settling properties of the sludge. In general, the data suggest that the various groups of protozoa may not be necessary for the formation of granules while the presence of fungi could enhance the settleability of sludge.

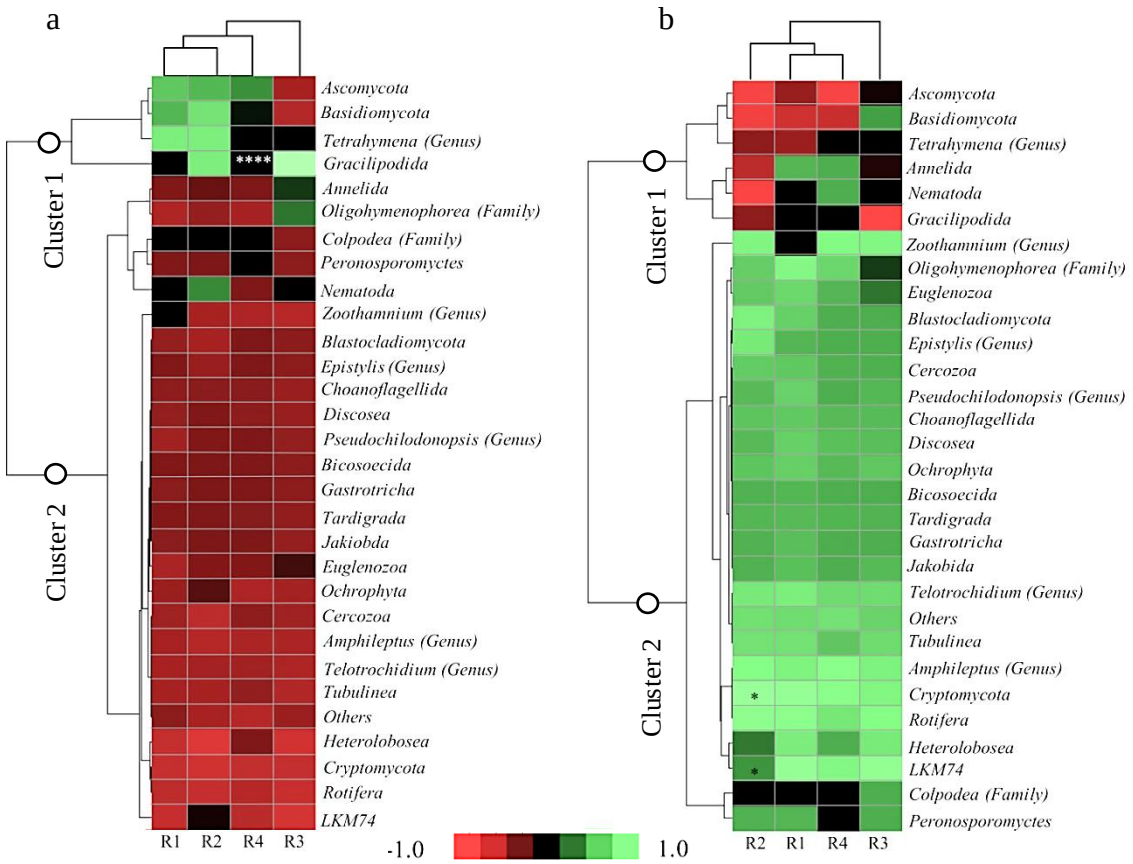

Figure 2.13: Clustering of the top 100 eukaryotic OTUs in each SBR with two measurements of granulation namely (a) 50th percentile of particle size and (b) SVI_5. The relationship between the abundance of the top 100 eukaryotic OTUs and granulation measurements over 11 weeks (12 time points) were determined using Pearson's correlation coefficient. The correlation matrixes were clustered based on Euclidean distance with the complete linkage method. The correlation matrixes are color-coded where green and red indicate positive and negative correlations, respectively. False discovery rate corrections were also performed for multiple correlations. * and **** denote significant difference where *P*-value $\leq$ 0.05 and 0.0001, respectively.

2.4. Discussion

The implementation of well-studied physical factors such as shear force and settling time greatly enhances aerobic granulation of floccular sludge. However, the instability of aerobic granules often results in disintegration after prolonged operations. Hence, it is important to better understand the biological factors that govern granulation as they are still poorly understood. One of these factors is protozoan predation, which is known to enhance the formation of biofilms (Hahn and Höfle 2001) and in activated sludge, it has also been suggested to enhance flocculation of wastewater bacteria (Bossier and Verstraete 1996).

To study the role of protozoa in the granulation process, four SBRs inoculated with floccular sludge were operated according to standard procedures, e.g. gradual reduction in settling time and introduction of hydrodynamic shear force from intermittent sparging of air and nitrogen during aerobic and anaerobic/anoxic phases, respectively. As a consequence of the reduction in settling time, a decline of the MLSS and VSS was observed during week 1, which was consistent with other granulation studies (Barr et al. 2010a, Lemaire et al. 2008b). However, the MLSS and VSS of the floccular sludge started to increase again as the aggregates continued to increase in particle size. This was likely to be due to the increase in density and compactness of the flocs as indicated by the decreasing SVI_5, which allowed them to settle and be retained in the SBRs before being discharged.

The initiation of granulation was characterized by the appearance of dense and compact aggregates with decreasing SVI_5 coupled with increasing particle sizes. Aerobic granules are characterized by a minimum particle size of 100 µm and a SVI_5 of 50 mL g^{-1}or less (Barr et al. 2010a) and based on this definition, the biomass was deemed to have

transformed into aerobic granules by week 7 in these experiments. All four reactors were performing SNDPR with a total P removal between 55 to 75% and total N removal ranged between 65 to 75%. These values were generally lower than those typically observed for SNDPR bioreactors (He et al. 2017, Lemaire et al. 2008a, Yilmaz et al. 2008). For example, Lemaire et al. (2008) reported a total N and P removal of 85% and 99% respectively. The increased efficiency of those reactors may be due to the fact that they had been operated and optimized for SNDPR over the course of 1 year compared to the 11 weeks of operation for the experiments reported here. The formation of aerobic granules capable of efficient nutrient removal may require several months of cultivation. For example, 170 days were required to adapt aerobic granules treating synthetic wastewater to abattoir wastewater which contained higher levels of ammonia and organic nitrogen (Yilmaz et al. 2008).

As the flocs developed into granules and began to remove nutrients, a shift in bacterial communities was observed in each SBR over time (Figure 2.4b). It was in the floccular phase where the bacteria community was the most diverse, as reflected by the Ribotagger profiling of OTUs (Figure 2.5) and the Shannon-Wiener Index (Figure 2.7a). Previous sequencing studies also revealed a high level of bacteria diversity in activated sludge flocs (Ibarbalz et al. 2013, Ju et al. 2014, Shchegolkova et al. 2016, Yu and Zhang 2012). Bacterial communities in activated sludge were found to be commonly dominated by several major phyla such as *Proteobacteria*, *Bacteroidetes*, *Firmicutes* and *Actinobacteria* (Liu 2008, Yu and Zhang 2012, Zhang et al. 2012). As granulation took place in the four SBRs, the diversity of the bacteria decreased over time and dominant bacterial species emerged. The loss of diversity and emergence of dominant bacterial species can be attributed to the extensive discharge of biomass due to a low settling time and short hydraulic retention time, which was necessary to convert flocs to aerobic granules

(Weissbrodt et al. 2012). A study by Weissbrodt et al. (2012) also reported this pattern of decreasing diversity and emergence of new dominant bacterial members during early stages of aerobic granulation. A highly diverse bacterial community dominated by *Tetrasphaera* during inoculation was replaced by *Zoogloea* and *Dechloromonas* after 5 days of operations (Weissbrodt et al. 2012). This process of settling reduction and biomass discharge exerted strong selection pressure for flocs that could settle within the given time. Hence, only the retained biomass in the SBRs were analyzed since the discharged biomass had little role in the formation of granules.

During the early phase of granulation, the phylum *Proteobacteria* was the most dominant in the bacterial communities in the four SBRs. The dominance and abundance of *Proteobacteria* was also typically observed in other activated sludge studies (Gonzalez-Martinez et al. 2016, Kämpfer et al. 1996). Two important groups of *Proteobacteria, Candidatus Accumulibacter* and *Candidatus Competibacter* were observed to increase in relative abundance despite significant washout of biomass during the phase of settling time reduction The abundance of both *Candidatus Accumulibacter* and *Candidatus Competibacter* was likely due to the use of synthetic wastewater that had both acetate and propionate as carbon sources. The use of propionate had been shown to provide a selective growth advantage to *Candidatus Accumulibacter* as *Candidatus Competibacter* was less proficient in propionate uptake (Oehmen et al. 2005b). Unlike the *Gammaproteobacteria* GAOs such as *Candidatus Competibacter,* only *Alphaproteobacteria* GAOs are more efficient at propionate uptake (Oehmen et al. 2005b). In contrast, the use of acetate as a carbon source favored the growth of *Candidatus Competibacter*, which would out-compete *Candidatus Accumulibacter,* leading to very poor phosphorous removal (Barr et al. 2010a, Zhou et al. 2010). Here, the carbon concentration of the synthetic wastewater was 200 mg L^{-1} with a 3:1 ratio of

acetate and propionate. Despite of the previous observations by Zhou et al. (2010), both propionate and acetate in the synthetic wastewater feed used in this current study possibly enriched for the growth of both *Candidatus Accumulibacter* and *Candidatus Competibacter*. Here, *Nitrospira* was also found to be a less dominant member. This strongly suggested that *Candidatus Accumulibacter, Candidatus Competibacter* and *Nitrospira* were closely associated with the denser flocs that settled before being discharged.

As granules formed during the maturation phase, *Candidatus Accumulibacter* became increasingly more abundant than *Candidatus Competibacter*. Previous studies on mature aerobic granules in SNDPR systems also showed that *Candidatus Accumulibacter* and *Candidatus Competibacter* were typically the most abundant among all bacteria (Barr et al. 2010a, Lemaire et al. 2008b). In general, PAOs such as *Candidatus Accumulibacter* were localized on the outer layers ranging from the aerobic to the anoxic layers of the granules while GAOs such as *Candidatus Competibacter* were localized at the anoxic layers (Winkler et al. 2013). As the aerobic granules were formed under SNDPR conditions, it was expected that *Candidatus Accumulibacter* would be highly abundant on the aerobic zone as *Candidatus Accumulibacter* plays an essential in phosphorus removal. The anoxic zone within the granules would be dominated by *Candidatus Competibacter* (Lemaire et al. 2008b). The decrease in *Candidatus Competibacter* during the maturation phase could be due to expansion of the granules which could have limited the diffusion of substrate such as acetate into the inner anoxic zone where *Candidatus Competibacter* resided. Previous studies have found that granules larger than 0.5 mm in radius had limitations in the diffusion of both dissolved oxygen (DO) and acetate beyond the aerobic zone of the granules (Jang et al. 2003, Li and Liu 2005, Li et al. 2008). As the penetration depth of DO decreased in granules, aerobic activities within the granules would be limited

and hence resulting in a poor diffusion of acetate (Jang et al. 2003, Li and Liu 2005, Li et al. 2008). The dead cells which form the core of the aerobic granules were suggested to be a result of diffusion limitations and plugging of channels within the granules (Tay et al. 2002). Therefore, without a carbon source, it is likely that *Candidatus Competibacter* would either die or beome metabolically inactive within the granules. Although the localization of *Candidatus Accumulibacter* and *Candidatus Competibacter* on flocs and aerobic granules was not performed here, the high abundance of both *Candidatus Competibacter* and *Candidatus Accumulibacter* appeared to be essential for the formation of granules. Future studies could also analyse the discharged liquid phase since the discharged effluent may contain bacteria that were dislodged or dispersed from the surfaces of aggregates or granules, which may have led to the increase in abundance of *Candidatus Competibacter* and *Candidatus Accumulibacter*.

Although bacteria have important roles in the formation of granules and nutrient removal, the abundance of eukaryotes in sludge also indicate their potential role in these processes. Eukaryotes in sludge consist of a variety of microorganisms such as fungi, protozoa, metazoa, and algae. Fungi are typically minor community members of activated sludge as they are unable to compete with bacteria except during toxic or acidic environments (Cooke and Pipes 1970, Seviour and Nielsen 2010). Under these unfavorable conditions, fungi will be able to compete with bacteria and cause undesirable bulking in the activated sludge (Jenkins and Richards 2003, Seviour and Nielsen 2010). However, fungi have been shown to enhance the settleability and biodegradability of sewage sludge (Fakhru'l-Razi et al. 2002, Mannan et al. 2005). In addition, fungi were also found to provide better denitrifying capabilities than denitrifying bacteria (Guest and Smith 2002). In the current study, fungi were not detected during the floccular phase in any of the SBRs. However, fungi from the phyla *Ascomycota* and *Basidiomycota* were detected at low relative

abundance in all 4 SBRs during the initiation phase. The understanding of the role of fungi in aerobic granulation is limited. A study by Weber et al. (2007) suggested that filamentous fungi could play a role in the expansion of aggregates and granules where sludge bacteria utilize the fungal hyphae as a substratum for colonization. This process allowed fungal hyphae to form the core of the granule over time as the granules expanded. Other studies also proposed that fungi formed the initial aggregates during aerobic granulation as they could form mycelial pellets that had good settling properties (Beun et al. 1999, Etterer and Wilderer 2001). However, these fungal pellets often lyse due to oxygen limitation in the inner core of the pellet as they grow in size (Beun et al. 1999). Thereafter, bacteria would colonize these pellets and expand into granules. Hence, there is a possibility that *Ascomycota* and *Basidiomycota* detected in all 4 SBRs during the initiation phase could have been useful in initiating the formation of compact aggregates. However, more work is still required (e.g. FISH) to determine the localization of the fungi within the compact aggregates during the initiation phase.

Previous efforts in investigating the fungal diversity in aerobic granules also found representatives from both *Ascomycota* and *Basidiomycota* in flocs and mature granules (Weber et al. 2009). Hence, it was suggested that fungi could contribute to the early formation of aggregates and particularly towards the biofilm structure of aerobic granules (Weber et al. 2009). Moreover, both of these fungal species were positively correlated with the increase of particle size over time, suggesting their close association with flocs and granules. However, the specific interactions between bacteria and fungi were not identified. Unlike fungi-bacteria interactions, protozoa-bacteria behaviors such as predation are well established factors for the formation of biofilms and promoting flocculation in wastewater sludge (Bossier and Verstraete 1996, Hahn et al. 2000, Hahn and Höfle 2001).

With respect to the protozoa, ciliated protozoa were the most abundant group throughout the aerobic granulation process as reflected by the relative abundance of the phylum *Ciliophora*. In the floccular phase, there was a higher diversity of ciliates including swimming, crawling and sessile ciliates compared to the maturation phase. There was a succession of ciliated protozoa as the floccular sludge converted to granules. For example, as the flocs started to aggregate at the initiation phase, swimming ciliates became less abundant due to a decrease in the availability of suspended bacteria due to biomass discharge and floccular aggregation. Protozoan predation exerted by swimming ciliates on the suspended bacteria would have been significant in altering the morphology of bacteria, causing the formation of microcolonies or filaments (Hahn et al. 2000, Hahn and Höfle 2001, Michaela et al. 2005). However, the abundance of swimming ciliates, such as *Paramecium*, was found to be of very low abundance in this current study. Hence, the loss of swimming ciliates due to biomass discharge would have limited their influence on the aggregation process.

During the initiation phase, compact aggregates formed and continued to expand. This allowed for the dominance of both crawling ciliates and sessile ciliates as swimming ciliates are not adapted to feed on compact and larger particles. The motility of crawling ciliates such as *Chilodonella* has been suggested to cause dislodgement of cells from biofilms (Böhme et al. 2009, Dopheide et al. 2011a). The dislodged surface-associated cells could also act as a form of food source for the filter-feeding sessile ciliates. Grazing by these crawling ciliates was also reported to stimulate the growth of microcolonies (Dopheide et al. 2011a). The outgrowth or aggregation of microcolonies was previously suggested to be mechanisms of granule formation (Barr et al. 2010a). The presence of crawling ciliates on flocs and aggregates would contribute to the compactness and possibly, the growth of aggregates into granules. The appearance of compact and dense

granules by maturation phase reduced the availability of loose bacteria on the surfaces. Hence, crawling ciliates would be outcompeted by sessile ciliates whose growth is favored by an increase in surface area due to granulation. These trends of succession and decreased diversity of ciliates was observed for all four SBRs during aerobic granulation.

During the early stages of granulation, there were a variety of sessile ciliates which could be differentiated into colonial or singular ciliates. These different groups of sessile ciliates were also observed frequently in other activated sludge studies (Al-Shahwani and Horan 1991, Augustin and Foissner 1992, Madoni 2003, Madoni 2010). Here, several genera of sessile ciliates identified by Ribotagger such as *Telotrochidium*, *Epistylis*, *Carchesium* and *Vorticella* belonged to the class of *Peritrichia* which falls under the family *Oligohymenophorea*. In the current protozoa dataset, the majority of the *Oligohymenophorea* reads could not be resolved beyond the family classification. The genus *Telotrochidium* was detected by Ribotagger during the early stages of granulation. As *Telotrochidium* is a stalkless peritrich which is free swimming, *Telotrochidium* would have been being unable to colonize the surface area of the granules and aggregates. Hence it was likely that they were generally washed out over time and replaced by other sessile ciliates.

During the later stage of granulation, most of the sessile ciliates observed were highly likely to be *Vorticella*. This observation was based on their characteristic of a single body mounted on a single contractile stalk. Previous studies also showed that sessile ciliates such as *Vorticella* and *Epistylis* are found at high abundance on the aggregates and granules (Lemaire et al. 2008a, Li et al. 2013, Schwarzenbeck et al. 2004b, Weber et al. 2007). Here, the singular sessile ciliates observed on the surfaces of aggregates and granules revealed that the majority of these ciliates belonged to the genus of *Vorticella*.

Although *Vorticella* was not detected in the metacommunity data, it is possible that the majority of the *Oligohymenophorea* reads belonged to *Vorticella* during the maturation phase. This is likely due to the lack of *Vorticella* related data in the SILVA ARB database utilized for Ribotagger analysis.

Based on the data presented here, the changes in the protozoan community were not correlated with granulation. Hence, it can be suggested that protozoa do not play a dominant role in aerobic granulation. It is more likely that the change from flocs to granules acted as a form of selection pressure on the protozoan community. The formation of aggregates favoured the growth crawling and sessile ciliates while the compact and large granules favoured the colonization of sessile ciliates. The process of aerobic granulation also resulted in a less diverse bacterial community as there were strong selective pressures from the settling time and subsequent discharge of biomass. In the next chapter, both floccular and granular sludge were chemically treated to remove the protozoal community to test if the absence of protozoa results in either poor formation of granules or disintegration of granules.

Chapter 3: THE ROLE OF PROTOZOAN PREDATION IN THE FORMATION AND MAINTENANCE OF AEROBIC GRANULES

3.1. Introduction

Two distinct mechanisms for driving granulation have been suggested, the outgrowth of cells within microcolonies and the aggregation of microcolonies to form larger granules (Barr et al. 2010a). During microcolony outgrowth, a particular bacterial type is selected for and is enriched over time within the microcolony. Thereafter, the enriched microcolony starts growing and expanding in size, forming a large aggregate and eventually a large granular structure is formed. Another mechanism is microcolony aggregation where numerous small microcolonies or flocs aggregate and grow together as a single entity to form a large granular structure. However, the driving biological forces that push the microcolonies towards outgrowth and aggregation are still unknown.

Protozoan predation has been demonstrated to enhance biofilm formation in various species of bacteria (Matz et al. 2005b, Rychert and Neu 2010, Sun et al. 2013). Hence, it has been hypothesized that protozoan predation could play an important role in driving the formation of aerobic granules from activated floccular sludge. Protozoa are abundant in activated floccular sludge systems, and play an important role in the predation of suspended bacteria, which aids in the clarification of wastewater effluent (Li et al. 2013). In addition, previous studies of aerobic granulation systems demonstrated an abundance of sessile ciliates on the surface of aerobic granules (Lemaire et al. 2008a, Li et al. 2013, Schwarzenbeck et al. 2004b, Weber et al. 2007), where they reportedly feed on suspended bacteria in the wastewater. Electron microscopy of granular surfaces showed the attachment of bacteria on the stalks of sessile ciliates (Weber et al. 2007). Hence, Weber et al. (2007) further hypothesized that these sessile ciliates could also act as nucleating

agents for the attachment of bacteria. Taken together, these studies strongly suggest that protozoan predation may have a role in promoting aerobic granulation.

To better understand the role of protozoan predation in sequencing batch reactors (SBRs), eukaryotic metabolic inhibitors were added to both floccular and granular sludge in mini-SBRs that were designed and fabricated for aerobic granulation. Thiram, which is a eukaryotic inhibitor, has been shown to be effective against the natural assemblages of ciliates and flagellates in marine sediments (Shimeta and Cook 2011). Inhibition refers to either metabolic inactivation or death. Thiram has been shown to rapidly decrease intracellular glutathione and inhibit glutathione reductase in active growing yeast cells, which increases the sensitivity of cells to oxidative stress (Elskens and Penninckx 1997). Here, the concentration of thiram was optimized to ensure effective inhibition of protozoan communities whilst not affecting the metabolic activity of the sludge bacterial communities. The metabolic activity of bacteria was measured by the efficiency of ammonium removal from the synthetic wastewater as both floccular and granular sludge were operated for simultaneous nitrification, denitrification and phosphorus removal. Using the optimum concentration of thiram for inhibition of protozoa, the role of predators in the granulation process was investigated.

3.2. Materials and Methods

3.2.1. Optimization of concentration of thiram for removal of protozoa from floccular and granular sludge

Thiram was tested at concentration ranges of 0 to 200 mg L^{-1} for the removal of protozoa from floccular and granular sludge. Activated floccular sludge was collected from the Ulu Pandan Wastewater Treatment Plant (UPWTP) while granular sludge was obtained from this study in granulation reactors that were operating in the laboratory. Each thiram

treatment was performed in duplicate. For each microfuge tube, 500 µL of well-mixed sludge was added to 200 µL of synthetic wastewater and 290 µL of filtered deionized MilliQ water. Varying concentrations of thiram were added to the tubes in a volume of 10 µL to obtain the required working concentrations. As DMSO was the solvent used to dissolve thiram, the effect of DMSO on both bacterial and protozoan communities was also investigated by the addition of 10 µL of DMSO as controls. For tubes without thiram, 300 µL of filtered deionized MilliQ water was added instead of 290 µL. The tubes were incubated at room temperature for 72 h with constant shaking at 120 rpm. Used medium was replaced with fresh medium every 24 h. The viability of the flocs and granules were assessed by Live/Dead Cell Viability Assays (Thermo Fisher Scientific, Singapore) as per the manufacturer's guidelines using confocal microscopy (LSM780, Carl Zeiss, Germany). In addition, to determine the efficiency of ammonia removal, the concentration of ammonia was determined after 72 h. Poor ammonia removal efficiency would indicate that the concentration of thiram used had a negative effect on the bacterial community. Three confocal micrographs were captured for each control and treated sample and biomass quantification of confocal micrographs was performed using Imaris (Bitplane AG, Belfast, UK) to obtain the volume of both flocs and granules. For the quantification of sludge protozoa, triplicate aliquots of 10 µL were removed from each tube and the numbers of sludge protozoa determined using light microscopy (Primo Star, Carl Zeiss, Germany). These optimization studies were performed in triplicates.

3.2.2. Operation of mini-sequencing batch reactors

Mini-SBRs (mSBR) were seeded with either activated floccular sludge from the UPWTP or laboratory cultivated aerobic granules. For floccular sludge experiments, both controls and treatments were performed in triplicate and for granular sludge experiments, duplicate experiments were performed. Each SBR had a final working volume of 30 mL

and was enhanced for simultaneous nitrification, denitrification and phosphorous removal (SNDPR) at 21 to 22^{o}C (Zhou et al. 2010). For the floccular sludge experiments, each mSBR was operated in a 6 h cycle comprising of feeding (10 min), anaerobic (100 min), aerobic (110 min at Day 0, with a gradual increase to 120 min by the end of Week 1) and anoxic (100 min) phases. Each cycle was completed with a settling stage (30 min at Day 0, with a gradual decrease to 20 min by the end of Week 1) and a 10 min decanting stage. The settling time was maintained at 20 min per cycle from the end of Week 1 onwards. For the granular sludge experiments, the mSBRs were also operated in a 6 h cycle comprised of feeding (10 min), anaerobic (105 min), aerobic (125 min) and anoxic (105 min) phases. However, the settling time for each cycle was fixed at 5 min followed by 10 min of decanting.

A volume (14.97 mL) of synthetic wastewater was fed to each SBR during the feeding stages of each phase and 15 mL of treated effluent was discharged at the end of the cycle. Synthetic wastewater was prepared as described previously (Smolders et al. 1994, Zhou et al. 2010). For the inhibition of eukaryotes, thiram was dissolved in dimethyl sulfoxide (DMSO) to obtain a stock solution of 20 g L^{-1} for treatment of the floccular sludge, or 5 g L^{-1} for the granular sludge. Based on optimisation studies, thirty µL of thiram was added to each reactor once per day after feeding to obtain a final concentration of 20 mg L^{-1} for treatment of floccular sludge or 5 mg L^{-1} for granular sludge. DMSO was also added to each control mSBR. Both DMSO and thiram treatment of sludge was completed by Week 2. Both control and treated mSBRs were operated from Week 3 to Week 8 without the addition of DMSO or thiram. Nitrogen was sparged intermittently into the mSBRs during feeding, anaerobic and anoxic phases while compressed air was sparged intermittently during aerobic phases, except during the settling and decanting stages. Sparging of both nitrogen and air provided complete mixing of the sludge and the hydrodynamic shear

force required for aerobic granulation and maintenance of granular sludge. Both floccular and granular sludge experiments were carried out for a total of 8 weeks and 5 weeks, respectively.

3.2.3. Performance (cycle) studies of mini-sequencing batch reactors

Cycle studies were performed on a weekly basis to evaluate the efficiency of nutrient removal of both floccular and granular sludge as detailed in Chapter 2, Section 2.2.2 with the following modifications. For both mixed liquor suspended solids (MLSS) and mixed liquor volatile suspended solids (MLVSS) analysis, 1 mL of sludge was obtained from each SBR instead of 5 mL to reduce overall sludge biomass loss. For particle size analysis, images of sludge were taken in triplicate for each reactor on a weekly basis. Each image was analyzed using ImageJ (National Institute of Health, USA) to obtain the mean diameter of all the particles within the image. An overall mean particle diameter was obtained from the three images for each mSBR, which represented the average particle size of that mSBR. For quantification of protozoa, 10 µL were removed in triplicate from a representative sludge sample of each mSBR and the numbers of protozoa were determined using light microscopy (Primo Star, Carl Zeiss, Germany).

3.2.4. Metatranscriptomic sequencing and analysis

RNA extractions were performed as detailed in Chapter 2, Section 2.2.3. Extracted RNA samples were sequenced and analyzed using Ribotagger as detailed in Chapter 2, Section 2.2.4.

3.2.5. Statistical analyses

PERMANOVA using distance matrices was performed as detailed in Chapter 2, Section 2.2.5. The three factors used for PERMANOVA were weeks, reactors and treatment. One-way and two-way ANOVA with Tukey's multiple comparisons tests were performed

using Prism (GraphPad 6.0) to determine the effectiveness of thiram for inhibition of protozoa in the sludge communities.

3.3. Results

3.3.1. Thiram concentration for treatment of floccular sludge

To determine the role of protozoan predation on aerobic granulation, thiram was added into floccular sludge to inhibit or kill sludge protozoa during the operation of the mSBRs. Here, a range of concentrations of thiram (0 to 200 mg L^{-1}) was tested to determine the optimal concentration for the treatment of floccular sludge. Active protozoa at a cell density of 1133 ± 219 cells mL^{-1} were found in the sludge that did not receive treatment (Figure 3.1a). The number of protozoa observed in the DMSO treated sludge, 1228 ± 279 cells mL^{-1}, was not significantly different from the untreated control (Figure 3.1a). This indicated that DMSO did not inhibit the activity of the protozoa. Thiram addition at concentrations of 5 and 10 mg L^{-1} resulted in 311 ± 62 cells mL^{-1} and 147 ± 53 cells mL^{-1} of protists, respectively (Figure 3.1a). The density of active protozoa was determined to be 6 ± 8 cells mL^{-1} when the thiram concentration was increased to 20 mg L^{-1} (Figure 3.1a). No active protozoa were observed at thiram concentrations $\geq$ 50 mg L^{-1}. Hence, the results showed that thiram treatment inhibited the protozoa under these conditions.

To ensure that bacterial activity was not negatively affected by the addition of DMSO and/or thiram, the efficiency of ammonia removal from the synthetic wastewater was measured. The untreated sludge showed 100% efficiency in removing ammonia (Figure 3.1b). Sludge treated with DMSO and low concentrations of thiram, from 5 mg L^{-1} to 10 mg L^{-1}, also demonstrated a high level of ammonia removal, from 85.99 ± 6.83 to 95.63 ± 3.09% (Figure 3.1b). One-way ANOVA analysis suggested that there was no significant difference between the untreated sludge and thiram treated sludge. When the

concentration of thiram was increased to 20 mg L^{-1} and above, the efficiency of ammonia removal ranged from 80.68 ± 5.99 to 73.20 ± 2.01% (Figure 3.1b). These results showed that thiram treatment at 20 mg L^{-1} or more, significantly reduced the removal of ammonia, which indicates inhibition of bacterial activity.

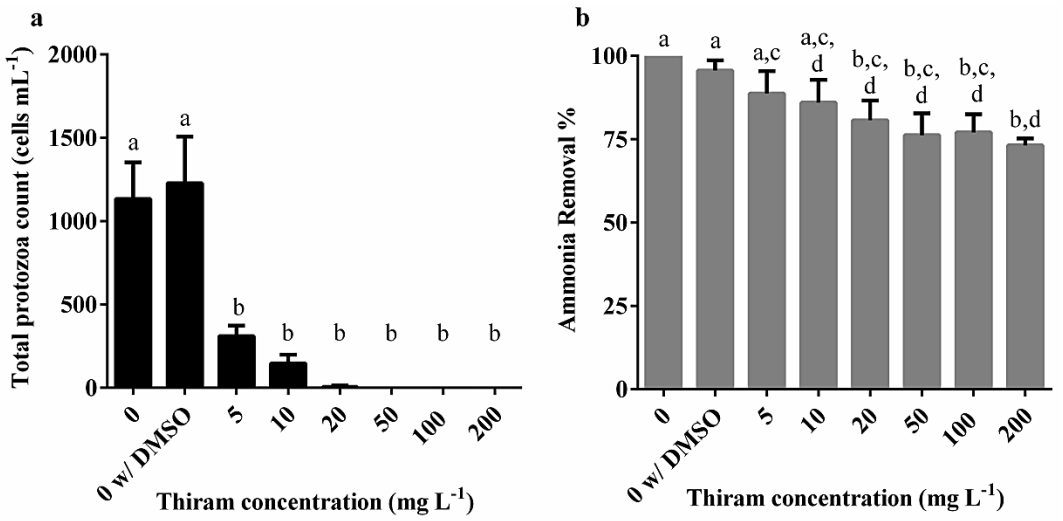

Figure 3.1: Optimization of thiram concentration for floccular sludge treatment. (a) Total protozoan numbers in floccular sludge. Significance values of comparisons between each group can be found in Table A3.1. (b) Efficiency of ammonia removal from floccular sludge. Significance values of comparisons between each group can be found in Table A3.2. Different letters indicate significant differences between groups in a one-way ANOVA. Error bars represent standard deviations (n = 3).

Confocal imaging was performed for all sludge samples to determine if thiram treatment negatively affected the viability of sludge (Figure 3.2), as assessed by the Live/Dead Cell staining. It was observed that untreated sludge samples had a similar ratio of live and dead cells to the DMSO and thiram treated samples after 72 h (Figure 3.2a to h). These observations demonstrated that thiram treatment did not reduce the viability of the treated sludge.

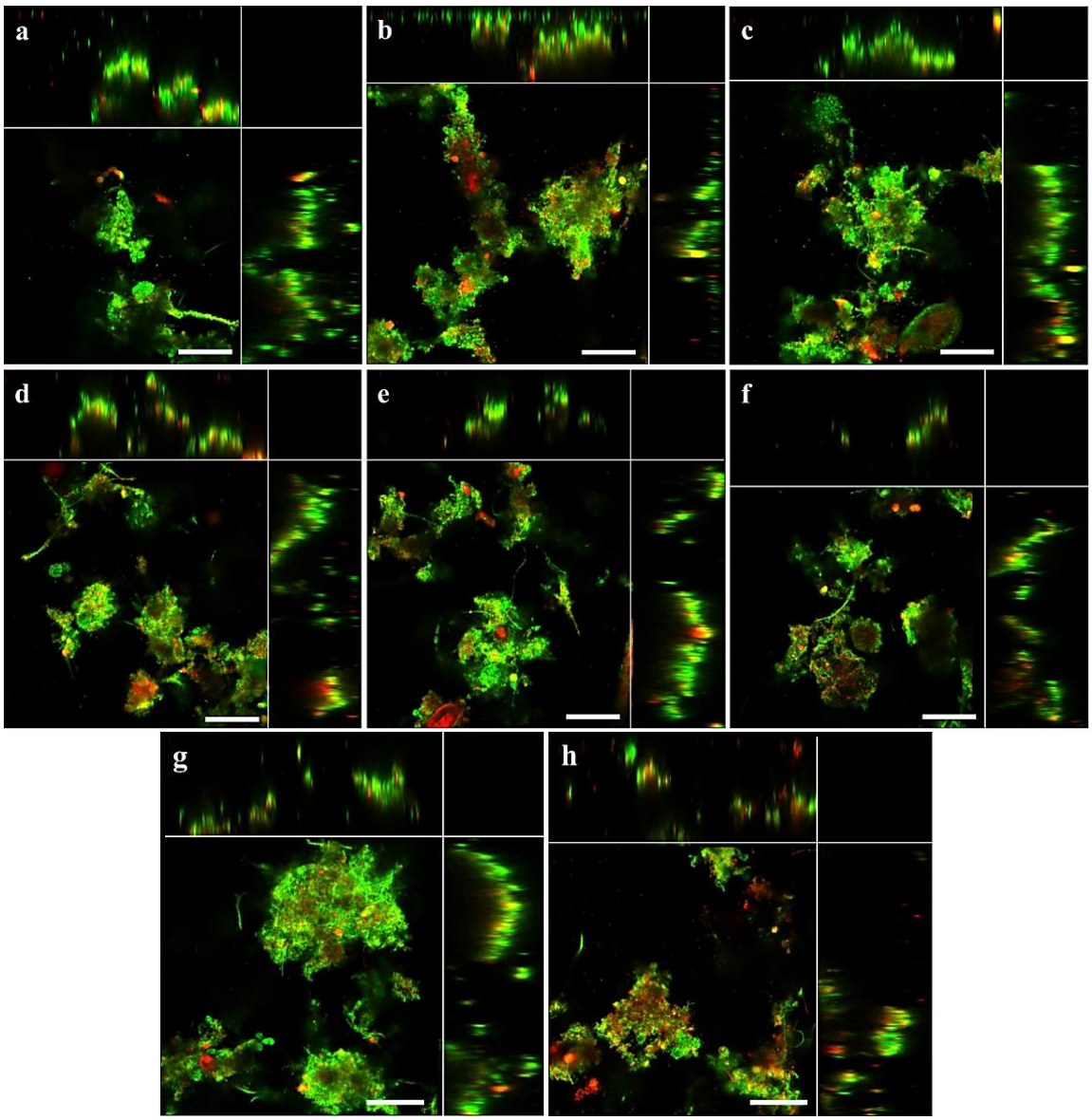

Figure 3.2: Confocal micrographs of Live/Dead stained sludge samples. (a) Untreated sludge (b) DMSO treated sludge (c to h) sludge treated with 5, 10, 20, 50, 100 and 200 mg L^{-1} of thiram. (Bar = 50 µm).

Quantification of fluorescence from the confocal micrographs revealed a higher percentage of live than dead sludge at 61.62 ± 0.04% and 38.38 ± 0.04%, respectively (Figure 3.3). The addition of various concentrations of thiram did not affect the viability of the sludge as there was an average of 59.68 ± 2.97% live and 40.32 ± 2.97% dead sludge (Figure 3.3). There was no significant differences in the ratio of live and dead cells

between untreated, DMSO treated and thiram treated sludge samples. The ratio of live sludge was significantly higher than the dead sludge in all untreated, DMSO treated and thiram treated sludge.

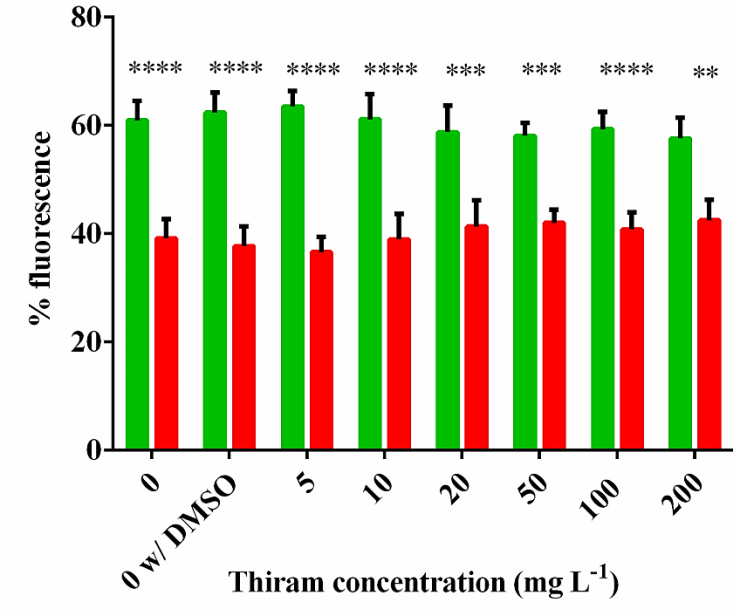

Figure 3.3: Quantification of Live/Dead stained sludge untreated or treated with thiram. ANOVA analysis showed that the quantity of live sludge (green bars) was significantly higher than the dead sludge (red bars) in all sludge samples. Error bars represent standard deviations (n = 3). **, *** and **** denote significant differences (One-way ANOVA: *P*-value ≤ 0.01, 0.001 and 0.0001, respectively).

Observations of the floccular sludge using light microscopy also showed that the untreated sludge, DMSO contol sludge or sludge treated with up to 20 mg L^{-1} of thiram did not show an increase in suspended bacteria (Figure 3.4a to c). In contrast, floccular sludge that was treated with thiram concentrations above 50 mg L^{-1} showed an increase in suspended bacteria (Figure 3.4d), which were likely to be bacteria that dispersed from the floccular sludge after 72 h. Although thiram concentrations of 20 mg L^{-1} showed some inhibition effect on nitrogen removal, it was selected for treatment of floccular sludge in

the mSBRs during aerobic granulation, as this concentration demonstrated the greatest inhibition or killing effect against protozoa while preserving the viability of bacteria.

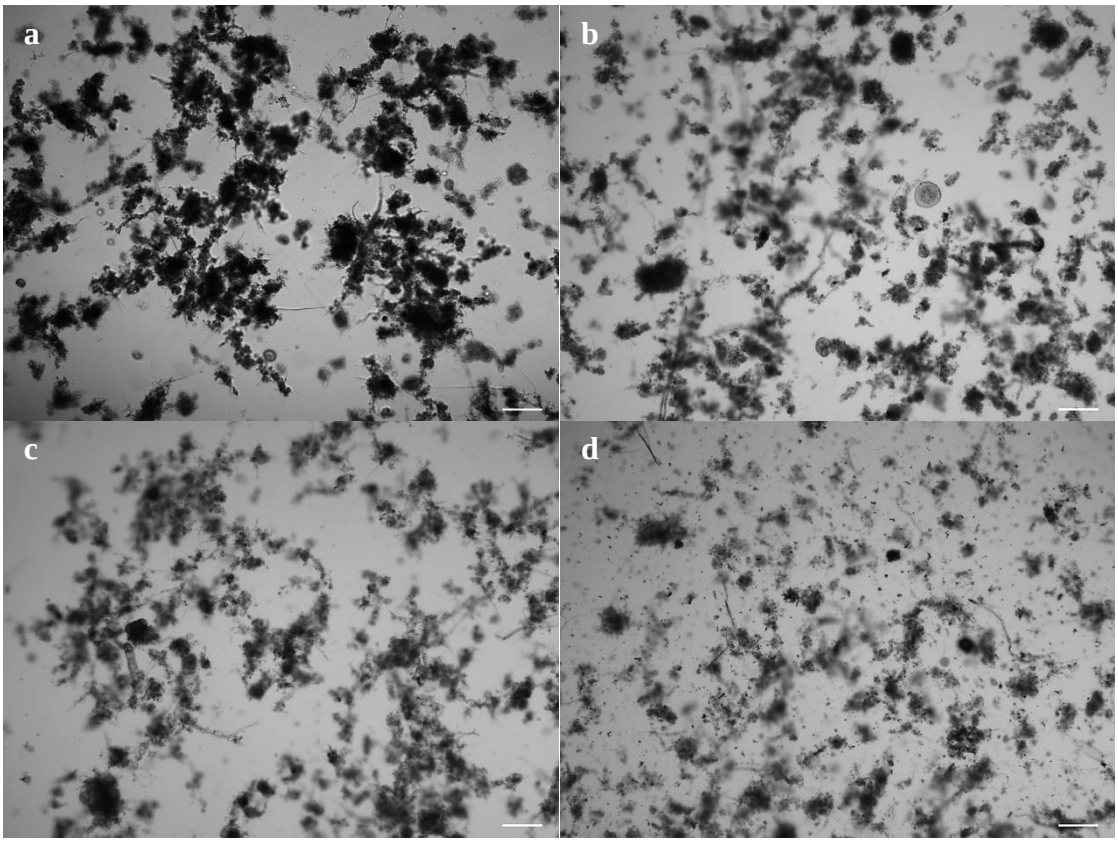

Figure 3.4: Micrographs of untreated and treated floccular sludge after 72 h incubation. (a) Untreated (b) DMSO treated (c) thiram treatment at 20 and (d) 200 mg L^{-1}.

3.3.2. Thiram concentration for treatment of granular sludge

Protozoa in the untreated and DMSO treated sludge were present at a density of 1369 ± 347 and 1125 ± 276 cells mL^{-1}, respectively (Figure 3.5a). No protozoa were observed in the sludge that was treated with 5, 50, 100 and 200 mg L^{-1} of thiram (Figure 3.5a). Although 5 mg L^{-1} of thiram was effective in inhibiting protozoa, inhibition was more effective at the higher concentrations of 10 and 20 mg L^{-1} as protozoa were present at densities of 94.44 ± 38.69 and 286.11 ± 259.12, respectively (Figure 3.5a). There were no significant differences in the number of protozoa between the untreated and DMSO

treated sludge (Figure 3.5a). However, the protozoan numbers were significantly higher in the untreated and DMSO treated sludge than thiram treated sludge.

The untreated and DMSO treated sludge showed 100% efficiency in ammonia removal. Granular sludge treated with 5 mg L^{-1} of thiram demonstrated a 99.06 ± 1.33% ammonia removal (Figure 3.5b). The increase in thiram from 10 to 20 mg L^{-1} resulted in a decline in ammonia removal efficiency to 87.50 ± 5.17 and 75.33± 2.12%, respectively (Figure 3.5b). Higher concentrations of thiram further reduced the ammonia removal efficiency to 54.93 ± 8.66 - 47.03 ± 9.23% (Figure 3.5b). Hence, sludge treated with 20 mg L^{-1} or more of thiram had significantly lower ammonia removal than untreated and DMSO treated sludge (Figure 3.5b).

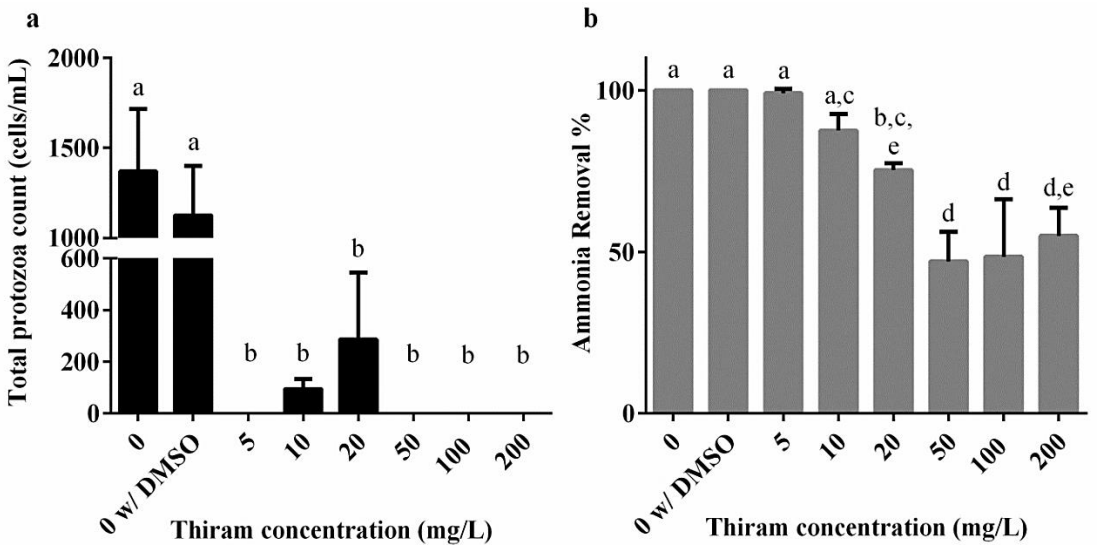

Figure 3.5: Optimization of thiram concentration for granular sludge treatment. (a) Total protozoa from granular sludge. Significance values of comparisons between each group can be found in Table A3.3 (b) Efficiency of ammonia removal from floccular sludge. Significance values of comparisons between each group can be found in Table A3.4. Different letters indicate significant differences between groups based on one-way ANOVA. Error bars represent standard deviations (n = 3).

Granular sludge samples were stained with Live/Dead Cell kit to determine the ratio of live and dead cells. Confocal micrographs of untreated, DMSO treated and sludge treated with 5, 10 and 20 mg L^{-1} of thiram showed that the viability of the sludge did not differ (Figure 3.6a to e). In contrast, sludge treated with 50 to 200 mg L^{-1} had relatively higher ratio of red fluorescence which indicated that these concentrations of thiram were toxic to the sludge biomass (Figure 3.6f - h).

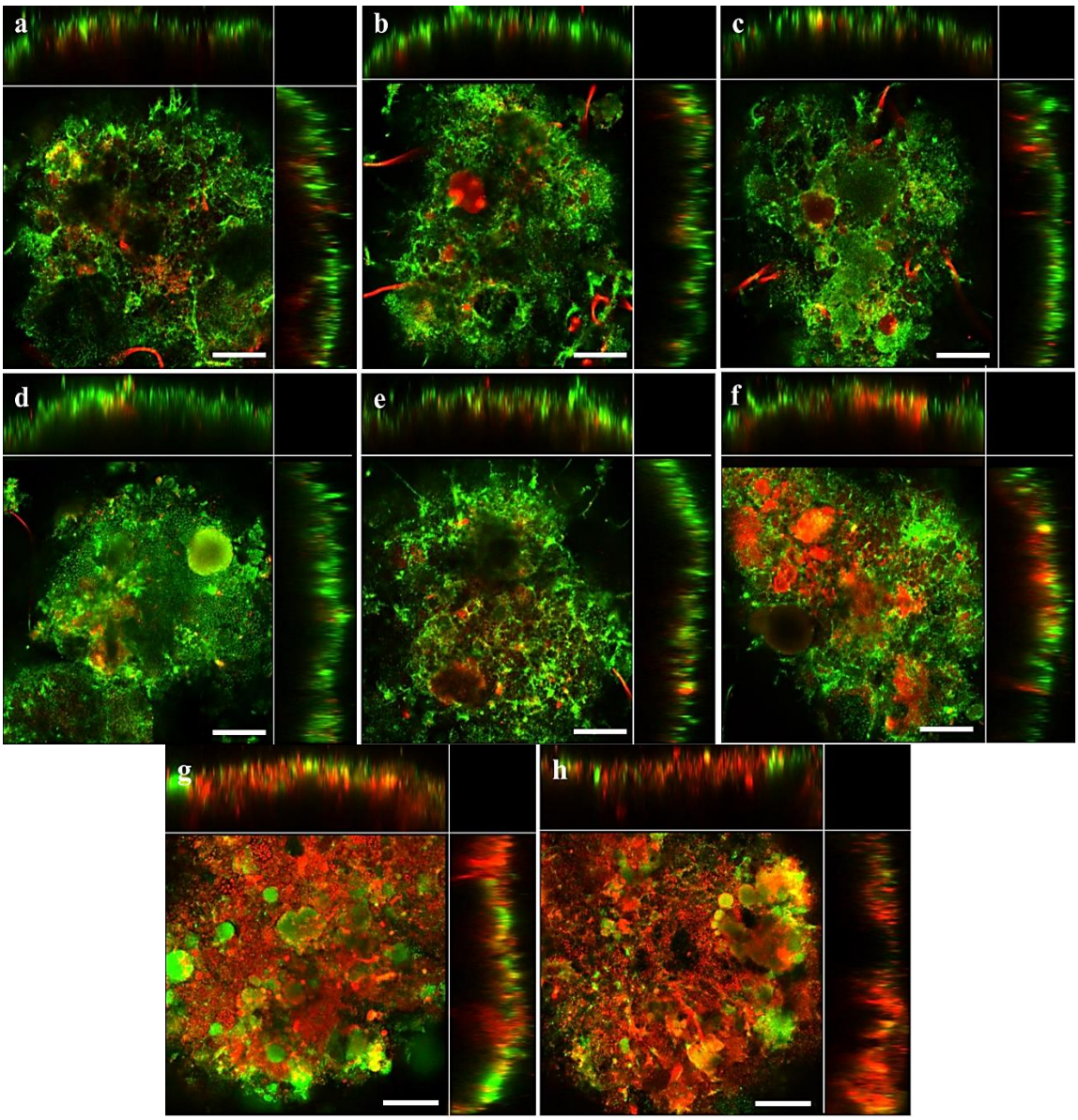

Figure 3.6: Confocal micrographs of Live/Dead stained sludge samples. (a) Untreated sludge (b) DMSO treated sludge (c to h) sludge treated with 5, 10, 20, 50, 100 and 200 mg L^{-1} of thiram, respectively. (Bar = 50 µm).

Quantification of fluorescence from the confocal micrographs showed that there was a higher percentage of live (63.63 ± 3.36%) than dead sludge (36.37 ± 3.33%) in the untreated sludge (Figure 3.7). Similarly, there was 64.87 ± 1.75% live sludge and 35.13 ± 1.78% dead sludge in the DMSO treated sludge (Figure 3.7). On average, there was 62.29 ± 4.13% of live sludge and 37.31 ± 4.13% of dead sludge in the sludge biomass treated with 5, 10 or 20 mg L^{-1} thiram, respectively (Figure 3.7). In contrast, there was an average of 42.93 ± 6.29% of live sludge in sludge samples treated with 50 mg L^{-1} or more of thiram (Figure 3.7). The percentage of dead sludge was significantly higher in the sludge samples treated with 200 mg L^{-1} (58.33 ± 1.76%).

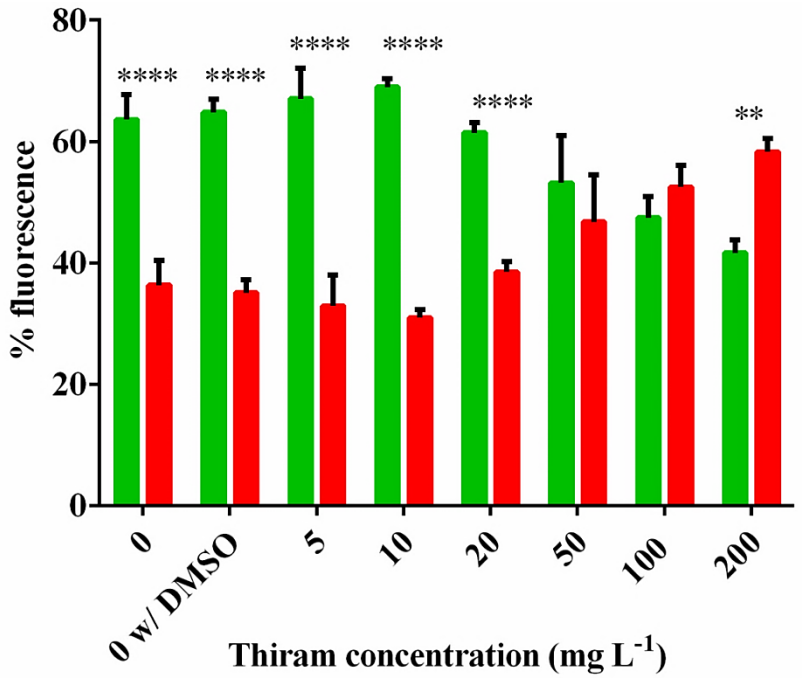

Figure 3.7: Quantification of Live/Dead stained sludge untreated or treated with thiram. ANOVA analysis showed that the quantity of live sludge (green bars) was significantly higher than the dead sludge (red bars) in all sludge samples. Error bars represent standard deviations (n =3). ** and **** denote significant differences (One-way ANOVA, *P*-value ≤ 0.01 and 0.0001, respectively).

Observations of the granular floccular sludge by light microscopy also showed that the untreated sludge, DMSO treated or treated with 5 mg L^{-1} of thiram did not show a significant increase in suspended bacteria (Figure 3.8a to c). In contrast, granular sludge that was treated with concentrations of thiram above 10 mg L^{-1} had an increase in suspended bacteria (Figure 3.8d to h). These suspended bacteria were likely to be dispersed bacteria from the granular sludge. Hence, the concentration of 5 mg L^{-1} was selected to treat the granular sludge in the mSBRs.

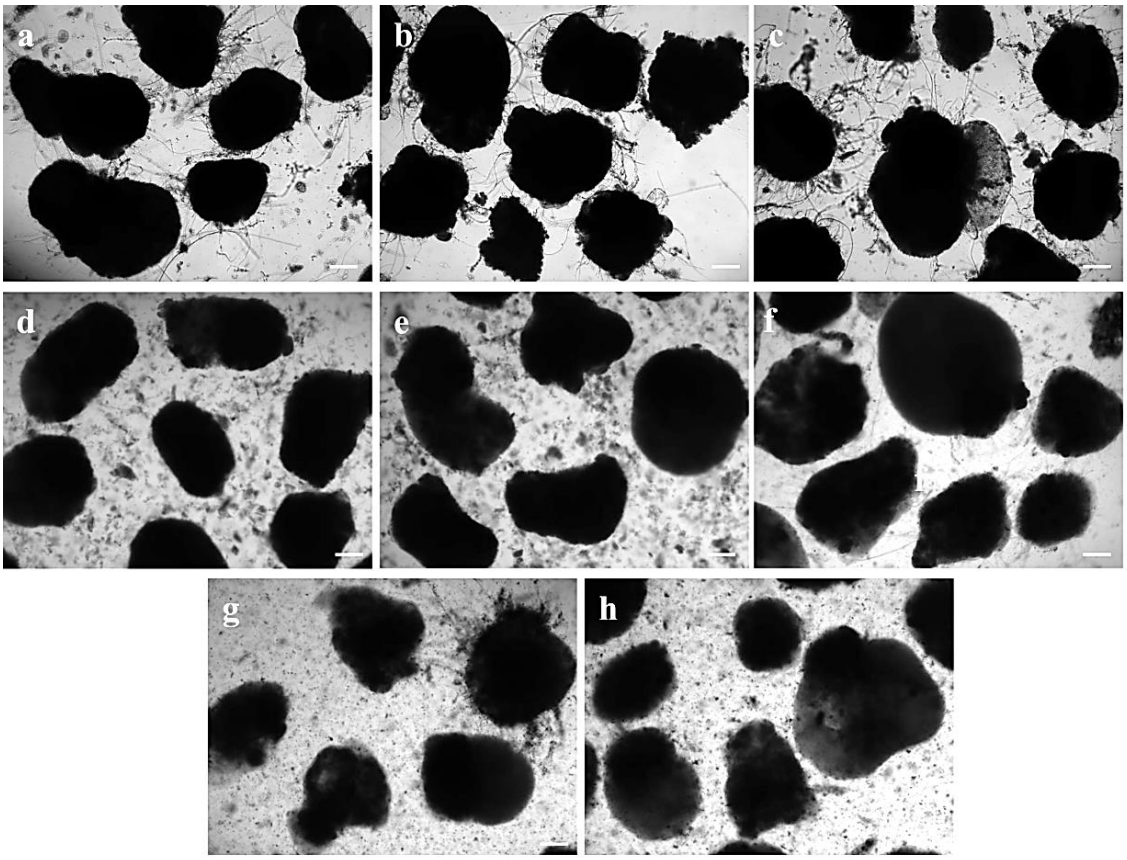

Figure 3.8: Micrographs of untreated and treated floccular sludge after 72 h incubation. (a) Untreated, (b) DMSO treated and (c) thiram treated at: (d) 5, (e) 10, (f) 20, (g) 50, 100 or (h) 200 mg L^{-1} (Bar = 200 µm).

3.3.3. Effectiveness of thiram inhibition of protozoa in floccular sludge

Six mSBRs were seeded with activated floccular sludge and operated under conditions optimal for the aerobic granulation process over a period of 8 weeks. To investigate the role of protozoan predation in aerobic granulation, protozoa were removed from the floccular sludge by the addition of thiram to the mSBRs and DMSO was added as a control. The effectiveness of thiram treatment was determined by comparing the total number of active protozoa in both control and thiram treated sludge. The seed sludge had approximately 5800 ± 816 cells mL^{-1} of protozoa (Figure 3.9a) and was dominated by sessile and crawling ciliates (Figure 3.9b). Both sessile and crawling ciliates were frequently found on the surfaces of flocs. Sessile ciliates feed on suspended bacteria while crawling ciliates slough off the surfaces of flocs to feed on loosely attached bacteria. Metazoa such as rotifers and gastrotrichs which predate on bacteria were also present at relatively low abundances (Figure 3.9b). At week 1, the control sludge had 3667 ± 554 cells mL^{-1} protozoa, while no protozoa were observed in the treated sludge (Figure 3.9a). Classification of the observed protozoa indicated that sessile ciliates, crawling ciliates, amoeba and rotifers were the most dominant at week 1. There were no protozoa observed in the treated sludge of any of the remaining weeks. From weeks 1 to 8, the control sludge had a protozoa density of 1455 ± 1023 to 2577 ± 632 cells mL^{-1} (Figure 3.9a). The relative abundance of the crawling ciliates continued to fluctuate from week 1 to 6 before declining sharply from week 7 onwards (Figure 3.9b). In contrast, sessile ciliates continuously increased in relative abundance from week 5 onwards. Amoeba with hard-shells (testate amoeba) were consistently present from weeks 1 to 8. Overall, the absence of protozoa in the treated sludge showed that the thiram treatment was effective in removing protozoa.

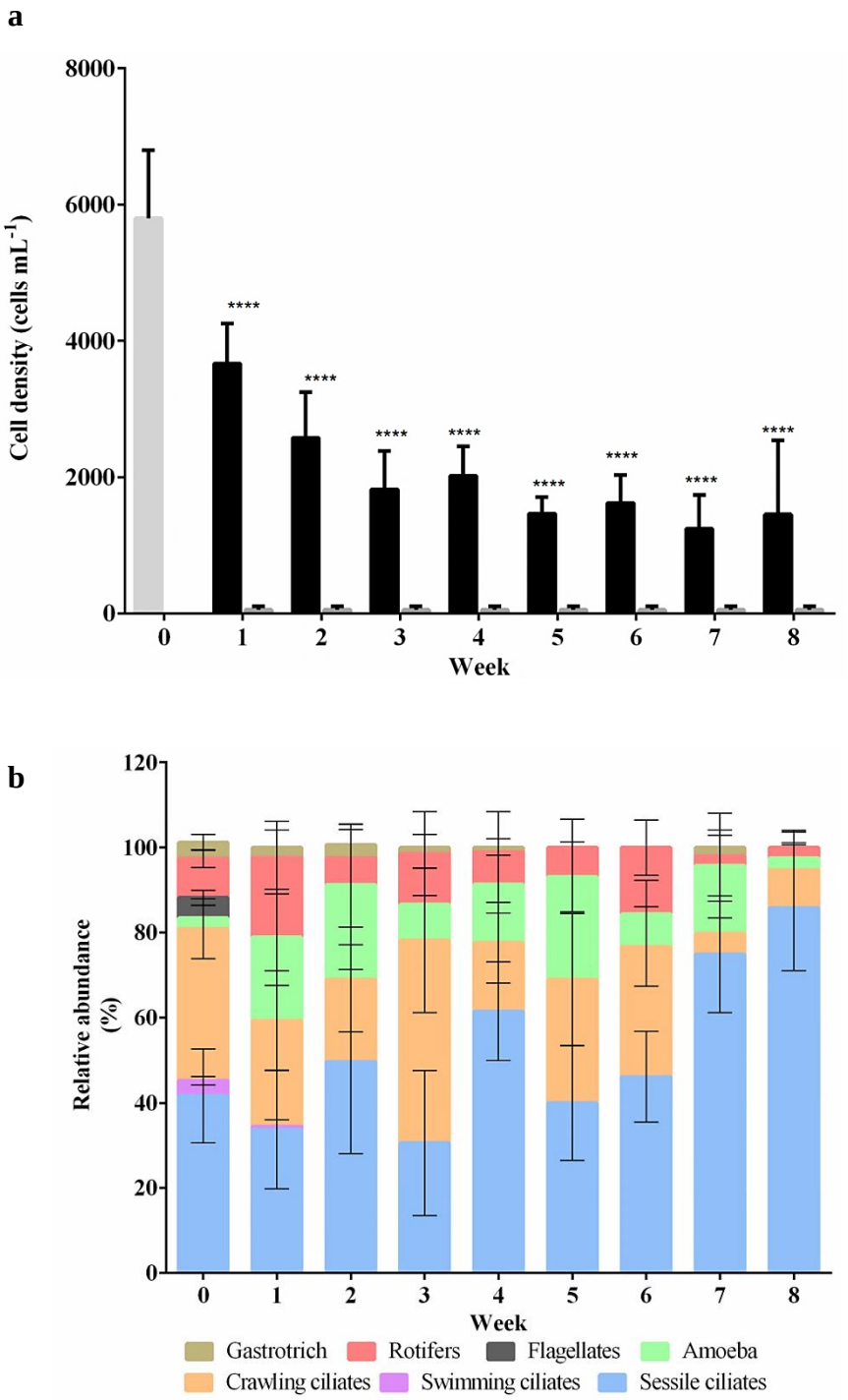

Figure 3.9: Total protozoa in floccular sludge. (a) Total protozoan density in seed (light grey), control (black) and treated (dark grey) floccular sludge. (b) Types of predators observed in seed (week 0) and control sludge (weeks 1 to 8). No protozoa was detected in the treated sludge. Error bars represent standard deviations (n = 2). **** denotes significant differences (One-way ANOVA: P-value $\leq$ 0.0001).

3.3.4. Development of aerobic granules from untreated and thiram treated floccular sludge

Microscopic observations of control floccular sludge indicated that the conversion of floccular into granular sludge began at week 4 (Figure 3.10a). Compact aggregates were observed in the initiation phase and these aggregates continued to expand in size. The sludge entered the maturation phase at week 6 and remained in this phase until week 8 (Figure 3.10a). In contrast, thiram treated sludge did not initiate granulation until week 6 and started to mature by week 8 (Figure 3.10b).

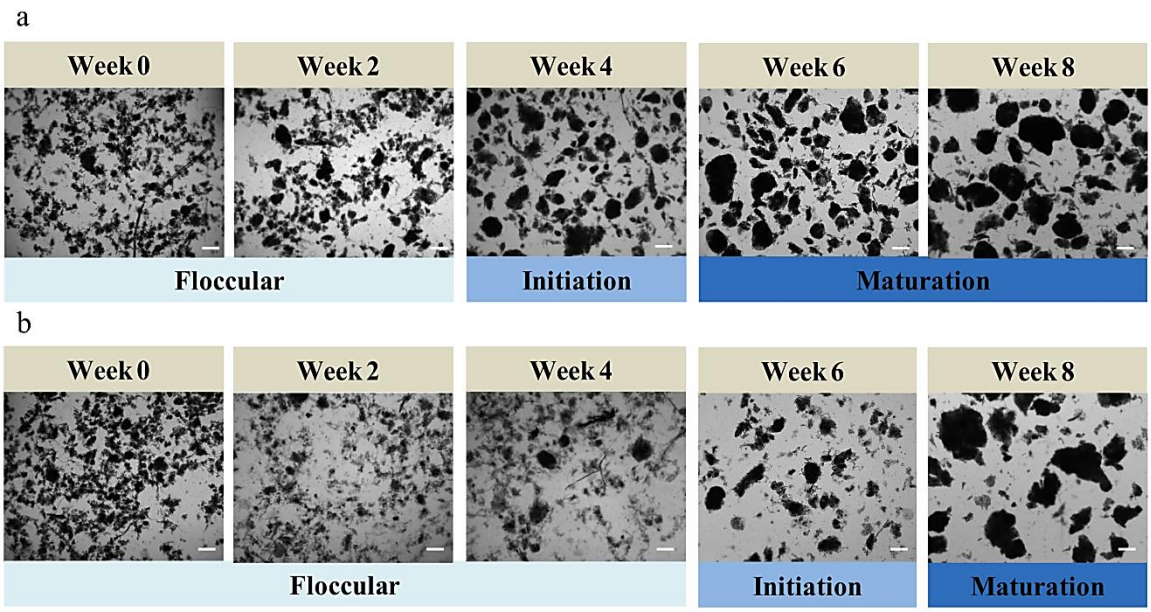

Figure 3.10: Development of granules from untreated and thiram treated floccular sludge. (a) Control floccular sludge (b) floccular sludge treated with 20 mg L^{-1} of thiram. Magnification x 40 (Bar, 200 µm).

Micrographs of sludge were also quantified using ImageJ to obtain the mean sludge particle size, which was 84.36 ± 12.41 µm (Figure 3.11a). By week 2, the control sludge mean particle size was 89.61 ± 5.94 µm, while the treated sludge was 67.02 ± 2.65 µm, which was significantly smaller than the control sludge (Figure 3.11a). By week 7, the particle size of the treated sludge was 125.42 ± 10.60 µm, which was similar to the size of the the control sludge particles, 122.71 ± 23.00 µm (Figure 3.11a). By week 8, there was a slight decrease in the particle size of the control sludge (104.60 ± 17.57 µm) while the thiram treated sludge particle size (119.36 µm ± 6.05 µm) was significantly larger (Figure 3.11a).

The sludge volumetric index (SVI_5) of the treated sludge was significantly higher than the control sludge from weeks 2 to 4 (Figure 3.11b). This suggested that the treated sludge was less dense and compact, hence required a longer settling time compared to the control sludge. However, from week 5 onwards, the SVI_5 for the treated sludge decreased and was not significantly different from the control sludge. The low SVI_5 indicated that the density of both control and treated sludge had increased, resulting in a shorter settling time. The sludge biomass was determined using measures of both MLSS and VSS, where the MLSS represented the total biomass and VSS represented the total organic biomass (Figure 3.11c and d). The MLSS of the control sludge showed gradual increases from week 1 whereas the treated sludge MLSS was decreasing from week 1 (Figure 3.11b). The loss of biomass in the treated sludge could be attributed to the slower expansion rate of flocs into larger aggregates (Figure 3.11a). Hence, the smaller flocs in the treated sludge were discharged from the mSBRs as the settling time was reduced over time to induce for granulation. Once granulation was initiated in the treated sludge at week 6, the MLSS continued to increase from weeks 6 to 8 (Figure 3.11c). The VSS of both control and treated sludge displayed a similar trend as the MLSS of both sludge (Figure 3.11d).

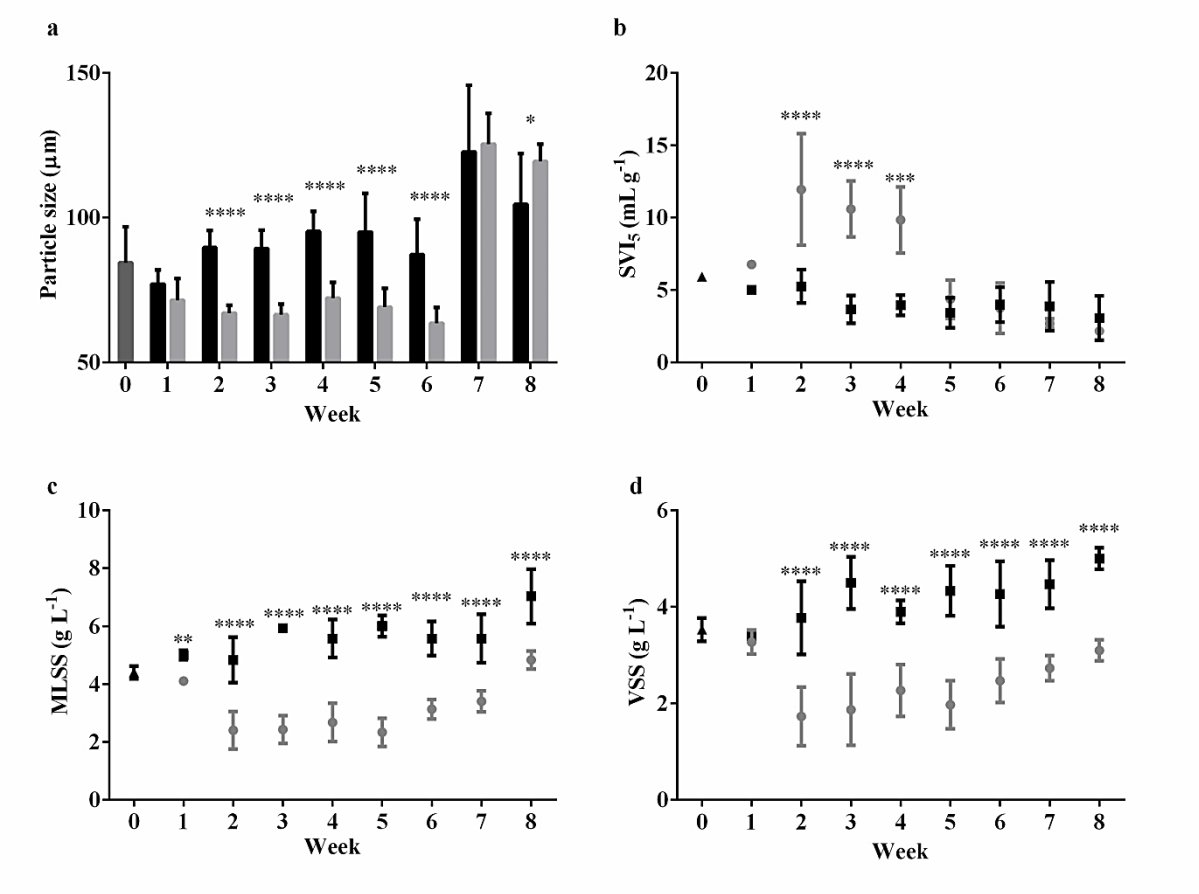

Figure 3.11: Analysis and measurement of floccular sludge during aerobic granulation. (a) Mean particle size of seed (dark grey, Week 0), control (black) and treated sludge (light grey) over 8 weeks. (b) Sludge volumetric index of seed (black triangle), control (black square) and treated (grey circle) sludge. (c) Mean mixed liquor suspended solids (MLSS) of seed (black triangle), control (black square) and treated (grey circle) sludge. (d) Mean volatile suspended solids (VSS) of seed (black triangle), control (black square) and treated (grey circle) sludge. Error bars represent standard deviation (n = 3) *, **, *** and **** denote significant differences (One-way ANOVA: *P*-value ≤ 0.05, 0.01, 0.001 and 0.0001, respectively).

Live-dead staining was also performed on the sludge to assess the viability of both untreated and treated sludge. The ratio of green (live) and red (dead) fluorescence ranged from 1.50 ± 0.40 to 2.49 ± 0.58 and 1.92 ± 0.58 to 2.76 ± 0.59 in the control and thiram treated sludge, respectively (Figure 3.12). This indicated that the majority of the bacterial cells were viable in both sludge types.

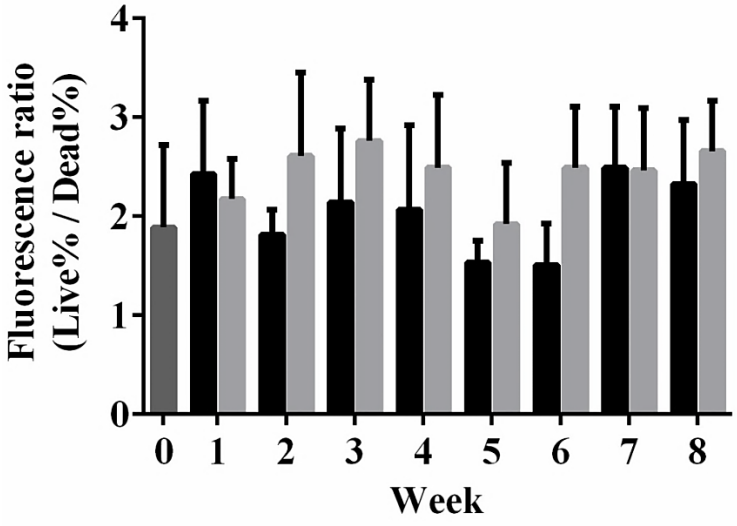

Figure 3.12: Fluorescence ratio of the Live/Dead staining for both control and treated sludge. The ratio was determined by the division of the fluorescence percentage of live cells against fluorescence percentage of dead cells. Error bars represent standard deviations (n = 3).

As the sludge was operated for SNDPR, the nutrient removal profiles for the control and treated sludge were also determined. The efficiency of phosphate removal was 75.05 ± 1.63% for the control sludge, which was significantly higher than that of the treated sludge with a removal efficiency of 10.79 ± 5.23% (Figure 3.13a). Phosphate removal in the control sludge continued to decrease and had a low removal efficiency of 11.67 ± 6.26%, at week 3 (Figure 3.13a), which was similar to the removal efficiency of the treated sludge. The removal efficiency for the control sludge improved at week 4 and was

maintained between 29.04 ± 15.76 and 53.64 ± 10.18% until week 8 (Figure 3.13a). The efficiency of phosphate removal in the treated sludge improved gradually from week 4 to 8. By week 8, phosphate removal in the treated sludge was significantly higher (72.69 ± 26.56%) than for the control sludge (Figure 3.13a). Nitrogen removal in the control sludge was between 44.06 ± 5.66 and 54.60 ± 6.03% from week 1 to 3 (Figure 3.13b). Nitrogen removal of the treated sludge was between 60.40 ± 2.32 and 67.06 ± 2.22% for weeks 1 to 3 (Figure 3.13b). Nitrogen removal was significantly higher in the treated sludge than the control sludge in week 3. From week 4 onwards, nitrogen removal was between 41.18 ± 7.68 and 60.63 ± 1.81% in the control sludge and were significantly lower than for the treated sludge for weeks 5, 7 and 8.

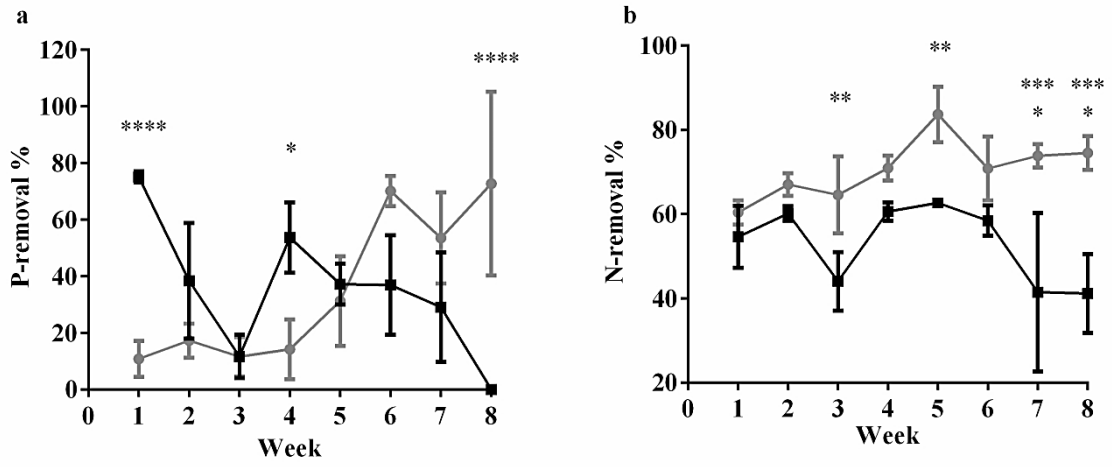

Figure 3.13: Nutrient removal profiles for control and treated sludge. (a) Percentage of total phosphate removed from wastewater by control (black) and treated (grey) sludge. (b) Percentage of total nitrogen removal from wastewater by control (black) and treated (grey) sludge. Error bars represent standard deviations (n=3). *, ** and **** denote significant differences (One-way ANOVA: *P*-value = 0.05, 0.01 and 0.0001, respectively).

3.3.5. Analysis of microbial communities in floccular control and treated sludges

3.3.5.1. Ribotagger analysis of 16S and 18S rRNA genes from sludge

The communities in the two sludge types were compared by metacommunity based sequencing of the V5 region of the 16S and 18S rRNA genes using the Ribotagger method (Xie et al. 2016). Sequencing reads numbered between 55289 ± 2401 and 74603 ± 4541 for the control sludge from week 0 to 8 (Table 3.1). An average of 48843 ± 5185 to 59381 ± 8941 sequencing reads was obtained from the treated sludge (Table 3.1). In both control and treated sludge, bacteria accounted for the majority of the sequencing reads. The number of eukaryotic sequencing reads from the control sludge was generally higher than in the treated sludge (Table 3.1). This was probably due to the inhibitory effect of thiram on protozoa. Each control and treated sludge dataset had 72 OTUs representing all eukaryotic reads. Both Archaea and Unidentified reads were not considered for further analysis in this Chapter.

Table 3.1: Mean sum and percentage of Bacteria, Eukarya, Archaea and Unidentified sequencing reads

Control					
Week	Mean Sum of Reads	% Bacteria	% Eukarya	% Archaea	% Unidentified
0	59381 ± 8941	36.50 ± 0.73	26.55 ± 0.71	0.10 ± 0.001	36.84 ± 0.013
1	74603 ± 4541	67.73 ± 4.09	7.56 ± 2.73	0.09 ± 0.02	24.62 ± 1.49
2	68569 ± 5086	80.89 ± 0.64	2.45 ± 0.47	0.06 ± 0.003	16.60 ± 0.52
3	60208 ± 7180	81.99 ± 1.77	1.75 ± 0.70	0.04 ± 0.01	16.22 ± 1.33
4	61126 ± 2491	80.43 ± 3.51	1.59 ± 0.84	0.03 ± 0.006	17.95 ± 2.90
5	61176 ± 1563	81.12 ± 2.19	0.92 ± 0.28	0.02 ± 0.004	17.94 ± 2.07
6	58875 ± 3082	82.46 ± 1.09	1.31 ± 0.67	0.02 ± 0.007	16.22 ± 1.04
7	56871 ± 3627	83.94 ± 1.31	1.79 ± 0.97	0.01 ± 0.004	14.26 ± 1.15
8	55289 ± 2401	83.12 ± 2.31	2.64 ± 1.43	0.01 ±0.004	14.24 ± 1.68
Treated					
Week	Mean Sum of Reads	% Bacteria	% Eukarya	% Archaea	% Unidentified
0	59381 ± 8941	36.50 ± 0.73	26.55 ± 0.71	0.10 ± 0.001	36.84 ± 0.013
1	57989 ± 7263	86.21 ± 3.16	0.74 ± 0.28	0.17 ± 0.04	12.88 ± 2.84
2	52556 ± 6121	92.65 ± 0.52	0.27 ± 0.14	0.11 ± 0.005	6.97 ± 0.36
3	55945 ± 3700	93.97 ± 0.96	0.30 ± 0.34	0.05 ± 0.02	5.68 ± 0.81
4	54071 ± 3449	89.42 ± 3.36	0.92 ± 1.02	0.02 ± 0.003	9.64 ± 3.79
5	48843 ± 5185	88.21 ± 2.25	0.49 ± 0.42	0.01 ± 0.004	11.30 ± 2.25
6	53818 ± 2984	91.29 ± 2.56	0.25 ± 0.23	0.00	8.45 ± 2.67
7	50761 ± 919	92.21 ± 0.78	0.59 ± 0.29	0.00	7.20 ± 0.88
8	57230 ± 2565	92.30 ± 0.44	0.54 ± 0.29	0.00	7.15 ± 0.63

3.3.5.2. Analysis of the eukaryotic communities in control and treated sludge

The low percentage (< 1.0%) of eukaryotic sequencing reads associated with the thiram treatment indicated that eukaryotes in the treated sludge were inhibited compared to the control sludge (Table 3.1). The top 72 Eukarya OTUs were selected for principal component analysis (PCoA) to understand the effects of thiram on the eukaryotic communities. The similarities and dissimilarities were visualized with MDS plots (Figure

3.14) For Eukarya, there was a dissimilarity of 39.16% between the control and treated sludge (Figure 3.14). The divergence of all control and treated replicates from the seed sludge at week 0 indicated that the composition of the eukaryotic community changed over time (Figure 3.14). All control replicates showed close clustering for most weeks except for mSBR 2, which diverged during weeks 7 and 8 (Figure 3.14). Comparisons between control and treated replicates showed that all treated replicates clustered separately from the control replicates (Figure 3.14). Within the treated sludge, close clustering of the three replicates was observed during week 1, which subsequently diverged from each other until week 5. These three replicates started to converge from week 6 onwards which indicated that the eukaryotic communities could have been similar in composition (Figure 3.14). PERMANOVA analysis also indicated that the microbial communities were highly dissimilar due to thiram treatment ($Pr = 0.001$) and between weeks ($Pr = 0.001$). However, there were no dissimilarities between the replicates ($Pr = 0.16$).

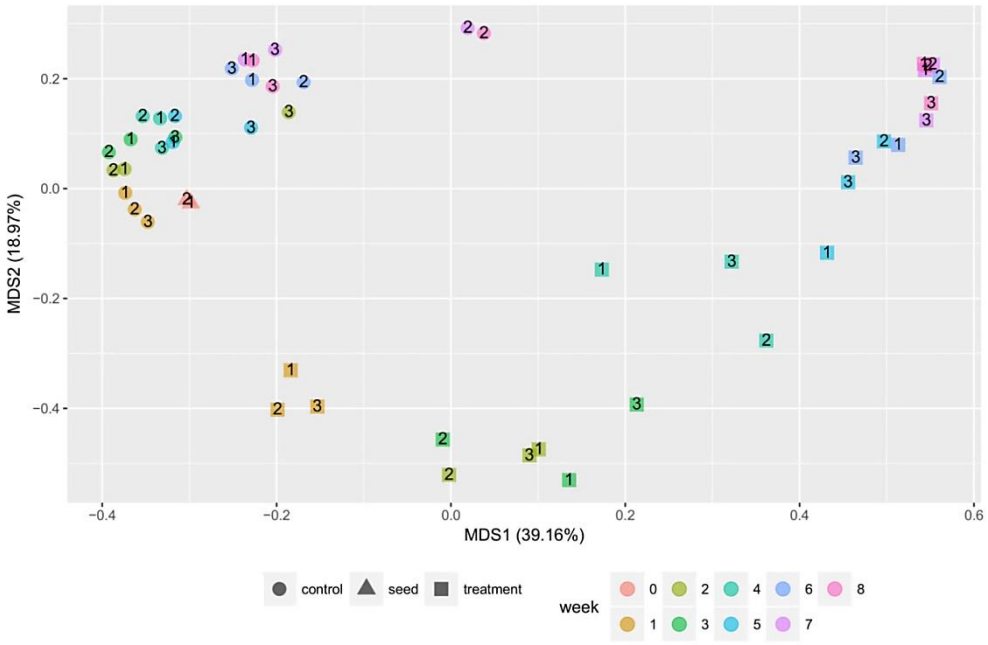

Figure 3.14: Multi-dimensional scaling (MDS) plots for principal component analysis of different groups of eukaryotic microorganisms in control and treated sludge during the aerobic granulation process. The data were transformed by the square root function for principal component analysis. The three factors used for analysis were weeks, replicates and treatment. Each symbol labelled 1 to 3 represents a replicate. Triangles, circles and squares represent the seed, control and treated sludge, respectively. Each week is represented by a unique colour.

There was a total of 59381 ± 8941 sequencing reads from the seed sludge at week 0, 26.55 ± 0.71% of which were of eukaryotic origin (Table 3.1). Within the seed sludge, the phyla *Ciliophora* and *Rotifera* were the most dominant (Figure 3.15a). The phylum *Ciliophora* consists of ciliated protozoa which are characterized by the presence of hair-like organelles known as cilia on their bodies. The phylum *Rotifera* consists of metazoan predators that predate on both bacteria and other small eukaryotes, including protozoa.

By week 1, 7.56 ± 2.73% of the total 74603 ± 4541 sequencing reads were from eukaryotes (Table 3.1). At week 1, the *Rotifera* started to decline while *Ciliophora*

continued to gain dominance over time (Figure 3.15a). Other less abundant eukaryotes in the seed sludge were from the class *Tubulinea* and the phylum of *Ochrophyta,* which are made up of amoeba and algae, respectively (Figure 3.15a). In addition, there was an increase in members of the phylum *Cercozoa* from weeks 1 to 6 and the phylum LKM 74 from Week 1 to 8 (Figure 3.15a). The phylum *Cercozoa* consists of flagellates and amoeba that feed by the constant retraction and extensions of their filamentous pseudopodia (Bass et al. 2009). The phylum LKM74 is an amoebozoan clade which has been recently characterized (Blandenier et al. 2017). By week 8, eukaryotes accounted for 2.64 ± 1.43% of the total 55289 ± 2401 sequencing reads with *Ciliophora* as the most dominant group (Table 3.15a). Within *Ciliophora,* there were four groups of ciliates that were dominant at week 0 (Figure 3.15b). The relative abundance of these ciliates was derived by dividing the number of sequencing reads of each unique OTU against the total number of *Ciliophora* sequencing reads. The most dominant group was the family of *Oligohymenophorea* which consists of a wide variety of swimming, crawling and sessile ciliates.

Other groups of ciliates were from the genus of *Paramecium* and *Carchesium,* which are swimming ciliates and sessile ciliates, respectively (Figure 3.15b). Swimming ciliates typically feed by swimming and intercepting their prey before ingestion. In contrast, sessile ciliates are attached onto surfaces and feed by creating feeding currents with oral cilia for ingestion of prey through their oral region. In the subsequent weeks, the family *Oligohymenophorea* continued to be the most dominant group in the control sludge (Figure 3.15b). There were other minor *Ciliophora* groups such as *Epistylis, Vorticella,* and *Telotrochidium,* which are sessile ciliates that grow on surfaces of flocs or granules (Figure 3.15b).

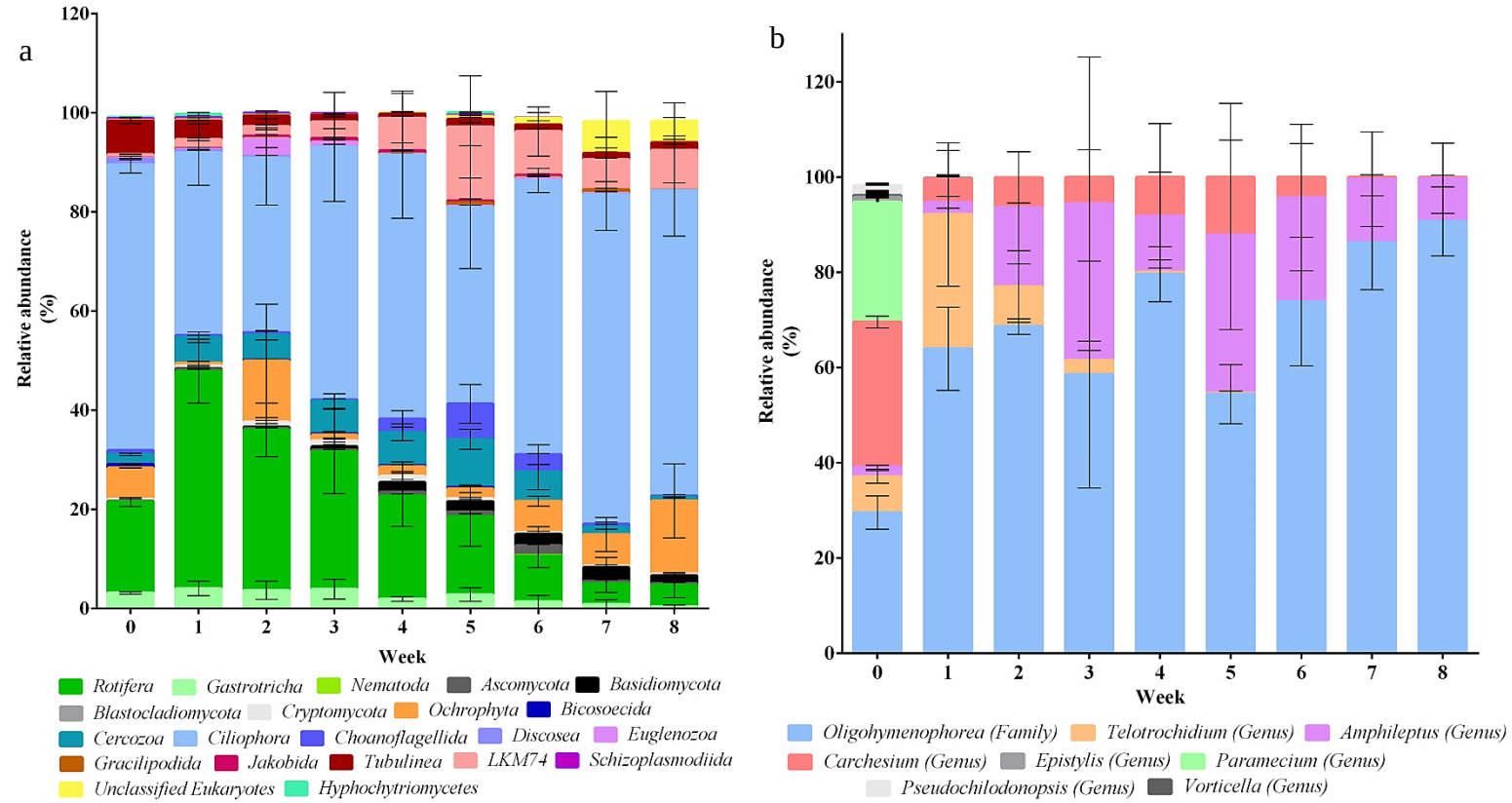

Figure 3.15: Relative abundance of eukaryotes in (a) control sludge and (b) the relative abundance of *Ciliophora* OTUs from the control sludge. A total of 72 OTUs were analyzed for the relative abundance of eukaryotes. The percentage of eukaryotic reads ranged between 0.92 and 7.56% from weeks 1 to 8 (Table 3.1). Error bars represent standard deviations (n = 3).

Members of the genus *Telotrochidium* were only present from weeks 1 to 3 where it increased in abundance from 0.25 ± 0.35 to 2.95 ± 3.32%. However, this genus was not observed from week 4 onwards. Another genera, *Amphileptus* was present during weeks 1 to 8 (Figure 3.15b) and consisted of pleurostomatid ciliates that can feed on sessile ciliates, particularly on the zooids which are essential for colonization of new surfaces and reproduction (Lin and Song 2004).

In contrast to the control sludge, the total number of sequencing reads from the treated sludge ranged from 48843 ± 5185 to 57989 ± 7263 with < 1% of eukaryotic origin. Unlike the *Ciliophora*-dominated control sludge, the treated sludge was dominated by members of the phylum of fungi, *Basidiomycota* from weeks 1 to 3 (Figure 3.16). Members of the phyla, *Cryptomycota* and *Ascomycota* were also present during these three weeks (Figure 3.16). The phylum *Ciliophora* was only observed from weeks 1, 3 and 4 at very low abundance. This indicated that the thiram treatment was highly effective in removing ciliated protozoan predators.

The phylum of *Rotifera* was also present with decreasing abundance from weeks 1 to 4 (Figure 3.16). From weeks 4 to 5, the class of amoeba, *Tubulinea* was found to be the dominant group in the sludge microbial community (Figure 3.16). However, subsequent weeks showed that the percentage of *Tubulinea* reads had decreased, while members of the phyla of algae, *Ochrophyta* and *Unclassified Eukarya* had increased (Figure 3.16).

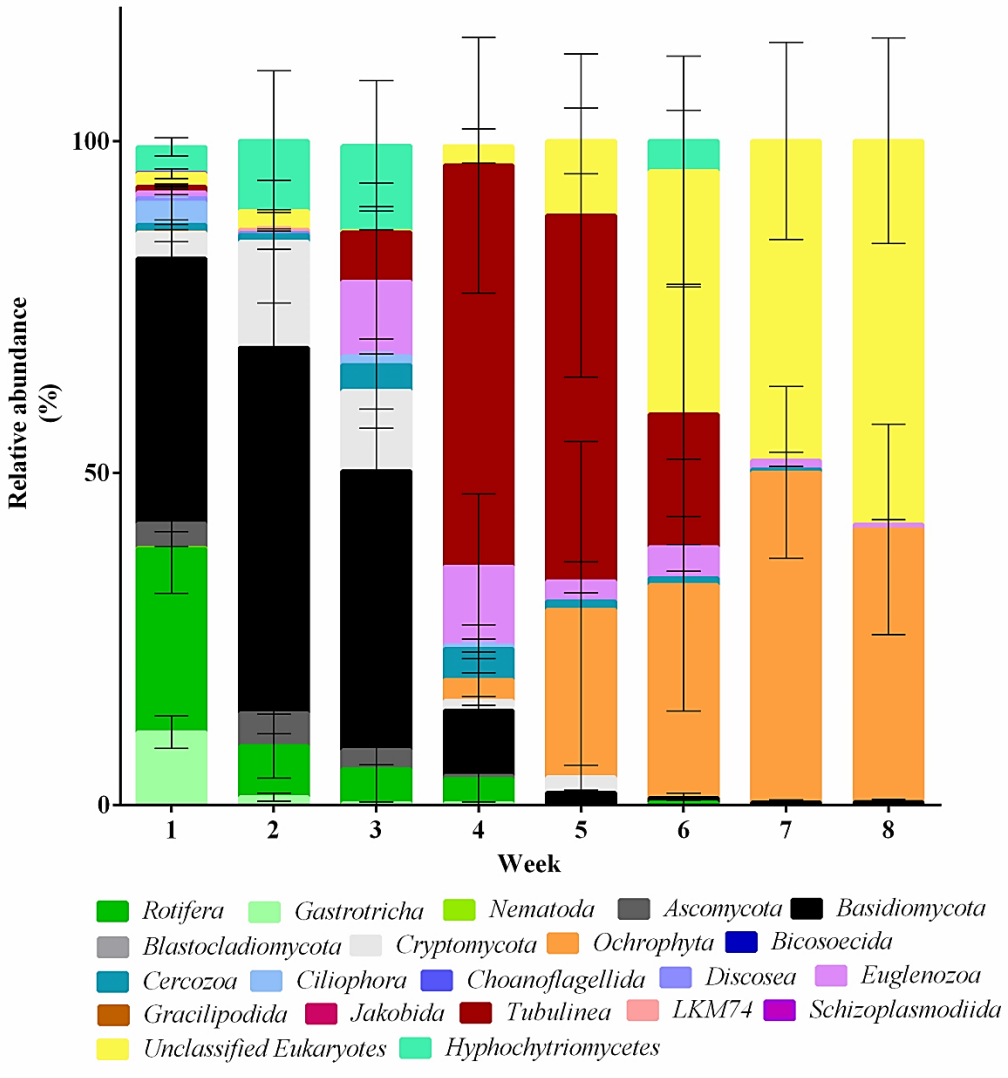

Figure 3.16: Relative abundance of eukaryotes in the treated sludge**.** A total of 72 OTUs which represented all eukaryotic reads were analyzed for the relative abundance of eukaryotes. The number of eukaryotic reads was less than 1% in the entire sequencing dataset from weeks 1 to 8 (Table 3.1). Error bars represent standard deviations (n = 3).

3.3.5.3. Analysis of bacterial communities in control and treated sludge

As thiram was effective in removing most protozoan predators and eukaryotes, it was important to investigate if the absence of protozoan predators and changes in eukaryotic communities had an impact on bacterial communities. Based on the MDS plot for the bacterial communities, there was a dissimilarity of 52.79% between the control and

treated sludge in all mSBRs (Figure 3.17). Based on PERMANOVA analysis, bacterial communities were significantly dissimilar between weeks (Pr = 0.001) and treatment (Pr = 0.001) but not between mSBRs (Pr = 0.16). This suggested that the absence of protozoan predators and eukaryotes correlated with a shift of the bacterial community composition during aerobic granulation.

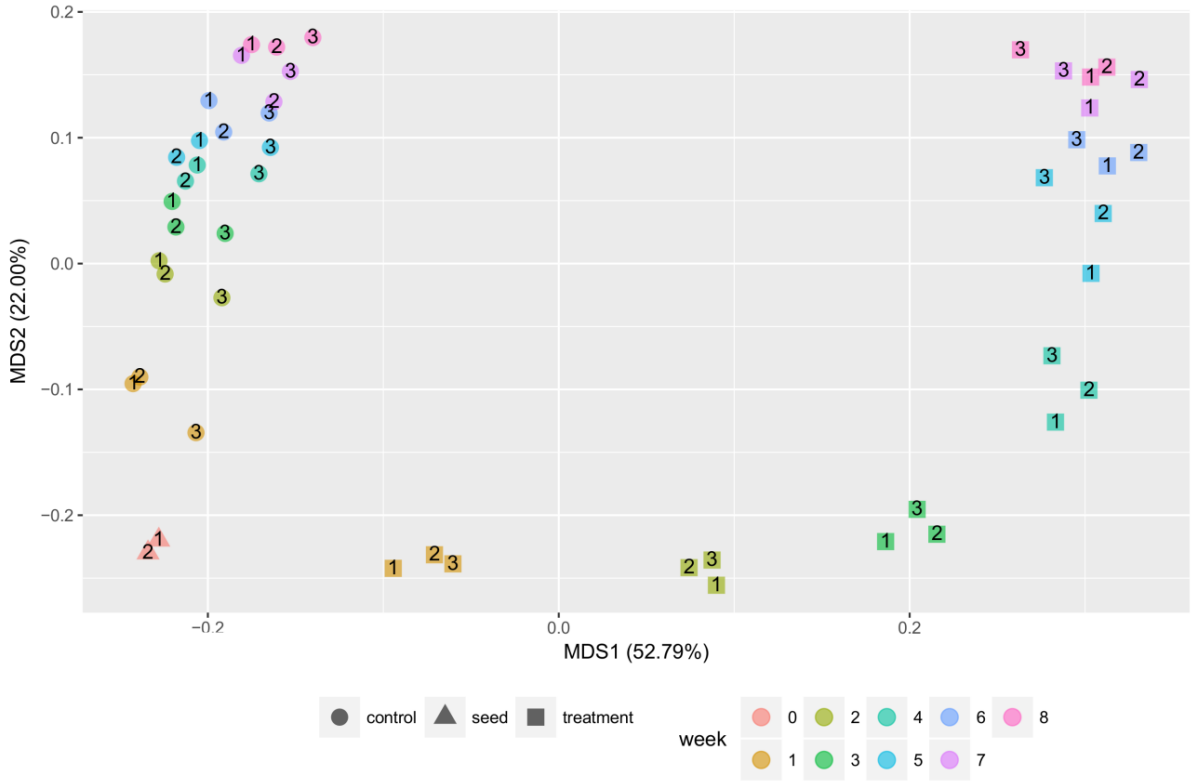

Figure 3.17: Multi-dimensional scaling (MDS) plots for principal component analysis of different groups of bacteria in control and treated sludge during aerobic granulation process. The data were transformed by the square root function for principal component analysis. The three factors used for analysis were weeks, replicates and treatment. Each symbol labelled 1 to 3 represents a replicate. Triangles, circles and squares represent the seed, control and treated sludge, respectively. Each week was represented by a unique colour.

To determine the differences in the bacterial communities of the control and treated sludge, the top 400 OTUs representing 90 to 95% of the bacterial reads were analyzed. The phylum *Proteobacteria* was the most dominant group in seed, control and treated sludge (Figure 3.18a and b) and accounted for an average of 69.95 ± 0.05, 81.35 ± 4.86and 91.52 ± 3.02% in seed, control and treated sludge, respectively (Figure 3.18a and b).

In addition to *Proteobacteria*, members of the *Acidobacteria, Actinobacteria, Bacteriodetes, Chloroflexi, Firmicutes, Nitrospira, Planctomycetes, Spirochaetes* and *Verrucomicrobia* were also present (Figure 3.19a). These non-*Proteobacteria* reads accounted for 20-30% of the bacterial community in the seed and control sludge. Although the thiram treated sludge was also dominated by *Proteobacteria*, non-*Proteobacteria* reads accounted for <10% of the community, and were primarily *Actinobacteria, Bacteriodetes, Chloroflexi, Nitrospira*, and *Planctomycetes* (Figure 3.18b).

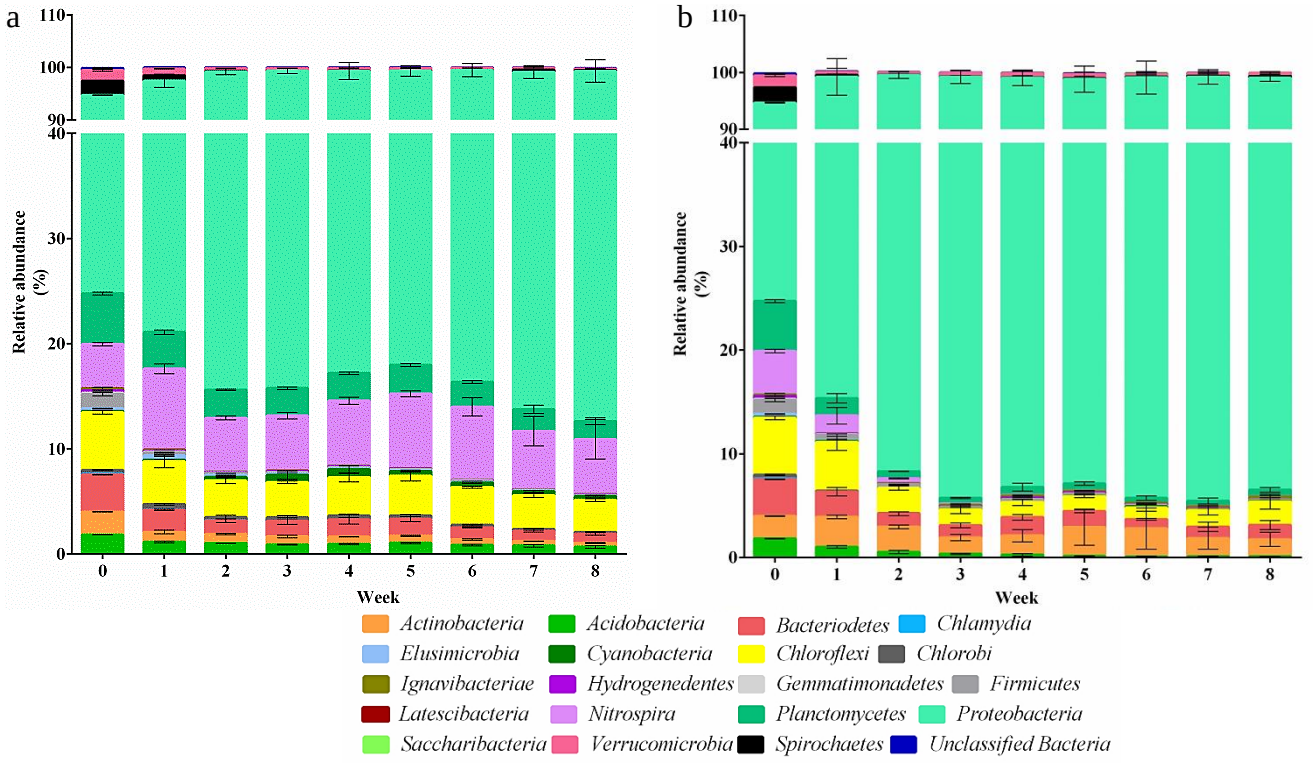

Figure 3.18: Relative abundance of the dominant bacteria groups in (a) seed, control and (b) treated sludge. A total of 400 OTUs were selected from each SBR which represented approximately 90 to 95% of the bacterial sequencing reads. Error bars represent standard deviations (n = 3).

Profiling of the *Proteobacteria* OTUs showed significant differences between the bacterial communities for the seed, control and treated sludge. The two core groups of bacteria, *Candidatus Accumulibacter* and *Candidatus Competibacter* accounted for only 13.11 ± 0.62 and 9.39 ± 0.33% in the seed sludge, respectively (Figure 3.19a). There were other dominant bacteria groups such as *Myxococcales, Comamonadaceae* and *Pseudomonadales* which had a relative abundance of approximately 56% in the seed sludge (Figure 3.19a). However at week 1, the abundance of both *Candidatus Accumulibacter* and *Candidatus Competibacter* in the control sludge increased to 23.07 ± 1.70 and 38.23 ± 5.76%, respectively (Figure 3.19a).

Both *Candidatus Accumulibacter* and *Candidatus Competibacter* continued to increase in relative abundance over the remaining seven weeks to 46.31 ± 5.11 and 32.11 ± 8.20%, respectively (Figure 3.19a). Other bacterial groups such as *Myxococcales, Comamonadaceae* and *Pseudomonadales* decreased in relative abundance (Figure 3.19a). Interestingly, the relative abundance of *Thauera* increased from 1.40 ± 1.11 at week 1 to 8.03 ± 3.19% by week 8 (Figure 3.19a). The increase in *Thauera* abundance appeared to be correlated with the decline in the abundance of *Myxococcales, Comamonadaceae* and *Pseudomonadales*.

The dissimilarity between the control and treated sludge were signified by differences in dominant bacterial groups. At week 1, the treated sludge were dominated by *Comamonadaceae, Rhodocyclaceae*, *Thauera* and *Zoogloea* which were present in relative abundances of 18.45 ± 2.79, 11.21 ± 1.67, 17.21 ± 3.90 and 21.45 ± 2.69% respectively (Figure 3.19b). Unlike the control sludge, both *Candidatus Accumulibacter* and *Candidatus Competibacter* were present at a low relative abundance at weeks 1 to 4. During this period, the particle size of the flocs in the treated sludge was significantly lower than the control sludge (Figure 3.11a). In addition, the relative abundance *Thauera* continued to increase from weeks 1 to 4 and only decreased in relative abundance from week 5 onwards (Figure 3.19b).

This trend was also observed for *Zoogloea*. The decreases in the relative abundances of *Thaurea* and *Zoogloea* in the treated sludge were correlated with a gradual increase in relative abundance for *Candidatus Accumulibacter* (Figure 3.19b). Although the relative abundance of *Candidatus Accumulibacter* had increased by week 5, this was not reflected in an increase in particle size in the treated sludge. By week 7, the relative abundance of *Candidatus Accumulibacter* had increased to more than 68% in the treated sludge, which was higher than the relative abundance in the control sludge. The increase in *Candidatus Accumulibacter* abundance in the treated sludge was positively correlated with an increase in particle size (Figure 3.11a). The particle size of the treated sludge was not significantly different to the control sludge. However, the relative abundance of *Candidatus Competibacter* was maintained between 3.90 ± 0.55 and 4.75 ± 1.46% from weeks 5 to 8 in the treated sludge (Figure 3.19b). This was significantly different from the control sludge where the relative abundance of *Candidatus Competibacter* was 32.11 ± 8.20% at week 8 (Figure 3.19b). Based on the observations from the treated sludge, the data suggested that a high abundance of *Candidatus Accumulibacter* was essential for the formation of granules. Furthermore as seen in the controls, it appeared that the presence of both *Candidatus Accumulibacter* and *Candidatus Competibacter* at high abundances were necessary for the increase in floccular size and aggregation for the formation of granules.

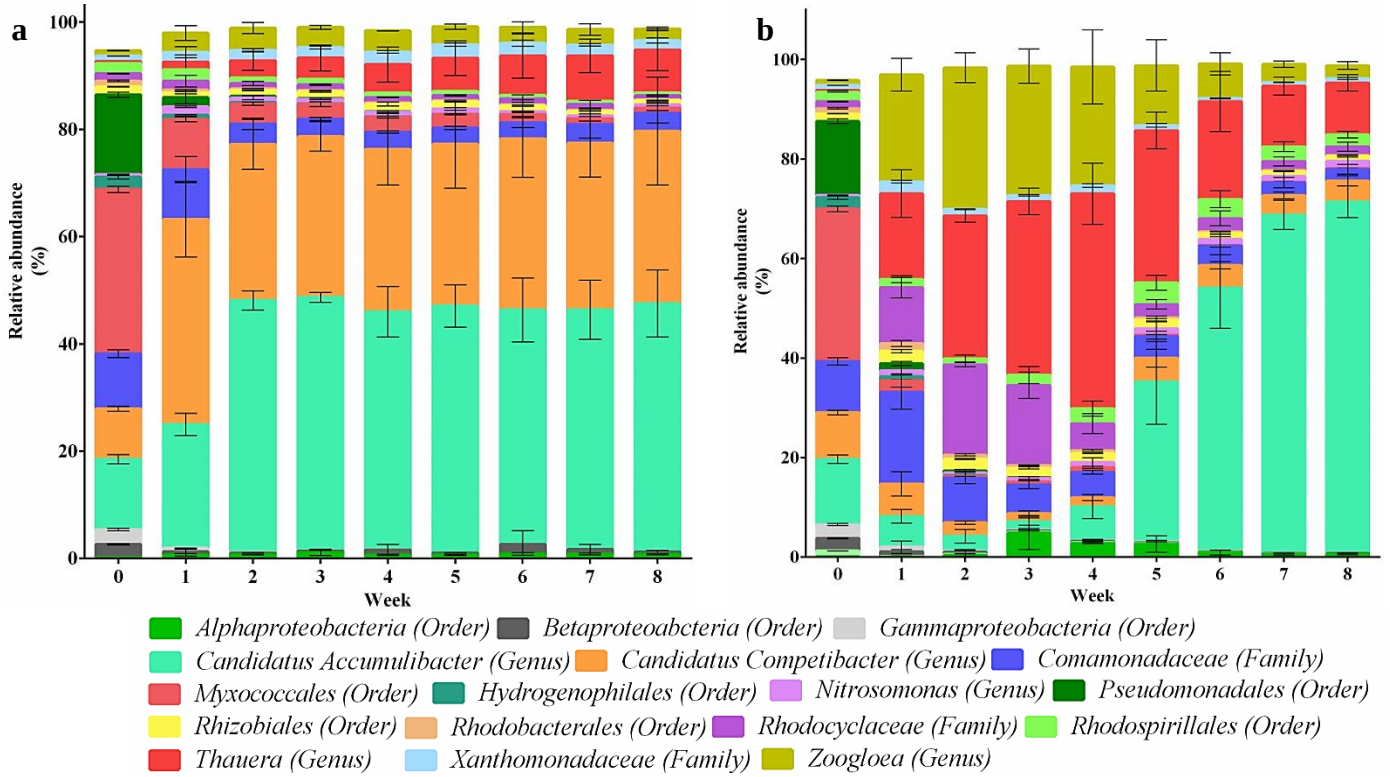

Figure 3.19: Relative abundance of dominant bacteria groups within *Proteobacteria*. (a) Dominant *Proteobacteria* groups in control and (b) treated sludge. Error bars represent standard deviations (n = 3).

3.3.6. Role of protozoa in the expansion and maintenance of aerobic granules

The role of protozoa in the formation of granules from floccular sludge was tested by the addition of thiram to inhibit protozoa. Sessile ciliates were hypothesized to play a role in the expansion and structural maintenance of aerobic granules. Therefore, to test this hypothesis, preformed granules were also treated with thiram to inhibit protozoa on granules, which were predominantly sessile ciliates.

Here, four mSBRs were seeded with mature granules and operated for five weeks. Enumeration of protozoa from both control and treated sludge also indicated that thiram treatment was effective in removing protozoa. The cell density of protozoa was 2916 ± 469 cells mL^{-1} at week 0 (Figure 3.20a). Sessile ciliates were the only type of protozoa observed in the seed sludge at week 0 (Figure 3.20b). Although the discharge of biomass and reduced settling time was associated with a loss of protozoa at week 1, the cell density of protozoa in the control sludge increased in the subsequent weeks from 866.67 ± 237.46 to 1558.33 ±229.89 cells mL^{-1} (Figure 3.20a). More than 95% of protozoa observed in the granular sludge from week 1 to 5 were sessile ciliates (Figure 3.20b). Swimming ciliates which were only observed in weeks 1 and 2 accounted for less than 5% of the protozoa observed (Figure 3.20b). There were no protozoa detected in the treated granular reactors. Rotifers were only observed during weeks 3 and 4 at very low abundance. Microscopic observations revealed no differences in the particle sizes of the control and treated granules (Figure 3.21a and b).

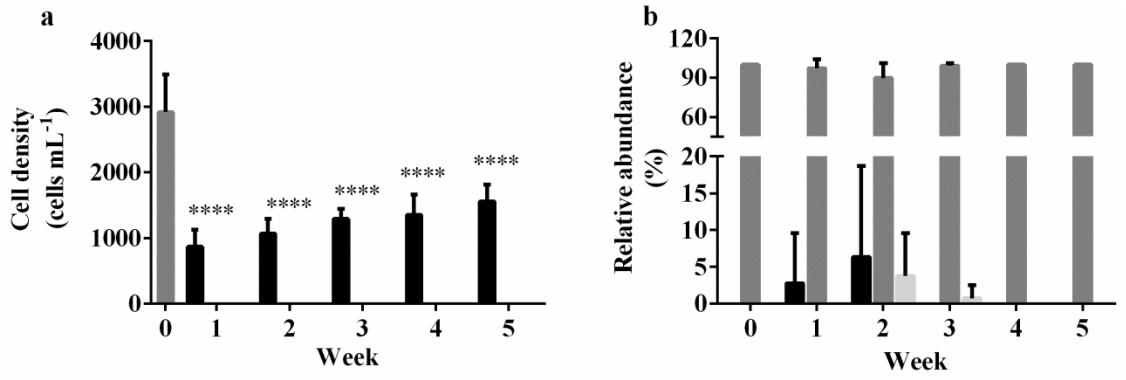

Figure 3.20: Protozoan numbers in granular sludge. (a) Total protozoan density in seed (dark grey), control (black) and treated (light grey) granular sludge. (b) Types of predators observed in seed (week 0) and control sludge (week 1 to 5); rotifers (light grey), swimming ciliates (black) and sessile ciliates (dark grey). Error bars represent standard deviations (n = 2). **** denote significant differences (One-way ANOVA: *P*-value ≤ 0.0001).

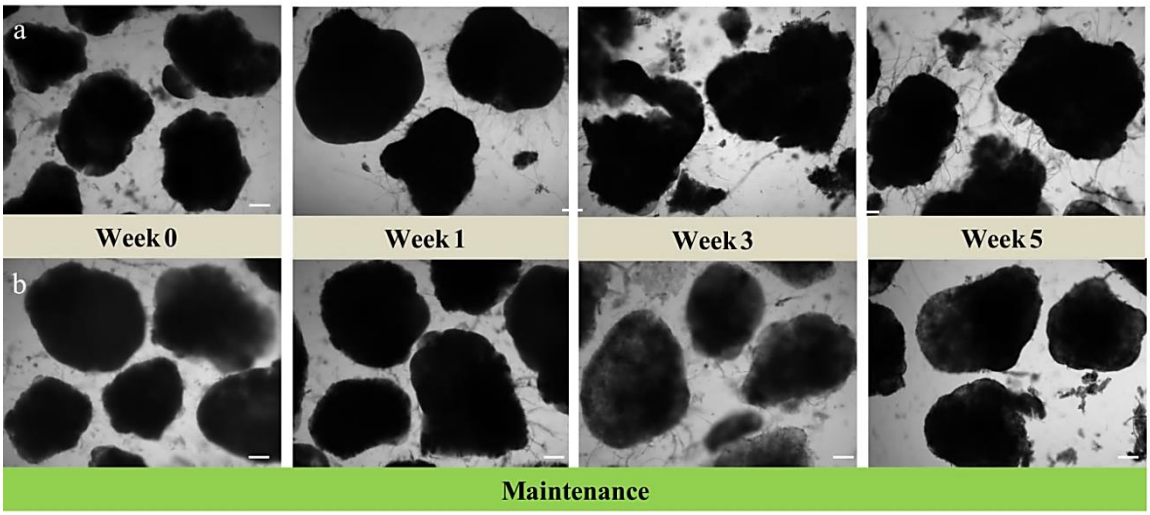

Figure 3.21: Micrographs of granules from seed, control and thiram treated granular sludge during the maintenance phase. (a) Control granular sludge and (b) floccular sludge treated with 5 mg L^{-1} of thiram. Magnification x 40 (Bar, 200 µm).

The seed sludge had a mean particle size of 972.61 ± 53.39 µm (Figure 3.22a) while both control and treated granules had similar mean particle sizes of 1208.50 ± 129.04 and 1135.00 ± 108.81 µm at week 5, respectively (Figure 3.22a). The sludge volumetric index (SVI_5) of control and treated granular sludge was not significantly different (Figure 3.22b). There was also no significant loss of biomass (MLSS and VSS) in either control or treated granular sludge, despite the lack of protozoa in the treated sludge (Figure 3.22c and d).

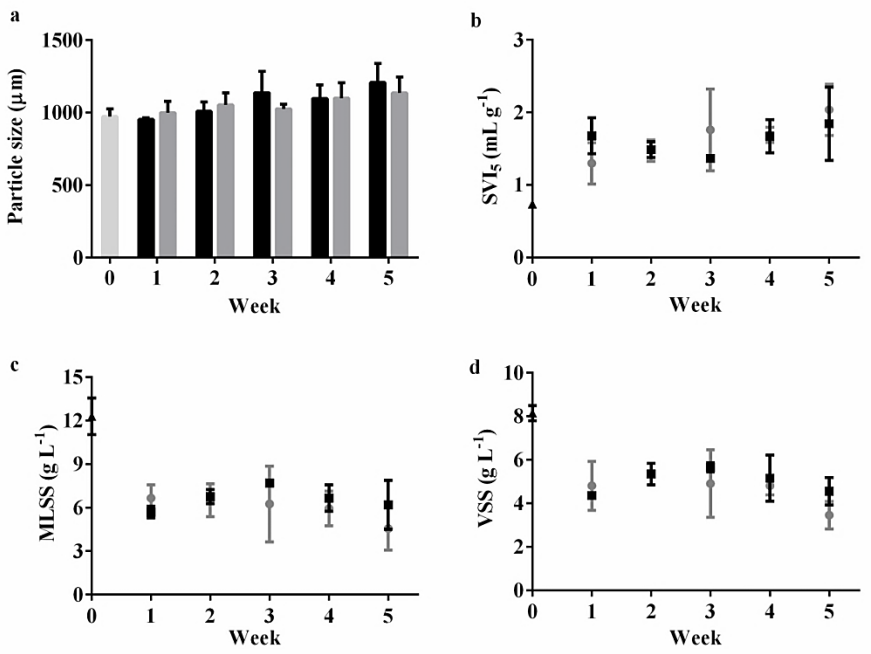

Figure 3.22: Analysis and measurements of granular sludge. (a) Mean particle size of seed (light grey, Week 0), control (black) and treated sludge (dark grey) over 5 weeks. (b) SVI_5 of seed (black triangle), control (black square) and treated (grey circle) sludge. (c) MLSS of seed (black triangle), control (black square) and treated (grey circle) sludge. (d) VSS of seed (black triangle), control (black square) and treated (grey circle) sludge. Error bars represent standard deviations (n = 3).

There were some differences between the control and treated granular sludge in terms of the efficiency of nutrient removal. The P removal of control sludge was significantly

lower (6.29 ± + 6.29%) than the treated sludge (33.11 ± 2.89%) at week 2 (Figure 3.23). However, the P removal improved from week 3 onwards and reached 68.34% at week 5, which was significantly higher than 31.30% for the treated sludge (Figure 3.23). The N removal in control sludge also decreased sharply from 65.34 ± 6.10 ± 3.44% in week 1 to 49.20% in week 2 (Figure 3.23). However, N removal also improved from week 3 to 55.75 ± 0.46 % in week 5 (Figure 3.23).

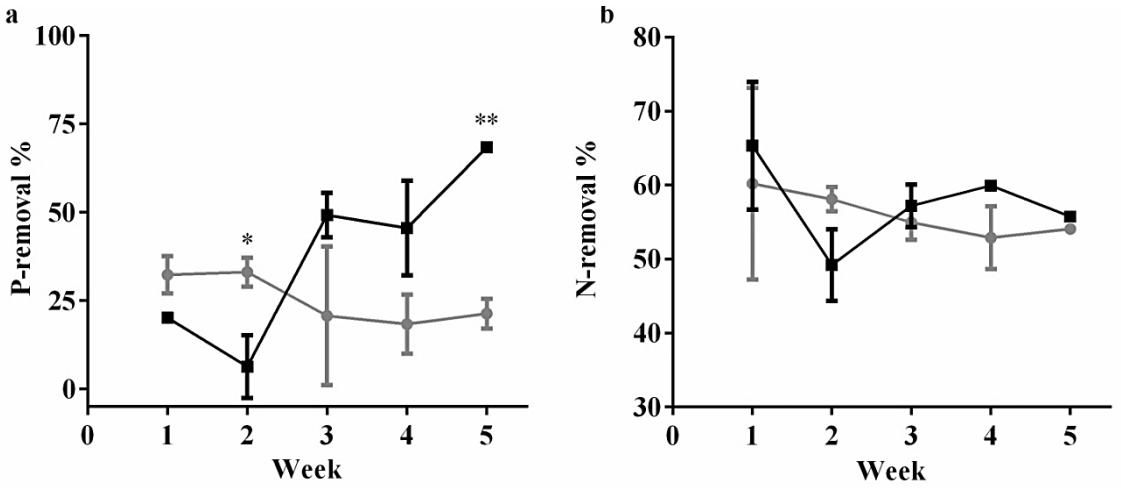

Figure 3.23: Nutrient removal profiles for control and treated sludge. (a) Percentage of total phosphate removed from wastewater by control (black) and treated (grey) sludge. (b) Percentage of total nitrogen removal from wastewater by control (black) and treated (grey) sludge. Error bars represent standard deviations (n=3). * and ** denote significant differences (One-way ANOVA: *P*-value = 0.05, 0.01 and 0.0001, respectively).

3.3.6.1. Analysis of eukaryotic communities in control and treated granular sludge

In the seed sludge, the mean number of sequencing reads was 62483 ± 2535 with the percentage of eukaryotes being 6.99 ± 0.42% (Table 3.2). The percentage of eukaryotes remained within the range of 3.63 ± 1.44 to 17.68 ± 5.99% in the control sludge from weeks 1 to 5 (Table 3.2). In contrast, the percentage of eukaryotes in the treated sludge

was < 1% from weeks 1 to 5 (Table 3.2). Each control and treated sludge dataset had 72 OTUs which represented all eukaryotic reads. The reduced percentage of eukaryotic reads in the treated sludge indicated that thiram was effective in removing eukaryotes from sludge.

Table 3.2: Mean sum and percentage of Bacteria, Eukarya, Archaea and Unidentified sequencing reads

Control				
Week	Mean Sum of Reads	% Bacteria	% Eukarya	% Unidentified
0	62483 ± 2535	73.03 ± 0.24	6.99 ± 0.42	19.98 ± 0.18
1	55683 ± 221	77.30 ± 0.71	3.63 ± 1.44	19.07 ± 0.73
2	59291 ± 262	66.72 ± 0.29	10.07 ± 2.20	23.22 ± 1.91
3	51088 ± 3356	65.31 ± 7.95	14.78 ± 9.27	19.91 ± 132
4	66567 ± 3056	67.93 ± 3.04	11.35 ± 5.47	20.73 ± 2.43
5	64824 ± 7388	59.27 ± 1.61	17.68 ± 5.99	23.05 ± 4.37
Treated				
Week	Mean Sum of Reads	% Bacteria	% Eukarya	% Unidentified
0	62483 ± 2535	73.03 ± 0.24	6.99 ± 0.42	19.98 ± 0.18
1	55753 ± 3584	80.15 ± 1.49	0.63 ± 0.31	19.23 ± 1.18
2	68266 ± 3553	81.78 ± 2.37	0.77 ± 0.58	17.45 ± 2.96
3	53820 ± 3250	86.09 ± 7.67	0.30 ± 0.20	13.61 ± 7.87
4	64976 ± 6875	81.27 ± 4.03	0.38 ± 0.09	18.35 ± 4.12
5	59454 ± 3040	83.02 ± 2.94	0.90 ± 0.56	16.08 ± 2.38

The similarities and dissimilarities between the eukaryotic communities in the control and treated sludge were visualized on MDS plots (Figure 3.24). There was a dissimilarity of

46.33% between the control and treated sludge (Figure 3.24). For the control sludge, there was close clustering of the two replicates from week 1 with the seed sludge. The close clustering of the two control replicates were also observed from weeks 2 to 5 (Figure 3.24). Hence, these observations showed that the eukaryotic communities were highly similar between weeks 0 to 5 in the control sludge (Pr = 0.108). Comparisons between control and treated replicates showed that the treated replicates were distinctly divergent from the control replicates (Figure 3.24).

Within the treated sludge, there was close clustering of only the two replicates, weeks 1 and 2. These two treated replicates subsequently diverged from each other from weeks 3 to 5 to form individual clusters for each replicate (Figure 3.24). PERMANOVA analysis also indicated that the eukaryotic communities were highly dissimilar between the control and treated sludge due to thiram treatment (Pr = 0.001). However, comparison of the eukaryotic community between each control and treated replicate did not show any dissimilarities from weeks 0 to 5 (Pr = 0.395).

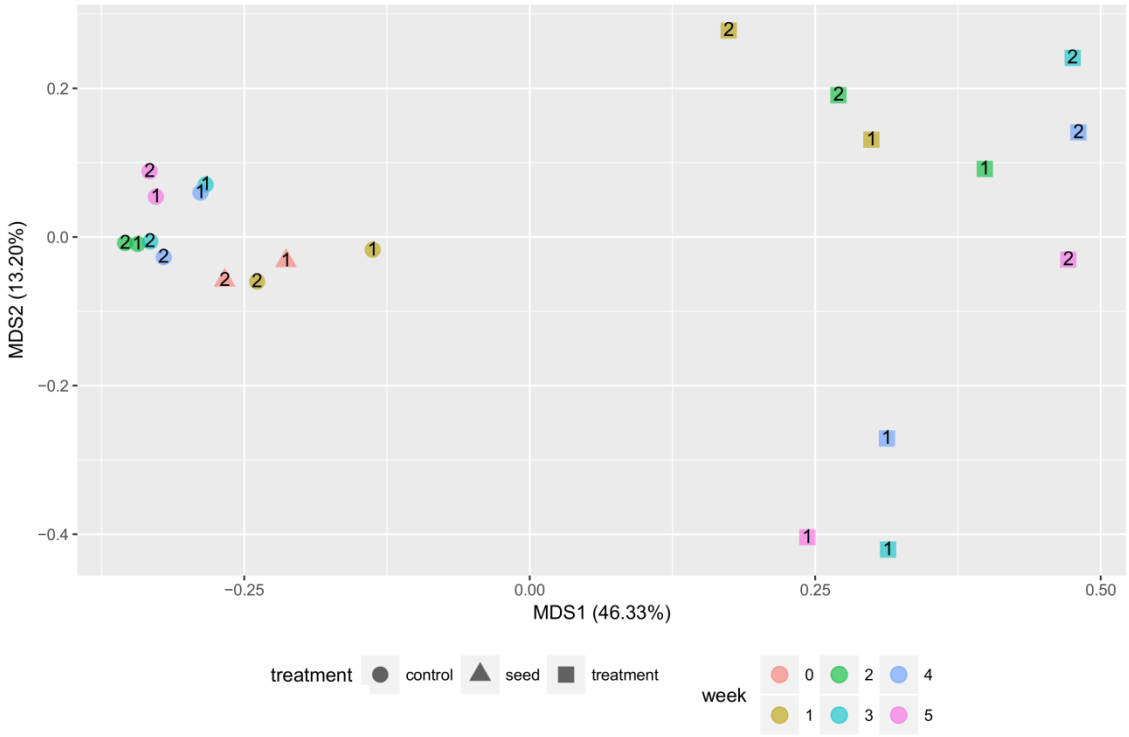

Figure 3.24: Multi-dimensional scaling (MDS) plots for principal component analysis of different groups of eukaryotic microorganisms in control and treated sludge during aerobic granulation process. The data were transformed by the square root function for principal component analysis. The three factors used for analysis were weeks, mSBRs and treatment. Each symbol labelled 1 to 2 is a mSBR replicate. Circles represent the control sludge while triangles represent the seed sludge and squares represent the treated sludge. Each week was represented by a unique colour.

For the seed sludge, the eukaryotes reads were primarily dominated by the phylum *Ciliophora* (92%) (Figure 3.25a). The most dominant member in *Ciliophora* was the genus *Vorticella* which accounted for > 90% the reads, while the genus *Carchesium* and phylum *Oligohymenophorea* accounted for the remaining reads at week 0 (Figure 3.25b). The genus *Vorticella* is a group of non-colonial stalked ciliates characterized by a singular head on a contractile stalk. These sessile ciliates filter feed primarily on suspended bacteria. The phylum *Ciliophora* continued to dominate the control granular sludge with

other minor groups such as the phyla *Tubulinea, Rotifera* and *Ochrophyta* from weeks 1 to 5 (Figure 3.25a). Within *Ciliophora* during week 1, *Oligohymenophorea*, *Vorticella* and *Amphileptus* were the three dominant groups of ciliates in the control sludge (Figure 3.25b). Although these three groups of ciliates continued to be dominant from weeks 2 to 5, the phylum *Oligohymenophorea* accounted for majority of the reads (Figure 3.25b).

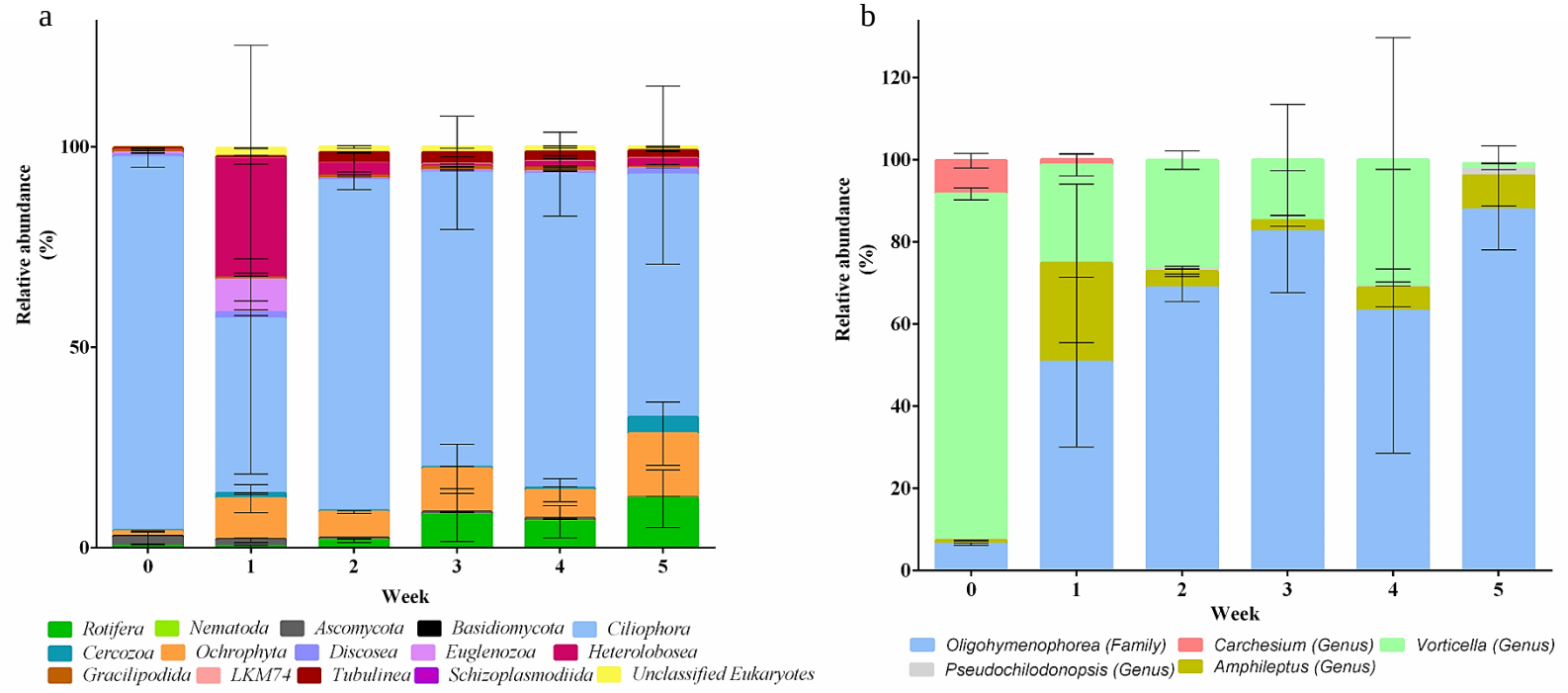

Figure 3.25: Relative abundance of eukaryotes in the (a) control sludge. (b) Relative abundance of various OTUs within *Ciliophora*. A total of 72 OTUs which represented all eukaryotic reads were analyzed for the relative abundance of eukaryotes. The percentage of eukaryotic reads ranged between 3.63 to 17.68% from weeks 1 to 5 (Table 3.1). A total of 16 OTUs which represented all *Ciliophora* reads were analyzed for their relative abundance in *Ciliophora*. Error bars represent standard deviations (n = 2).

In contrast to the control granular sludge, the treated granular sludge had a significantly different eukaryotic community. The treated sludge which had < 1% of eukaryotic reads was primarily dominated by the phyla *Ochrophyta*, *Ascomycota*, *Tubulinea* and unclassified eukaryotes (Figure 3.26). Although the phylum *Ciliophora* was present from weeks 1 to 5, it was of very low abundance at < 4% on average (Figure 3.26). Despite the absence of ciliated protozoa, the particle size of the granules did not decrease. In fact, the mean particle size of granules continued to increase from 999.00 ± 79.08 µm at week 1 to 1135.00 ± 108.81 µm at week 5, which was similar to the mean particle size of the control sludge.

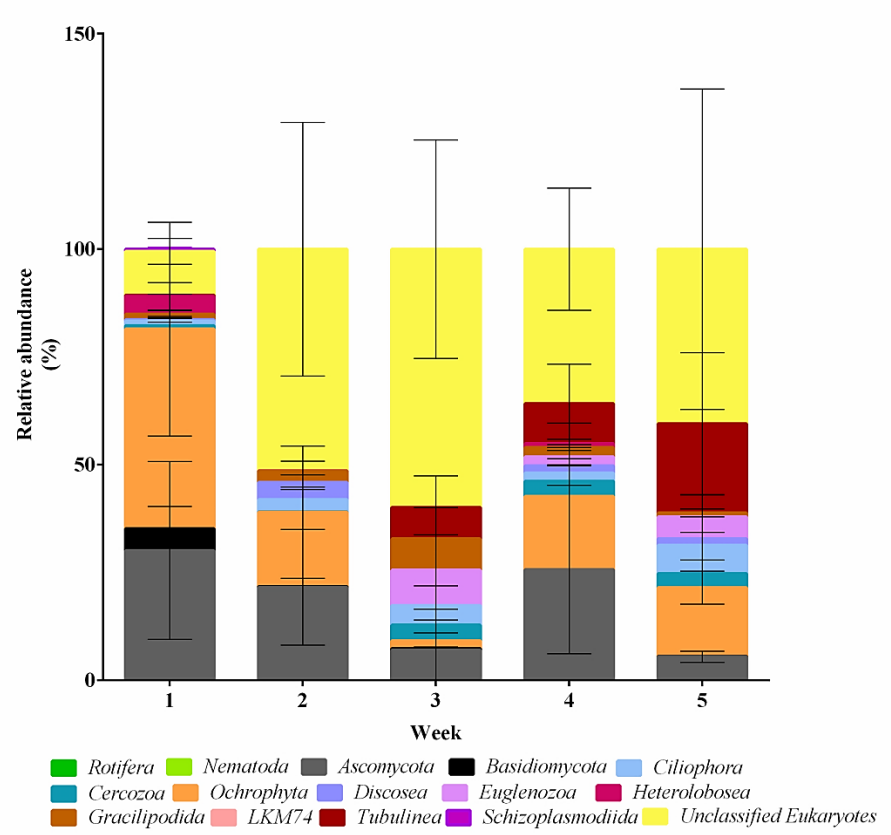

Figure 3.26: Relative abundance of eukaryotes in the treated sludge. A total of 72 OTUs which represented all eukaryotic reads were analyzed for the relative abundance of eukaryotes. The treated sludge had < 1% of eukaryotic reads (Table 3.1). Error bars represent standard deviations (n = 3).

3.3.6.2. Analysis of bacterial communities in control and treated granular sludge

As the eukaryotic communities were effectively removed in the treated granular sludge, it was essential to investigate the difference in the bacterial communities of the control and treated sludge. Based on the MDS plot for the bacterial communities, there was a dissimilarity of 54.52% between the control and treated sludge (Figure 3.27). Control replicates were closely clustered together from weeks 0 to 5. However, replicates of the treated samples diverged from week 1 to form individual clusters for each replicate. Based on PERMANOVA analysis, bacterial communities were significantly dissimilar due to the thiram treatment (Pr = 0.001) and between weeks (Pr = 0.001). However, there was no significant dissimilarity between each control and treated replicate. This suggested that the absence of protozoan predators resulted in a shift of bacterial communities during the maintenance phase of aerobic granulation.

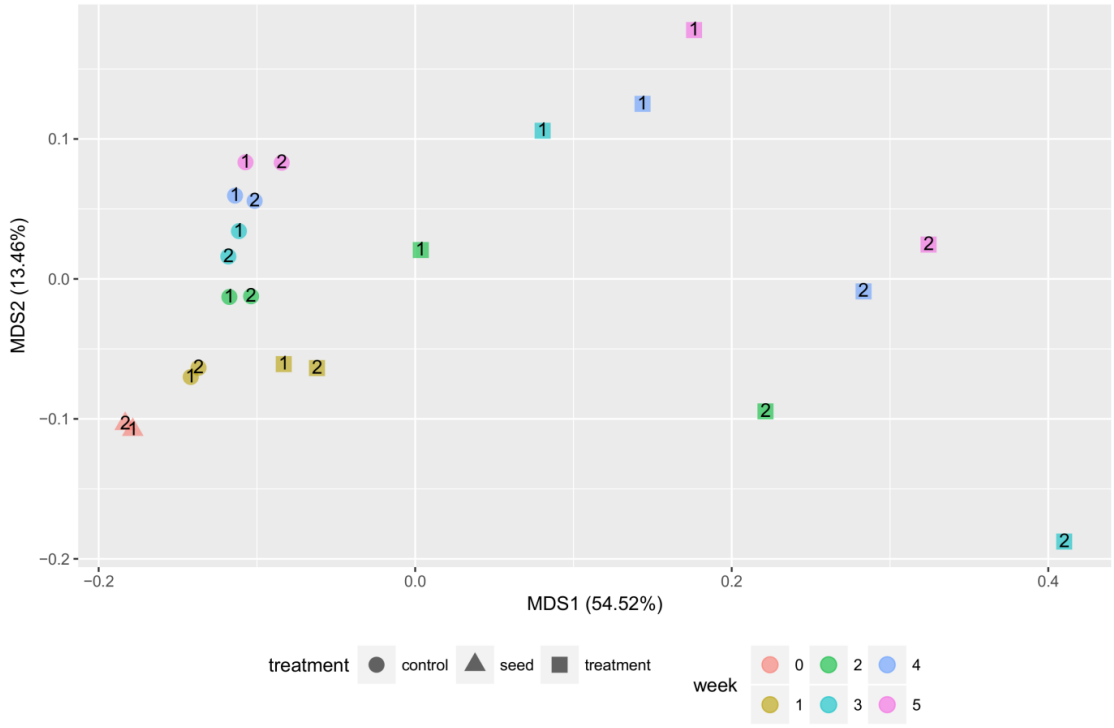

Figure 3.27: Multi-dimensional scaling (MDS) plots for principal component analysis of different groups of eukaryotic microorganisms in control and treated sludge during aerobic granulation process. The data were transformed by the square root function for principal component analysis. The three factors used for analysis were weeks, mSBRs and treatment. Each symbol labelled 1 to 3 represents a replicate. Triangles, circles and squares represent the seed, control and treated sludge, respectively. Each week was represented by a unique colour.

The top 400 OTUs representing 90 to 95% of the bacterial reads were analyzed to elucidate the differences in the bacterial communities that were observed in the MDS plot. The phylum *Proteobacteria* were the most dominant group in all sludge samples (Figure 3.28) and accounted for an average of 67.51 ± 4.21, 71.71 ± 10.74 and 75.14 ± 0.32% in seed, control and treated sludge, respectively (Figure 3.28). While *Proteobacteria* made up most of the reads, non-*Proteobacteria* groups such *Planctomycetes*, *Nitrospira*, *Chlorofexi*, *Bacteroidetes*, *Cyanobacteria* and *Acidobacteria* accounted for the remaining

sequencing reads. However, there was no significant difference in the relative abundance of various groups of bacteria between the control and treated sludge (Figure 3.28a and b). Interestingly, relative abundance of *Proteobacteria* OTUs suggested that the absence of protozoa could have played a role in the shift of bacterial communities in the treated sludge.

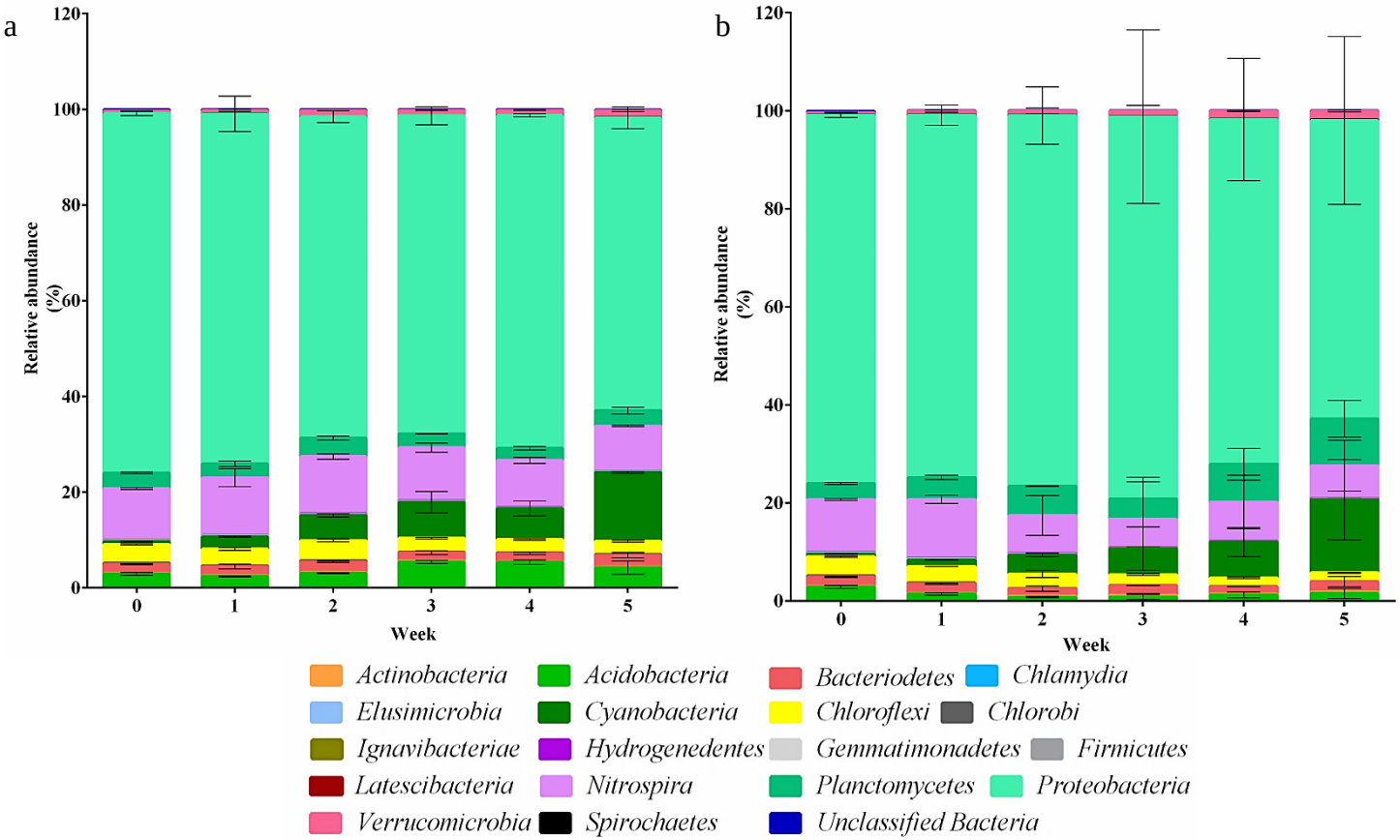

Figure 3.28: Relative abundance of the dominant bacteria groups in (a) control and (b) treated sludge. A total of 400 OTUs were selected from each SBR, which represented approximately 90% to 95% of the bacterial sequencing reads. Error bars represent standard deviations (n = 2).

Within the phylum *Proteobacteria* in control sludge, both *Candidatus Accumulibacter* and *Candidatus Competibacter* accounted for approximately 35% and between 30-40%, respectively. There were no significant fluctuations in the *Proteobacteria* community over 5 weeks except the slight increase in the relative abundance of the phyla *Nitrosomonas*, *Thauera* and *Zoogloea* (Figure 3.29a). Interestingly, the increase in these three phyla also coincided with an increase in P removal of the control sludge from 6.29 ± 6.29% at week 2 to 49.19 ± 4.43% by week 3 (Figure 3.24a). By week 5, P removal efficiency was 68.34 ± 0.22% (Figure 3.24a). The N removal of the control sludge also increased from 49.19 ± 3.44% at week 2 to 57.18 ± 2.06% at week 3 (Figure 3.24b). The particle size of the control sludge was observed to increase continually during these 5 weeks. In contrast, there was a decrease in the relative abundance of *Candidatus Competibacter* and *Candidatus Accumulibacter* from week 1 in the treated granular sludge (Figure 3.29b).

The bacterial community in the treated sludge appeared to be different from the control sludge from week 2 onwards. There were increases in the relative abundance of *Xanthomonadaceae*, *Thauera, Zoogloea*, *Rhizobales* and *Rhodospirillales* (Figure 3.29b). Increases in the relative abundance of *Xanthomonadaceae, Rhizobales*, and *Rhodospirillales* were not observed in the control sludge (Figure 3.29b). Despite the decrease in the relative abundance in *Candidatus Accumulibacter*, the P removal of the treated sludge remained at 18.35 ± 5.92 to 33.11 ± 2.89% (Figure 3.24a). In addition, N removal from the treated sludge did not change significantly (Figure 3.24b). The particle size of the treated granular sludge was not significantly different to the control sludge despite the absence of protozoa and decreases in relative abundance of *Candidatus Accumulibacter* and *Candidatus Competibacter*.

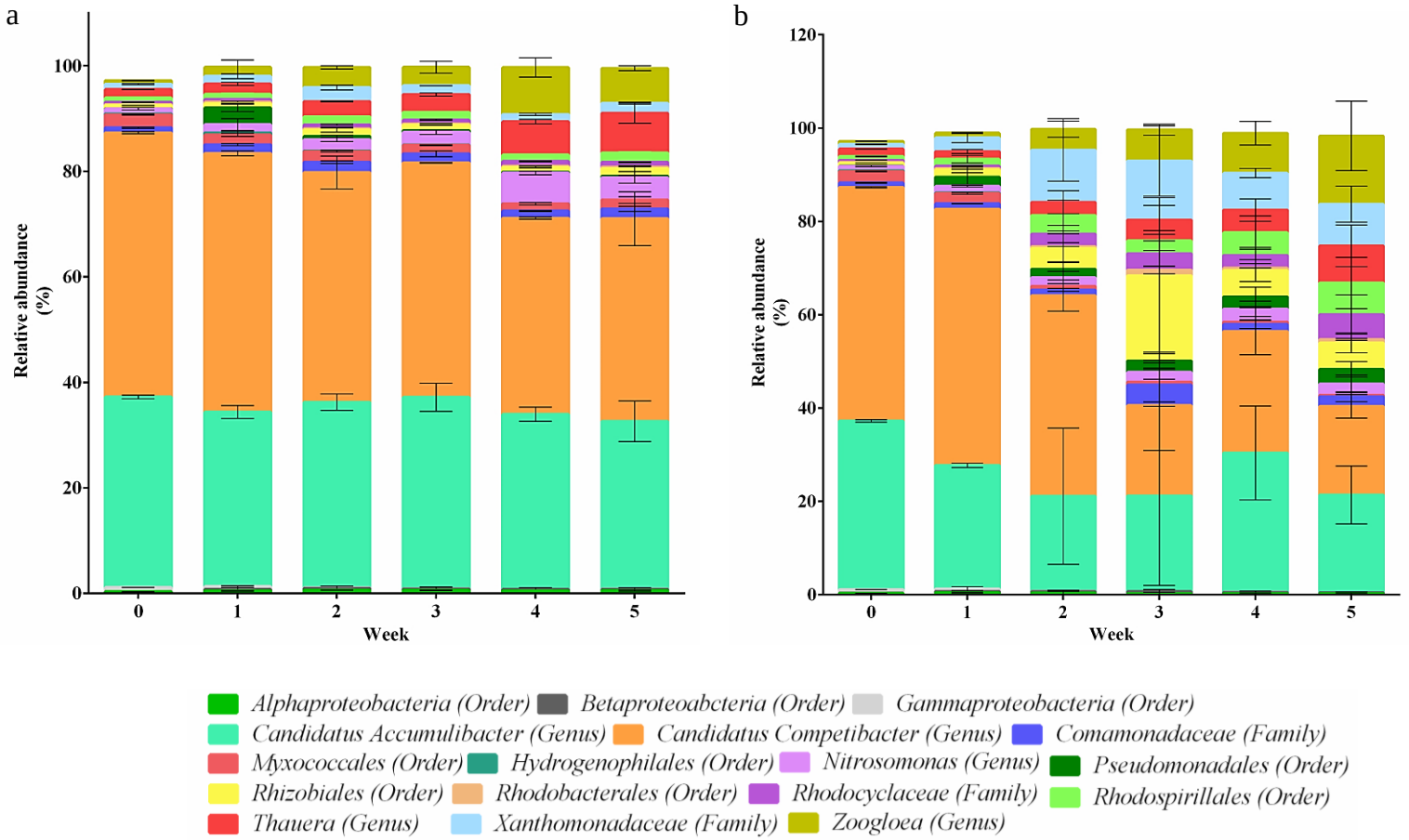

Figure 3.29: Relative abundance of dominant bacteria groups within *Proteobacteria*. (a) Dominant *Proteobacteria* groups in control and (b) treated sludge. Error bars represent standard deviations (n = 3) .

3.4. Discussion

Ciliated protozoa are the most dominant protozoa in activated sludge and they are essential in removing suspended bacteria which improves treated effluent (Madoni 2003, Madoni 2010). In wastewater environments, protozoa were also suggested to improve flocculation of bacteria (Bossier and Verstraete 1996, Curds 1963, Curds 1982). Sessile ciliates are also often observed in high abundance on the surfaces of aerobic granules (Lemaire et al. 2008a, Li et al. 2013, Schwarzenbeck et al. 2004b), which are generally formed from activated floccular sludge. The predatory role of sessile ciliates was confirmed by the presence of bacteria in food vacuoles found within the bodies of these ciliates (Lemaire et al. 2008a). A study by Weber et al. (2007) further hypothesized that the stalks of these sessile ciliates served as a form of substratum for the continual expansion of granules. These observations strongly suggested that protozoan predation had an important role in driving floccular sludge towards the aerobic granulation process. In addition, the presence of sessile ciliates was also hypothesized to have a structural role in maintaining the integrity of aerobic granules. However data presented in Chapter 2, revealed that protozoa did not play a dominant role in the granulation process here, based on the negative correlation between the abundance of protozoa and the particle sizes. In addition, the changes in the protozoan community during granulation were likely due to the selection pressure exerted by the change from flocs to granules.

To better investigate the role of protozoan predation in granule formation and maintenance of structural integrity, thiram was added into mSBRs that contained either floccular or granular sludge. Eukaryotic inhibitors are generally used for the inhibition of protozoan predators to study the rate of predation on bacteria, their effects on bacterial growth and their influence on bacterial activities (Ramirez and Alexander 1980, Shimeta

and Cook 2011). Thiram was selected as it was demonstrated to be highly effective against natural assemblages of ciliates (Shimeta and Cook 2011). Other inhibitors such as cycloheximide and nystatin caused an initial decline in ciliate count which was followed by a bloom of tolerant ciliates species (Shimeta and Cook 2011). In agreement with this, optimization experiments using cycloheximide performed in this study showed strong inhibition of both swimming and crawling ciliates but little effect on the inhibition of sessile ciliates (data not shown). In contrast, thiram was found to be highly effective for protozoan inhibition at 20 mg L^{-1} and 5 mg L^{-1} in floccular and granular sludge, respectively. Interestingly, both 10 and 20 mg L^{-1} of thiram was less effective in protozoan inhibition than 5 mg L^{-1} of thiram in granular sludge. However, it is unknown why these higher concentrations were less effective. Beyond these selected concentrations, thiram reduced the efficiency of N removal by the bacterial community although live dead staining indicated that thiram was not toxic. Previous studies also demonstrated that thiram (> 50 mg L^{-1}) caused a significant reduction in denitrification rate in sediments to less than 4% compared to the control (Acton 2012, Shimeta and Cook 2011). Here, 5 mg L^{-1} of thiram did not significantly reduce total N removal in the treated granular sludge as compared to the untreated sludge. Although optimization studies showed that 20 mg L^{-1} of thiram affected the total N removal in floccular sludge, this concentration demonstrated the greatest inhibition of protozoa with the least reduction in total N removal compared to the untreated floccular sludge. In addition, the efficiency of COD and phosphate removal can also be measured to better understand the effects of thiram on the metabolic activity of sludge.

To determine if protozoan predation had a role in driving floccular sludge towards aerobic granulation, six mSBRs were inoculated with floccular sludge and operated according to standard procedures to obtain aerobic granules with SNDPR functions. Eukaryotic

communities in the control and thiram treated mSBRs were significantly different. Similar to the observations presented in Chapter 2, there was a succession of protozoan groups where sessile ciliates became the most abundant protozoa as the floccular sludge changed to granules. These sessile ciliates were also observed to colonize the surfaces of granules. Furthermore, Ribotagger analysis also demonstrated that the phylum *Ciliophora* was consistently the dominant member in the control mSBRs, with the family *Oligohymenophorea* as the most dominant group. The dominance of *Ciliophora* and *Oligohymenophorea* was also observed in Chapter 2 during aerobic granulation and supports the observations made here. The abundance of sessile ciliates on granules was also observed in previous studies (Lemaire et al. 2008a, Li et al. 2013, Schwarzenbeck et al. 2004b, Weber et al. 2007).

As thiram was effective in inhibiting protozoa, the eukaryotic community in the treated sludge were dominated mostly by fungi from the phyla *Basidiomycota*, *Cryptomycota* and *Ascomycota* during the early stages of granulation (weeks 1 to 3) followed by testate amoeba (weeks 4 to 5). Algae and unidentified eukaryotes were the dominant members from weeks 6 to 8. Although fungi were previously suggested to form mycelial pellets with good settling properties (Beun et al. 1999, Etterer and Wilderer 2001), the overall abundance of these fungi was very low, i.e. less than 1% of sequencing reads were eukaryotic in the treated sludge. Hence, it was unlikely that fungi contributed significantly to the formation of granules from flocs. Previous studies also showed that protozoan predation could positively simulate biofilm growth (Arndt et al. 2003, Matz et al. 2005a, Rychert and Neu 2010). For example, the co-incubation of activated sludge bacteria with sludge protozoa composed of attached, crawling ciliates, flagellates and amoeba for 48 h, resulted in biofilms that had 2000% more biomass than the biofilms that were not exposed to protozoan predation (Rychert and Neu 2010).

Here, despite the implementation of strong granulation factors such as settling time and shear force, the absence of protozoa in the treated mSBRs resulted in a delay in the initiation phase which started at week 6 instead of week 4 in the control mSBRs. The delay in initiating granulation was likely due to the poor settling properties of treated sludge during the floccular phase, resulting in the loss of biomass indicated by MLSS and VSS. Although there was a delay in formation of granules, the particle size of the treated granules was similar to the control granules. The formation of granules without protozoa indicated that granulation from floccular sludge without protozoa is possible, albeit at a slower rate due to a delayed initiation phase.

Comparisons between the control and treated sludge revealed no significant differences in the bacterial communities except for the phylum *Proteobacteria*. In the absence of protozoa, the poor settling of the treated sludge in the floccular phase could be correlated to both genera *Thauera* and *Zoogloea* of *Proteobacteria*. These two groups of bacteria were the most dominant members in the treated sludge before the initiation phase. Without protozoa, the dominance of these two groups was likely due to the wash-out of PAOs and nitrifiers, which could lead to insufficient sludge retention time for the slow growing PAOs and nitrifiers (Weissbrodt et al. 2012). In addition, bacterial populations exposed to protozoan predation can develop larger grazing resistant morphologies such as filaments (Hahn et al. 1999) and microcolonies (Hahn et al. 2000, Scherwass et al. 2016), which may aid in the formation of granules. Predation was also found to induce the production of floc-associated EPS (Menniti and Morgenroth 2010). In contrast, bacteria grown in the absence of predation pressure did not develop grazing resistant morphologies. Hence, it was likely that the absence of predators further allowed the fast-growing *Zoogloea* and *Thauera* to outcompete the slower growing *Candidatus Accumulibacter*. Both *Zoogloea* and *Thauera* are known to produce EPS for the

flocculation of bacteria but without the presence of protozoan predators, the rate of EPS production would have been affected.

The granulation of the treated sludge could be largely attributed to the emergence of *Candidatus Accumulibacter* which dominated the bacterial community by week 7. In contrast to the treated sludge, the control sludge was dominated mainly by both *Candidatus Accumulibacter* and *Candidatus Competibacter* from week 1 onwards. The abundance of both *Candidatus Accumulibacter* and *Candidatus Competibacter* ensured that the control sludge entered the initiation phase by week 4. This was also observed in the formation of granules in week 6 as shown in Chapter 2. Hence, it was apparent that to achieve aerobic granules from flocs, the high abundance of both *Candidatus Accumulibacter* and *Candidatus Competibacter* was essential.

Based on these observations, we suggest that the presence of protozoa reduced the time required for the floccular sludge to initiate aerobic granulation. This was coupled with the high abundance of *Candidatus Accumulibacter* and *Candidatus Competibacter*. In the absence of protozoa, granulation could also occur spontaneously when *Candidatus Accumulibacter* became highly abundant. Here, the core of the treated granules could be formed by either *Thauera*, *Zoogloea* or a combination of both instead of *Candidatus Competibacter* as these bacteria were highly dominant during the floccular phase. As aerobic granulation occurred, *Candidatus Accumulibacter* could have enveloped the *Thauera* or *Zoogloea* dominated flocs to form granules. More work would be required to identify the localization of these groups of bacteria in the treated sludge during aerobic granulation. Importantly, it was clear that a high abundance of *Candidatus Accumulibacter* is necessary for the formation of aerobic granules. This study showed that protozoan predation during the floccular phase would decrease the time required for

floccular sludge to initiate granulation, although protozoa were not necessary for aerobic granulation.

The abundant sessile ciliates on mature granules were hypothesized to play an important structural role in aerobic granulation (Weber et al. 2007). Here, sessile ciliates that were found on the surfaces of granules were successfully inhibited by the addition of thiram. However, the absence of sessile ciliates on the treated granular sludge did not result in significant differences in the particle size compared to the control granular sludge. There was also no obvious break up of granules in the treated sludge over 5 weeks. Despite the lack of sessile ciliates, other physical properties of the granules such as SVI_5, MLSS and VSS remained similar to the control granular sludge. This was in contrast to a study by Li et al. (2013) where the physical removal of *Vorticella* from mature granules caused an increase in SVI_5. Unlike the *Ciliophora* dominated control sludge, the eukaryotic community of the treated sludge was comprised primarily of algae from the phylum *Ochrophyta,* fungi from the phylum of *Ascomycota,* testate amoeba of phylum *Tubulinea* and unidentified eukaryotes. However, loss of protozoa along with the associated increased dominance of algae and fungi did not result in disintegration of the treated granules.

Comparisons of the bacterial communities between the control and treated granular sludge did not show any significant differences. However, within the phylum *Proteobacteria,* it was observed that there was a decrease in the relative abundance of *Candidatus Competibacter* and *Candidatus Accumulibacter*. However, the decrease in relative abundance of both groups of bacteria did not cause any observable granular break up although there was a decline in total P removal. This was likely due to the decrease in the abundance of *Candidatus Accumulibacter*. Interestingly, for the control sludge, there

was nearly 0% of P removal at week 2. As *Candidatus Accumulibacter* are localized on the aerobic zone of granules, sessile ciliates could be responsible for the depletion of oxygen on the granular surface (Lemaire et al. 2008a). This could lead to poor P removal by *Candidatus Accumulibacter* in week 2. Sessile ciliates were consistently observed on the surface of granules from week 3 onwards. Interestingly, the total P removal in treated granular sludge continued to increase over time. However, the exact cause for the improvement of P removal still requires further investigation. The total N removal of both control and treated granular sludge was similar throughout 5 weeks.

Overall, the data suggested that sessile ciliates did not have an important structural role in the expansion and maintenance of aerobic granules. However, it was more likely that the high abundance of both *Candidatus Accumulibacter* and *Candidatus Competibacter* was responsible for the expansion and stability of aerobic granules instead.

Chapter 4: PROTOZOAN PREDATION ON SINGLE AND MIXED SPECIES BIOFILMS

4.1. Introduction

Grazing by protozoa constitutes a major mortality factor for bacteria in natural environments (Matz and Kjelleberg 2005) and thus, predation plays an important role in shaping the composition and structure of bacterial communities (Jurgens and Matz 2002). Protozoan grazing exerts a strong selective pressure on bacteria to develop anti-predator mechanisms such as the formation of bacterial aggregates and grazing resistant microcolonies (Hahn and Hofle 2001, Matz et al. 2004). For example, the suspension feeder, *Cafeteria roenbergensis*, effectively feeds on planktonic cells of *Vibrio cholerae*, while biofilms are resistant to predation by surface feeding protozoa (Matz et al. 2005b). In addition, protozoan grazing has been shown to activate the secretion of antiprotozoal compounds, which are effective against amoeba and flagellates (Matz et al. 2004, Matz et al. 2005b, Sun et al. 2013, Sun et al. 2015).

Biofilms are complex communities organized in a matrix of extracellular polysaccharide that provides protection to biofilm cells from a variety of stresses, such as antibiotics (Fux et al. 2005) and grazing by protists (Chavez-Dozal et al. 2013, Erken et al. 2012). Biofilms in the environment exist as mixed species communities that are known to display greater resistance against various stresses than single species biofilms (Burmølle et al. 2006, Lee et al. 2014, Schwering et al. 2013). The ubiquity of mixed species biofilms and their ability to resist various stresses highlights the importance of investigating the influence of protozoan grazing on these biofilms.

Predation resistance of *Pseudomonas aeruginosa* biofilms has been demonstrated to be due to both chemical and physical defenses. When exposed to the amoeba, *Acanthamoeba castellanii*, *P. aeruginosa* was shown to induce the type III secretion system which

resulted in lysis of the predator (Matz et al. 2008a). In addition, in the presence of the flagellate, *Rhynchomonas nasuta*, undifferentiated early biofilms of *P. aeruginosa* formed microcolonies that were protected from predation (Matz et al. 2004).

Here, the grazing resistance of both single and mixed species biofilms consisting of *P. aeruginosa* (PAO1), *Klebsiella pneumoniae* (KP-1) and *Pseudomonas protegens* (Pf-5) to the heterotrophic ciliate, *Tetrahymena pyriformis*, a ciliate that feeds both on planktonic cells as well as biofilms, was examined. The results demonstrate that the grazing sensitive strains *K. pneumoniae* and *P. protegens* gain associational resistance from the grazing resistant *P. aeruginosa*. The ability of *P. aeruginosa* to protect both mono and mixed species biofilms was examined to further elucidate the underlying resistance mechanism(s). While this resistance was partly due to the production of rhamnolipids, results show that there are other yet unidentified factors that provide *P. aeruginosa* resistance to predation. This work highlights the importance of using mixed species systems to investigate protozoan predation.

4.2. Materials and Methods

4.2.1. Bacterial and protozoal strains

Bacterial strains (Table 4.1) were cultured on Luria-Bertani (LB) agar with either 100 µg ml^{-1} gentamicin or 30 µg ml^{-1} tetracycline. Prior to inoculation for biofilm grazing assays, single colonies were inoculated into M9 minimal medium (48 mM Na_2HPO_4, 22 mM KH_2PO_4, 9mM NaCl, 19 mM NH_4Cl, 2 mM $MgSO_4$, 0.1 mM $CaCl_2$, and 0.04% w/v glucose) supplemented with 0.2% casamino acids and incubated for 24 h at room temperature. *T. pyriformis* was cultured axenically in PYG medium (20 g of peptone, 1 g of yeast extract and 50 mL of 2 M glucose) at room temperature.

Table 4.1: Bacterial and protozoal strains and plasmid used for biofilm grazing assays.

Strains and plasmid	Relevant characteristic*	Source or reference
Bacteria		
P. aeruginosa PAO1	eYFP, Gm^R	(Lee et al. 2014)
P. protegens Pf-5	eCFP, Gm^R	(Lee et al. 2014)
K. pneumonia KP-1	DsRedExpress, Gm^R	(Lee et al. 2014)
P. aeruginosa Δ*rhlA*	eYFP, Gm^R, Δ*rhlA*	(Rahim et al. 2001), (Pamp and Tolker-Nielsen 2007)
P aeruginosa Δ*rhlA*, Δ*pscJ*	eYFP, $Gm^{R,}$, Tc^R, Δ*rhlA*, Δ*pscJ*	This study
P. aeruginosa Δ*pscJ*	eYFP, $Gm^{R,}$, Tc^R, Δ*pscJ*	This study
Protozoa		
T. pyriformis	Wild type, planktonic and biofilm lifestyle	CCAP/1630/1F; Culture Collection of Algae and Protozoa, UK
Plasmids		
pEX18ApGW	Ap^R, Cm^R	(Choi and Schweizer 2005)

*Gm^R: gentamicin resistant; Tc^R, tetracycline resistant: Ap^R; ampicillin/carbenicillin resistant: Cm^R; chloramphenicol resistant: Δ*rhlA*; rhamnolipid deficient: Δ*pscJ*; Type III secretion system deficient.

4.2.2. Construction of *P. aeruginosa* type III secretion mutants

To generate a mutant lacking the type III secretion system, *pscJ* was deleted using allelic exchange (Hmelo et al. 2015). The flanking regions of the *pscJ* gene of *P. aeruginosa* were amplified by PCR and *tetA* was amplified using pBR322 as template. The three PCR

fragments were fused by second-round SOE PCR using primers with overhangs, introducing *Sac*I and *Xba*l restriction sites. The SOE PCR product was introduced into pEX18ApGw that had been digested with S*acI* and X*bal* (Choi and Schweizer 2005). The pEX18Ap-Δ*pscJ*::*tet* plasmid was transformed into *E. coli* S17 and subsequently introduced into *P. aeruginosa* $PAO1_{YFP}$ and $PAO1_{YFP}$ Δ*rhl* by conjugative DNA transfer (Simon et al. 1983). The resulting *pscJ* deletion mutants were selected on M9 medium supplemented with 0.2% glucose and 100 μg mL^{-1} tetracycline and LB medium supplemented with 100 μg mL^{-1} tetracycline. The *pscJ* deletion mutants were verified by Sanger Sequencing. These mutants were generated by Ms. Henriette L. Roeder from University of Copenhagen, Denmark.

4.2.3. Biofilm grazing assays

Grazing assays were established in 24 well microtitre plates as described in Matz et al. (2004) with modifications. Bacterial strains grown for 24 h at room temperature were adjusted to approximately 1×10^8 cfu mL^{-1}. Single species biofilms were established by inoculating well plates with a 1:10 dilution of the bacterial strain in 1 mL of M9. Mixed species biofilms of *P. aeruginosa* wild type or mutant strains, *P. protegens* and *K. pneumoniae* were established by mixing the cultures at a ratio of 5:5:1 to account for the faster growth rate of *K. pneumoniae* (Lee et al. 2014). Biofilms were grown at room temperature (21 to 23°C) for 48 h with gentle shaking (50 rpm). Spent medium was replaced with fresh M9 medium after 24 h in both single and mixed species biofilms and the biofilms incubated for another 24 h before *T. pyriformis* was introduced at a final cell density of 10^3 cells mL^{-1}. Controls for the biofilm assays were made up of M9 medium with heat killed bacteria (HKB) added at a cell density of 10^8 cells mL^{-1} and *T. pyriformis* with a final cell density of 10^3 cells mL^{-1}. Ungrazed and grazed biofilms were prepared in duplicate. Biofilms were examined with confocal laser scanning microscopy (CLSM)

(LSM 780, Carl Zeiss, Germany) to observe the grazing effects after 48 h. For quantification of *T. pyriformis*, triplicates of 10 µL were removed from each well and the numbers of *T. pyriformis* determined using light microscopy (Primo Star, Carl Zeiss, Germany).

4.2.4. Supernatant toxicity assay

Cell-free supernatants were obtained from ungrazed and grazed biofilms by filtration (0.22 µm) and added to 24 well microtitre plates containing *T. pyriformis* at 10^3 cells mL^{-1}. Controls for the supernatant assays were *T. pyriformis* at a final cell density of 10^3 cells mL^{-1} in M9 medium. *T. pyriformis* was enumerated by light microscopy after 24 h.

4.2.5. Rhamnolipid toxicity assay

The toxicity of purified rhamnolipids (AGAE Technologies, USA) (0.01 to 0.5 g $L^{-1)}$ to *T. pyriformis* (10^3 cells mL^{-1}) was tested in 96 well microtitre plates. These purified rhamnolipids were made up of 95% di-rhamnolipid. Controls consisted of 10^3 cells mL^{-1} of *T. pyriformis* in M9 media. Both controls and treatments were prepared in triplicates with a working volume of 100 µL each. Ciliates were enumerated after 24 h using light microscopy. Inactive *T. pyriformis* were considered to be dead.

4.2.6. Rhamnolipid quantification

The concentration of rhamnolipids from the single and mixed species biofilms were determined by the orcinol assay as previously described (Gutierrez et al. 2013). Supernatants from 48 h grazed and ungrazed biofilms were filtered (0.22 µm) and 0.5 mL was extracted twice with 2 volumes of diethyl ether. The ether fractions were evaporated until dry and reconstituted in 100 µL dH_2O. For each 100 µL sample, 100 µL of 1.71% orcinol solution and 800 µL of 60% (vol/vol) H_2SO_4 were added. The samples were

heated at 80°C for 30 min, cooled for 15 min at room temperature and the absorbance ($A_{421\ nm}$) measured and compared to rhamnose standards (0 to 40 g L^{-1}). Rhamnolipid concentrations were determined as 1.0 mg of rhamnose corresponds to 2.5 mg of rhamnolipid (Pearson et al. 1997, Pesci et al. 1997).

4.2.7. Microscopy, image and statistical analyses

A confocal light scanning microscope (LSM 780, Carl Zeiss) with the multi-track mode was utilized for image acquisition. Excitation and emission wavelengths for eCFP, eYFP and DsRedExpress were 458 / 476, 514 / 527 and 561 / 584 nm, respectively. Image stacks were obtained from each well, starting from the center and 2.0 mm towards the top and bottom. Quantification of confocal micrographs was performed using Imaris (Bitplane AG, Belfast, UK) to obtain values for biofilm biomass volume and area. One-way ANOVA was performed using Prism (Graphpad 6.0) to determine the effectiveness of protozoan grazing on biofilm biomass reduction.

4.3. Results

4.3.1. The effect of predation on single and mixed species biofilms

Predator-prey interactions between *T. pyriformis* and single and mixed species biofilms of wild type *P. aeruginosa*, *P. protegens* and *K. pneumoniae* were examined by co-incubation for 48 h. Confocal imaging of the grazed *K. pneumoniae* biofilms revealed that there was approximately a 9-fold reduction in biomass compared to the ungrazed biofilm (Figure 4.1a and e). Red fluorescence observed in *T. pyriformis* indicated that the loss of biofilm biomass was due to *T. pyriformis* grazing (Figure 4.1i). Although there was no observable reduction in biomass of the grazed biofilms of *P. protegens* (Figure 4.1b and f), cyan fluorescence of *T. pyriformis* food vacuoles indicated that the biofilm was being grazed (Figure 4.1k). In contrast to the *K. pneumoniae* and *P. protegens*

biofilms, single species biofilms of *P. aeruginosa* (Figure 4.1c and g) and the mixed species biofilms (Figure 4.1d and h) were unaffected by grazing, and thus were predation resistant. Furthermore, no protozoa were observed on either biofilm (Figure 4.1k and l), indicating that these biofilms were toxic to the predator.

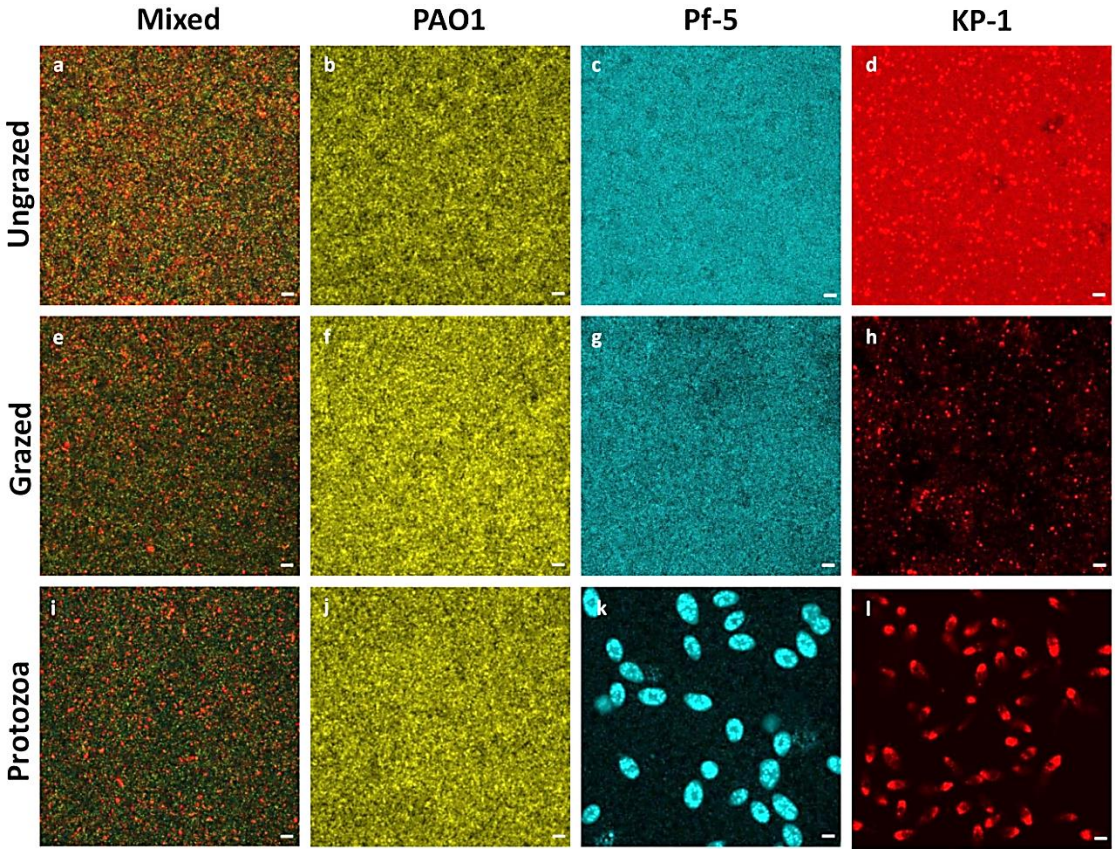

Figure 4.1: Confocal micrographs of ungrazed and grazed single and mixed species biofilms formed by *P. aeruginosa* (PAO1 WT, yellow), *P. protegens* (Pf-5, cyan) and *K. pneumoniae* (KP-1, red). Ungrazed biofilms were grown for 96 h while grazed biofilms were grown for 48 h before *T. pyriformis* was added and co-incubated for 48 h. Panels (a to h) show the difference in biomass between the ungrazed and grazed single and mixed species biofilms and (i to l) panels show the presence or absence of *T. pyriformis* after grazing. No *T. pyriformis* were observed in the mixed or single species *P. aeruginosa* biofilms. Magnification: 20 ×. Scale bar: 20 µm.

One-way analysis of variance (ANOVA) of the biofilm images indicated that there was no significant difference for the biovolumes of ungrazed and grazed biofilms of *P. aeruginosa*, *P. protegens* or the mixed species biofilm (Figure 4.2a). However, there were significant differences in the biovolumes of the ungrazed and grazed biofilms of *K. pneumoniae* (Figure 4.2a). Quantitative image analysis of the mixed species biofilm revealed that the biofilm biomass was 13% *K. pneumoniae*, 47% *P. protegens* and 40% *P. aeruginosa* (Figure 4.2b). Enumeration of *T. pyriformis* co-incubated with the *P. protegens* and *K. pneumoniae* biofilms revealed there were 9166 ± 678 and 49,577 ± 2272 cells mL^{-1}, respectively (Figure 4.2c). In addition, there were 37,000 ± 3300 cells mL^{-1} of *T. pyriformis* enumerated from controls consisting of M9 media and HKB (Figure 4.2c). In contrast, no *T. pyriformis* remained after co-incubation with the *P. aeruginosa* or mixed species biofilms, indicating toxicity of these biofilms towards the predator.'

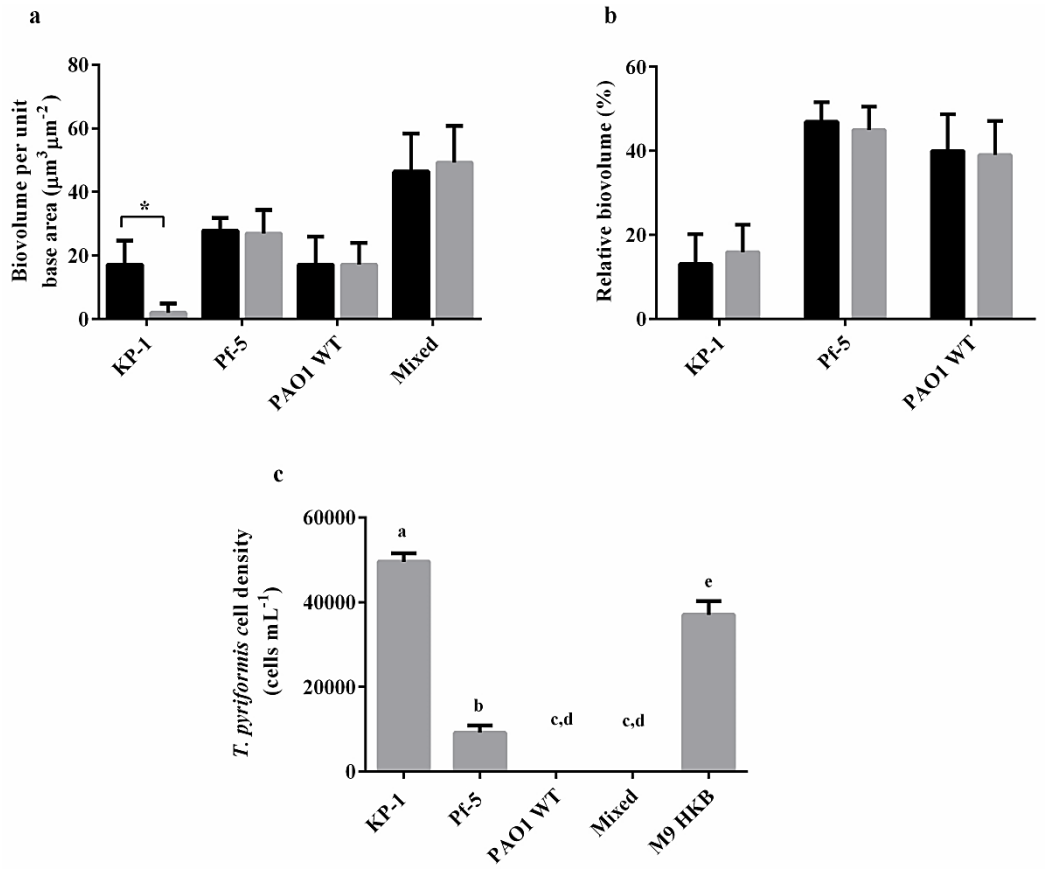

Figure 4.2: Predation of single and mixed species biofilms by *T. pyriformis*. (a) Biovolume per unit base area ($\mu m^3/\mu m^2$) of single and mixed species ungrazed (black bars) and grazed (grey bars) biofilms after 48 h (* $p < 0.05$). **(b)** Relative percent biovolume of *P. aeruginosa* PAO1, *P. protegens* Pf-5 and *K. pneumoniae* KP-1 in the mixed species biofilm after 48 h of grazing by *T. pyriformis*. **(c)** Enumeration of *T. pyriformis* in the grazed biofilms and M9 media controls with 10^8 cells mL^{-1} of HKB. Different letters indicate significant differences between groups in a one-way ANOVA. ($n = 3$) ($p \leq 0.0001$)

4.3.2. Toxicity of biofilm cell-free supernatants to *T. pyriformis*

To test for the presence of a secreted toxin that affects the survival of *T. pyriformis*, cell-free supernatants from single and mixed species biofilms were collected and added to cultures of *T. pyriformis*. Exposure to supernatants from ungrazed or grazed *P. aeruginosa* biofilms resulted in the death of the protist (Figure 4.3). In contrast, supernatants obtained from the mixed species biofilms containing *P. aeruginosa* did not demonstrate toxicity towards *T. pyriformis* (Figure 4.3). Enumeration of ciliates exposed to single species *P. protegens* or *K. pneumoniae* supernatants indicated that those supernatants were not toxic to *T. pyriformis* (Figure 4.3).

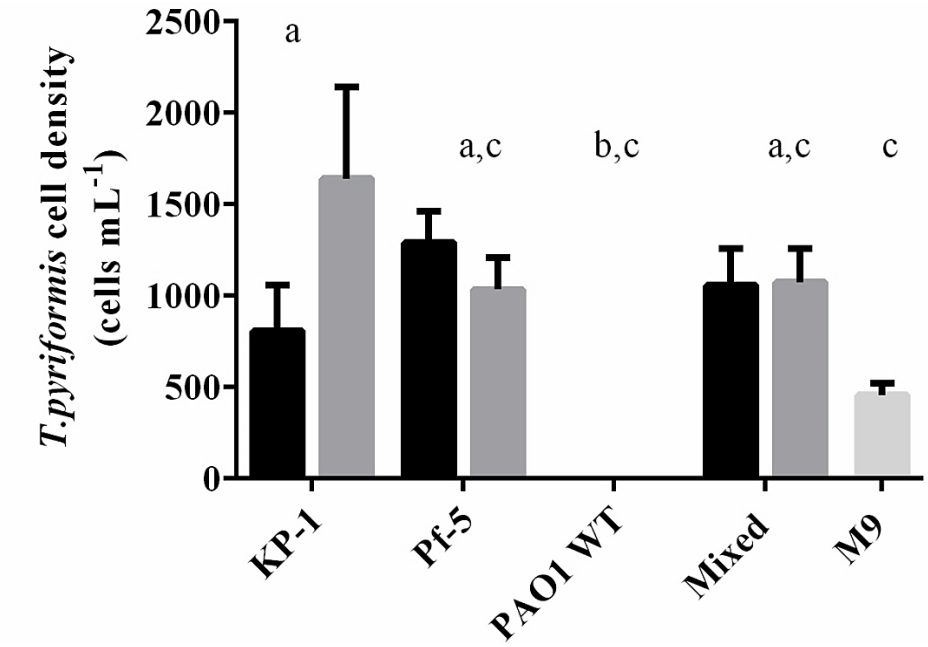

Figure 4.3: Enumeration of *T. pyriformis* exposed to cell-free supernatants from single and mixed species biofilms. Different letters indicate significant differences between groups in a one-way ANOVA. ($n = 3$) ($p \leq 0.0001$).

4.3.3. The effect of rhamnolipids on the predation resistance of biofilms

The toxicity of the cell-free supernatants from *P. aeruginosa* biofilms indicated that the anti-protozoan activity was due to a secreted factor. It is known that rhamnolipids are secreted by *P. aeruginosa* biofilms, thus, to determine if rhamnolipid production is the anti-protozoal compound, *T. pyriformis* was exposed to a biofilm of a *P. aeruginosa ΔrhlA* strain that is defective for rhamnolipid production. Confocal imaging of the single and mixed species biofilms of *P. aeruginosa ΔrhlA* revealed that there was no observable reduction in biomass of the grazed biofilms (Figure 4.4a and b).

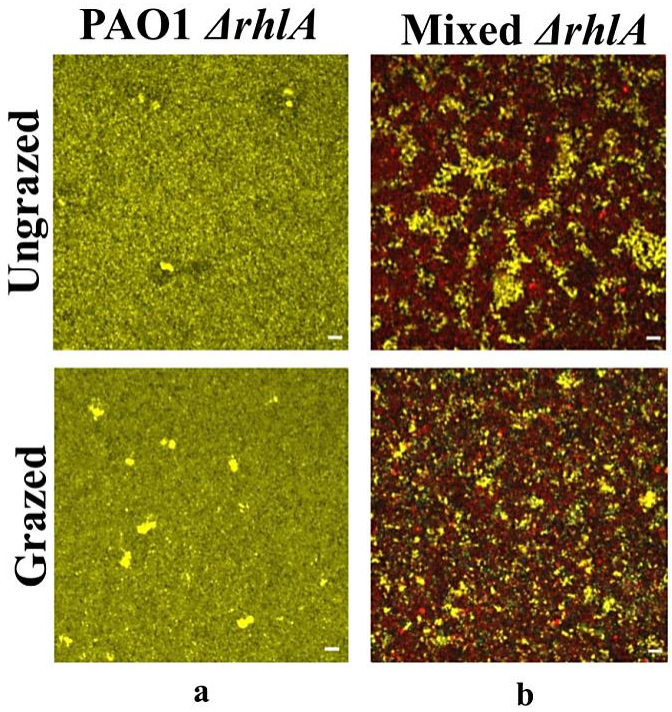

Figure 4.4: Confocal micrographs of ungrazed and grazed single and mixed species biofilms of *P. aeruginosa* (PAO1 ΔrhlA, yellow) *P. protegens* (Pf-5, cyan) and *K. pneumoniae* (KP-1, red). Ungrazed biofilms were grown for 96 h while grazed biofilms were grown for 48 h before *T. pyriformis* was added and co-incubated for 48 h. Panels (a and b) show the differences in biomass between the ungrazed and grazed single and mixed species biofilms. Magnification: 20 ×. Scale bar: 20 µm.

Quantitative image analysis showed that despite the lack of rhamnolipid production, the biovolumes of ungrazed and grazed single species biofilms of *P. aeruginosa ΔrhlA* were not significantly different (Figure 4.5a), indicating that these biofilms are resistant to predation. In contrast to the single species biofilm, the mixed species biofilm containing *P. aeruginosa ΔrhlA* did not exhibit the same level of toxicity, as the number of *T. pyriformis* was 750 ± 876 cells mL^{-1} after co-incubation for 48 h (Figure 4.5b). The *P. aeruginosa ΔrhlA* mutant strain comprised only 22% of the biofilm biomass in the mixed biofilm compared to 39 % for the WT strain (Figure 4.5c). There was also no significant difference in the proportion of *P. aeruginosa*, *P. protegens* or *K. pneumoniae* in the ungrazed and grazed biofilms. Cell-free supernatants obtained from both *P. aeruginosa ΔrhlA* ungrazed and grazed biofilms were less toxic to *T. pyriformis* than the wild type *P. aeruginosa* (Figure 4.5d), indicating that rhamnolipids do conferring grazing resistance to the single species biofilms. Interestingly, the single species biofilm of *P. aeruginosa ΔrhlA* was still grazing resistant despite the loss of rhamnolipid production (Figure 4.5a), suggesting that there is another mechanism for predation resistance expressed by *P. aeruginosa ΔrhlA* biofilms.

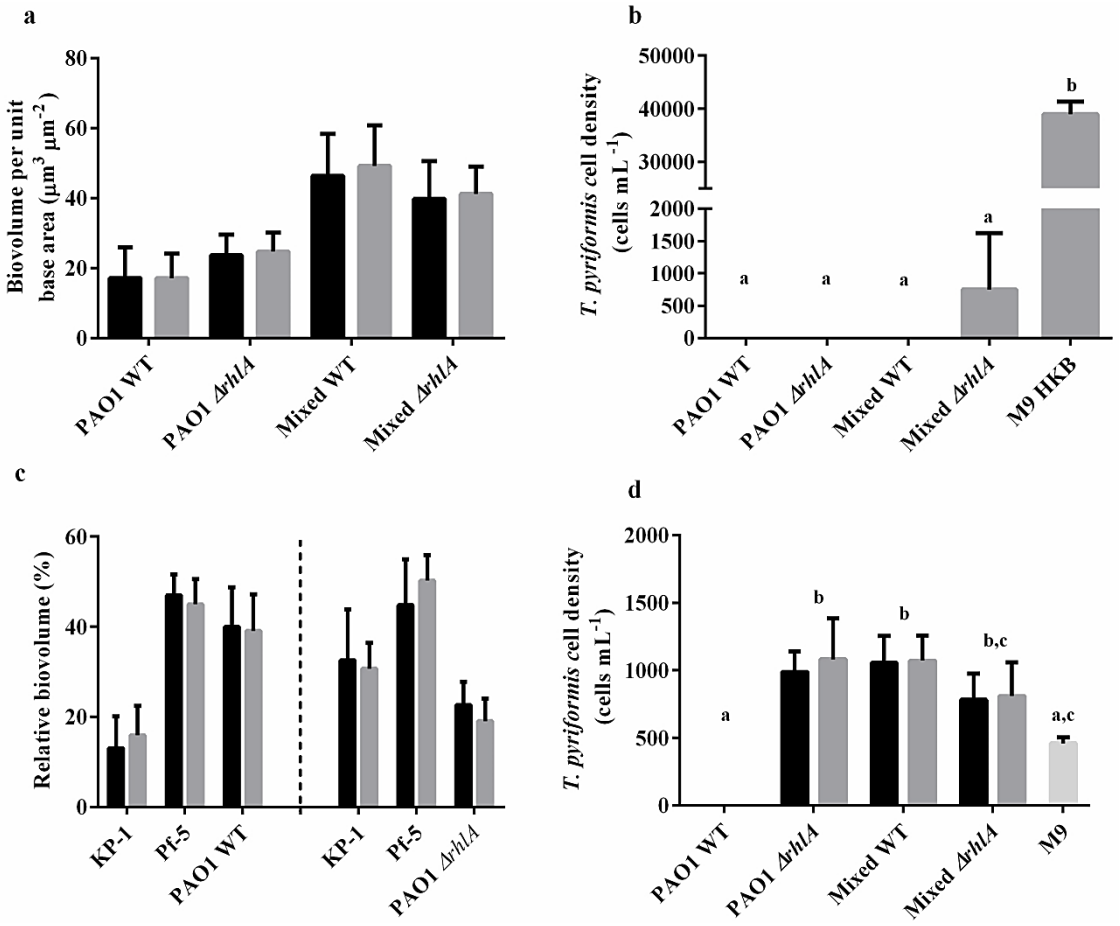

Figure 4.5: *T. pyriformis* predation on single and mixed species biofilms containing the *P. aeruginosa ΔrhlA* mutant. (a) Biovolume per unit base area ($\mu m^3/\mu m^2$) of ungrazed (black bars) and grazed (grey bars) biofilms after 48 h. (b) Enumeration of *T. pyriformis* in the grazed biofilms and M9 media controls with 10^8 cells mL^{-1} of HKB. (c) Relative percent biovolume of *P. aeruginosa* PAO1, *P. protegens* Pf-5 and *K. pneumoniae* KP-1 in the mixed species biofilm after 48 h of grazing by *T. pyriformis***.** (d) Enumeration of *T. pyriformis* exposed to cell-free supernatants from single and mixed species biofilms. Different letters indicate significant differences between groups in a one-way ANOVA. (n = 3) ($p \leq 0.0001$) (n = 3) ($p \leq 0.0001$).

4.3.4. Role of type III secretion system in predation resistance

Despite the absence of rhamnolipids, a single species biofilm formed by the *P. aeruginosa ΔrhlA* mutant was grazing resistant. Supernatants from the *ΔrhlA* strain were

not toxic to *T. pyriformis,* which suggested the possibility of a contact-dependent resistance mechanism. It has been previously reported that the type III secretion system was important for protecting *P. aeruginosa* late stage biofilms from predation by amoebae (Matz et al. 2008a). Hence, a mutant defective in the type III secretion system (*pscJ*) and a double mutant in *rhlA* and *pscJ* were constructed and their grazing resistance in single and mixed species biofilms tested. Confocal imaging of the single and mixed species biofilms of *P. aeruginosa ΔrhlA ΔpscJ* revealed that there was no observable reduction in biomass of the grazed biofilms (Figure 4.6a to d).

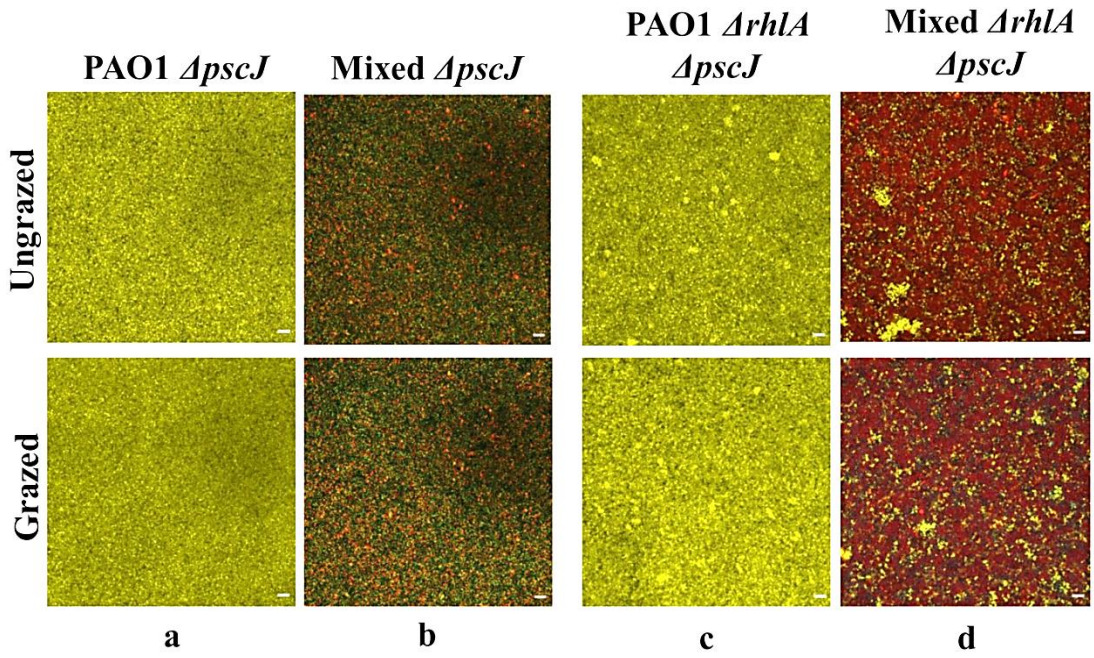

Figure 4.6: Confocal micrographs of ungrazed and grazed single and mixed species biofilms of *P. aeruginosa* (PAO1 Δ*pscJ*, PAO1 *ΔrhlA ΔpscJ* yellow), *P. protegens* (Pf-5, cyan) and *K. pneumoniae* (KP-1, red). Ungrazed biofilms were grown for 96 h while grazed biofilms were grown for 48 h before *T. pyriformis* was added and co-incubated for 48 h. Panels (a to d) show the differences in biomass between the ungrazed and grazed single and mixed species biofilms. Magnification: 20 ×. Scale bar: 20 µm.

Quantitative image analysis with one-way ANOVA comparisons of the biovolumes of the ungrazed and grazed biofilms indicated no significant differences (Figure 4.7a). The proportion of *P. aeruginosa ΔpscJ* in the mixed species biofilm consortia was 37%, which was similar to 39% for the *P. aeruginosa* WT in the mixed species biofilms. In contrast, the proportion of the *P. aeruginosa ΔrhlA ΔpscJ* strain was 13% in the mixed species biofilms compared to 22% and 39% for the *P. aeruginosa ΔrhlA* and *P. aeruginosa* WT strains, respectively (Figure 4.7b). No *T. pyriformis* were detected after co-incubation with the single or mixed species biofilms of the *pscJ* mutant (Figure 4.7c). Similarly, there were no viable *T. pyriformis* in the *P. aeruginosa ΔrhlA ΔpscJ* single species biofilms. However, when *P. aeruginosa ΔrhlA ΔpscJ* was grown as part of a mixed species biofilm, the number of *T. pyriformis* was 749 ± 150 cells mL^{-1}. Furthermore, filtered supernatants obtained from the *P. aeruginosa ΔrhlA ΔpscJ* single and mixed species biofilms were not toxic for *T. pyriformis* (Figure 4.7d). In contrast, filtered supernatants obtained from the *P. aeruginosa ΔpscJ* single species biofilm remained toxic towards *T. pyriformis* (Figure 4.7d) which was probably due to the production of rhamnolipids by the *pscJ* mutant.

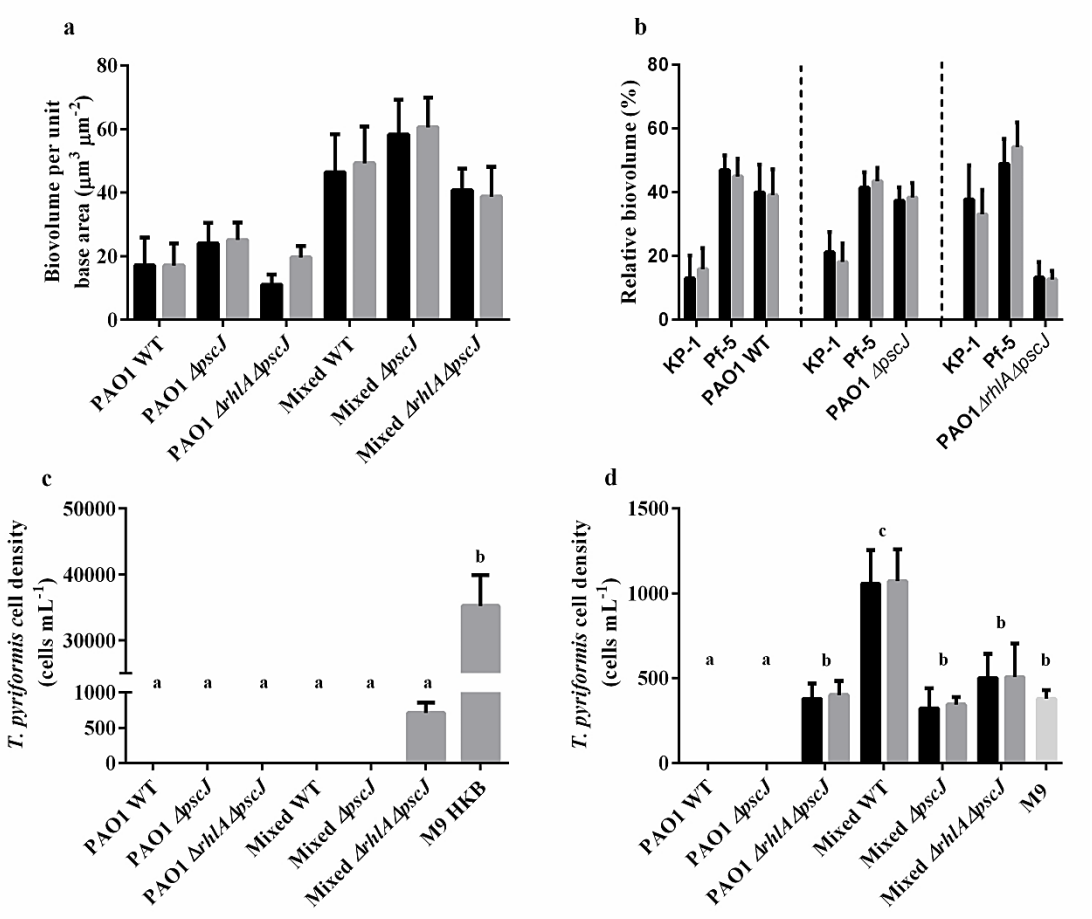

Figure 4.7: *T. pyriformis* predation on single and mixed species biofilms containing the *P. aeruginosa ΔrhlA ΔpscJ* mutant. (a) Biovolume per unit base area ($\mu m^3/\mu m^2$) of ungrazed (black bars) and grazed (grey bars) biofilms after 48 h. (b) Relative percent biovolume of *P. aeruginosa* PAO1, *P. protegens* Pf-5 and *K. pneumoniae* KP-1 in the mixed species biofilm after 48 h of grazing by *T. pyriformis*. (c) Enumeration of *T. pyriformis* in the grazed biofilms and M9 media controls with 108 cells mL^{-1} of heat killed bacteria (HKB). (d) Enumeration of *T. pyriformis* exposed to cell-free supernatants from single and mixed species biofilms. Different letters indicate significant differences between groups in a one-way ANOVA ($n = 3$) ($p \leq 0.0001$).

4.3.5. Toxicity of purified rhamnolipids to *T. pyriformis*

To confirm the toxicity of rhamnolipids to *T. pyriformis*, the minimum inhibition concentration (MIC) of rhamnolipids for *T. pyriformis* was determined and found to be 0.03 g L^{-1} (Figure 4.8). At this concentration of rhamnolipids, the *T. pyriformis* cells swelled and lysed immediately upon contact.

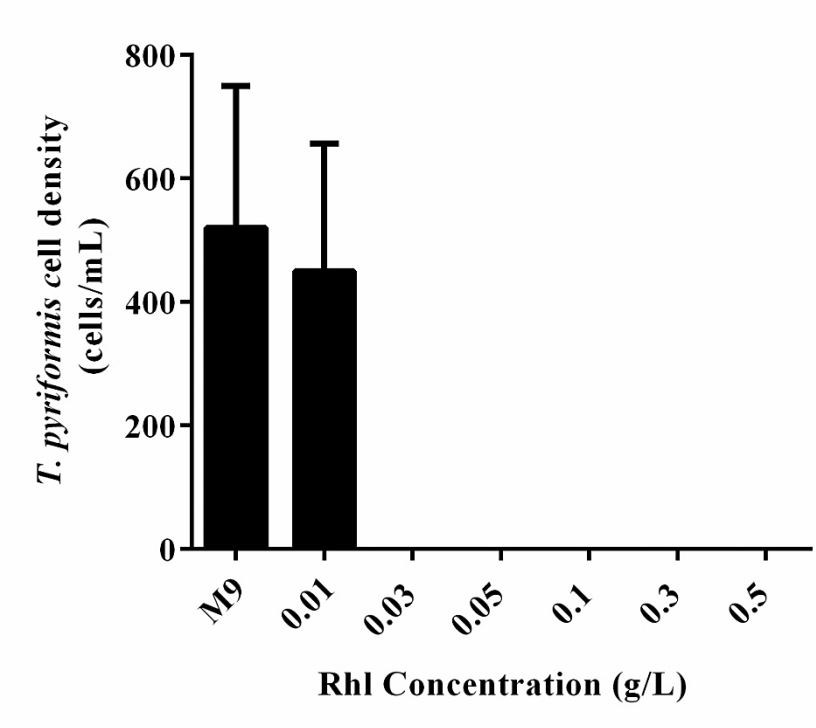

Figure 4.8: The effectiveness of purified rhamnolipids at lysing *T. pyriformis*. A minimum concentration of 0.03 g L^{-1} was found to be effective in lysing the ciliate (n =3).

4.3.6. Quantification of biofilm rhamnolipids

The amount of rhamnolipids produced by the single and mixed species biofilms were quantified using the orcinol assay (Choi and Schweizer 2005). No rhamnolipids were detected in the biofilms containing *P. aeruginosa ΔrhlA,* with the exception of the mixed species biofilm where minute quantities were detected (Figure 4.9). Mixed species

biofilms formed with either *P. aeruginosa ΔpscJ* or WT strains produced rhamnolipids ranging from approximately 5 to 8 g L^{-1} (Figure 4.9). The levels of rhamnolipid did not differ significantly between grazed and ungrazed biofilms. The amount of rhamnolipids produced in the single species biofilms was at least 10 fold greater than in the mixed species biofilms. While single species biofilms of *K. pneumoniae* did not produce any rhamnolipids, *P. protegens* biofilms produced 6.94 ± 5.12 g L^{-1} and 8.03 ± 8.33 g L^{-1} of rhamnolipids in the ungrazed and grazed biofilms respectively.

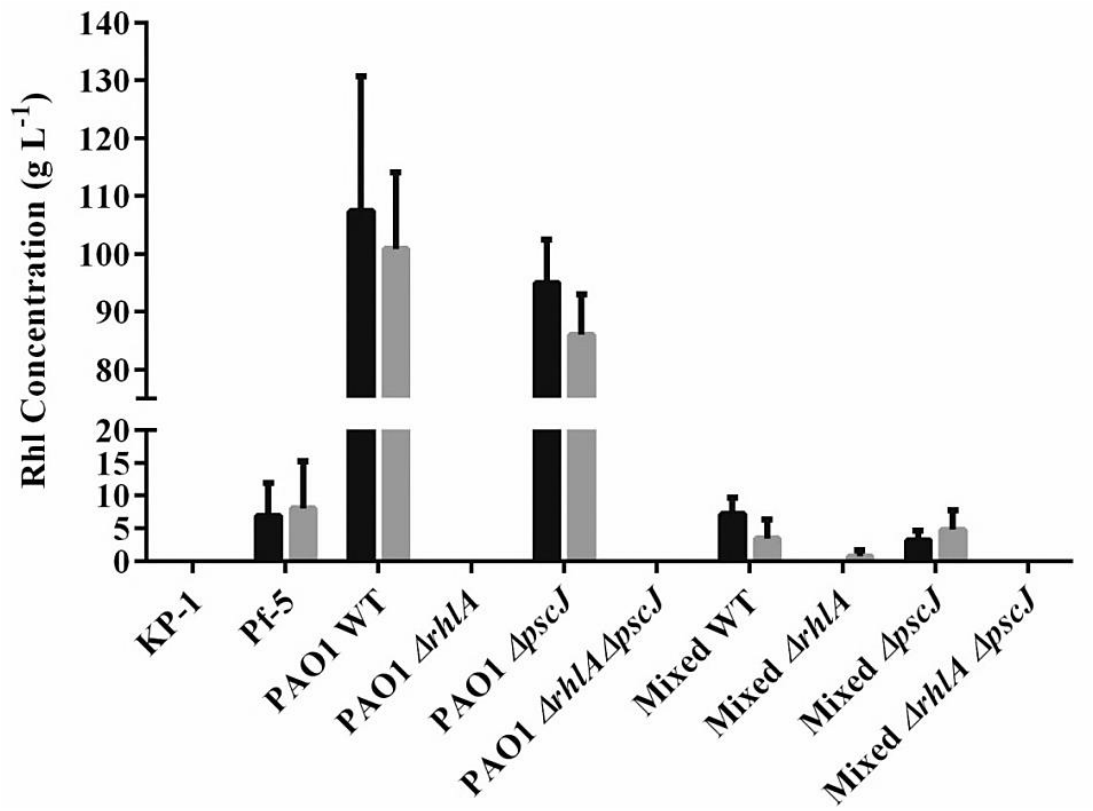

Figure 4.9: Rhamnolipid quantification from single and mixed species biofilms. Ungrazed biofilms were grown for 96 h while grazed biofilms were grown for 48 h before *T. pyriformis* was added and co-incubated for 48 h. The concentration of rhamnolipids produced by the biofilms was subsequently quantified by orcinol assays (n =3).

4.4. Discussion

Biofilms typically exist as mixed species consortia, which can lead to increased biofilm biomass. When *P. aeruginosa*, *P. protegens* and *K. pneumoniae* were grown together as a mixed species biofilm, the resulting biomass was greater than the sum of the single species biofilms, which agrees with previous observations (Lee et al. 2014) and of others (Madsen et al. 2016, Røder et al. 2015). Mixed species biofilms have also been found to have increased resistance to a variety of stresses compared to single species biofilms (Burmølle et al. 2006, Lee et al. 2014, van der Veen and Abee 2011). Here , the ability of a mixed species microbial community containing *P. aeruginosa*, *P. protegens* and *K. pneumoniae* to withstand protozoan grazing by the filter-feeding ciliate, *T. pyriformis* were investigated.

It has previously been shown that 3 d *P. aeruginosa* biofilms co-incubated with the surface feeding flagellate, *R. nasuta,* resulted in the death of the flagellate within 24 h (Matz et al. 2004). The grazing resistance of the *P. aeruginosa* WT biofilm was attributed to the formation of microcolonies and possible expression of virulence factors (e.g. rhamnolipids and pyocyanins) that are regulated by the *las* and *rhl* quorum sensing systems (Pesci et al. 1997). Results presented here demonstrate that single species biofilms of *P. aeruginosa* are also resistant to predation by *T. pyriformis*, as the biofilm biomass was unaffected by grazing (Figures 4.1c, 4.1g, 4.1k and 4.2a). When *P. aeruginosa* was grown together with the grazing sensitive *P. protegens* and *K. pneumoniae* in a mixed species biofilm, all species in the biofilm were protected, indicating that *P. aeruginosa* provides associational resistance in mixed species biofilms. In contrast, a mixed species biofilm consisting of *K. pneumoniae, P. protegens* and *Staphylococcus epidermidis* was found to be sensitive to protozoan grazing by both *Acanthamoeba castellanii* and *Colpoda maupasi* (Huws et al. 2005). Here, it was

demonstrated that *P. aeruginosa* may be a beneficial member in a mixed species biofilm under predation pressure, as *T. pyriformis* has been shown to be an effective predator of biofilms (Dopheide et al. 2011b, Parry 2004) (Figure 4.2a).

Cell-free supernatants obtained from *P. aeruginosa* biofilms were found to be toxic for *T. pyriformis* (Figure 4.3), suggesting the presence of secreted antiprotozoal compounds. Rhamnolipids secreted by *P. aeruginosa* have been shown to cause lysis of polymorphonuclear leukocytes (PMNs) (Jensen et al. 2007, Van Gennip et al. 2009) and monocyte macrophages (McClure 1992). Rhamnolipids have also been suggested to function as a "biofilm shield", which significantly reduces the ability of PMNs to attack biofilm cells (Van Gennip et al. 2009). It was reported that 0.01 g L^{-1} of purified rhamnolipids from *P. aeruginosa* resulted in the lysis of the amoeba, *Dictyostelium discoideum*, while supernatant obtained from a *rhlA* mutant strain did not cause lysis (Cosson et al. 2002). In addition, epithelial cells exposed to rhamnolipids demonstrated a loss of cilia and alterations to the tight junctions between epithelial cells, which resulted in increased permeability of the epithelia (Zulianello et al. 2006). Hence, it was likely that the swelling and subsequent lysis of *T. pyriformis* was due to the increased permeability of the cell membranes after rhamnolipid exposure. Thus, the role of rhamnolipids produced by *P. aeruginosa* in providing overall biofilm grazing resistance was investigated.

The results presented here confirm that the production of rhamnolipids by *P. aeruginosa* biofilms is a defense mechanism against *T. pyriformis* grazing, as 0.03 g L^{-1} of purified rhamnolipids (di-rhamnolipid dominant) was sufficient to kill *T. pyriformis* (Figure 4.8). The amount of rhamnolipids present in the supernatants of single and mixed species biofilms greatly exceeded the amount of rhamnolipids required to kill *T. pyriformis*

(Figure 4.9). *P. protegens* has not been shown to produce rhamnolipids, however, the orcinol extraction of the biofilm supernatant indicated that rhamnolipids were present. *P. protegens* produces a class of *amphiphilic* molecules known as cyclic lipopeptides (CLPs) which are similar to rhamnolipids. These CLPs are known to negatively affect protozoan predators such as *A. castellanii* (Jousset et al. 2010). Hence, these lipopeptides may have been detected in the orcinol assay.

The supernatant from the mixed species biofilm was not as toxic as the supernatant from the *P. aeruginosa* biofilms (Figure 4.3), as there was 10 fold less rhamnolipid in the mixed biofilm supernatant (Figure 4.9). *P. aeruginosa* has been demonstrated to upregulate rhamnolipid synthesis in the presence of PMNs (Alhede et al. 2009). In contrast, no significant difference was detected between the concentration of rhamnolipids produced by ungrazed and grazed biofilms, indicating that rhamnolipid production was not induced by the presence of *T. pyriformis*. Regardless, it is clear that production of rhamnolipid by *P. aeruginosa* plays a partial role in protecting the biofilm against *T. pyriformis* grazing.

Despite the lack of rhamnolipid production, the single species biofilms of *P. aeruginosa ΔrhlA* was resistant to *T. pyriformis* grazing (Figure 4.5a), while the cell-free supernatant from the *ΔrhlA* mutant strain was non-toxic (Figures 4.5d). Thus, the role of the type III secretion system (T3SS) in predation resistance was investigated. The T3SS is a contact-based defense system that has been shown to be involved in killing the amoeba *A. castellanii* and *D. discoideum* (Matz et al. 2008a, Pukatzki et al. 2002). The T3SS produces needle-like structures on the bacterial cell surface that injects effector proteins into eukaryotic cells that they come in contact with (Hauser 2009). These effector proteins, i.e. ExoT and ExoU, are associated with rapid cell death of eukaryotic cells

(Hauser 2009). Here, both mixed and single species biofilms containing a *P. aeruginosa* strain deficient in both T3SS and rhamnolipid production remained grazing resistant (Figure 4.7a). It is unlikely that the observed resistance could be attributed to any secreted compounds as the supernatant of both the single and mixed species biofilms containing the double mutant showed no signs of toxicity towards *T. pyriformis* (Figure 4.7d). Although the specific mechanism of resistance is still unknown, it is likely that the resistance observed in the biofilm could be mediated by the type VI secretion system (T6SS).

Although the total biovolume for all combinations of the mixed species consortia remained the same, the defect in *rhlA* resulted in a reduction in the ratio of *P. aeruginosa* from 39 % in the mixed species WT to 22% and 13% for *ΔrhlA* and *ΔrhlA ΔpscJ* biofilms respectively (Figures 4.2b, 4.5c, 4.7b). Rhamnolipids are known to affect microbial adhesion and biofilm development (Pamp and Tolker-Nielsen 2007). Inactivating the *rhlA* gene would inhibit swarming motility and reduce twitching motility (Caiazza et al. 2005), both forms of which are essential for the initial development of *P. aeruginosa* microcolonies (Pamp and Tolker-Nielsen 2007). Furthermore, rhamnolipids also exhibit antibacterial properties (El-Sheshtawy and Doheim 2014). Thus, the lack of rhamnolipids may have affected the ability of *P. aeruginosa* to form a mixed species biofilm. Furthermore, the decline in *P. aeruginosa* biomass resulted in an increase in *K. pneumoniae* biomass on the surface of the biofilm (Figure 4.4b) Therefore, it is possible that the localization of *K. pneumoniae* reduced the contact between *P. aeruginosa* and *T. pyriformis*, which resulted in lowered mortality of the predators.

In conclusion, the presence of *P. aeruginosa* within the mixed species biofilm provides associational resistance to other members of the microbial community against protozoan

grazing. Additionally, rhamnolipids were demonstrated to be a protective mechanism against the predation, although additional unidentified protective mechanisms also exist. These protective mechanisms in *P. aeruginosa* also play a role in the interspecies interactions indicating that diverse factors influence mixed microbial communities.

Chapter 5: GENERAL DISCUSSION AND CONCLUSIONS

5.1. General Discussion

Protozoan predation is one of the major contributors towards bacterial mortality in many environments. In activated sludge, protozoa are suggested to play a primary role in predation of suspended bacteria, which is essential for clarification of the effluent (Luxmy et al. 2000, Madoni 2003). Bacteria may respond to protozoan predation by changing their morphology, e.g. formation of inedible filaments and microcolonies, which promotes the formation of biofilms (Hahn and Höfle 2001, Matz et al. 2004, Michaela et al. 2005). In addition, mucus and waste material secreted by protozoa may accumulate in the surrounding environment and act to nucleate bacterial interactions (Curds 1963, Neville 1946). Hence, protozoan predation is suggested to improve flocculation of bacteria and the formation of biofilms (Bossier and Verstraete 1996, Curds 1963, Curds 1982). Previous studies have also demonstrated that sessile ciliates are the most dominant type of protozoa on the surfaces of granules (Lemaire et al. 2008a, Li et al. 2013, Weber et al. 2007, Winkler et al. 2012). These sessile ciliates were hypothesized to be the primary consumers of suspended bacteria and were suggested to act as a substratum for the attachment of bacteria, which would lead to granule initiation and further expansion. However, these hypotheses have not been fully explored as they were based mainly on microscopic observations and physical measurements of effluent quality such as turbidity. Hence, more studies are needed to better elucidate the role of protozoa in the formation of granules from floccular sludge.

In addition, despite the implementation of well-defined operating conditions, the use of aerobic granules remains restricted for full-scale wastewater treatment due to their instability and the long time required for initial granule formation (Adav et al. 2010a,

Adav et al. 2010b). The dense and compact structure of granules have been hypothesized to provide increased protection for bacterial communities against predation (Feng et al. 2017). However, predation by predatory bacteria resulted in significant reductions in both microbial activity and total biomass in floccular and granular sludge, which could negatively affect the performance of the wastewater treatment process (Feng et al. 2017). Other predators of bacteria, such as bacteriophage, also exist in high abundance in wastewater treatment systems (Shapiro et al. 2009, Wu and Liu 2009). In enhanced biological phosphorus removal (EBPR) systems, *Candidatus Accumulibacter* is often enriched as they have a key role in phosphorus removal (Lu et al. 2006, Martin et al. 2006). However, enrichments of *Candidatus Accumulibacter* are highly susceptible to phage predation. Floccular and granular sludge infected with *Candidatus Accumulibacter*-associated phages rapidly caused a decline in *Candidatus Accumulibacter* populations, which subsequently resulted in significant deterioration in phosphorus removal. These studies demonstrated that predation have significant impacts on both floccular and granular sludge. Hence, experimental studies on how protozoan predation affects biofilm development and stability would potentially provide insights on improving the aerobic granulation process.

Here, the diversity and abundance of both protozoa and bacteria were characterized and monitored throughout the process of aerobic granulation via both microscopic analyses and total RNA sequencing (Chapter 2). Both methods indicated that the diversity of protozoa was the greatest during the floccular phase and gradually declined as the sludge transited into the granule maturation phase. Total RNA sequencing indicated that the most dominant group of protozoa was *Ciliophora*, i.e. ciliated protozoa. During the granulation process, there was a continual shift in the type and abundance of ciliates. This was likely to have been due to the increase in compactness and size of particles as the flocs changed

to granules. The development of granules also resulted in the emergence of sessile ciliates as the dominant group of protozoa which colonized the surface of granules. The abundance of sessile ciliates on the surface of granules was consistent with other studies (Lemaire et al. 2008a, Li et al. 2013, Schwarzenbeck et al. 2004b, Weber et al. 2007). However, the changes in the protozoan community and dominance of sessile ciliates on granules had no correlation with the process of granulation. The role of protozoan predation in aerobic granulation was further investigated by the comparison between thiram treated and non-treated floccular sludge in mini-SBRs (Chapter 3). The inhibition of protozoa by thiram showed that the absence of protozoa resulted in a delay in the initiation phase of the treated floccular sludge (Chapter 3). However, the delay in the progression to initiation did not ultimately affect the formation of aerobic granules. Furthermore, the inhibition or killing off of protozoa, sessile ciliates in particular, on granules did not result in disintegration of granules.

The data presented in Chapters 2 and 3 show that the formation of granules was found to be linked strongly with the abundance of *Candidatus Accumulibacter* and *Candidatus Competibacter*. However, correlation studies demonstrated that only *Candidatus Accumulibacter* was positively correlated with granulation (Chapter 2). Based on the localization studies of SNDPR granules from Lemaire et al. (2008), it was hypothesized that the anoxic/anaerobic granular core would be dominated by *Candidatus Competibacter* while the outer aerobic layer would be dominated by *Candidatus Accumulibacter*. Indeed, the high abundance of *Candidatus Accumulibacter* was also observed in both the untreated and thiram treated sludge, particularly when the treated sludge granulated (Chapter 3). To better understand the difference in the untreated and treated sludge, the structure of both flocs and granules by fluorescence in situ hybridization (FISH) on flocs and cryosectioned granules. This method would provide

insight on the microbial distribution on the different layers within both flocs and granules during the granulation process (Lemaire et al. 2008a, Weber et al. 2007). Extracellular polysaccharides (EPS) have also been demonstrated to contribute positively towards the formation and stability of granules (Adav et al. 2008a, Adav et al. 2008b, Tay et al. 2001b). Granules subjected to EPS hydrolysis were observed to undergo fragmentation (Adav et al. 2008b). Hence, future work could include both FISH on sludge particles throughout granulation and also the tracking of the production of EPS during aerobic granulation.

Quorum sensing may also be involved in the granulation of treated sludge, i.e. in the absence of protozoan predation. Quorum sensing has been described previously to be an important mediating factor for biofilm development (Li and Tian 2012, Ng and Bassler 2009, Tan et al. 2014). Specific N-acyl-homoserine-lactones (AHL) were previously shown to be at high concentration and strongly associated with the initiation of aerobic granulation (Tan et al. 2014). Furthermore, exogenous addition of AHLs that were highly abundant during aerobic granulation, resulted in an increased in floc-associated EPS (Tan et al. 2014). In contrast, quorum quenching was found to suppress quorum sensing signal accumulation in floccular sludge, which inhibited the formation of aerobic granules (Tan et al. 2015). Exogenous addition of quorum quenchers quenched AHLs and delayed the development of biofilms on membranes (Yeon et al. 2009). The data presented here indicated that bacteria, particularly *Candidatus Accumulibacter,* coupled with well-established physical factors, such as settling time and hydrodynamic shear force, were highly important for the formation of granules in SNDPR systems. It was more likely the morphological change from flocs to granules that resulted in a form of selection pressure on the protozoan community, rather than predation that enhanced the formation of granules. While protozoan predation was not necessary for the formation of granules from

floccular sludge, the presence of protozoa may enhance and speed up this process. This is supported by the observations above, where granulation was slightly delayed in the absence of predators.

Traditionally, the majority of predation studies have been performed on single species biofilms. However, both activated floccular sludge and aerobic granular sludge are complex engineered ecosystems that consist of highly diverse microbial communities. Hence, to better represent and define how protozoan predation affects the development of highly diverse biofilms, a mixed species biofilm consisting of *Pseudomonas aeruginosa*, *Klebsiella pneumoniae* and *Pseudomonas protegens* were subjected to grazing to the heterotrophic ciliate, *Tetrahymena pyriformis,* that feeds both on planktonic cells and early biofilms (Chapter 4). In essence, grazing sensitive strains were able to gain associational grazing resistance from defended strains. Previous studies have also demonstrated that a single resistant species was able to confer protection to sensitive members within a biofilm (Burmølle et al. 2006, Kara et al. 2006, Lee et al. 2014). Here, the grazing resistance provided by the *P. aeruginosa* was not only limited to a single mechanism. It would be interesting to elucidate the yet unidentified factors that provided resistance to the grazing resistance strain. One possible mechanism of resistance could be the type VI secretion system, which resembles a phage tail and is capable of transporting toxic proteins from the host bacterial cell into eukaryotic cells (Schwarz et al. 2010). The expression of type VI secretion system in *P. aeruginosa* was found to be regulated by quorum sensing (Hood et al. 2010, Lesic et al. 2009). Quorum-mediated defense mechanisms were also demonstrated in *P. aeruginosa* where grazing resistant microcolonies were formed in the presence of predatory flagellates (Matz et al. 2004). In contrast, quorum sensing mutants formed fewer and smaller microcolonies when co-incubated with predatory flagellates (Matz et al. 2004).

Quorum sensing could also regulate the morphology and architecture in biofilms as observed in *Serratia marcescens* (Rice et al. 2005). In the presence of rich media, *S. marcescens* biofilms displayed a filamentous morphology while microcolonies were formed under low nutrient conditions (Rice et al. 2005). In floccular and granular sludge which are constantly fed with nutrient rich wastewater, it is likely that groups of different bacteria will be able to convert into the filamentous or microcolony phenotype. The formation of filaments and microcolonies can increase the resistance of bacteria to protozoan predation (Hahn et al. 1999, Rønn et al. 2002). Moreover, these filaments or microcolonies could aid in the initiation of biofilm formation, such as the initial conversion from flocs to aggregates. Hence, predation studies on single or mixed species biofilms provide insights on the interactions between bacteria and protozoa, which can be applied to improve the stability of complex biofilm systems such as aerobic granules.

5.2. Conclusions

Protozoa predation has been demonstrated to be a non-significant factor in the development of aerobic granules from activated sludge. In contrast, it was *Candidatus Accumulibacter* from the phylum *Proteobacteria* and other major bacterial groups coupled with operating conditions of the SBRs that appeared to be the primary drivers of the aerobic granulation process. The findings here further the current understanding of the role that protozoa play in driving initiation and maintenance of aerobic granules. The role of fungi in aerobic granulation remains to be further investigated as they were also shown to correlate positively with granulation.

The role of protozoan predation in the development of biofilms was also evaluated using less complex defined biofilms. The results from single and mixed species biofilms also demonstrated that a single grazing resistant species was able to protect other sensitive

members in the biofilms. However, only one mechanism of resistance has been elucidated. More work would have to be done to elucidate the remaining mechanisms of resistance. Ultimately, the understanding of the interactions between protozoa and bacteria would be useful in enhancing the stability of granules for long term operations in full-scale wastewater treatment plants.

References

Acton QA (2012). *Issues in Global Environment: Pollution and Waste Management: 2011 Edition*. ScholarlyEditions.

Adav SS, Lee D-J, Show K-Y, Tay J-H (2008a). Aerobic granular sludge: Recent advances. *Biotechnology Advances* **26:** 411-423.

Adav SS, Lee D-J, Tay J-H (2008b). Extracellular polymeric substances and structural stability of aerobic granule. *Water Research* **42:** 1644-1650.

Adav SS, Lee D-J, Lai J-Y (2010a). Potential cause of aerobic granular sludge breakdown at high organic loading rates. *Applied Microbiology and Biotechnology* **85:** 1601-1610.

Adav SS, Lee D-J, Lai JY (2010b). Microbial community of acetate utilizing denitrifiers in aerobic granules. *Applied Microbiology and Biotechnology* **85:** 753-762.

Al-Shahwani SM, Horan NJ (1991). The use of protozoa to indicate changes in the performance of activated sludge plants. *Water Research* **25:** 633-638.

Alhede M, Bjarnsholt T, Jensen PO, Phipps RK, Moser C, Christophersen L *et al* (2009). *Pseudomonas aeruginosa r*ecognizes and responds aggressively to the presence of polymorphonuclear leukocytes. *Microbiology* **155:** 3500-3508.

Anderson OR (2001). Protozoan Ecology. *eLS*. John Wiley & Sons, Ltd.

Aqeel H, Basuvaraj M, Hall M, Neufeld JD, Liss SN (2016). Microbial dynamics and properties of aerobic granules developed in a laboratory-scale sequencing batch reactor with an intermediate filamentous bulking stage. *Applied Microbiology and Biotechnology* **100:** 447-460.

Arndt H, Schmidt-Denter K, Auer B, Weitere M (2003). Protozoans and Biofilms. In: Krumbein WE, Paterson DM, Zavarzin GA (eds). *Fossil and Recent Biofilms: A Natural History of Life on Earth*. Springer Netherlands: Dordrecht. pp 161-179.

Arnold E, Böhm B, Wilderer PA (2000). Application of activated sludge and biofilm sequencing batch reactor technology to treat reject water from sludge dewatering systems: a comparison. *Water Science and Technology* **41:** 115.

Augustin H, Foissner W (1992). Morphology and ecology of some ciliates (Protozoa Ciliophora) from activated sludge. *Archiv für Protistenkunde* **141:** 243-283.

Barbeau J, Buhler T (2001). Biofilms augment the number of free-living amoebae in dental unit waterlines. *Research in Microbiology* **152:** 753-760.

Barcina I, Ayo B, Muela A, Egea L, Iriberri J (1991). Predation rates of flagellate and ciliated protozoa on bacterioplankton in a river. *FEMS Microbiology Letters* **85:** 141-149.

Barr JJ, Cook AE, Bond PL (2010a). Granule formation mechanisms within an aerobic wastewater system for phosphorus removal. *Applied and Environmental Microbiology* **76:** 7588-7597.

Barr JJ, Slater FR, Fukushima T, Bond PL (2010b). Evidence for bacteriophage activity causing community and performance changes in a phosphorus-removal activated sludge. *FEMS Microbiology Ecology* **74:** 631-642.

Bass D, Chao EEY, Nikolaev S, Yabuki A, Ishida K-i, Berney C *et al* (2009). Phylogeny of novel naked filose and reticulose *Cercozoa*: *Granofilosea* cl. n. and *Proteomyxidea* revised. *Protist* **160:** 75-109.

Bassin JP, Kleerebezem R, Dezotti M, van Loosdrecht MCM (2012). Simultaneous nitrogen and phosphate removal in aerobic granular sludge reactors operated at different temperatures. *Water Research* **46:** 3805-3816.

Bertanza G (1997). Simultaneous nitrification-denitrification process in extended aeration plants: pilot and real scale experiences. *Water Science and Technology* **35:** 53-61.

Beun JJ, Hendriks A, Van Loosdrecht MCM, Morgenroth E, Wilderer PA, Heijnen JJ (1999). Aerobic granulation in a sequencing batch reactor. *Water Research* **33:** 2283-2290.

Biswas K, Turner SJ (2012). Microbial community composition and dynamics of moving bed biofilm reactor systems treating municipal sewage. *Applied and Environmental Microbiology* **78:** 855-864.

Blandenier Q, Seppey CVW, Singer D, Vlimant M, Simon A, Duckert C *et al* (2017). *Mycamoeba gemmipara* nov. gen., nov. sp., the first cultured member of the environmental *Dermamoebidae* clade LKM74 and its unusual life cycle. *Journal of Eukaryotic Microbiology* **64:** 257-265.

Boenigk J, Stadler P, Wiedlroither A, Hahn MW (2004). Strain-specific differences in the grazing sensitivities of closely related ultramicrobacteria affiliated with the polynucleobacter cluster. *Applied and Environmental Microbiology* **70:** 5787-5793.

Böhme A, Risse-Buhl U, Küsel K (2009). Protists with different feeding modes change biofilm morphology. *FEMS Microbiology Ecology* **69:** 158-169.

Bossier P, Verstraete W (1996). Triggers for microbial aggregation in activated sludge? *Applied Microbiology and Biotechnology* **45:** 1-6.

Branda SS, Vik Å, Friedman L, Kolter R (2005). Biofilms: the matrix revisited. *Trends in Microbiology* **13:** 20-26.

Breitbart M (2012). Marine viruses: Truth or dare. *Annual Review of Marine Science* **4:** 425-448.

Brüssow H, Hendrix RW (2002). Phage genomics: Small is beautiful. *Cell* **108:** 13-16.

Burmølle M, Webb JS, Rao D, Hansen LH, Sørensen SJ, Kjelleberg S (2006). Enhanced biofilm formation and increased resistance to antimicrobial agents and bacterial invasion are caused by synergistic interactions in multispecies biofilms. *Applied and Environmental Microbiology* **72:** 3916-3923.

Caiazza NC, Shanks RM, O'Toole GA (2005). Rhamnolipids modulate swarming motility patterns of *Pseudomonas aeruginosa*. *Journal of Bacteriology* **187:** 7351-7361.

Chang HT, Rittmann BE, Amar D, Heim R, Ehlinger O, Lesty Y (1991). Biofilm detachment mechanisms in a liquid-fluidized bed. *Biotechnology and Bioengineering* **38:** 499-506.

Chavez-Dozal A, Gorman C, Erken M, Steinberg PD, McDougald D, Nishiguchi MK (2013). Predation response of Vibrio fischeri biofilms to bacterivorus protists. *Applied and Environmental Microbiology* **79:** 553-558.

Choi J, Kotay SM, Goel R (2011). Bacteriophage-based biocontrol of biological sludge bulking in wastewater. *Bioengineered Bugs* **2:** 214-217.

Choi K-H, Schweizer HP (2005). An improved method for rapid generation of unmarked *Pseudomonas aeruginosa* deletion mutants. *BMC Microbiology* **5:** 1-11.

Chrzanowski TH, Šimek K (1990). Prey-size selection by freshwater flagellated protozoa. *Limnology and Oceanography* **35:** 1429-1436.

Cloete TE, Bosch M (1994). Acinetobacter cell biomass, growth stage and phosphorus uptake from activated sludge mixed liquor. *Water Science and Technology* **30:** 219-230.

Cooke WB, Pipes WO (1970). The occurrence of fungi in activated sludge. *Mycopathologia et mycologia applicata* **40:** 249-270.

Cosson P, Zulianello L, Join-Lambert O, Faurisson F, Gebbie L, Benghezal M *et al* (2002). *Pseudomonas aeruginosa* virulence analyzed in a *Dictyostelium discoideum* host system. *Journal of Bacteriology* **184:** 3027-3033.

Crocetti GR, Banfield JF, Keller J, Bond PL, Blackall LL (2002). Glycogen-accumulating organisms in laboratory-scale and full-scale wastewater treatment processesb. *Microbiology* **148:** 3353-3364.

Curds CR (1963). The flocculation of suspended matter by *Paramecium caudatum*. *Microbiology* **33:** 357-363.

Curds CR (1982). The ecology and role of protozoa in aerobic sewage treatment processes. *Annual Review of Microbiology* **36:** 27-46.

Dashiff A, Junka RA, Libera M, Kadouri DE (2010). Predation of human pathogens by the predatory bacteria *Micavibrio aeruginosavorus* and *Bdellovibrio bacteriovorus*. *Journal of Applied Microbiology* **110**.

Davies DG, Parsek MR, Pearson JP, Iglewski BH, Costerton JW, Greenberg EP (1998). The involvement of cell-to-cell signals in the development of a bacterial biofilm. *Science* **280:** 295-298.

de Bruin LMM, de Kreuk MK, van der Roest HFR, Uijterlinde C, van Loosdrecht MCM (2004). Aerobic granular sludge technology: an alternative to activated sludge? *Water Science and Technology* **49:** 1-7.

de Hoon MJL, Imoto S, Nolan J, Miyano S (2004). Open source clustering software. *Bioinformatics* **20:** 1453-1454.

de Kievit TR, Iglewski BH (2000). Bacterial quorum sensing in pathogenic relationships. *Infection and Immunity* **68:** 4839-4849.

de Kreuk MK, Heijnen JJ, van Loosdrecht MCM (2005). Simultaneous COD, nitrogen, and phosphate removal by aerobic granular sludge. *Biotechnology and Bioengineering* **90:** 761-769.

de Kreuk MK, Picioreanu C, Hosseini M, Xavier JB, van Loosdrecht MCM (2007). Kinetic model of a granular sludge SBR: Influences on nutrient removal. *Biotechnology and Bioengineering* **97:** 801-815.

Dopheide A, Lear G, Stott R, Lewis G (2011a). Preferential feeding by the ciliates *Chilodonella* and *Tetrahymena* spp. and effects of these protozoa on bacterial biofilm structure and composition. *Applied and Environmental Microbiology* **77:** 4564-4572.

Dopheide A, Lear G, Stott R, Lewis G (2011b). Preferential feeding by the ciliates *Chilodonella* and *Tetrahymena* spp. and effects of these protozoa on bacterial biofilm structure and composition. *Applied & Environmental Microbiology* **77:** 4564-4572.

Eaton AD, Franson MAH, Association APH, Association AWW, Federation WE (2005). *Standard Methods for the Examination of Water and Wastewater*. American Public Health Association: Washington, DC, USA.

Edwards SJ, Kjellerup BV (2013). Applications of biofilms in bioremediation and biotransformation of persistent organic pollutants, pharmaceuticals/personal care products, and heavy metals. *Applied Microbiology and Biotechnology* **97:** 9909-9921.

El-Sheshtawy HS, Doheim MM (2014). Selection of Pseudomonas aeruginosa for biosurfactant production and studies of its antimicrobial activity. *Egyptian Journal of Petroleum* **23:** 1-6.

Elskens MT, Penninckx MJ (1997). Thiram and dimethyldithiocarbamic acid interconversion in Saccharomyces cerevisiae: a possible metabolic pathway under the control of the glutathione redox cycle. *Applied and Environmental Microbiology* **63:** 2857-2862.

Erken M, Farrenschon N, Speckmann S, Arndt H, Weitere M (2012). Quantification of individual flagellate - bacteria interactions within semi-natural biofilms. *Protist* **163:** 632-642.

Esteban G, Téllez C, Bautista LM (1991). Dynamics of ciliated protozoa communities in activated-sludge process. *Water Research* **25:** 967-972.

Etterer T, Wilderer PA (2001). Generation and properties of aerobic granular sludge. *Water Science and Technology* **43:** 19.

Fakhru'l-Razi A, Zahangir Alam M, Idris A, Abd-Aziz S, Molla AH (2002). Filamentous fungi in Indah Water Konsortium Sewage Treatment Plant for biological treatment of domestic wastewater sludge *Journal of Environmental Science and Health, Part A* **37:** 309-320.

Feiner R, Argov T, Rabinovich L, Sigal N, Borovok I, Herskovits AA (2015). A new perspective on lysogeny: prophages as active regulatory switches of bacteria. *Nature Reviews Microbiology* **13:** 641-650.

Fenchel T (2001). Eppur si muove: many water column bacteria are motile. *Aquatic Microbial Ecology* **24:** 197-201.

Feng S, Tan CH, Cohen Y, Rice SA (2016). Isolation of *Bdellovibrio bacteriovorus* from a tropical wastewater treatment plant and predation of mixed species biofilms assembled by the native community members. *Environmental Microbiology* **18:** 3923-3931.

Feng S, Tan CH, Constancias F, Kohli GS, Cohen Y, Rice SA (2017). Predation by *Bdellovibrio bacteriovorus* significantly reduces viability and alters the microbial community composition of activated sludge flocs and granules. *FEMS Microbiology Ecology* **93:** fix020-fix020.

Finlay BJ (2001). Protozoa A2 - Levin, Simon Asher. *Encyclopedia of Biodiversity*. Elsevier: New York. pp 901-915.

Flemming H-C, Neu TR, Wozniak DJ (2007). The EPS matrix: The "House of Biofilm Cells". *Journal of Bacteriology* **189:** 7945-7947.

Flemming H-C, Wingender J (2010). The biofilm matrix. *Nature Reviews Microbiology* **8:** 623-633.

Fu Z, Yang F, An Y, Xue Y (2009). Simultaneous nitrification and denitrification coupled with phosphorus removal in an modified anoxic/oxic-membrane bioreactor *Biochemical Engineering Journal* **43:** 191-196.

Fuhrman JA (1999). Marine viruses and their biogeochemical and ecological effects. *Nature* **399:** 541-548.

Fux CA, Costerton JW, Stewart PS, Stoodley P (2005). Survival strategies of infectious biofilms. *Trends in Microbiology* **13:** 34-40.

Gebara F (1999). Activated sludge biofilm wastewater treatment system. *Water Research* **33:** 230-238.

Gjaltema A, van Loosdrecht MCM, Heijnen JJ (1997). Abrasion of suspended biofilm pellets in airlift reactors: Effect of particle size. *Biotechnology and Bioengineering* **55:** 206-215.

Gonzalez-Martinez A, Rodriguez-Sanchez A, Lotti T, Garcia-Ruiz M-J, Osorio F, Gonzalez-Lopez J *et al* (2016). Comparison of bacterial communities of conventional and A-stage activated sludge systems **6:** 18786.

Gonzalez JM, Suttle CA (1993). Grazing by marine nanoflagellates on viruses and virus-sized particles - ingestion and digestion. *Marine Ecology Progress Series* **94:** 1-10.

Guest RK, Smith DW (2002). A potential new role for fungi in a wastewater MBR biological nitrogen reduction system. *Journal of Environmental Engineering and Science* **1:** 433-437.

Gutierrez M, Choi MH, Tian B, Xu J, Rho JK, Kim MO *et al* (2013). Simultaneous inhibition of rhamnolipid and polyhydroxyalkanoic acid synthesis and biofilm formation in *Pseudomonas aeruginosa* by 2-bromoalkanoic acids: Effect of inhibitor alkyl-chain-length. *PLOS ONE* **8:** e73986.

Hahn MW, Moore ERB, Höfle MG (1999). Bacterial filament formation, a defense mechanism against flagellate grazing, is growth rate controlled in bacteria of different phyla. *Applied and Environmental Microbiology* **65:** 25-35.

Hahn MW, Moore ER, Hofle MG (2000). Role of microcolony formation in the protistan grazing defense of the aquatic bacterium *Pseudomonas* sp. MWH1. *Microbial Ecology* **39:** 175-185.

Hahn MW, Hofle MG (2001). Grazing of protozoa and its effect on populations of aquatic bacteria. *FEMS Microbiology Ecology* **35:** 113-121.

Hahn MW, Höfle MG (2001). Grazing of protozoa and its effect on populations of aquatic bacteria. *FEMS Microbiology Ecology* **35:** 113-121.

Hall-Stoodley L, Costerton JW, Stoodley P (2004). Bacterial biofilms: from the natural environment to infectious diseases. *Nature Reviews Microbiology* **2:** 95-108.

Hans-Peter G, Lasse R, Farooq A (2001). Bacterial motility in the sea and its ecological implications. *Aquatic Microbial Ecology* **25:** 247-258.

Hauser AR (2009). The type III secretion system of *Pseudomonas aeruginosa*: infection by injection. *Nature Reviews Microbiology* **7:** 654-665.

He Q, Zhang W, Zhang S, Wang H (2017). Enhanced nitrogen removal in an aerobic granular sequencing batch reactor performing simultaneous nitrification, endogenous denitrification and phosphorus removal with low superficial gas velocity. *Chemical Engineering Journal* **326:** 1223-1231.

He S, Gall DL, McMahon KD (2007). *Candidatus Accumulibacter* population structure in enhanced biological phosphorus removal sludges as revealed by polyphosphate kinase genes. *Applied and Environmental Microbiology* **73:** 5865-5874.

He S, McMahon KD (2011). Microbiology of *Candidatus Accumulibacter* in activated sludge. *Microbial Biotechnology* **4:** 603-619.

Helmer C, Kunst S (1998). Simultaneous nitrification/denitrification in an aerobic biofilm system. *Water Science and Technology* **37:** 183-187.

Hense BA, Kuttler C, Muller J, Rothballer M, Hartmann A, Kreft J-U (2007). Does efficiency sensing unify diffusion and quorum sensing? *Nature Reviews Microbiology* **5:** 230-239.

Hmelo LR, Borlee BR, Almblad H, Love ME, Randall TE, Tseng BS *et al* (2015). Precision-engineering the *Pseudomonas aeruginosa* genome with two-step allelic exchange. *Nature Protocols* **10:** 1820-1841.

Hood RD, Singh P, Hsu F, Güvener T, Carl MA, Trinidad RRS *et al* (2010). A Type VI Secretion System of *Pseudomonas aeruginosa* Targets a Toxin to Bacteria. *Cell Host & Microbe* **7:** 25-37.

Hughes AL, Piontkivska H (2003). Molecular phylogenetics of *Trypanosomatidae*: contrasting results from 18S rRNA and protein phylogenies. *Kinetoplastid Biology and Disease* **2:** 15.

Huws SA, McBain AJ, Gilbert P (2005). Protozoan grazing and its impact upon population dynamics in biofilm communities. *Journal of Applied Microbiology* **98:** 238-244.

Ibarbalz FM, Figuerola ELM, Erijman L (2013). Industrial activated sludge exhibit unique bacterial community composition at high taxonomic ranks. *Water Research* **47:** 3854-3864.

Isanta E, Suárez-Ojeda ME, Val del Río Á, Morales N, Pérez J, Carrera J (2012). Long term operation of a granular sequencing batch reactor at pilot scale treating a low-strength wastewater. *Chemical Engineering Journal* **198–199:** 163-170.

Jang A, Yoon Y-H, Kim IS, Kim K-S, Bishop PL (2003). Characterization and evaluation of aerobic granules in sequencing batch reactor. *Journal of Biotechnology* **105:** 71-82.

Jassim SAA, Limoges RG, El-Cheikh H (2016). Bacteriophage biocontrol in wastewater treatment. *World Journal of Microbiology and Biotechnology* **32:** 70.

Jenkins D, Richards MD (2003). Manual on the causes and control of activated sludge bulking, foaming, and other solids separation problems. Lewis Publishers.

Jensen PO, Bjarnsholt T, Phipps R, Rasmussen TB, Calum H, Christoffersen L *et al* (2007). Rapid necrotic killing of polymorphonuclear leukocytes is caused by quorum-sensing-controlled production of rhamnolipid by *Pseudomonas aeruginosa*. *Microbiology* **153:** 1329-1338.

Jeuck A, Arndt H (2013). A short guide to common heterotrophic flagellates of freshwater habitats based on the morphology of living organisms. *Protist* **164:** 842-860.

Jousset A, Rochat L, Scheu S, Bonkowski M, Keel C (2010). Predator-prey chemical warfare determines the expression of biocontrol genes by rhizosphere-associated *Pseudomonas fluorescens*. *Applied and Environmental Microbiology* **76:** 5263-5268.

Ju F, Guo F, Ye L, Xia Y, Zhang T (2014). Metagenomic analysis on seasonal microbial variations of activated sludge from a full-scale wastewater treatment plant over 4 years. *Environ Microbiol Rep* **6:** 80-89.

Jurgens K, Matz C (2002). Predation as a shaping force for the phenotypic and genotypic composition of planktonic bacteria. *Antonie Van Leeuwenhoek* **81:** 413-434.

Jürgens K, Matz C (2002). Predation as a shaping force for the phenotypic and genotypic composition of planktonic bacteria. *Antonie Van Leeuwenhoek* **81:** 413-434.

Jürgens K (2007). Predation on Bacteria and Bacterial Resistance Mechanisms: Comparative Aspects Among Different Predator Groups in Aquatic Systems. In: Jurkevitch E (ed). *Predatory Prokaryotes: Biology, Ecology and Evolution*. Springer Berlin Heidelberg: Berlin, Heidelberg. pp 57-92.

Justice SS, Hunstad DA, Cegelski L, Hultgren SJ (2008). Morphological plasticity as a bacterial survival strategy. *Nature Reviews Microbiology* **6:** 162-168.

Kadouri D, Venzon NC, O'Toole GA (2007). Vulnerability of pathogenic biofilms to *Micavibrio aeruginosavorus*. *Applied and Environmental Microbiology* **73:** 605-614.

Kämpfer P, Erhart R, Beimfohr C, Böhringer J, Wagner M, Amann R (1996). Characterization of bacterial communities from activated sludge: Culture-dependent numerical identification versus in situ identification using group- and genus-specific rRNA-targeted oligonucleotide probes. *Microbial Ecology* **32:** 101-121.

Kaplan JB (2010). Biofilm dispersal: mechanisms, clinical implications, and potential therapeutic uses. *Journal of Dental Research* **89:** 205-218.

Kara D, Luppens SBI, ten Cate JM (2006). Differences between single- and dual-species biofilms of *Streptococcus mutans* and *Veillonella parvula* in growth, acidogenicity and susceptibility to chlorhexidine. *European Journal of Oral Sciences* **114:** 58-63.

Kawakoshi A, Nakazawa H, Fukada J, Sasagawa M, Katano Y, Nakamura S *et al* (2012). Deciphering the genome of polyphosphate accumulating actinobacterium *Microlunatus phosphovorus*. *DNA Research: An International Journal for Rapid Publication of Reports on Genes and Genomes* **19:** 383-394.

Kerrn-Jespersen JP, Henze M, Strube R (1994). Biological phosphorus release and uptake under alternating anaerobic and anoxic conditions in a fixed-film reactor. *Water Research* **28:** 1253-1255.

Kragelund C, Caterina L, Borger A, Thelen K, Eikelboom D, Tandoi V *et al* (2007). Identity, abundance and ecophysiology of filamentous *Chloroflexi* species present in activated sludge treatment plants. *FEMS Microbiology Ecology* **59:** 671-682.

Kristiansen R, Nguyen HTT, Saunders AM, Nielsen JL, Wimmer R, Le VQ *et al* (2013). A metabolic model for members of the genus *Tetrasphaera* involved in enhanced biological phosphorus removal. *ISME Journal* **7:** 543-554.

Kuba T, Wachtmeister A, van Loosdrecht MCM, Heijnen JJ (1994). Effect of nitrate on phosphorus release in biological phosphorus removal systems. *Water Science and Technology* **30:** 263-269.

Kunin V, He S, Warnecke F, Peterson SB, Garcia Martin H, Haynes M *et al* (2008). A bacterial metapopulation adapts locally to phage predation despite global dispersal. *Genome Research* **18:** 293-297.

Lahr DJG, Kubik GM, Grant J, Anderson FR, Katz LA (2012). Morphological description of *Telaepolella tubasferens ng*, Isolate ATCC © 50593 ™, and filoe amoeba in *Gracilipodida, Amoebozoa*. *Acta Protozoologica* **51:** 305-318.

Law Y, Kirkegaard RH, Cokro AA, Liu X, Arumugam K, Xie C *et al* (2016). Integrative microbial community analysis reveals full-scale enhanced biological phosphorus removal under tropical conditions. *Scientific Reports* **6:** 25719.

Lee KWK, Periasamy S, Mukherjee M, Xie C, Kjelleberg S, Rice SA (2014). Biofilm development and enhanced stress resistance of a model, mixed-species community biofilm. *ISME Journal* **8:** 894-907.

Lemaire R, Meyer R, Taske A, Crocetti GR, Keller J, Yuan Z (2006). Identifying causes for N2O accumulation in a lab-scale sequencing batch reactor performing simultaneous nitrification, denitrification and phosphorus removal. *Journal of Biotechnology* **122:** 62-72.

Lemaire R, Webb RI, Yuan Z (2008a). Micro-scale observations of the structure of aerobic microbial granules used for the treatment of nutrient-rich industrial wastewater. *ISME Journal* **2:** 528-541.

Lemaire R, Yuan Z, Blackall LL, Crocetti GR (2008b). Microbial distribution of *Accumulibacter* spp. and *Competibacter* spp. in aerobic granules from a lab-scale biological nutrient removal system. *Environmental Microbiology* **10:** 354-363.

Lesic B, Starkey M, He J, Hazan R, Rahme LG (2009). Quorum sensing differentially regulates *Pseudomonas aeruginosa* type VI secretion locus I and homologous loci II and III, which are required for pathogenesis. *Microbiology* **155:** 2845-2855.

Li J, Ma L, Wei S, Horn H (2013). Aerobic granules dwelling vorticella and rotifers in an SBR fed with domestic wastewater. *Separation and Purification Technology* **110:** 127-131.

Li Y-H, Tian X (2012). Quorum sensing and bacterial social interactions in biofilms. *Sensors (Basel, Switzerland)* **12:** 2519-2538.

Li Y, Liu Y (2005). Diffusion of substrate and oxygen in aerobic granule. *Biochemical Engineering Journal* **27:** 45-52.

Li Y, Liu Y, Shen L, Chen F (2008). DO diffusion profile in aerobic granule and its microbiological implications. *Enzyme and Microbial Technology* **43:** 349-354.

Lima SL (1998). Nonlethal effects in the ecology of predator-prey interactions. *Bioscience* **48:** 25-34.

Lin X, Song W (2004). Establishment of a new *Amphileptid* genus, *Apoamphileptus* nov. gen. (*Ciliophora, Litostomatea, Pleurostomatida*), with description of a new marine species, *Apoamphileptus robertsi* nov. spec, from Qingdao, China. *Journal of Eukaryotic Microbiology* **51:** 618-625.

Liu M, Gill JJ, Young R, Summer EJ (2015). Bacteriophages of wastewater foaming-associated filamentous *Gordonia* reduce host levels in raw activated sludge. *Scientific Reports* **5:** 13754.

Liu Y, Liu Q-S (2006). Causes and control of filamentous growth in aerobic granular sludge sequencing batch reactors. *Biotechnology Advances* **24:** 115-127.

Liu Y (2008). *Wastewater purification: Aerobic granulation in sequencing batch reactors*. Taylor & Francis: Boca Raton.

Lu H, Oehmen A, Virdis B, Keller J, Yuan Z (2006). Obtaining highly enriched cultures of *Candidatus Accumulibacter* phosphates through alternating carbon sources. *Water Research* **40:** 3838-3848.

Lu Y-Z, Wang H-F, Kotsopoulos TA, Zeng RJ (2016). Advanced phosphorus recovery using a novel SBR system with granular sludge in simultaneous nitrification, denitrification and phosphorus removal process. *Applied Microbiology and Biotechnology* **100:** 4367-4374.

Luxmy BS, Nakajima F, Yamamoto K (2000). Predator grazing effect on bacterial size distribution and floc size variation in membrane-separation activated sludge. *Water Science and Technology* **42:** 211-217.

Lynn DH (2001). Ciliophora. *eLS*. John Wiley & Sons, Ltd.

Madoni P (1994). A sludge biotic index (SBI) for the evaluation of the biological performance of activated sludge plants based on the microfauna analysis. *Water Research* **28:** 67-75.

Madoni P (2003). Protozoa in activated sludge. *Encyclopedia of Environmental Microbiology*. John Wiley & Sons, Inc.

Madoni P (2010). Protozoa in wastewater treatment processes: A minireview. *Italian Journal of Zoology* **78:** 3-11.

Madsen JS, Roder HL, Russel J, Sorensen H, Burmolle M, Sorensen SJ (2016). Coexistence facilitates interspecific biofilm formation in complex microbial communities. *Environ Microbiol* **18:** 2565-2574.

Mannan S, Fakhru'l-Razi A, Alam MZ (2005). Use of fungi to improve bioconversion of activated sludge. *Water Research* **39:** 2935-2943.

Martin HG, Ivanova N, Kunin V, Warnecke F, Barry KW, McHardy AC *et al* (2006). Metagenomic analysis of two enhanced biological phosphorus removal (EBPR) sludge communities. *Nature Biotechnology* **24:** 1263-1269.

Maszenan AM, Liu Y, Ng WJ (2011). Bioremediation of wastewaters with recalcitrant organic compounds and metals by aerobic granules. *Biotechnology Advances* **29:** 111-123.

Matz C, Bergfeld T, Rice SA, Kjelleberg S (2004). Microcolonies, quorum sensing and cytotoxicity determine the survival of *Pseudomonas aeruginosa* biofilms exposed to protozoan grazing. *Environmental Microbiology* **6:** 218-226.

Matz C, Jurgens K (2005). High motility reduces grazing mortality of planktonic bacteria. *Applied Environmental Microbiology* **71:** 921-929.

Matz C, Kjelleberg S (2005). Off the hook--how bacteria survive protozoan grazing. *Trends in Microbiology* **13:** 302-307.

Matz C, McDougald D, Moreno AM, Yung PY, Yildiz FH, Kjelleberg S (2005a). Biofilm formation and phenotypic variation enhance predation-driven persistence of *Vibrio cholerae*. *Proceedings of the National Academy of Sciences* **102:** 16819-16824.

Matz C, McDougald D, Moreno AM, Yung PY, Yildiz FH, Kjelleberg S (2005b). Biofilm formation and phenotypic variation enhance predation-driven persistence of *Vibrio cholerae*. *Proceedings of the National Academy of Sciences* **102:** 16819-16824.

Matz C, Moreno AM, Alhede M, Manefield M, Hauser AR, Givskov M *et al* (2008a). *Pseudomonas aeruginosa* uses type III secretion system to kill biofilm-associated amoebae. *ISME Journal* **2:** 843-852.

Matz C, Webb JS, Schupp PJ, Phang SY, Penesyan A, Egan S *et al* (2008b). Marine biofilm bacteria evade eukaryotic predation by targeted chemical defense. *PLOS ONE* **3:** e2744.

McClure C (1992). Effects of *Pseudomonas aeruginosa* rhamnolipids on human monocyte-derived macrophages. *Journal of Leukocyte Biology* **51:** 97-102.

McDougald D, Rice SA, Barraud N, Steinberg PD, Kjelleberg S (2012). Should we stay or should we go: mechanisms and ecological consequences for biofilm dispersal. *Nature Reviews Microbiology* **10:** 39-50.

McIlroy SJ, Karst SM, Nierychlo M, Dueholm MS, Albertsen M, Kirkegaard RH *et al* (2016). Genomic and in situ investigations of the novel uncultured *Chloroflexi* associated with 0092 morphotype filamentous bulking in activated sludge. *ISME Journal* **10:** 2223-2234.

McSwain BS, Irvine RL, Wilderer PA (2004). The influence of settling time on the formation of aerobic granules. *Water Science and Technology* **50:** 195-202.

Menniti A, Morgenroth E (2010). The influence of aeration intensity on predation and EPS production in membrane bioreactors. *Water Research* **44:** 2541-2553.

Meyer RL, Zeng RJ, Giugliano V, Blackall LL (2005). Challenges for simultaneous nitrification, denitrification, and phosphorus removal in microbial aggregates: mass transfer limitation and nitrous oxide production. *FEMS Microbiology Ecology* **52:** 329-338.

Michaela MS, Jakob P, Roland P, Thomas P (2005). Succession of bacterial grazing defense mechanisms against protistan predators in an experimental microbial community. *Aquatic Microbial Ecology* **38:** 215-229.

Mitchell GC, Baker JH, Sleigh MA (1988). Feeding of a freshwater flagellate, *Bodo saltans*, on diverse bacteria. *The Journal of Protozoology* **35:** 219-222.

Mitchell JG, Pearson L, Bonazinga A, Dillon S, Khouri H, Paxinos R (1995a). Long lag times and high velocities in the motility of natural assemblages of marine bacteria. *Applied and Environmental Microbiology* **61:** 877-882.

Mitchell JG, Pearson L, Dillon S, Kantalis K (1995b). Natural assemblages of marine bacteria exhibiting high-speed motility and large accelerations. *Applied and Environmental Microbiology* **61:** 4436-4440.

Monger B, Landry M (1992). Size-selective grazing by heterotrophic nanoflagellates: an analysis using live-stained bacteria and dual-beam flow cytometry. *Archiv für Hydrobiologie–BeiheftErgebnisse der Limnologie* **37:** 173-185.

Morales N, Figueroa M, Fra-Vázquez A, Val del Río A, Campos JL, Mosquera-Corral A *et al* (2013). Operation of an aerobic granular pilot scale SBR plant to treat swine slurry. *Process Biochemistry* **48:** 1216-1221.

More TT, Yan S, Tyagi RD, Surampalli RY (2010). Potential use of filamentous fungi for wastewater sludge treatment. *Bioresource Technology* **101:** 7691-7700.

Morgenroth E, Sherden T, van Loosdrecht MCM, Heijnen JJ, Wilderer PA (1997). Aerobic granular sludge in a sequencing batch reactor. *Water Research* **31:** 3191-3194.

Münch EV, Lant P, Keller J (1996). Simultaneous nitrification and denitrification in bench-scale sequencing batch reactors. *Water Research* **30:** 277-284.

Murnleitner E, Kuba T, van Loosdrecht MCM, Heijnen JJ (1997). An integrated metabolic model for the aerobic and denitrifying biological phosphorus removal. *Biotechnology and Bioengineering* **54:** 434-450.

Nealson KH, Platt T, Hastings JW (1970). Cellular control of the synthesis and activity of the bacterial luminescent system. *Journal of Bacteriology* **104:** 313-322.

Neville A (1946). The ecology and function of Protozoa in sewage purification. *Annals of Applied Biology* **33:** 314-325.

Ng W-L, Bassler BL (2009). Bacterial quorum-sensing network architectures. *Annual Review of Genetics* **43:** 197-222.

Nielsen JL, Nguyen H, Meyer RL, Nielsen PH (2012). Identification of glucose-fermenting bacteria in a full-scale enhanced biological phosphorus removal plant by stable isotope probing. *Microbiology* **158:** 1818-1825.

Oehmen A, Teresa Vives M, Lu H, Yuan Z, Keller J (2005a). The effect of pH on the competition between polyphosphate-accumulating organisms and glycogen-accumulating organisms. *Water Research* **39:** 3727-3737.

Oehmen A, Yuan Z, Blackall LL, Keller J (2005b). Comparison of acetate and propionate uptake by polyphosphate accumulating organisms and glycogen accumulating organisms. *Biotechnology and Bioengineering* **91:** 162-168.

Oehmen A, Saunders AM, Vives MT, Yuan Z, Keller J (2006). Competition between polyphosphate and glycogen accumulating organisms in enhanced biological phosphorus removal systems with acetate and propionate as carbon sources. *Journal of Biotechnology* **123:** 22-32.

Ong YH, Chua ASM, Huang YT, Ngoh GC, You SJ (2016). The microbial community in a high-temperature enhanced biological phosphorus removal (EBPR) process. *Sustainable Environment Research* **26:** 14-19.

Orias E, Cervantes MD, Hamilton EP (2011). *Tetrahymena thermophila*, a unicellular eukaryote with separate germline and somatic genomes. *Research in Microbiology* **162:** 578-586.

Pamp SJ, Tolker-Nielsen T (2007). Multiple roles of biosurfactants in structural biofilm development by *Pseudomonas aeruginosa*. *Journal of Bacteriology* **189:** 2531-2539.

Parry JD (2004). Protozoan grazing of freshwater biofilms. *Advances in Applied Microbiology* **54:** 167-196.

Patterson DJ (2001). Protozoan diversity and biogeography. *eLS*. John Wiley & Sons, Ltd.

Pearson JP, Pesci EC, Iglewski BH (1997). Roles of *Pseudomonas aeruginosa las* and *rhl* quorum-sensing systems in control of elastase and rhamnolipid biosynthesis genes. *Journal of Bacteriology* **179:** 5756-5767.

Pearson JP, Feldman M, Iglewski BH, Prince A (2000). *Pseudomonas aeruginosa* cell-to-cell signaling ss required for virulence in a model of acute pulmonary infection. *Infection and Immunity* **68:** 4331-4334.

Peng Y-z, Wang X-l, Li B-k (2006). Anoxic biological phosphorus uptake and the effect of excessive aeration on biological phosphorus removal in the A2O process. *Desalination* **189:** 155-164.

Pernthaler J, Sattler B, Simek K, Schwarzenbacher A, Psenner R (1996). Top-down effects on the size-biomass distribution of a freshwater bacterioplankton community. *Aquatic Microbial Ecology* **10:** 255-263.

Pesci EC, Pearson JP, Seed PC, Iglewski BH (1997). Regulation of *las* and *rhl* quorum sensing in *Pseudomonas aeruginosa*. *Journal of Bacteriology* **179:** 3127-3132.

Pettitt ME, Orme BAA, Blake JR, Leadbeater BSC (2002). The hydrodynamics of filter feeding in choanoflagellates. *European Journal of Protistology* **38:** 313-332.

Pijuan M, Werner U, Yuan Z (2011). Reducing the startup time of aerobic granular sludge reactors through seeding floccular sludge with crushed aerobic granules. *Water Research* **45:** 5075-5083.

Pochana K, Keller J (1999). Study of factors affecting simultaneous nitrification and denitrification (SND). *Water Science and Technology* **39:** 61-68.

Pronk M, de Kreuk MK, de Bruin B, Kamminga P, Kleerebezem R, van Loosdrecht MCM (2015). Full scale performance of the aerobic granular sludge process for sewage treatment. *Water Research* **84:** 207-217.

Pukatzki S, Kessin RH, Mekalanos JJ (2002). The human pathogen *Pseudomonas aeruginosa* utilizes conserved virulence pathways to infect the social amoeba *Dictyostelium discoideum*. *Proceedings of the National Academy of Sciences* **99:** 3159-3164.

Qin L, Liu Y, Tay J-H (2004). Effect of settling time on aerobic granulation in sequencing batch reactor. *Biochemical Engineering Journal* **21:** 47-52.

Rahim R, Ochsner UA, Olvera C, Graninger M, Messner P, Lam JS *et al* (2001). Cloning and functional characterization of the *Pseudomonas aerugiosa rhlC* gene that encodes rhanmosyltransferase 2, an enzyme responsible for di-rhamnolipid biosynthesis. *Molecular Microbiology* **40:** 708-718.

Rahimi Y, Torabian A, Mehrdadi N, Shahmoradi B (2011). Simultaneous nitrification–denitrification and phosphorus removal in a fixed bed sequencing batch reactor *Journal of Hazardous Materials* **185:** 852-857.

Ramirez C, Alexander M (1980). Evidence suggesting protozoan predation on rhizobium associated with germinating seeds and in the rhizosphere of eans (*Phaseolus vulgaris*). *Applied and Environmental Microbiology* **40:** 492-499.

Ren T-t, Yu H-q, Li X-y (2010). The quorum-sensing effect of aerobic granules on bacterial adhesion, biofilm formation, and sludge granulation. *Applied Microbiology and Biotechnology* **88:** 789-797.

Rendulic S, Jagtap P, Rosinus A, Eppinger M, Baar C, Lanz C *et al* (2004). A predator unmasked: Life cycle of *Bdellovibrio bacteriovorus* from a genomic perspective. *Science* **303:** 689-692.

Rice SA, Koh KS, Queck SY, Labbate M, Lam KW, Kjelleberg S (2005). Biofilm formation and sloughing in *Serratia marcescens* are controlled by quorum sensing and nutrient cues. *Journal of Bacteriology* **187:** 3477-3485.

Røder HL, Raghupathi PK, Herschend J, Brejnrod A, Knøchel S, Sørensen SJ *et al* (2015). Interspecies interactions result in enhanced biofilm formation by co-cultures of bacteria isolated from a food processing environment. *Food Microbiology* **51:** 18-24.

Ronn R, Vestergard M, Ekelund F (2012). Interactions between bacteria, protozoa and nematodes in soil. *Acta Protozoologica* **51:** 223-235.

Rønn R, McCaig AE, Griffiths BS, Prosser JI (2002). Impact of protozoan grazing on bacterial community structure in soil microcosms. *Applied and Environmental Microbiology* **68:** 6094-6105.

Rutherford ST, Bassler BL (2012). Bacterial quorum sensing: Its role in virulence and possibilities for its control. *Cold Spring Harbor Perspectives in Medicine* **2:** a012427.

Rychert K, Neu T (2010). Protozoan impact on bacterial biofilm formation. *Biological Letters*. p 3.

Sadrzadeh F, Dulekgurgen E (2014). Improving the settling properties of activated sludge by gradually decreasing the settling time. *Desalination and Water Treatment* **52:** 2465-2471.

Saldanha AJ (2004). Java Treeview—extensible visualization of microarray data. *Bioinformatics* **20:** 3246-3248.

Samson JE, Magadan AH, Sabri M, Moineau S (2013). Revenge of the phages: defeating bacterial defences. *Nature Reviews Microbiology* **11:** 675-687.

Sanders RW (1991). Trophic strategies among heterotrophic flagellates. *Biology of Free-Living Heterotrophic Flagellates* **45:** 21-38.

Saunders AM, Oehmen A, Blackall LL, Yuan Z, Keller J (2003). The effect of GAOs (glycogen accumulating organisms) on anaerobic carbon requirements in full-scale Australian EBPR (enhanced biological phosphorus removal) plants. *Water Science and Technology* **47:** 37-43.

Scherwass A, Erken M, Arndt H (2016). Grazing effects of ciliates on microcolony formation in bacterial biofilms. In: Dhanasekaran D, Thajuddin N (eds). *Microbial Biofilms - Importance and Applications*. InTech: Rijeka. p Ch. 05.

Schwarz S, Hood RD, Mougous JD (2010). What is type VI secretion doing in all those bugs? *Trends in Microbiology* **18:** 531-537.

Schwarzenbeck N, Erley R, Mc Swain BS, Wilderer PA, Irvine RL (2004a). Treatment of malting wastewater in a granular sludge sequencing batch reactor (SBR). *Acta Hydrochimica et Hydrobiologica* **32:** 16-24.

Schwarzenbeck N, Erley R, Wilderer PA (2004b). Aerobic granular sludge in an SBR-system treating wastewater rich in particulate matter. *Water Science and Technology* **49:** 41-46.

Schwarzenbeck N, Borges JM, Wilderer PA (2005). Treatment of dairy effluents in an aerobic granular sludge sequencing batch reactor. *Applied Microbiology and Biotechnology* **66:** 711-718.

Schwering M, Song J, Louie M, Turner RJ, Ceri H (2013). Multi-species biofilms defined from drinking water microorganisms provide increased protection against chlorine disinfection. *Biofouling* **29:** 917-928.

Seviour R, Nielsen PH (2010). *Microbial ecology of activated sludge*. IWA Publishing.

Sezgin M, Jenkins D, Parker DS (1978). A unified theory of filamentous activated sludge bulking. *Journal - (Water Pollution Control Federation)***:** 362-381.

Shapiro OH, Kushmaro A, Brenner A (2009). Bacteriophage predation regulates microbial abundance and diversity in a full-scale bioreactor treating industrial wastewater. *ISME Journal* **4:** 327-336.

Shchegolkova NM, Krasnov GS, Belova AA, Dmitriev AA, Kharitonov SL, Klimina KM *et al* (2016). Microbial community structure of activated sludge in treatment plants with different wastewater compositions. *Frontiers in Microbiology* **7:** 90.

Sherr EB, Sherr BF (1987). High rates of consumption of bacteria by pelagic ciliates. *Nature* **325:** 710-711.

Shimada K, Itoh Y, Washio K, Morikawa M (2012). Efficacy of forming biofilms by naphthalene degrading *Pseudomonas stutzeri* T102 toward bioremediation technology and its molecular mechanisms. *Chemosphere* **87:** 226-233.

Shimeta J, Cook PLM (2011). Testing assumptions of the eukaryotic inhibitor method for investigating interactions between aquatic protozoa and bacteria, applied to marine sediment. *Limnology and Oceanography: Methods* **9:** 288-295.

Simon R, Priefer U, Puhler A (1983). A broad host range mobilization system for in vivo genetic engineering: Transposon mutagenesis in Gram negative bacteria. *Nature Biotechnology* **1:** 784-791.

Singh R, Paul D, Jain RK (2006). Biofilms: Implications in bioremediation. *Trends in Microbiology* **14:** 389-397.

Smolders GJF, van der Meij J, van Loosdrecht MCM, Heijnen JJ (1994). Model of the anaerobic metabolism of the biological phosphorus removal process: Stoichiometry and pH influence. *Biotechnology and Bioengineering* **43:** 461-470.

Sockett RE (2009). Predatory lifestyle of *Bdellovibrio bacteriovorus*. *Annual Review of Microbiology* **63:** 523-539.

Solano C, Echeverz M, Lasa I (2014). Biofilm dispersion and quorum sensing. *Current Opinion in Microbiology* **18:** 96-104.

Stewart PS, William Costerton J (2001). Antibiotic resistance of bacteria in biofilms. *The Lancet* **358:** 135-138.

Stolp H, Starr MP (1963). *Bdellovibrio bacteriovorus* gen. et sp. n., a predatory, ectoparasitic, and bacteriolytic microorganism. *Antonie Van Leeuwenhoek* **29:** 217-248.

Sun S, Kjelleberg S, McDougald D (2013). Relative contributions of *Vibrio* polysaccharide and quorum sensing to the resistance of *Vibrio cholerae* to predation by heterotrophic protists. *PLOS ONE* **8:** e56338.

Sun S, Tay QXM, Kjellberg S, Rice SA, McDougald D (2015). Quorum sensing-regulated chitin metabolism provides grazing resistance to *Vibrio cholerae* biofilms. *ISME Journal* **9:** 1812-1820.

Tan CH, Koh KS, Xie C, Tay M, Zhou Y, Williams R *et al* (2014). The role of quorum sensing signalling in EPS production and the assembly of a sludge community into aerobic granules. *ISME Journal* **8:** 1186-1197.

Tan CH, Koh KS, Xie C, Zhang J, Tan XH, Lee GP *et al* (2015). Community quorum sensing signalling and quenching: microbial granular biofilm assembly. *npj Biofilms and Microbiomes* **1:** 15006.

Tay JH, Liu QS, Liu Y (2001a). Microscopic observation of aerobic granulation in sequential aerobic sludge blanket reactor. *Journal of Applied Microbiology* **91:** 168-175.

Tay JH, Liu QS, Liu Y (2001b). The role of cellular polysaccharides in the formation and stability of aerobic granules. *Letters in Applied Microbiology* **33:** 222-226.

Tay JH, Liu QS, Liu Y (2001c). The effects of shear force on the formation, structure and metabolism of aerobic granules. *Applied Microbiology and Biotechnology* **57:** 227-233.

Tay JH, Ivanov V, Pan S, Tay STL (2002). Specific layers in aerobically grown microbial granules. *Letters in Applied Microbiology* **34:** 254-257.

Toyofuku M, Inaba T, Kiyokawa T, Obana N, Yawata Y, Nomura N (2016). Environmental factors that shape biofilm formation. *Bioscience, Biotechnology, and Biochemistry* **80:** 7-12.

Trap J, Bonkowski M, Plassard C, Villenave C, Blanchart E (2016). Ecological importance of soil bacterivores for ecosystem functions. *Plant and Soil* **398:** 1-24.

Tsuneda S, Miyauchi R, Ohno T, Hirata A (2005). Characterization of denitrifying polyphosphate-accumulating organisms in activated sludge based on nitrite reductase gene. *Journal of Bioscience and Bioengineering* **99:** 403-407.

Turk O, Mavinic DS (1986). Preliminary assessment of a shortcut in nitrogen removal from wastewater. *Canadian Journal of Civil Engineering* **13:** 600-605.

Turk O, Mavinic DS (1989). Maintaining nitrite build-up in a system acclimated to free ammonia. *Water Research* **23:** 1383-1388.

van der Veen S, Abee T (2011). Mixed species biofilms of *Listeria monocytogenes* and *Lactobacillus plantarum* show enhanced resistance to benzalkonium chloride and peracetic acid. *International Journal of Food Microbiology* **144:** 421-431.

Van Gennip M, Christensen LD, Alhede M, Phipps R, Jensen PO, Christophersen L *et al* (2009). Inactivation of the *rhlA* gene in *Pseudomonas aeruginosa* prevents rhamnolipid production, disabling the protection against polymorphonuclear leukocytes. *APMIS* **117:** 537-546.

Van Houdt R, Michiels CW (2010). Biofilm formation and the food industry, a focus on the bacterial outer surface. *Journal of Applied Microbiology* **109:** 1117-1131.

van Loosdrecht MCM, Tijhuis L, van Loosdrecht MCM, Eikelboom D, Gjaltema A, Mulder A *et al* (1995). Biofilm structure, growth and dynamics biofilm structures. *Water Science and Technology* **32:** 35-43.

van Loosdrecht MCM, Brandse FA, de Vries AC (1998). Upgrading of waste water treatment processes for integrated nutrient removal-the BCFS® process. *Water Science and Technology* **37:** 209-217.

Wang S, Shi W, Tang T, Wang Y, Zhi L, Lv J *et al* (2017). Function of quorum sensing and cell signaling in the formation of aerobic granular sludge. *Reviews in Environmental Science and BioTechnology* **16:** 1-13.

Wang Z, Liu L, Yao J, Cai W (2006). Effects of extracellular polymeric substances on aerobic granulation in sequencing batch reactors. *Chemosphere* **63:** 1728-1735.

Wang Z, Kadouri DE, Wu M (2011). Genomic insights into an obligate epibiotic bacterial predator: *Micavibrio aeruginosavorus* ARL-13. *BMC Genomics* **12:** 453.

Wang ZW, Liu Y, Tay JH (2005). Distribution of EPS and cell surface hydrophobicity in aerobic granules. *Applied Microbiology and Biotechnology* **69:** 469-473.

Wang ZW, Liu Y, Tay JH (2007). Biodegradability of extracellular polymeric substances produced by aerobic granules. *Applied Microbiology and Biotechnology* **74:** 462-466.

Weber SD, Ludwig W, Schleifer KH, Fried J (2007). Microbial composition and structure of aerobic granular sewage biofilms. *Applied Environmental Microbiology* **73:** 6233-6240.

Weber SD, Hofmann A, Pilhofer M, Wanner G, Agerer R, Ludwig W *et al* (2009). The diversity of fungi in aerobic sewage granules assessed by 18S rRNA gene and ITS sequence analyses. *FEMS Microbiology Ecology* **68:** 246-254.

Weinbauer MG (2004). Ecology of prokaryotic viruses. *FEMS Microbiology Reviews* **28:** 127-181.

Weissbrodt D, Lochmatter S, Ebrahimi S, Rossi P, Maillard J, Holliger C (2012). Bacterial selection during the formation of early-stage aerobic granules in wastewater treatment systems operated under wash-out dynamics. *Frontiers in Microbiology* **3**.

Weitere M, Bergfeld T, Rice SA, Matz C, Kjelleberg S (2005). Grazing resistance of *Pseudomonas aeruginosa* biofilms depends on type of protective mechanism, developmental stage and protozoan feeding mode. *Environmental Microbiology* **7:** 1593-1601.

Wilderer PA, Arnz P, Arnold E (2000). Application of biofilms and biofilm support materials as a temporary sink and source. *Water, Air, and Soil Pollution* **123:** 147-158.

Wilmes P, Andersson AF, Lefsrud MG, Wexler M, Shah M, Zhang B *et al* (2008). Community proteogenomics highlights microbial strain-variant protein expression within activated sludge performing enhanced biological phosphorus removal. *ISME Journal* **2:** 853-864.

Winkler M-KH, Kleerebezem R, de Bruin LMM, Verheijen PJT, Abbas B, Habermacher J *et al* (2013). Microbial diversity differences within aerobic granular sludge and activated sludge flocs. *Applied Microbiology and Biotechnology* **97:** 7447-7458.

Winkler MKH, Kleerebezem R, Khunjar WO, de Bruin B, van Loosdrecht MCM (2012). Evaluating the solid retention time of bacteria in flocculent and granular sludge. *Water Research* **46:** 4973-4980.

Withey S, Cartmell E, Avery LM, Stephenson T (2005). Bacteriophages-potential for application in wastewater treatment processes. *Science of the Total Environment* **339:** 1-18.

Wu Q, Liu W-T (2009). Determination of virus abundance, diversity and distribution in a municipal wastewater treatment plant. *Water Research* **43:** 1101-1109.

Xie C, Goi CLW, Huson DH, Little PFR, Williams RBH (2016). RiboTagger: fast and unbiased 16S/18S profiling using whole community shotgun metagenomic or metatranscriptome surveys. *BMC Bioinformatics* **17:** 508.

Yang Q, Shen N, Lee ZM-P, Xu G, Cao Y, Kwok B *et al* (2016). Simultaneous nitrification, denitrification and phosphorus removal in a full-scale water reclamation plant located in warm climate. *Water Science and Technology*.

Yang S-F, Tay J-H, Liu Y (2004). Inhibition of free ammonia to the formation of aerobic granules. *Biochemical Engineering Journal* **17:** 41-48.

Yang SF, Li XY, Yu HQ (2008). Formation and characterisation of fungal and bacterial granules under different feeding alkalinity and pH conditions. *Process Biochemistry* **43:** 8-14.

Yeon K-M, Cheong W-S, Oh H-S, Lee W-N, Hwang B-K, Lee C-H *et al* (2009). Quorum sensing: A new biofouling control paradigm in a membrane bioreactor for advanced wastewater treatment. *Environmental Science & Technology* **43:** 380-385.

Yilmaz G, Lemaire R, Keller J, Yuan Z (2008). Simultaneous nitrification, denitrification, and phosphorus removal from nutrient-rich industrial wastewater using granular sludge. *Biotechnology and Bioengineering* **100:** 529-541.

Yoo H, Ahn K-H, Lee H-J, Lee K-H, Kwak Y-J, Song K-G (1999). Nitrogen removal from synthetic wastewater by simultaneous nitrification and denitrification via nitrite in an intermittently-aerated reactor. *Water Research* **33:** 145-154.

Yu K, Zhang T (2012). Metagenomic and metatranscriptomic analysis of microbial community structure and gene expression of activated sludge. *PLOS ONE* **7:** e38183.

Zeng RJ, Lemaire R, Yuan Z, Keller J (2003). Simultaneous nitrification, denitrification, and phosphorus removal in a lab-scale sequencing batch reactor. *Biotechnology and Bioengineering* **84:** 170-178.

Zhang T, Shao M-F, Ye L (2012). 454 Pyrosequencing reveals bacterial diversity of activated sludge from 14 sewage treatment plants. *ISME Journal* **6:** 1137-1147.

Zheng Y-M, Yu H-Q, Liu S-J, Liu X-Z (2006). Formation and instability of aerobic granules under high organic loading conditions. *Chemosphere* **63:** 1791-1800.

Zhou D, Liu M, Wang J, Dong S, Cui N, Gao L (2013). Granulation of activated sludge in a continuous flow airlift reactor by strong drag force. *Biotechnology and Bioprocess Engineering* **18:** 289-299.

Zhou Y, Ganda L, Lim M, Yuan Z, Kjelleberg S, Ng W (2010). Free nitrous acid (FNA) inhibition on denitrifying poly-phosphate accumulating organisms (DPAOs). *Applied Microbiology and Biotechnology* **88:** 359-369.

Zubkov MV, Sleigh MA (1999). Growth of amoebae and flagellates on bacteria deposited on filters. *Microbial Ecology* **37:** 107-115.

Zulianello L, Canard C, Köhler T, Caille D, Lacroix J-S, Meda P (2006). Rhamnolipids are virulence factors that promote early infiltration of primary human airway epithelia by *Pseudomonas aeruginosa Infection and Immunity* **74:** 3134-3147.

Appendix

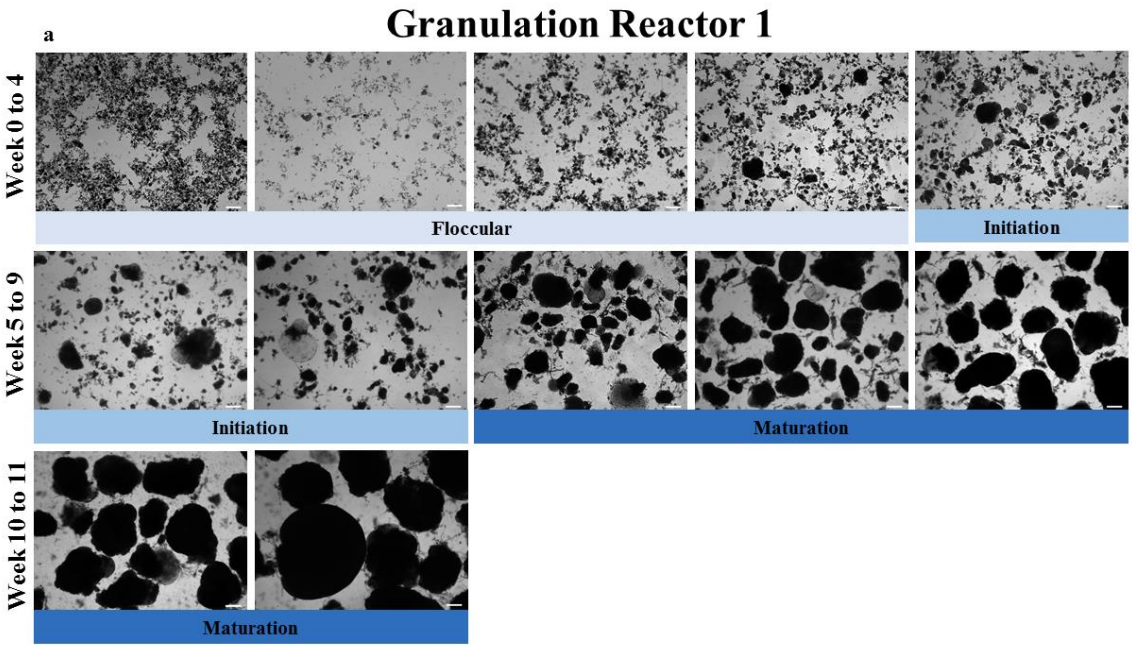
a
Granulation Reactor 1
Week 0 to 4
Floccular
Initiation
Week 5 to 9
Initiation
Maturation
Week 10 to 11
Maturation

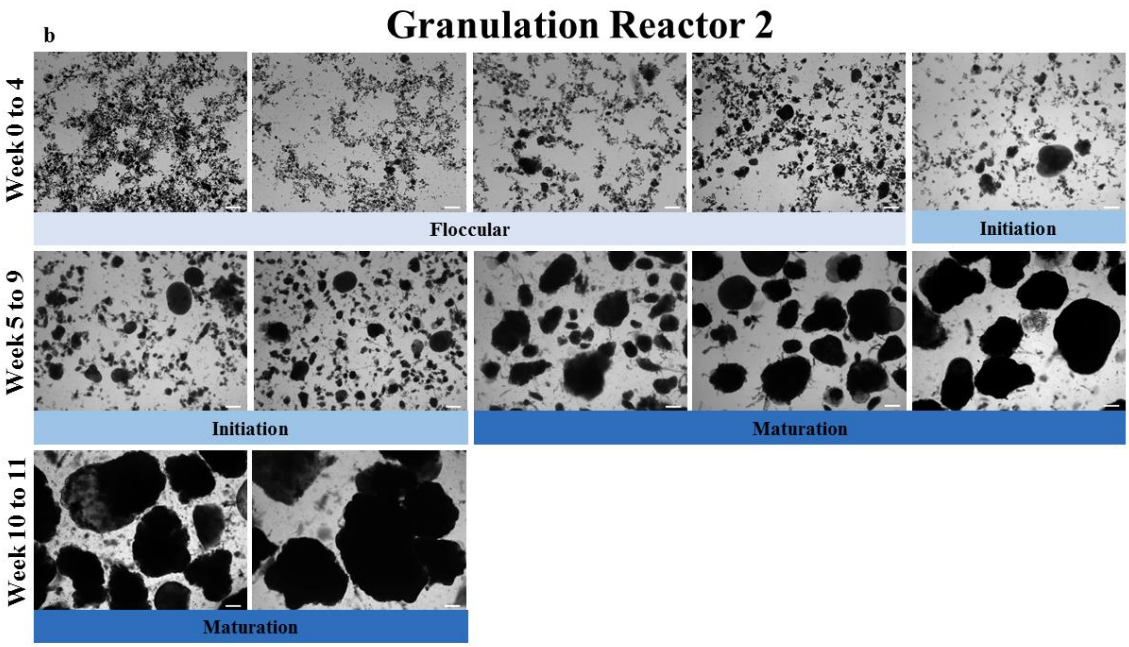
b
Granulation Reactor 2
Week 0 to 4
Floccular
Initiation
Week 5 to 9
Initiation
Maturation
Week 10 to 11
Maturation

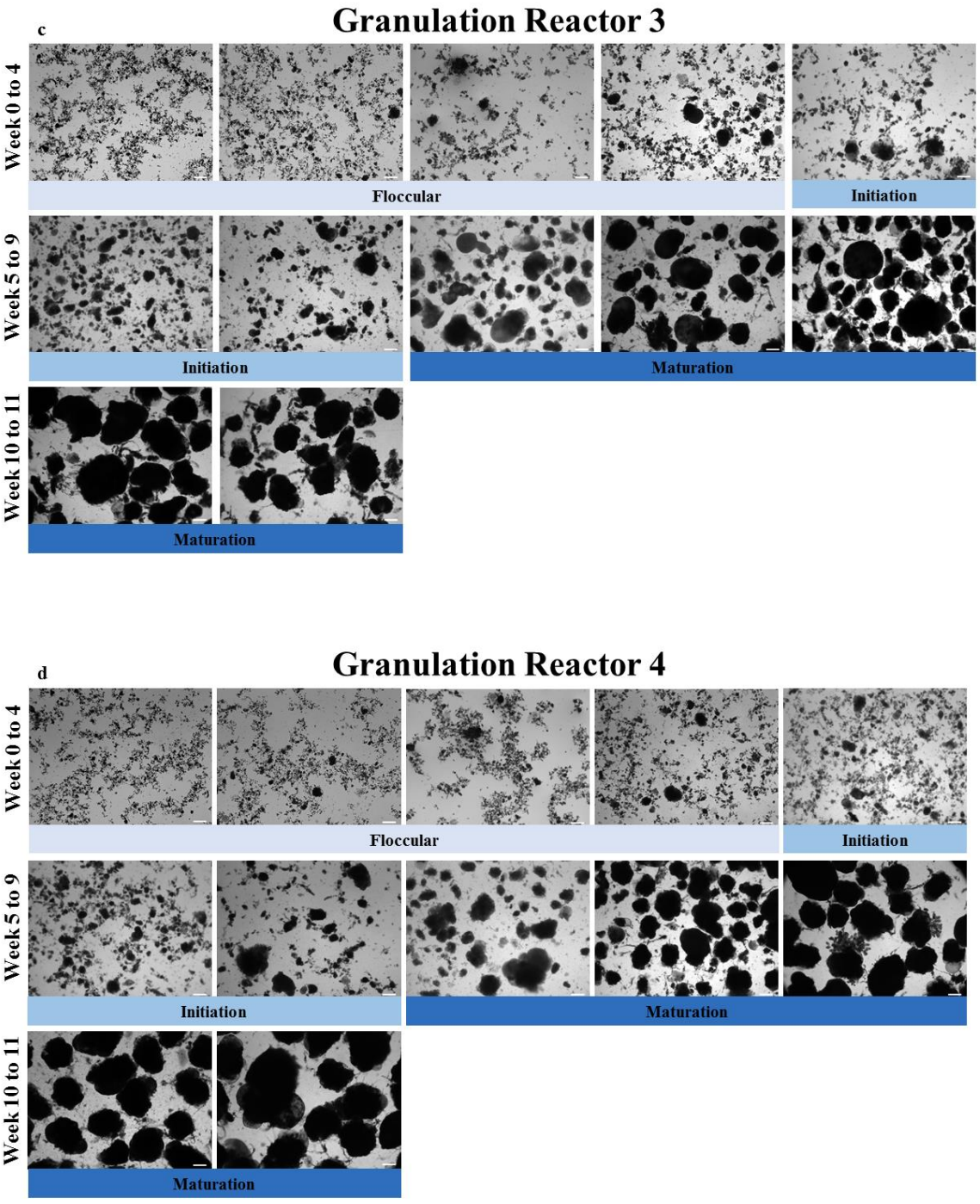

Figure A2.1: Weekly micrographs of floccular sludge development into granular sludge. (a-d) Floccular sludge in all SBRs had undergone aerobic granulation where aerobic granules were observed by the end of week 11. Magnification x 40 (bar, 200 µm)

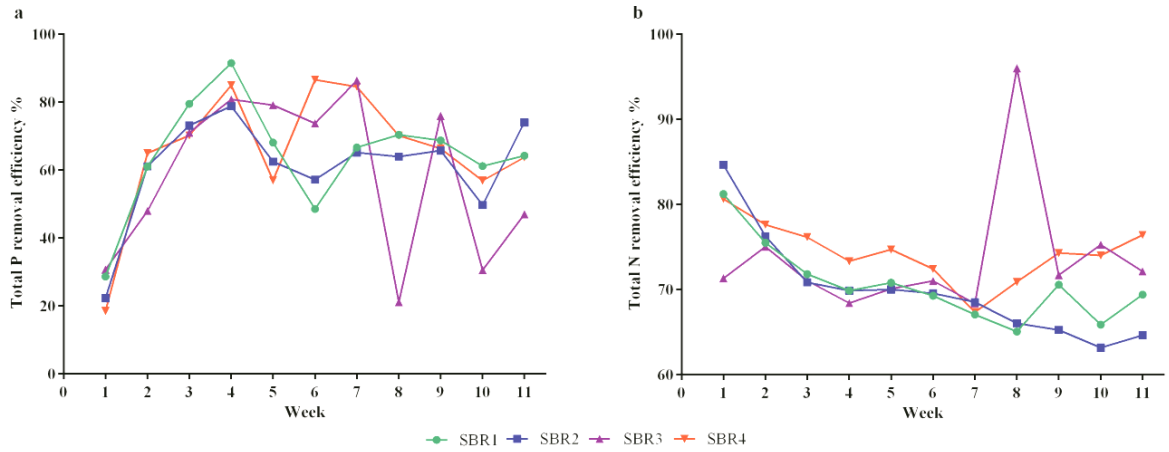

Figure A2.2: Weekly nutrient removal profile of the sludge community in each SBR**.** (a) Efficiency of the sludge community in removing phosphorous and (b) ammonia from synthetic influent as determined on a weekly basis.

Table A2.1: Total sum and percentage of sequencing reads for Bacteria, Eukarya, Archaea for SBR 1

SBR 1					
Week	Total reads	% Bacteria	% Eukarya	% Archaea	% Unidentified
0	182856	35.10	42.48	0.43	21.98
1	165151	56.85	24.78	0.15	18.23
2	147335	76.40	4.43	0.11	19.06
3	127442	74.30	4.74	0.05	20.92
4	159110	75.68	2.25	0.02	22.05
5	132967	83.18	3.00	0.01	13.80
6	149583	81.95	5.05	0.01	12.99
7	129893	88.08	3.00	0.00	8.91
8	139003	87.64	2.77	0.00	9.60
9	119907	88.39	2.30	0.00	9.31
10	151429	84.53	5.51	0.00	9.96
11	171021	86.47	2.84	0.00	10.69

Table A2.2: Total sum and percentage of sequencing reads for Bacteria, Eukarya, Archaea for SBR 2

SBR 2					
Week	Total reads	% Bacteria	% Eukarya	% Archaea	% Unidentified
0	186809	38.17	40.79	0.36	20.68
1	167064	52.70	31.67	0.13	15.51
2	122683	77.72	3.79	0.12	18.36
3	193256	75.04	1.79	0.06	23.11
4	219781	69.69	8.38	0.02	21.91
5	136727	85.08	2.24	0.01	12.68
6	135670	83.79	4.30	0.01	11.91
7	160050	83.70	8.16	0.00	8.13
8	149155	79.69	12.53	0.00	7.79
9	198922	87.96	4.47	0.00	7.57
10	188749	86.22	6.41	0.00	7.37
11	159953	89.48	1.54	0.00	8.98

Table A2.3: Total sum and percentage of sequencing reads for Bacteria, Eukarya, Archaea for SBR 3.

SBR 3					
Week	Total reads	% Bacteria	% Eukarya	% Archaea	% Unidentified
0	202338	35.06	42.06	0.42	22.46
1	161100	58.52	23.68	0.16	17.64
2	116584	77.40	3.64	0.14	18.82
3	147652	76.31	2.24	0.04	21.40
4	147460	76.19	2.82	0.02	20.97
5	198303	82.49	2.93	0.01	14.57
6	142990	82.57	2.52	0.00	14.91
7	133311	81.70	6.02	0.00	12.28
8	163426	81.13	7.72	0.00	11.15
9	157894	78.40	11.57	0.00	10.03
10	165228	78.79	10.57	0.00	10.64
11	157886	75.77	13.65	0.00	10.58

Table A2.4: Total sum and percentage of sequencing reads for Bacteria, Eukarya, Archaea for SBR 4.

SBR 4					
Week	Total reads	% Bacteria	% Eukarya	% Archaea	% Unidentified
0	207848	32.78	46.51	0.38	20.33
1	149188	64.00	19.49	0.14	16.38
2	125037	76.41	4.83	0.13	18.63
3	152048	83.78	0.56	0.04	15.62
4	129892	79.71	0.43	0.04	19.83
5	130700	85.85	1.17	0.01	12.97
6	136618	86.04	1.24	0.01	12.72
7	136628	81.96	4.88	0.00	13.16
8	158869	81.93	1.45	0.00	16.62
9	157567	79.63	0.36	0.00	20.01
10	155930	82.18	0.08	0.00	17.74
11	169759	84.52	0.10	0.00	15.38

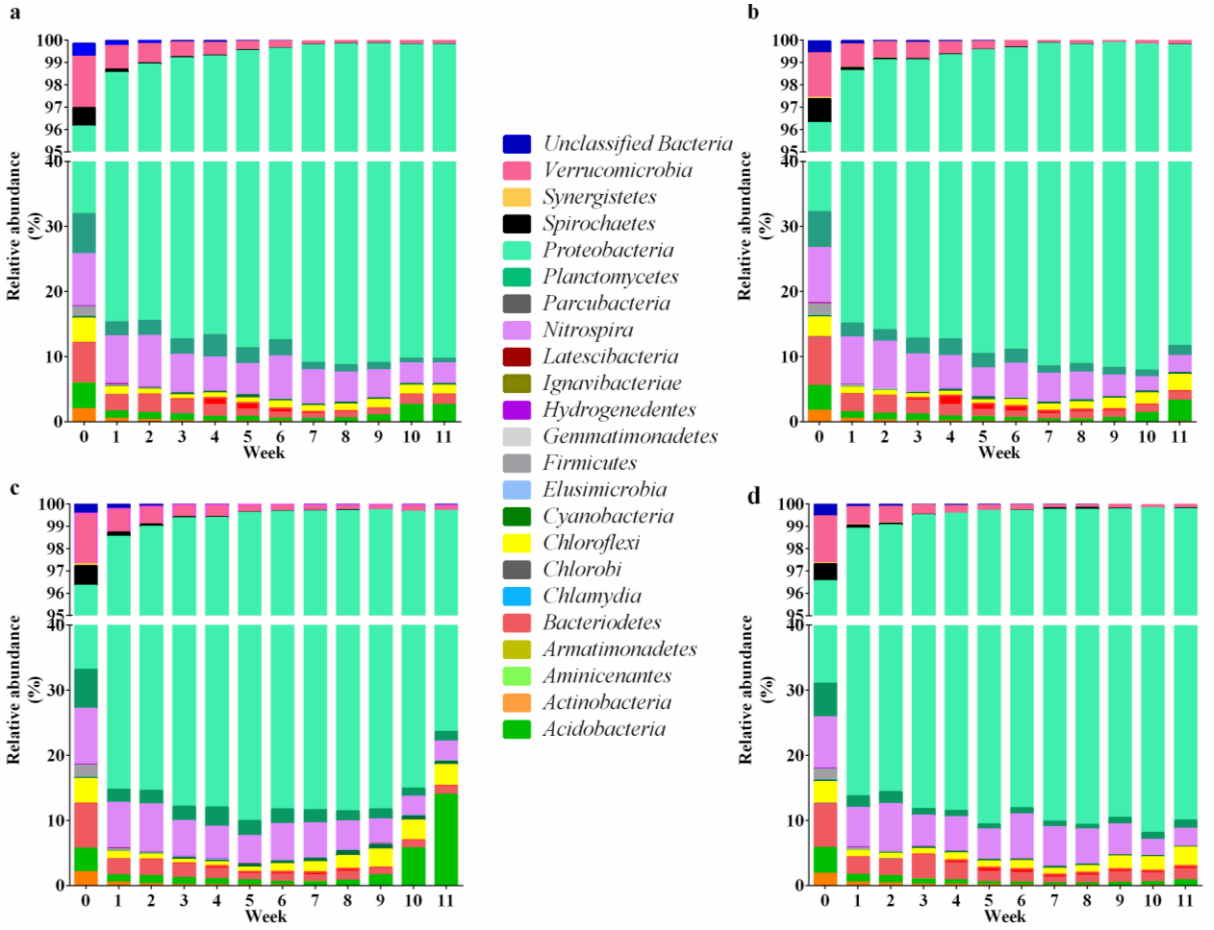

Figure A2.3: Ribotagger analysis of the microbial community composition of each SBR based on the different phases of aerobic granulation. (a) SBR 1 (b) SBR 2 (c) SBR 3 (d) SBR 4.

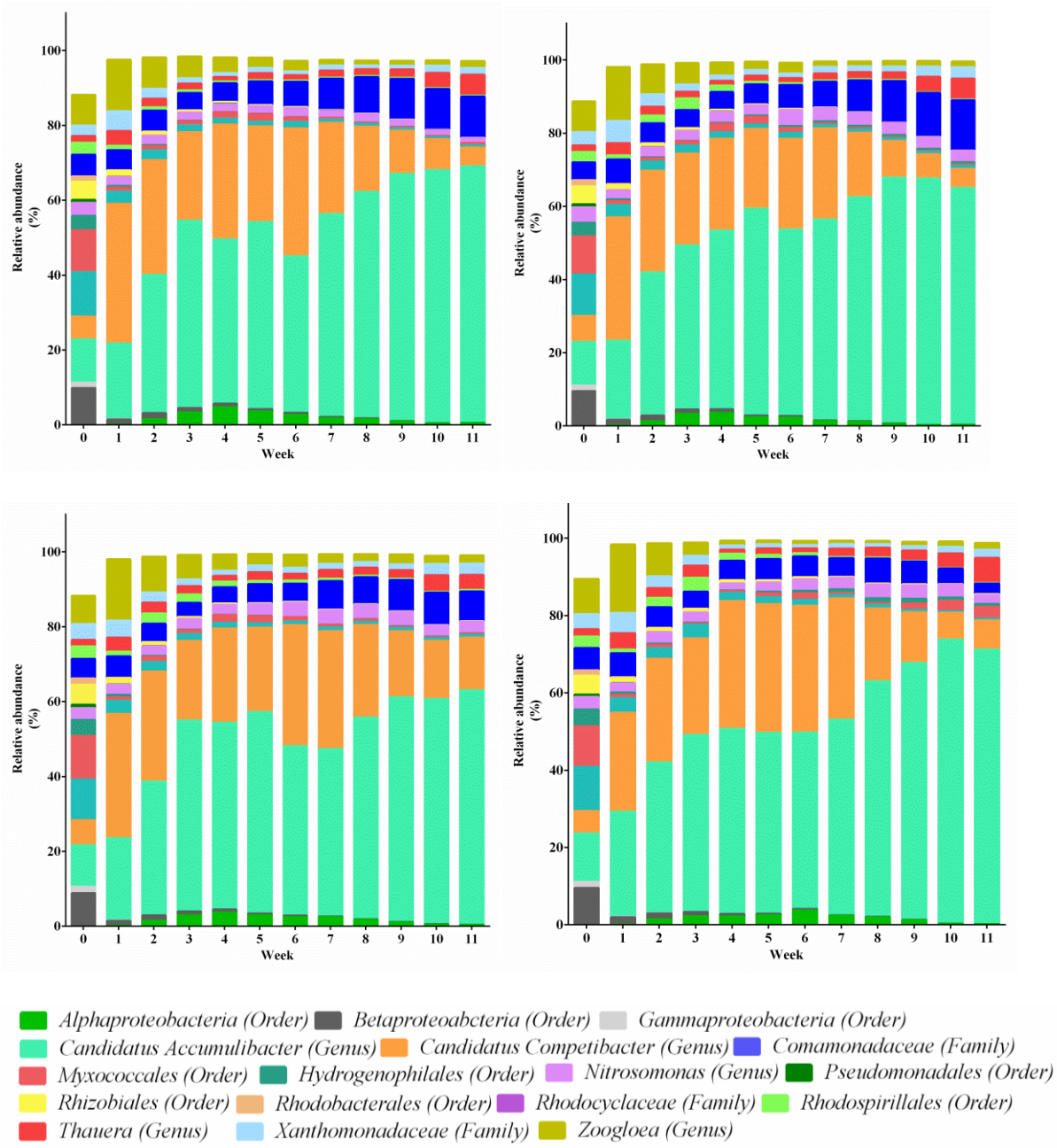

Figure A2.4: Ribotagger analysis of the microbial community composition of each SBR based on the different phases of aerobic granulation**.** (a) SBR 1 (b) SBR 2 (c) SBR 3 (d) SBR 4.

Table A3.1: One-way ANOVA with Tukey's multiple comparison test of total protozoa numbers in untreated, DMSO treated and thiram treated floccular sludge.

Tukey's multiple comparisons test	Mean Difference	95% CI of diff.	Significant?
0 mg L^{-1} vs. 0 mg L^{-1} w/DMSO	-94.45	-458.3 to 269.4	ns
0 mg L^{-1} vs. 5 mg L^{-1}	822.2	458.4 to 1186	****
0 mg L^{-1} vs. 10 mg L^{-1}	986.1	622.3 to 1350	****
0 mg L^{-1} vs. 20 mg L^{-1}	1128	764.0 to 1492	****
0 mg L^{-1} vs. 50 mg L^{-1}	1133	769.5 to 1497	****
0 mg L^{-1} vs. 100 mg L^{-1}	1133	769.5 to 1497	****
0 mg L^{-1} vs. 200 mg L^{-1}	1133	769.5 to 1497	****
0 mg L^{-1} w/DMSO mg L^{-1} vs. 5 mg L^{-1}	916.7	552.9 to 1280	****
0 mg L^{-1} w/DMSO mg L^{-1} vs. 10 mg L^{-1}	1081	716.7 to 1444	****
0 mg L^{-1} w/DMSO mg L^{-1} vs. 20 mg L^{-1}	1222	858.4 to 1586	****
0 mg L^{-1} w/DMSO mg L^{-1} vs. 50 mg L^{-1}	1228	864.0 to 1592	****
0 mg L^{-1} w/DMSO mg L^{-1} vs. 100 mg L^{-1}	1228	864.0 to 1592	****
0 mg L^{-1} w/DMSO mg L^{-1} vs. 200 mg L^{-1}	1228	864.0 to 1592	****
5 mg L^{-1} vs. 10 mg L^{-1}	163.9	-199.9 to 527.7	no
5 mg L^{-1} vs. 20 mg L^{-1}	305.6	-58.27 to 669.4	no
5 mg L^{-1} vs. 50 mg L^{-1}	311.1	-52.71 to 674.9	no
5 mg L^{-1} vs. 100 mg L^{-1}	311.1	-52.71 to 674.9	no
5 mg L^{-1} vs. 200 mg L^{-1}	311.1	-52.71 to 674.9	no
10 mg L^{-1} vs. 20 mg L^{-1}	141.7	-222.2 to 505.5	no
10 mg L^{-1} vs. 50 mg L^{-1}	147.2	-216.6 to 511.0	no
10 mg L^{-1} vs. 100 mg L^{-1}	147.2	-216.6 to 511.0	no
10 mg L^{-1} vs. 200 mg L^{-1}	147.2	-216.6 to 511.0	no
20 mg L^{-1} vs. 50 mg L^{-1}	5.560	-358.3 to 369.4	no
20 mg L^{-1} vs. 100 mg L^{-1}	5.560	-358.3 to 369.4	no
20 mg L^{-1} vs. 200 mg L^{-1}	5.560	-358.3 to 369.4	no
50 mg L^{-1} vs. 100 mg L^{-1}	0.0	-363.8 to 363.8	no
50 mg L^{-1} vs. 200 mg L^{-1}	0.0	-363.8 to 363.8	no
100 mg L^{-1} vs. 200 mg L^{-1}	0.0	-363.8 to 363.8	no

Table A3.2: One-way ANOVA with Tukey's multiple comparison test of total ammonia removal in untreated, DMSO treated and thiram treated floccular sludge.

Tukey's multiple comparisons test	Mean Difference	95% CI of diff.	Significant?
0 mg L^{-1} vs. 0 mg L^{-1} w/DMSO	4.370	-10.22 to 18.96	no
0 mg L^{-1} vs. 5 mg L^{-1}	11.23	-3.355 to 25.82	no
0 mg L^{-1} vs. 10 mg L^{-1}	14.01	-0.5753 to 28.60	no
0 mg L^{-1} vs. 20 mg L^{-1}	19.32	4.735 to 33.91	**
0 mg L^{-1} vs. 50 mg L^{-1}	23.75	9.165 to 38.34	***
0 mg L^{-1} vs. 100 mg L^{-1}	22.92	8.335 to 37.51	**
0 mg L^{-1} vs. 200 mg L^{-1}	26.80	12.21 to 41.39	***
0 mg L^{-1} w/DMSO mg L^{-1} vs. 5 mg L^{-1}	6.860	-7.725 to 21.45	no
0 mg L^{-1} w/DMSO mg L^{-1} vs. 10 mg L^{-1}	9.640	-4.945 to 24.23	no
0 mg L^{-1} w/DMSO mg L^{-1} vs. 20 mg L^{-1}	14.95	0.3647 to 29.54	*
0 mg L^{-1} w/DMSO mg L^{-1} vs. 50 mg L^{-1}	19.38	4.795 to 33.97	**
0 mg L^{-1} w/DMSO mg L^{-1} vs. 100 mg L^{-1}	18.55	3.965 to 33.14	**
0 mg L^{-1} w/DMSO mg L^{-1} vs. 200 mg L^{-1}	22.43	7.845 to 37.02	**
5 mg L^{-1} vs. 10 mg L^{-1}	2.780	-11.81 to 17.37	no
5 mg L^{-1} vs. 20 mg L^{-1}	8.090	-6.495 to 22.68	no
5 mg L^{-1} vs. 50 mg L^{-1}	12.52	-2.065 to 27.11	no
5 mg L^{-1} vs. 100 mg L^{-1}	11.69	-2.895 to 26.28	no
5 mg L^{-1} vs. 200 mg L^{-1}	15.57	0.9847 to 30.16	*
10 mg L^{-1} vs. 20 mg L^{-1}	5.310	-9.275 to 19.90	no
10 mg L^{-1} vs. 50 mg L^{-1}	9.740	-4.845 to 24.33	no
10 mg L^{-1} vs. 100 mg L^{-1}	8.910	-5.675 to 23.50	no
10 mg L^{-1} vs. 200 mg L^{-1}	12.79	-1.795 to 27.38	no
20 mg L^{-1} vs. 50 mg L^{-1}	4.430	-10.16 to 19.02	no
20 mg L^{-1} vs. 100 mg L^{-1}	3.600	-10.99 to 18.19	no
20 mg L^{-1} vs. 200 mg L^{-1}	7.480	-7.105 to 22.07	no
50 mg L^{-1} vs. 100 mg L^{-1}	-0.8300	-15.42 to 13.76	no
50 mg L^{-1} vs. 200 mg L^{-1}	3.050	-11.54 to 17.64	no
100 mg L^{-1} vs. 200 mg L^{-1}	3.880	-10.71 to 18.47	no

Table A3.3: One-way ANOVA with Tukey's multiple comparison test of total protozoa numbers in untreated, DMSO treated and thiram treated granular sludge.

Tukey's multiple comparisons test	Mean Difference	95% CI of diff.	Significant?
0 mg L^{-1} vs. 0 mg L^{-1} w/DMSO	244.4	-270.6 to 759.5	no
0 mg L^{-1} vs. 5 mg L^{-1}	1369	854.4 to 1884	****
0 mg L^{-1} vs. 10 mg L^{-1}	1275	760.0 to 1790	****
0 mg L^{-1} vs. 20 mg L^{-1}	1083	568.3 to 1598	****
0 mg L^{-1} vs. 50 mg L^{-1}	1369	854.4 to 1884	****
0 mg L^{-1} vs. 100 mg L^{-1}	1369	854.4 to 1884	****
0 mg L^{-1} vs. 200 mg L^{-1}	1369	854.4 to 1884	****
0 mg L^{-1} w/DMSO mg L^{-1} vs. 5 mg L^{-1}	1125	610.0 to 1640	****
0 mg L^{-1} w/DMSO mg L^{-1} vs. 10 mg L^{-1}	1031	515.5 to 1546	****
0 mg L^{-1} w/DMSO mg L^{-1} vs. 20 mg L^{-1}	838.9	323.9 to 1354	***
0 mg L^{-1} w/DMSO mg L^{-1} vs. 50 mg L^{-1}	1125	610.0 to 1640	****
0 mg L^{-1} w/DMSO mg L^{-1} vs. 100 mg L^{-1}	1125	610.0 to 1640	****
0 mg L^{-1} w/DMSO mg L^{-1} vs. 200 mg L^{-1}	1125	610.0 to 1640	****
5 mg L^{-1} vs. 10 mg L^{-1}	-94.44	-609.5 to 420.6	no
5 mg L^{-1} vs. 20 mg L^{-1}	-286.1	-801.1 to 228.9	no
5 mg L^{-1} vs. 50 mg L^{-1}	0.0	-515.0 to 515.0	no
5 mg L^{-1} vs. 100 mg L^{-1}	0.0	-515.0 to 515.0	no
5 mg L^{-1} vs. 200 mg L^{-1}	0.0	-515.0 to 515.0	no
10 mg L^{-1} vs. 20 mg L^{-1}	-191.7	-706.7 to 323.4	no
10 mg L^{-1} vs. 50 mg L^{-1}	94.44	-420.6 to 609.5	no
10 mg L^{-1} vs. 100 mg L^{-1}	94.44	-420.6 to 609.5	no
10 mg L^{-1} vs. 200 mg L^{-1}	94.44	-420.6 to 609.5	no
20 mg L^{-1} vs. 50 mg L^{-1}	286.1	-228.9 to 801.1	no
20 mg L^{-1} vs. 100 mg L^{-1}	286.1	-228.9 to 801.1	no
20 mg L^{-1} vs. 200 mg L^{-1}	286.1	-228.9 to 801.1	no
50 mg L^{-1} vs. 100 mg L^{-1}	0.0	-515.0 to 515.0	no
50 mg L^{-1} vs. 200 mg L^{-1}	0.0	-515.0 to 515.0	no
100 mg L^{-1} vs. 200 mg L^{-1}	0.0	-515.0 to 515.0	no

Table A3.4: One-way ANOVA with Tukey's multiple comparison test of total ammonia removal in untreated, DMSO treated and thiram treated granular sludge.

Tukey's multiple comparisons test	Mean Difference	95% CI of diff.	Significant?
0 mg L^{-1} vs. 0 mg L^{-1} w/DMSO	0.0	-22.62 to 22.62	no
0 mg L^{-1} vs. 5 mg L^{-1}	0.9400	-21.68 to 23.56	no
0 mg L^{-1} vs. 10 mg L^{-1}	12.50	-10.12 to 35.12	no
0 mg L^{-1} vs. 20 mg L^{-1}	24.67	2.052 to 47.29	*
0 mg L^{-1} vs. 50 mg L^{-1}	52.97	30.35 to 75.59	****
0 mg L^{-1} vs. 100 mg L^{-1}	51.50	28.88 to 74.12	****
0 mg L^{-1} vs. 200 mg L^{-1}	45.07	22.45 to 67.69	****
0 mg L^{-1} w/DMSO mg L^{-1} vs. 5 mg L^{-1}	0.9400	-21.68 to 23.56	no
0 mg L^{-1} w/DMSO mg L^{-1} vs. 10 mg L^{-1}	12.50	-10.12 to 35.12	no
0 mg L^{-1} w/DMSO mg L^{-1} vs. 20 mg L^{-1}	24.67	2.052 to 47.29	*
0 mg L^{-1} w/DMSO mg L^{-1} vs. 50 mg L^{-1}	52.97	30.35 to 75.59	****
0 mg L^{-1} w/DMSO mg L^{-1} vs. 100 mg L^{-1}	51.50	28.88 to 74.12	****
0 mg L^{-1} w/DMSO mg L^{-1} vs. 200 mg L^{-1}	45.07	22.45 to 67.69	****
5 mg L^{-1} vs. 10 mg L^{-1}	11.56	-11.06 to 34.18	no
5 mg L^{-1} vs. 20 mg L^{-1}	23.73	1.112 to 46.35	*
5 mg L^{-1} vs. 50 mg L^{-1}	52.03	29.41 to 74.65	****
5 mg L^{-1} vs. 100 mg L^{-1}	50.56	27.94 to 73.18	****
5 mg L^{-1} vs. 200 mg L^{-1}	44.13	21.51 to 66.75	****
10 mg L^{-1} vs. 20 mg L^{-1}	12.17	-10.45 to 34.79	no
10 mg L^{-1} vs. 50 mg L^{-1}	40.47	17.85 to 63.09	***
10 mg L^{-1} vs. 100 mg L^{-1}	39.00	16.38 to 61.62	***
10 mg L^{-1} vs. 200 mg L^{-1}	32.57	9.952 to 55.19	**
20 mg L^{-1} vs. 50 mg L^{-1}	28.30	5.682 to 50.92	**
20 mg L^{-1} vs. 100 mg L^{-1}	26.83	4.212 to 49.45	*
20 mg L^{-1} vs. 200 mg L^{-1}	20.40	-2.218 to 43.02	no
50 mg L^{-1} vs. 100 mg L^{-1}	-1.470	-24.09 to 21.15	no
50 mg L^{-1} vs. 200 mg L^{-1}	-7.900	-30.52 to 14.72	no
100 mg L^{-1} vs. 200 mg L^{-1}	-6.430	-29.05 to 16.19	no